Phase II Low Intensity Chemical Dosing (LICD): Development of Management Practices

Final Report submitted to Florida Department of Environmental Protection in fulfillment of Contract No. WM720

By P.A.M. Bachand, P. Vaithiyanathan and C.J. Richardson

DUWC

Duke University Wetland Center

December, 2000

This project and the preparation of this report was funded in part by a Section 319 Nonpoint Source Management Program grant from the U.S. Environmental Protection Agency through a contract with the Stormwater/Nonpoint Management Section of the Florida Department of Environmental Protection. The total cost of First Year Phase II LICD was $600,096 of which $300,000 or 50% was provided by U.S.E.P.A. The remaining $300,096 or 50% was provided by the Everglades Agricultural Area Everglades Protection District (EAA EPD).

Executive Summary

Low Intensity Chemical Dosing (LICD) is defined as the *in situ* marsh addition of low concentrations of chemicals to enhance and accelerate phosphorus removal from the water column through precipitation, coagulation and settling of chemically formed and naturally occurring particulate phosphorus (Peer Consulting, P.C./Brown and Caldwell, 1996). These processes would be augmented by the natural phosphorus removal processes in the marsh which include biotic uptake (e.g. periphyton, phytoplankton, plants) and soil adsorption (Craft and Richardson, 1993). As LICD is defined as *in situ* marsh dosing, LICD thus includes both the processes associated with chemical dosing and those associated with marsh uptake.

Essentially, LICD is a five-step process comprised of several physical, chemical and biological processes. These processes are:

- **Precipitation** (chemical),
- **Floc aggregation** (chemical),
- **Settling and filtering** (physical, chemical and biological),
- **Uptake** (biological), and
- **Burial** (physical, biological and chemical).

The investigation LICD by the Duke University Wetland Center (DUWC) has progressed in two phases, a feasibility study and an optimization study. The feasibility study was conducted under previous grants during Phase I to determine if LICD had promise or potential for decreasing phosphorus concentrations or loads to downstream Everglades waters (Richardson et al, 1997). Phase I primarily focused on phosphorus removal through the chemical processes of precipitation, aggregation and settling. Gradient effects such as filtering or biotic uptake that would occur in larger-scale marsh were not investigated.

Phase I studies showed that LICD can very effectively decrease dissolved phosphorus concentrations at metal dosing levels of 100 – 200 μM (Bachand et al., 1999). At those dosing levels, surface water dissolved phosphorus concentrations averaging near 30 μg L^{-1} were decreased to 5 – 10 μg L^{-1}. Approximately 75% of the decrease occurred immediately after chemical dosing through the conversion of dissolved phosphorus to particulate phosphorus. LICD also decreased total phosphorus concentrations in the water column. Aluminum dosing levels of 100 and 200 μM achieved mean total phosphorus concentrations between 20 and 30 μg L^{-1}, representing a 33 – 50% reduction below background phosphorus concentrations of 40 – 45 μg L^{-1} (Bachand et al., 1999). Finally, LICD led to an accumulation of metal-rich sediments. Deposited sediments had higher mineral content and excess phosphorus storage capacity as compared to background marsh soils (Bachand et al., 1999). As LICD is defined as *in situ*

chemical dosing in a full-scale marsh and not defined as a stand-alone chemical dosing system, these results, which primarily elucidated phosphorus removal through chemical but not marsh processes, were very promising.

The second phase of the LICD investigation, Phase II, had the primary goal of developing management practices to enhance LICD performance. Phase I studies recommended this approach in order to make LICD a more robust and more reliable technology. Phase II was initially intended as a three-year study incorporating field studies at multiple scales. This grant supported the first year of Phase II investigations. For First Year Phase II studies, a series of eight jar studies were used to investigate process mechanisms and three mesocosm studies were used to field validate jar test findings and to further develop the technology for *in situ* applications at a larger-scale. As with Phase I studies, the field experiments used during Phase II could not test large-scale marsh gradient effects such as filtering, settling and some types of biotic uptake.

Phase II studies have demonstrated that polymers in combination with improved mixing regimes dramatically improve phosphorus removal by LICD. In jar tests, the addition of cationic polymers to iron and aluminum coagulants further decreased dissolved phosphorus concentrations in the water column and improved total phosphorus removal. For background total phosphorus concentrations of 31.4 $\mu g\ L^{-1}$, ferric sulfate in combination with 20% cationic polymer decreased total phosphorus concentrations to 7 $\mu g\ L^{-1}$ as opposed to only 13 $\mu g\ L^{-1}$ when ferric chloride was used. Alum in combination with 10% cationic polymer decreased total phosphorus to 7 $\mu g\ L^{-1}$ as opposed to only 18 $\mu g\ L^{-1}$ when alum was used alone.

Jar test studies also showed that under effective mixing regimes and chemical dosing protocols, anionic polyacrylamides (PAMs) greatly aided floc aggregation and subsequent settling. Flocs produced under PAM addition were up to several orders of magnitude greater in size than when PAMs were not used, especially when used in combination with iron coagulants. Larger flocs settled more quickly. For instance, under iron dosing, flocs formed from the use of PAMs began settling immediately and reached a steady state condition within 5 minutes. This was approximately one-tenth the time for steady state conditions to be achieved under iron dosing without PAMs. For aluminum, flocs settled more quickly though the difference with and without PAMs was less. Improved floc settling rates especially under iron dosing held great promise in improving total phosphorus settling rates under *in situ* marsh conditions. Small pin flocs formed under metal dosing and hindered settling had been identified by Bachand et al. (1999) as a problem needing to be addressed if LICD were to be made more robust. In jar tests, better rapid and slow mixing regimes further improved phosphorus removal though those improvements were not always statistically significant and generally less dramatic than the improvements gained through utilizing polymers.

Polymers utilization and improved mixing regimes were incorporated into the field studies based upon the jar test results. Mesocosm studies were conducted in June 1999, October 1999 and February/March 2000. Each study had different goals and each study led to further optimization in the LICD treatments. The February/March study therefore represents the most optimal *in situ* LICD treatments to date. In that study, mesocosms were operated under continuous flow at a 2.5-day hydraulic retention time (HRT). Both metal/cationic polymer blends and PAMS were used. PAMs were dosed at 0.5 and 1.0 mg L^{-1}. *In situ* PAM addition at 1.0 mg L^{-1} greatly improved phosphorus removal. When PAMs were dosed at 1 mg L^{-1} in combination with iron dosing levels of 200 μM (11.2 mg L^{-1}), mean total phosphorus concentrations in the mesocosms decreased by 72% from 105 μg L^{-1} to 29 μg L^{-1}. When PAMs were used at a lower dose of 0.5 mg L^{-1}, iron dosing at 200 μM only decreased total phosphorus concentrations 20% from 129 μg L^{-1} to 103 μg L^{-1}. This trend was similar for aluminum at 200 μM (5.4 mg L^{-1}), with PAM dosing at 1 mg L^{-1} resulting in mean phosphorus concentrations in the mesocosms of 39 μg L^{-1} as opposed to only 77 μg L^{-1} when the lower PAM dose was utilized.

In general, PAMs greatly improved settling and this was most apparent at lower metal doses. In previous mesocosm studies at metal dosing concentration of 200 μM, water column total phosphorus concentrations decreased by only 21 – 48% (Bachand et al, 1999). This finding is very important for LICD process. Metal dosing levels of 100 and 200 μM have effectively and consistently converted dissolved phosphorus to particulate phosphorus (Bachand et al., 1999). However, hindered settling of pin floc was identified as a problem for settling the particulate phosphorus. PAMs apparently convert the pin floc formed under metal dosing to larger aggregates that settle more effectively. Thus, *in situ* PAM dosing of 1 mg L^{-1} holds promise for effective total phosphorus removal at metal dosing levels below 200 μM.

Total phosphorus concentrations were also measured in the mixing tanks upstream of the mesocosms. Mixing tanks which were hydrologically isolated from the marsh were sampled after a quiescent period of 18 – 24 hours as opposed to a 2.5 day HRT in the mesocosms. Mean total phosphorus concentrations achieved in the mixing tanks ranged from 12 – 31 μg L^{-1}. At iron dosing of 200 μM (11.2 mg L^{-1}) in combination with PAM at 1 mg L^{-1}, a median total phosphorus concentration of 24 μg L^{-1} was achieved. For aluminum at the same molar metal dosing level (200 μM, 5.4 mg L^{-1}) and PAM concentrations, a median total phosphorus concentration of 19 μg L^{-1} was achieved.

On average, lower total phosphorus concentrations were achieved in the mixing tanks as opposed to the mesocosms despite much shorter hydraulic retention times in the mixing tanks. Some differences between the resulting total phosphorus concentrations in the mixing tanks and the mesocosms can be attributed to the presence of vegetation and other confounding factors in the

mesocosms. However, dilution of mesocosm water with high phosphorus marsh water was also a major factor. Bromide tracer data demonstrated that approximately 80% of the water within the mesocosm was chemically dosed marsh water and 20% was non-dosed marsh water. This likely occurred through diel water level fluctuations in the marsh forcing water in and out of the mesocosms through the outlet valves. When this factor is incorporated into the mass balance analyses, the predicted phosphorus concentration achieved by LICD in the mesocosms is very near that achieved in the mixing tanks. For PAM dosing levels of 1 mg L^{-1}, the calculated resulting phosphorus concentrations range from 12 – 28 μg L^{-1}. For mesocosms dosed with iron at 200 μM (11.2 mg L^{-1}) and PAM at 1 mg L^{-1}, a mean total phosphorus concentration of 12 μg L^{-1} was calculated. For mesocosms dosed with aluminum at 200 μM (5.4 mg L^{-1}) and PAM at 1 mg L^{-1}, a mean total phosphorus concentration of 29 μg L^{-1} was calculated. The optimum aluminum treatment in the mesocosm study was aluminum dosing at 400 μM (10.8 mg L^{-1}) and PAM dosing at 0.5 mg L^{-1}. This achieved a mean phosphorus concentration of 9 μg L^{-1}. These calculated values represent phosphorus levels that would be expected under hydrologically-isolated conditions. These values were calculated against a mean background phosphorus concentrations of 117 μg L^{-1}. Thus, many of these treatments would be expected to achieve total phosphorus removal of over 80%.

The mass balance analyses when considered in combination with anticipated full-scale marsh processes strongly suggest that LICD can meet threshold phosphorus concentrations when incorporated *in situ* in a larger-scale mature marsh operating under non-ideal plug flow conditions. Under hydrologically isolated conditions in the mixing tanks and when utilizing both cationic polymers and PAMs, LICD has decreased total phosphorus concentrations by over 80%. Mass balance calculations for the mesocosm data predict similar phosphorus levels would be achieved in the mesocosms under hydrologically-isolated conditions. Phosphorus removal in these experimental systems occurred primarily through chemical precipitation, floc aggregation and floc settling. Importantly though, these experiments could not test gradient effects that would occur for the treatment in a full-scale application and therefore these analyses exclude any such gradient effect.

Large-scale marshes dominated by emergent macrophytes such as sawgrass or cattails more closely resemble non-ideal plug flow reactor (PFR) as opposed to completely mixed systems such as the mesocosm systems used in this study (e.g. Continuous-Flow stirred tank reactor – CFSTR). For first-order substrate removal kinetics such as would be the case for biological uptake of nutrients, PFRs are much more efficient at pollutant removal than CFSTRs and this is fundamentally related to the decrease in nutrient concentrations as water passes through the systems (Metcalf and Eddy, 1979). Thus, the configuration of a full-scale marsh favors more efficient nutrient removal than that which can occur in a cylindrical mesocosm system such as was used in this study. Additionally, marshes have lower hydraulic conductivity and higher resistance to flow than

open water systems. This increased resistance is due to the presence of marsh plants. In flow through marsh systems, high plant density and accompanying high frictional resistance lead to more efficient particulate settling and filtering, greater surface area for colonization of biota, and more efficient biological uptake (Bachand and Horne, 2000; Phipps and Crumpton, 1994). These full-scale marsh characteristics should lead to higher particulate settling rates, better filtration and higher biotic uptake rates than can be achieved in the mesocosm systems used in this study. These are the gradient effects associated with large-scale non-ideal plug flow marshes.

Florida marshes are phosphorus limited and can decrease total phosphorus to levels at or below 10 $\mu g\ L^{-1}$ (Vaithiyanathan and Richardson, 1997). Dense submerged and emergent marsh vegetation aid with particle filtering and settling. Because Florida marshes alone can decrease total phosphorus concentrations to 10 $\mu g\ L^{-1}$, than a LICD marsh should also be able to achieve the same phosphorus levels. However, because LICD would decrease by approximately 80% the phosphorus load required for treatment by the accompanying marsh, the use of LICD would enable higher flows through the marsh and lengthen the effective life of the marsh. This will allow the marsh to be operated at a much shorter hydraulic retention time (HRT). Vaithiyanathan and Richardson (1997) showed that in the Water Conservation Areas (WCAs), total phosphorus concentrations under 10 $\mu g\ L^{-1}$ are reached 9 kilometers from the inflow structures. Inflow phosphorus concentrations are decreased by 80% to the range of 25 – 30 $\mu g\ L^{-1}$ 5 to 6 kilometers beyond the inflow structures. Thus, in the WCAs, 55 – 67% of the enriched marsh area is required to decrease the phosphorus loads by 80% to concentration levels in the range of 25 – 30 $\mu g\ L^{-1}$. This data set represents the time periods of 1986 – 1991 and 1993 – 1995. With a full-scale LICD marsh, our data suggests that 80% of the load will be removed by LICD and that only 20% of the load will need to be removed by associated marsh processes typical to those in the WCAs. Thus, the WCA data from Vaithiyanathan and Richardson (1997) predicts that the marsh area can be decreased by 55 – 67%. Conversely, flows to a LICD marsh can be on the order of 2 to 3 times higher than a treatment wetland without LICD.

In addition to enabling shorter HRTs, an LICD marsh will likely be less apt to become saturated with regard to phosphorus uptake. Richardson and Qian (1999) showed in the WCAs that once phosphorus loading saturate short-term uptake and storage mechanisms as is typical in the enriched zones of the WCAs, a phosphorus front begins moving down the gradient. This sediment saturation with phosphorus is indicated by soil phosphorus concentrations two to three times higher in the enriched zone of the WCAs as compared to the unenriched zones (Vaithiyanathan and Richardson, 1997). These soil concentrations exponentially decrease downstream from inflow structures. In an LICD marsh, the marsh is expected to be less likely to become saturated with regard to phosphorus because chemical processes are expected to decrease the phosphorus load by around 80%. This reduced phosphorus loading will lead to

lower water and sediment phosphorus concentrations and effectively extend the marsh life.

Thus, we believe an LICD marsh can potentially reduce phosphorus concentrations to near 10 $\mu g\ L^{-1}$. We believe that LICD chemical processes will decrease phosphorus concentrations to around 20 $\mu g\ L^{-1}$ and that the remaining phosphorus removal will occur through typical marsh processes such as settling, filtering and biotic uptake. We believe that a LICD marsh will be able to operate at a HRT approximately 2 to 3 times shorter than a treatment marsh without LICD and that LICD will extend the life of the marsh with regard to phosphorus removal. This conclusion is based upon the performance of LICD in the mesocosm systems under CFSTR conditions; an understanding of reactor kinetics related to wetlands, PFRs and CFSTRs; and WCAs phosphorus removal characteristics (Vaithiyanathan and Richardson, 1997; Craft and Richardson, 1993; Richardson and Qian, 1999). Effective implementation will require the incorporation of polymers and likely require some consideration of mixing regimes. Given the natural characteristics of the marsh, some of these requirements may be relatively simple and cost-effective to employ. Thus, we recommend testing LICD at a larger pilot-scale with incorporation of polymers and improved mixing regimes.

Other findings from this study further support our recommendation to continue pursuing the LICD model as presented by us. This study has shown that:

- LICD nearly eliminates dissolved phosphorus from the water column,
- Sediments formed under LICD prevent the release of phosphorus from the sediments back into the water column, and
- LICD has minor effects on the marsh readiness of waters and minimally affects the aquatic environment in the dosed regions.

Each of these is discussed below.

LICD nearly eliminates dissolved phosphorus from surface waters and this should positively affect the marsh biota. LICD has previously removed dissolved phosphorus from the water column (Bachand et al., 1999). With the addition of cationic polymers, improved conversion of dissolved phosphorus to particulate phosphorus occurs and lower dissolved phosphorus concentrations are achieved. Dissolved phosphorus concentrations in the water column are consistently decreased by 80 – 90% to near 5 $\mu g\ L^{-1}$ when metal/cationic polymer blends are utilized. As dissolved phosphorus is likely more biologically available than particulate phosphorus, the near total elimination of dissolved phosphorus from the water column will likely reduce downstream eutrophication in the Everglades.

Sediments formed under LICD are phosphorus deficient and should prevent the release of phosphorus from the sediments back into the water column. During LICD floc formed under metal dosing is primarily composed of the dosed metal, carbon, calcium and other non-measured parameters which are likely to be

oxygen, sulfur and hydrogen. The metal:phosphorus ratio in these flocs are approximately 100:1 which are twenty times higher than the metal:phosphorus ratio of 4:1 found for aluminum and iron in the peat sediments of the Everglades Nutrient Removal Project (ENRP). This higher ratio represents excess phosphorus storage capacity in the formed flocs. Mesocosm field studies supported this by showing that sediments in mesocosms receiving low aluminum and iron dosing levels of 100 μM suppressed the release of phosphorus from the sediments back into the water column during periods of exfiltration. Thus, LICD sediments effectively cap phosphorus release from the marsh sediments.

Finally, LICD minimally affects marsh readiness of the water. LICD did not affect temperature; specific conductance; concentrations of calcium, magnesium, potassium, sodium, copper, zinc, nitrate, ammornia or chloride; total suspended solids; and hardness. Both iron and aluminum dosing affected pH and alkalinity. However, iron effects were very minor. LICD did increase DO concentrations in the treated mesocosms though this was opposite to what had occurred during Phase I (Bachand et al., 1999). Thus, LICD effects on DO are very dependent upon the resident flora and fauna. Both iron and aluminum dosing increased sulfated concentrations and decreased color, and aluminum dosing decreased total dissolved nitrogen. Overall, LICD only slightly affected the marsh readiness of the water.

Several results from LICD are relevant to the other technologies. Higher dosing levels do not necessarily improve phosphorus removal. Better gains in improving phosphorus removal are achieved through the implementation of other practices rather than through higher metal doses. Fundamentally, the primary role of both aluminum and iron with regard to phosphorus removal from these organic waters is to convert dissolved phosphorus to particulate phosphorus. The role of aluminum and iron in creating large and settleable flocs in the Everglades water is generally negligible. That role is better met by the use of PAMs. At higher metal dosing levels, several causal results should be considered.

First, higher dosing levels may lead to higher residual concentrations of total aluminum and total iron in the water column. LICD has slightly elevated residual concentrations of total iron and aluminum. The incorporation of polymers and blending has generally reduced those concentrations to less than 1 mg L^{-1}. However, inefficient chemical usage would increase residual concentrations and possibly to levels as high or higher than 5 mg L^{-1}. Higher residual concentrations could lead to the carry over of either aluminum or iron into downstream marshes. Efficient chemical mixing should help reduce the levels of residual metals.

Second, higher dosing levels may require post-treatment for the purpose of providing marsh ready water. Both aluminum and iron affected pH and alkalinity though the effects at dosing concentrations of 200 μM and below were negligible. However, higher dosing concentrations and primarily those above 400 μM will

greatly affect alkalinity and pH. Thus higher dosing levels may require post-treatment to minimize those deleterious effects.

Third, other chemical treatments may require substantial investment in sludge management. During this study, when chemical application was near an optimum for producing settleable flocs, the metal:phosphorus ratio in the flocs was approximately 100:1. In floc formed under these conditions, phosphorus was on the order of 0.1 to 0.2% of the total dry weight. Under LICD, this material forms a mineral-organic sediment as discussed earlier and the formed sediment accretes over time. However, in other chemical application technologies, the material formed from chemical addition will need to be removed from the site. This requirement that is inherent in all other chemical treatment technologies creates disposal issues and costs. Thus, under optimal dosing conditions, for each ton of phosphorus removed, 500 to 1000 tons of dry sludge are produced. This material is stored as sediments in LICD though it will require disposal from the site in all other chemical treatment technologies. Of course, less efficient chemical utilization would increase sludge production, and increase sludge management costs.

In LICD, sludge remains in the marsh as formed sediments and accretes with the peat. With no chemical dosing in an enriched marsh as would be the case with the STAs, a one foot increase in sediment bed elevation would occur over 68 years. Chemical dosing at 100 μM would decrease that period to about 46 years. Dosing at 200 μM would decrease that period to about 34 years. Thus, the LICD marsh would provide long-term storage of the formed precipitates and require little if any management costs. Because of the excess phosphorus storage capacity of the LICD sediments, it is possible that dosing concentrations could be decreased over time. Thus, it is possible that this accretion rate could be further reduced.

All these implications (higher residual metal concentrations, the possible need for post-treatment to meet marsh readiness requirements and sludge disposal) increase costs. These costs are not borne by LICD.

Under the approach undertaken for Phase II, LICD remains unique from other technologies because of three primary and important characteristics. First, the LICD efforts focused on minimizing chemical usage by intensive investigation of methods to optimize chemical effectiveness. Second, under LICD metal-phosphorus precipitates would settle in the marsh as opposed to settling in upstream basins. For all the chemical treatment technologies, this characteristic is unique to LICD and could potentially minimize capital and O&M costs. Finally, in LICD the marsh is used to provide additional phosphorus removal through improved settling and biotic uptake. The marsh is simply not there for polishing. Phosphorus removal occurs in the Water Conservation Areas as demonstrated by total phosphorus concentrations in the downstream sections of Water Conservation Area-2A near and below 10 μg L^{-1} (Vaithiyanathan and Richardson,

1997). Florida marshes are phosphorus limited and able to remove total phosphorus to very low levels. Thus, chemical removal of phosphorus as demonstrated by the mesocosm studies and phosphorus uptake as demonstrated by the Water Conservation Areas-2A together suggests that LICD when applied in a larger-scale marsh could achieve total phosphorus concentrations near 10 $\mu g\ L^{-1}$.

We have developed a conceptual design for LICD implementation at the larger-scale. This design is based upon the findings of this study and expands upon the original vision of LICD as proposed by Peer Consulting, P.C./Brown and Caldwell (1996). Peer Consulting, P.C. recognized the need for mixing for LICD. In their presentation of LICD, they describe chemical injection at the water pumps. The pumps would provide the turbulence and energy necessary for effective chemical utilization (Berger, 1987). Peer Consulting, P.C./Brown and Caldwell (1996) do not discuss the use of polymers but they do not dismiss it either. Peer Consulting P.C./Brown and Caldwell recommend low chemical dosing levels to minimize chemical sludge accumulation. Thus any step to maintain low metal dosing levels would seem pertinent in achieving this goal.

In our proposed conceptual design, three mixing zones are recommended:

- A rapid mixing zone for blending metals provided by a pump,
- A rapid mixing zone for blending PAMs provided by a static mixer or equivalent, and
- A slow mixing zone for enhancing floc aggregation provided by either passive dispersion of high energy water into the marsh or by mechanical mixers.

Three chemical blends at dosing levels of 100 and 200 μM are recommended for initial testing at the larger scale. These blends are:

- FerriPlus-D (includes a 20% cationic polymer),
- Ferric chloride, and
- Clarion 4100 (alum plus 10% cationic polymer).

The use of PAMs is considered critical for this technology and an *in situ* dosing level of 1 $mg\ L^{-1}$ is recommended though that concentration may vary somewhat with PAM used. For these different chemical blends, the estimated treatment costs vary greatly with metal blends. Assuming the same metal dosing levels, 50-year Present Worth costs are approximately three times higher for metal blends with cationic polymers added than those without (e.g. FerriPlus-D vs. Ferric Iron; Clarion 4100 vs. alum). This underscores the need to optimize mixing regimes and to utilize PAMs in order to minimize chemical usage, improve floc aggregation, and possibly reduce the advantages of using cationic polymers. For LICD, the marsh is recommended to be operated at a 5 - 7.5 day HRT and to be divided into two zones. The first zone is primarily for floc aggregation and should be operated at an HRT of 2 days. The second zone is primarily for filtering less settleable particulates and biotic uptake. This zone is operated at 3 to 5 days. Testing LICD at a pilot-scale is recommended to further refine the methodology,

enable more efficient chemical usage. A pilot-scale marsh would have non-ideal plug flow characteristics which would improve settling, increase filtration rates and promote more efficient biotic uptake.

Table of Contents

List of Tables

List of Figures

List of Acronyms and Abbreviations

Al	Aluminum
ANOVA	Analyses of Variance
Br	Bromide
Ca	Calcium
CFSTR	Continuous Flow Stirred Tank Reactor
Cl	Chlorine
Cu	Copper
d	day
DO	Dissolved oxygen
DOC	Dissolved organic carbon
DUWC	Duke University Wetland Center
ENRP	Everglades Nutrient Removal Project
EPA	U.S. Environmental Protection Agency
FDEP	Florida Department of Environmental Protection
Fe	iron
FeCl	Ferric chloride
FPB	Ferriplus-B (© Kemiron, Inc.)
FPD	Ferriplus-D (© Kemiron, Inc.)
ft	feet
gpm	gallons per minute
h	hour
HRT	Hydraulic retention time
K	Potassium
kg	kilogram
L	Liter
LICD	Low Intensity Chemical Dosing
m	minute
mg	milligram
Mg	Mangnesium
ml	milliliter
Mn	Maganese
mgd	million gallons per day
N	Nitrogen
Na	Sodium
p	p-value; probability coefficient
P	Phosphorus
PAM	Anionic polyacrylamides
PFR	Plug flow reactor
ppb	parts per billion; equivalent to $\mu g\ L^{-1}$ for liquids and $\mu g\ kg^{-1}$ for solids
ppm	parts per million; equivalent to $mg\ L^{-1}$ for liquids and $mg\ kg^{-1}$ for solids
ppt	parts per thousand; equivalent to $g\ L^{-1}$ for liquids and $g\ kg^{-1}$ for solids
QAPP	Quality assurance project plan

r	correlation coefficient
s	second
SD	standard deviation
SE	standard error
Si	Silica
SO_4	Sulfate
SOW	Scope of work
STA	Stormwater Treatment Area
µg	microgram
µM	micromole
WCA	Water Conservation Area
Zn	zinc

Analyte Codes

FTP	Filtered total phosphorus. Equivalent to dissolved phosphorus.
UTP	Unfiltered total phosphorus
FOP	Filtered ortho-phosphate. Equivalent to soluble reactive phosphorus
FOC	Filtered organic carbon. Equivalent to dissolved organic carbon.
UFE	Unfiltered total iron
FFE	Filtered total iron
UAL	Unfiltered total aluminum
FAL	Filtered total aluminum
FBr	Filtered total bromide
NH_4	Ammonia (as nitrogen)
NO_X	Nitrate + nitrite (as nitrogen)
TDN	Total dissolved nitrogen (filtered)
TN	Total nitrogen (unfiltered)
Ca	Calcium (filtered)
Na	Sodium (filtered)
Mg	Magnesium (filtered)
Mn	Manganese (filtered)
K	Potassium (filtered)
Zn	Zinc (filtered)
Cu	Copper (filtered)
Si	Silica (filtered)
Cl	Cloride (filtered)
SO_4	Sulfate (filtered)
TSS	Total suspended solids
DO	Dissolved oxygen

Acknowledgements

We appreciate the efforts of the dedicated Wetland Center Staff for implementing and persevering with this work through many difficult situations. We would like to thank our Florida staff of Sean Cimilluca, Jeff Johnson, Lea Karppi and Ron Durham for their dedicated and excellent field support, and for their intellectual contributions which were crucial for implementing and running a complex field experiment from over one thousand miles away. We would also like to thank the excellent laboratory staff of Troy Rogers, Wes Willis, Julie Rice and Paul Heine for their precise and prompt data analyses; for their vigilance in maintaining high quality standards; and for their ideas and thoughtful feedback. We have also benefited from the ideas of others outside the Wetland Center. Of those, we would like to especially thank Fred Sims of Kemiron; Amir Abtahi of GeoSolar Energy Systems and Florida Atlantic University; Steve Faigan and Tom Coughlin of General Chemical; Kevin Locher of AMJ Equipment Corporation; Kerry Prugh of Atlantic Environmental Systems, Dave Jenkins of Atlantic Technology Group, and Steve Zimmerman of Robert E. Mason. All donated their expertise or services at one time or another. We also appreciate the efforts of Professor Yongxing Yang, a Visiting Scholar from the Changchun Institute of Geography who greatly aided with implementation of our final field studies. Finally, we appreciate the efforts of Sandra Bachand who provided feedback on this project throughout and aided with preparation of this document.

This study was jointly funded by the Everglades Agricultural Area Everglades Protection District and the Florida Department of Environmental Protection. Access to the ENRP was provided by the South Florida Water Management District.

Chapter 1. Introduction

Over the last decade, the State of Florida has embarked upon an ambitious plan to restore the Everglades. Flora and fauna species shifts that have occurred in the Everglades over the last few decades have been attributed in large part to high phosphorus loads from agricultural runoff and the subsequent phosphorus enrichment of the Everglades. In 1994, the Everglades Forever Act mandated the construction of Stormwater Treatment Areas (STAs). The STAs were envisioned to be large treatment marshes designed and operated to lower phosphorus concentrations in waters passing through them. They would be placed in the landscape to intercept upstream Everglade Agricultural Area runoff and Lake Okeechobee outflows. In this way, the STAs would lower phosphorus concentrations and loadings to the downstream Everglade Water Conservation Areas. Over 45,000 acres of former agricultural land has or is currently being converted to STAs.

However, the STAs are not expected to sufficiently lower inflow phosphorus concentrations (Walker, 1995). Current research efforts suggest that the threshold P concentration required to prevent further shifts in flora and fauna will be in the range of 9 – 25 $\mu g\ L^{-1}$ (Richardson et al., 1999; Nearhoof et al., 1999; SFWMD, 1999). These concentrations are not likely possible without the implementation of supplemental technologies.

Several chemical and biological treatment methods are being investigated as initially set forth by Peer Consultants, P.C./Brown and Caldwell 1996. All of the proposed chemical treatment methods involve the use of iron (Fe) or aluminum (Al) salts (Peer Consultants, P.C./Brown and Caldwell 1996). Low Intensity Chemical Dosing (LICD) was initially suggested by Peer Consultants, P.C./Brown and Caldwell (1996). In the original concept, Peer Consultants, P.C./Brown and Caldwell (1996) described the LICD process as such:

"This treatment process is similar to the STAs except that a low intensity dose of chemical (i.e., ferric chloride) is applied to the STAs to enhance and accelerate the rate of P removal through the precipitation of soluble P and coagulation of chemically formed and naturally occurring particulate P. The STAs act as settling basins and filters. Chemical precipitation provides an additional mechanism for P removal, and may enhance the P-retention capability of the sediments. The range of chemical dosing is limited to less than 5 mg L^{-1} to promote P removal without any significant accumulation of chemical sludge in the STAs.

A chemical feed system would be incorporated into the inlet pumping system for the STAs. Feed pumps would be paced to the stormwater pumps. Mixing of chemical with the drainage water would occur as the water flows through the pumps and the supply canal and into the STAs. It is expected that the light floc particles produced by the chemical addition would not settle out in the supply canal, but rather, would be filtered out or settled in the STA. It is not expected

that deposition of solids would be significant enough to adversely impact the growth of vegetation in the STA."

In this original concept, LICD was defined as *in situ* marsh dosing of low concentrations of ferric iron or aluminum. Under LICD, existing marsh biota (e.g. bacteria, algae, macrophytes) would provide some phosphorus uptake while LICD would precipitate and settle out most of the remaining phosphorus (Figure 1). Peer Consultants, P.C./Brown and Caldwell (1996) hypothesized that the addition of low chemical dosage could enhance the P removal performance of the STAs and improve their ability to sustain performance over the long term.

LICD has been investigated in two phases. Phase 1 was initiated primarily as a feasibility study to determine if LICD had promise or potential for decreasing phosphorus concentrations or loads to downstream waters in the Everglades. Phase I consisted of both laboratory and field studies. For the field studies, three remote mesocosm sites were constructed in the Everglades Nutrient Removal Project (ENRP) during 1997 and 1998 (Figures 2 and 3). Each site consisted of eight mesocosms and included pumps, solar panels, data loggers and flow sensors for remote operation and monitoring of the experiments. *In situ* alum and ferric chloride dosing at various concentrations were tested in Phase 1 for their potential to decrease surface water phosphorus concentrations. Process variables (e.g. total phosphorus, total dissolved phosphorus, iron, aluminum and dissolved organic carbon concentrations) and important water quality variables (e.g. temperature, dissolved oxygen, conductivity, pH) were closely monitored during these experiments.

Bachand et al. (1999) presented a final report for Phase I to the Florida Department of Environmental Protection (FDEP) which included the data, results and findings from that study. The major findings are summarized as follows:

- LICD effectively decreased dissolves phosphorus (filtered total phosphorus) concentrations at metal dosing levels of 100 – 200 μM. *In situ* mean dissolved P concentrations less than 15 $\mu g\ L^{-1}$ have been achieved. These reductions can be sustained.
- Total phosphorus concentrations below marsh background levels can be achieved and this has been primarily attributed to floc precipitation and settling.
- Deposited sediments have higher mineral content and excess phosphorus storage capacity than background marsh soils.
- Mean total phosphorus concentrations near 20 – 30 $\mu g\ L^{-1}$ have been achieved for some chemical dosing treatments, representing a 33 – 50% reduction below background phosphorus concentrations of 40 – 45 $\mu g\ L^{-1}$.

Figure 1. Low Intensity Chemical Dosing Model.
Under LICD, ferric iron and aluminum additions were hypothesized to reduce phosphorus concentrations through the formation and subsequent settling of precipitates. Phosphorus would be incorporated into or adsorbed onto the precipitate depending upon the solid formed.

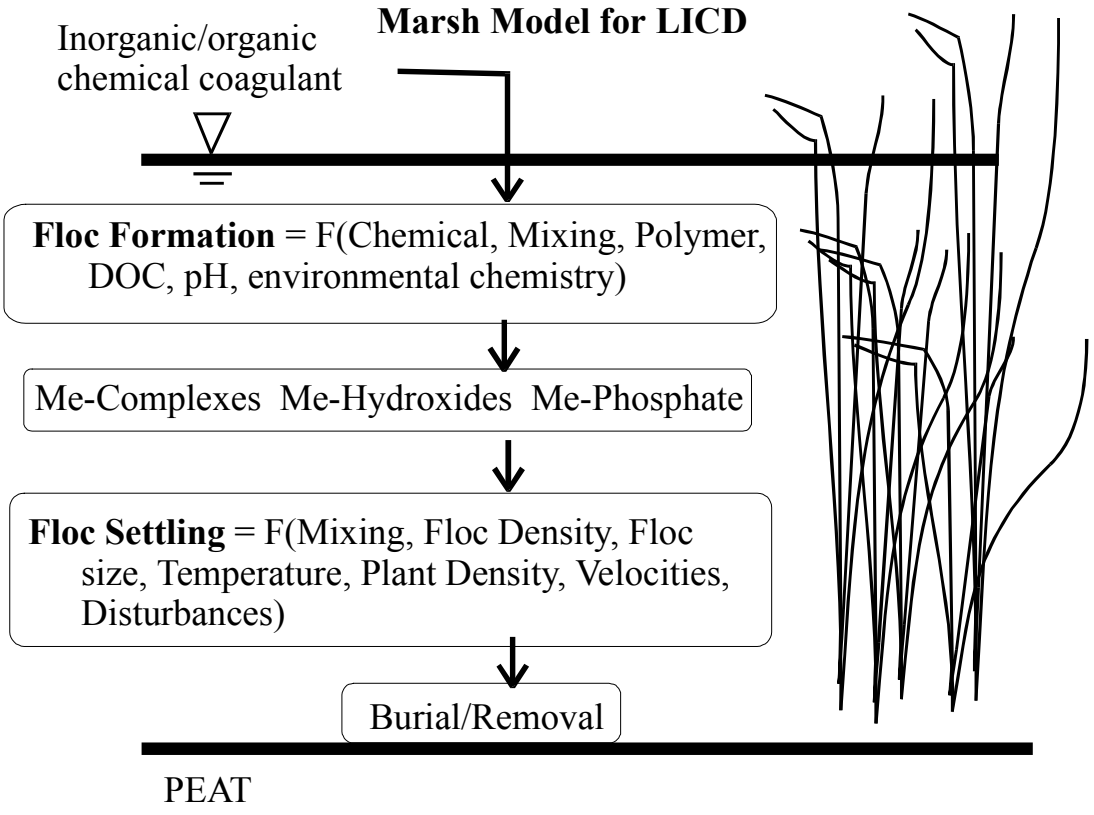

Phase 1 findings strongly suggested that LICD has promise for reducing phosphorus concentrations and eutrophication in waters downstream of its application. However, Phase I results also support a more sophisticated approach. Simply dosing marsh waters with ferric iron or aluminum coagulants as foreseen by Peer Consultants, P.C./ Brown and Caldwell in their original concept without optimizing the application process will provide sub-optimal performance. Inefficient and excessive chemical use, unnecessarily high outflow phosphorus concentrations, and lower reliability will likely result from that approach. Optimizing chemical usage in this technology will likely provide improved and more reliable performance and may require only slightly higher absolute capital costs. These costs when standardized for phosphorus mass removal may in fact be lower than the costs associated with the original concept.

Phase 2 LICD continues the study of LICD. During the writing of the original proposal for Phase 2, Phase 2 LICD was described as a three-year demonstration project that would utilize *in situ* mesocosm and macrocosm sites towards developing management practices for enhancing phosphorus removal (DUWC, 1999). The objective was to develop LICD management practices for enhancing phosphorus removal. First year Phase 2 studies were to be continued in the mesocosms and additionally incorporate laboratory studies. Second and third year studies were to incorporate larger-scale test cells for full-scale demonstration of LICD. The Scope of Work (SOW) for this work is presented in Appendix B to help clarify the objectives and evolution of this study.

The goals in SOW for the Phase II study (DUWC, 1999) are as follows:

- Investigate general changes in water quality (e.g. P, N, DOC, pH, temperature, anions, cations) associated with LICD.
- Develop phosphorus and metal mass balances to determine their fate.
- Determine water column phosphorus concentrations that can be achieved with *in situ* LICD under improved process implementation.

Objectives and strategies were expected to evolve as the study progressed (DUWC, 1999).

As this project has progressed through Phase I and into Phase II, LICD complexity has become more apparent. Parameters in this study were monitored for two purposes. The first purpose was to assess and enhance the LICD process. The second purpose was to assess outflow marsh readiness. Table 1 shows this and further divides the process parameters into dependent and independent variables. Dependent variables of interest for LICD were primarily total and total dissolved phosphorus. Independent variables were considered those that affect total and total dissolved phosphorus. These independent variables could be affect by either process manipulations or non-controllable environmental conditions (Table 2). Understanding the parameters and the goals behind monitoring the different parameters drove the experiments conducted for the study to development management practices to enhance LICD.

Table 1. Process and Marsh Readiness LICD Variables

Process variables were defined as dependent and independent variables.

LICD Variables	Analyte Code	Process		Phase I Marsh Readiness Screening (FDEP 1997)
		Primary variables of interest (Dependent)	Secondary (Independent)	
Surface Water Quality Parameters				
Grab samples				
Ortho-phosphate	FOP		X	X
Total dissolved phosphorus	FTP	X	X	X
Total phosphorus	UTP	X	X	X
Total iron	UFE		X	
Dissolved iron	FFE		X	X
Total aluminum	UAL		X	
Dissolved aluminum	FAL		X	X
Bromide	FBr			
Dissolved organic carbon	FOC		X	
Nitrate	NO3			X
Ammonia	NH4			X
Total nitrogen	TN			X
Dissolved nitrogen	TDN			
Alkalinity	ALK			X
Color	COL			X
Calcium	FCa			X
Dissolved sodium	FNa			X
Dissolved magnesium	FMn			X
Dissolved manganese	FMg			X
Dissolved potassium	FKa			
Dissolved zinc	FZn			
Dissolved copper	FCu			
Dissolved silica	FSi			X
Chloride	CL			X
Sulfate	SO4			X
Sondes[4]				
pH	pH			X
Temperature	T			X
Conductivity				X
Turbidity				X
Dissolved Oxygen	DO			X
Process Data (CR10X)[5]				
Flow rates[6]	Q		X	
Water Depth	Depth		X	
Precipitation	Rain		X	
Evapotranspiration (calculated)	ET		X	
Dosing methods				
Cationic polymers	CAT		X	
Anionic polyacrylamides	PAM		X	
Slow Mixing Rates	Mxslow		X	
Rapid Mixing Rates	Mxrapid		X	
Sediment/Soil/Floc				
Total Phosphorus (TP)	TP		X	
Extractable Phosphorus	ExtP		X	
Carbon	TC		X	
Nitrogen	TN			
Aluminum	TAL		X	
Extractable Aluminum	ExtAl		X	
Iron	TFe		X	
Extractable Iron	ExpFe		X	
Ca, Cu, Mg, Zn				

For this study, efforts were equally distributed between laboratory tests and field tests. Jar tests were implemented to initially screen different process variables (Table 2). Various metal dosing concentrations, cationic polymer blends, anionic polymer types and concentrations, slow mixing times and rapid mixing times were first screened under laboratory conditions. Jar tests provided a better understanding of the mechanisms and kinetics behind precipitation, floc aggregation and floc settling. Field studies were implemented to field verify certain findings and provide insights into improving the process. In total, eight jar tests and three field studies were implemented during the First Year Phase 2 studies. The dual approach of laboratory and field studies was considered the only reasonable approach for expediting LICD process development with the available manpower and resources.

Table 2. Controllable and environmental process variables affecting LICD.

Controllable	Environmental
Chemical dosing blend	**Surface Water Quality**
Dissolved iron concentrations	Ortho-phosphate concentrations
Dissolved aluminum concentrations	Dissolved phosphorus concentrations
Cationic polymer types and concentrations	Total phosphorus concentrations
Anionic polymer types and concentrations	Dissolved organic carbon
Mixing	**Sediment/Soil/Floc**
Slow mixing rates	Phosphorus concentrations and forms
Rapid mixing rates	Carbon concentrations c
	Aluminum concentrations and forms
Hydrology	Iron concentrations and forms
Water depths	
Flow rates	**Hydrology**
	Precipitation
	Evapotranspiration

This report details in individual chapters the results of each of these various laboratory and field studies. These are discussed in Chapters 3 through 14. An early chapter provides an overview of the methods. Chapters have also been written addressing sediment changes, conceptual designs, costs, conclusions and references. In addition, three appendices are included:

- Appendix A: Database Description for Access File
- Appendix B: Scope of Work for FDEP Contract No. WM720 (excluding budget information).
- Appendix C: QAPP
- Appendix D: Database

1.1. Deliverables

The report presents the following deliverables:

- A complete electronic copy of the data from these experiments in an Access Database,
- Results from hydraulic, phosphorus and metal budgets developed for the analyses of these studies.
- Sediment accumulation and phosphorus settling rates.
- An analysis on effectiveness of chemical additions for phosphorus removal which will include a prediction of effluent phosphorus concentrations, sediment accumulation rates and projected costs per cubic meter of water.
- Sediment analysis which includes phosphorus fractionation data.
- An analysis of the long-term fate of phosphorus removed by low intensity chemical dosing will be determined.
- Conceptual design and operational information necessary to implement this technology at the macrocosm or STA scale.
- A rough estimate of full-scale costs of this technology.

These deliverables are integrated throughout and across chapters in presentation and discussion of LICD.

Chapter 2. Methods

Laboratory and field mesocosm studies were conducted during this study with each building upon results from the previous study.

2.1. Jar Tests

Jar tests goals were conducted to better understand and prioritize different process variables (Table 2). Jar tests are typically used in industry for both process development and optimization, and as a predictive tool for full-scale systems of flocculation and settling characteristics. As a process development tool, jar tests are performed under optimal mixing criteria and given those criteria are used to test different chemical blends and rank their performance. Thus jar tests can be used to identify and prioritize mechanisms that need to be considered at the full-scale.

In total, eight jar tests were conducted with their goals and objectives evolving throughout the study (Table 3). For all jar tests, similar methods were used. Jar tests were conducted under standard jar test procedures using a four paddle jar tester and 1000 ml glass beakers. Source water for the studies was collected from the mesocosm sites in the Everglades Nutrient Removal Project (ENRP) and shipped to the Duke University Wetland Center (DUWC) in Durham, NC. After chemical dosing, beakers were rapid mixed followed by slow mixing. After completion of mixing, water was sampled with a pipette 2 cm below the water surface.

Mixing times, sampling times, coagulants used and variables monitored varied depending upon the goals and objectives of the jar test and the findings from earlier jar tests. Table 4 summarizes the experimental designs for the eight jar tests. Variations in mixing times and speeds, coagulants, coagulant aids and replicates are shown. Additionally, sampling times for different parameters are presented.

Table 3. Summary of Experimental Goals for Jar Tests conducted during Phase II LICD.

No.	Month	Goals
1	April	Target metal blends and doses 1. Identify most promising coagulants 2. Identify metal dosing effects 3. Identify percent cationic polymers which most enhance coagulation 4. Identify necessary settling time for jar test environment
2	April	Investigate mixing times. Replicates. 1. Identify most promising coagulants 2. Optimize rapid mix time 3. Optimize slow mix time 4. Identify necessary settling times for rapid and possible removal
3	July	Determine jar tests use as a predictor of mesocosm performance. 1. Replicate Mesocosm Field Study at same chemical doses
4	July	Investigate higher doses and metal/metal blends 1. Identify most promising coagulants 2. Investigate interactions between coagulants 3. Investigate metal dosing effects at higher levels
5	August	Investigate most effective PAMs and possible use of calcium/metal blends 1. Does calcium improve precipitate settling with different coagulants 2. Will calcium alone remove phosphorus 3. Does PAMs improve precipitate settling and flocculation
6	August	Replicate most promising treatments 1. Do PAM/metal treatments more effectively remove phosphorus (total, dissolved) then metal treatments alone? 2. Which metal dose is more promising with PAMs
7	August	Test low calcium doses 1. Do low doses of calcium improve settling rates
8	August	Replicate most promising treatments 1. Investigate settling times

Notes
1. Coagulants are listed by codes detailed in Table 1.
2. Percent polymer dependent upon metal used (e.g. ferric iron, aluminum).
3. Analyte codes can be found in Table 6.

Table 4. Experimental design for Jar Tests conducted during Phase 2 LICD.
Table shows various dosing regimes used, jar test operation, and sampling programs.

Jar Test No.		1	2	3	4	5	6	7	8
Month		April	June	July	July	August	August	August	August
Operation									
Rapid mix	time (s)	20	15, 30	15	15	15	15	15	15
	speed (rpm)	300	300	300	300	300	300	300	300
Slow mix	time (m)	20	0, 30	10	10	5	5	5	5
	speed (rpm)	30	30	30	30	30	30	30	30
Metal Coagulant Blends									
Iron	FeCl	FeCl	FeCl		FeCl	FeCl	FeCl	FeCl	FeCl
	FeSO4	FeSO4							
	PFS	PFS							
	PFS-a	PFS-a							
	FPA	FPA							
	FPB	FPB	FPB	FPB	FPB				
	FPC	FPC							
	FPD	FPD	FPD	FPD	FPD	FPD	FPD	FPD	FPD
Aluminum	Alum	Alum	Alum			Alum	Alum		Alum
	Cl4100	Cl4100	Cl4100	Cl4100	Cl4100	Cl4100			
	ClA410P	ClA410P							
Fe + Al	Alum + FeCl				Alum + FeCl				
	Alum + FPD				Alum + FPD				
	Cl4100 + FeCl				Cl4100 + FeCl				
Doses	uM	50, 100, 200	100, 200	100	100, 200, 400	100, 200	100, 200	100, 200	100, 200
Coagulant Aids									
Calcium	Ca(OH)2					Ca(OH)2	Ca(OH)2	Ca(OH)2	Ca(OH)2
	Dose (mg/L)					0, 25, 50, 100, 150	0, 25	0, 2.5, 5, 10, 25	0, 5, 10, 25
PAMs	A130					A130	A130	A130	A130
	A110					A110			
	A1894					A1894			
	Dose (mg/L)					0, 0.25, 0.75	0.25	0.25	0.25
Replicates	(N)	1	2	3	3	1	3	1	3
Sampled Parameters									
	Turbidity	2h, 4h, 1d, 3d		0m, 30m, 1h, 2h, 1d	0m, 30m, 1h, 2h, 4h	0m, 5m, 10m, 30m 1h	0m, 10m, 30, 1h	0m, 10m, 30m	
	FTP		2h	0m, 2h, 1d			0m, 10m, 30, 1h		0m, 10m, 30m, 2h
	UTP	2h	2h	0m, 30m, 2h, 1d			0m, 10m, 30, 1h		0m, 10m, 30m, 2h
	FOC		2h	0m, 2h, 1d					
	FFE		2h	0m, 2h, 1d			0m, 1h		0m, 30m, 2h
	UFE		2h						0m, 30m, 2h
	FAL		2h	0m, 2h, 1d			0m, 1h		0m, 30m, 2h
	UAL		2h						0m, 30m, 2h
	pH	0m					0m, 1h		

Notes
1. Coagulants are listed by codes detailed in Table 1.
2. Analyte codes can be found in Table 6.

2.2. Mesocosm Field Studies

Mesocosm studies were initiated during Phase I LICD to field assess the potential of this technology for reducing total phosphorus concentrations in waters entering the Everglades and for reducing eutrophication pressures on downstream waters. Field mesocosm studies were continued in this study for the purpose of:

- field testing and validating jar test findings,
- determining field conditions that either complement or complicate LICD,
- better modeling phosphorus concentrations targets that can be achieved *in situ,*
- identifying environmental and water quality effects from LICD, and
- assessing the long-term fate of phosphorus and added metals.

2.2.1. Construction

Mesocosm site construction which occurred from July 1997 through April 1999 was largely financed by funds outside this grant. This construction effort included design and installation of boardwalks, mesocosms, platforms, piping, solar power, pumps, chemical tubing, flow sensors and climate monitoring equipment. Details and photographs of the construction are presented in Bachand et al. (1999). The pertinent design and construction information is reviewed here.

At each site, mesocosms were positioned in a circular pattern around the central platform (Figures 2 and 3). This layout minimized infrastructure costs and made process variables (e.g. time since chemical injection, flow rates) similar for all mesocosms. This design allowed easy implementation of a LICD to all mesocosms locations while minimizing infrastructure and differences between mesocosms at each site (Figure 4). Mesocosms themselves were designed with six foot diameters and were constructed of polycarbonate to allow light to pass through the walls (Figures 5 and 6). Mesocosms were lowered into place with a portable crane as to minimally disturb site sediments and soils. Mesocosms were then driven into the peat as far down as possible to prevent leakage around the mesocosm cylinder walls. Leak tests were conducted after installation to ensure a tight seal in the surrounding peat.

Figure 2. Site Layout.
Plan view of LICD Site A showing mesocosm placement, weather station, solar grid, piping and chemical injection equipment. Sites B and C are functionally identical to Site A though they do not require weather stations. Figure is not drawn to scale.

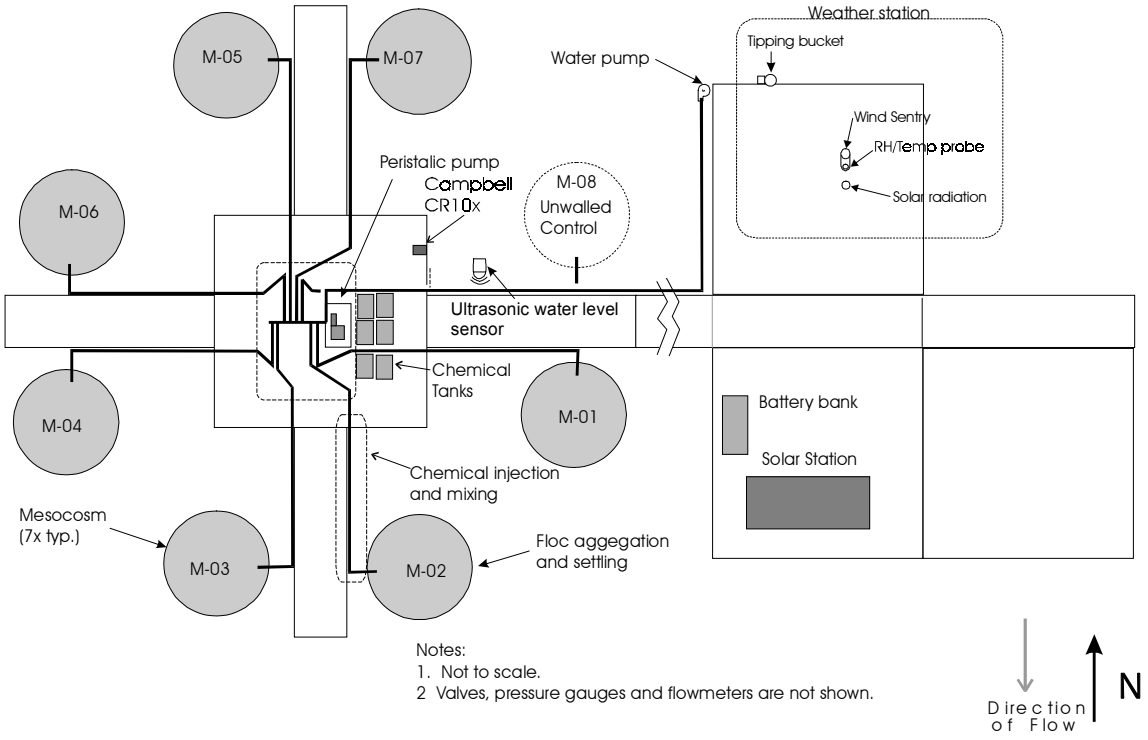

Figure 3: Aerial View of Site A in the ENRP on February 12, 1999.
Site A included equipment for mesocosm and field microcosm subtasks. Sites B and C included equipment for mesocosm subtasks. Sites B and C did not require weather station as Site A weather data was used for all sites. All sites were located in ENRP Cell 2 with the platforms oriented in an East-West direction. Background photograph was courtesy of Drew Campbell of SFWMD.

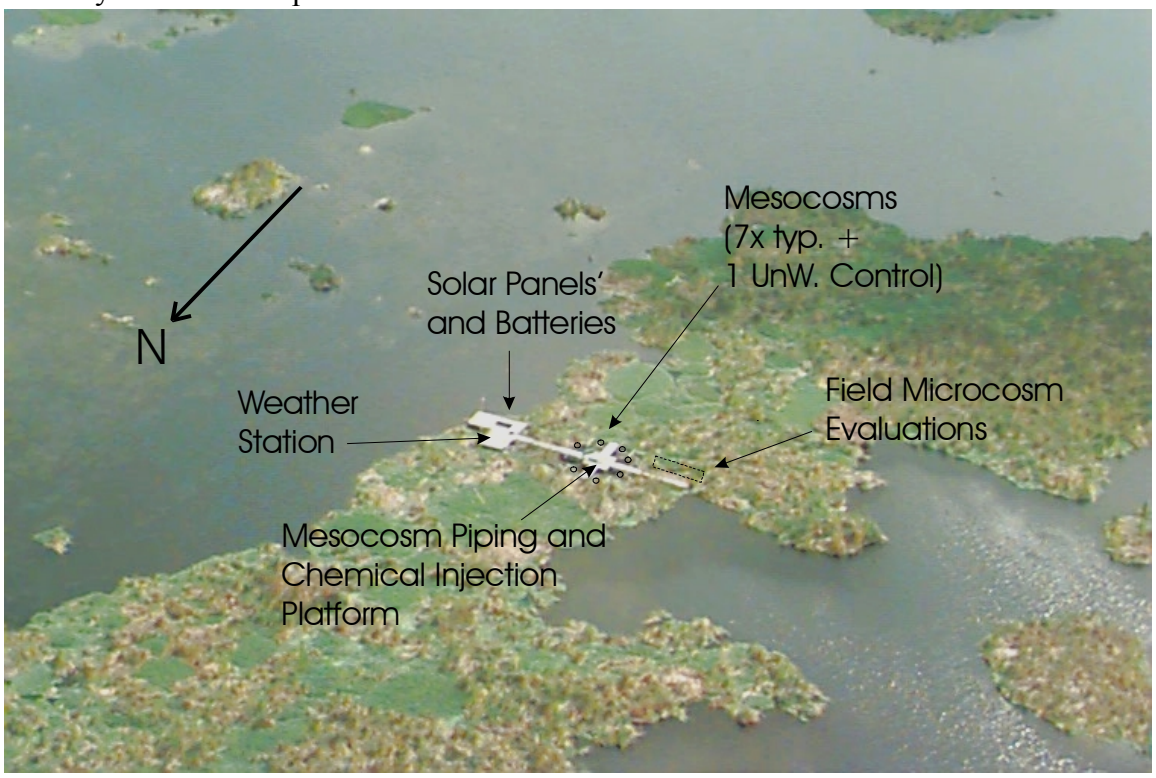

Figure 4. Process Train for LICD.
Water is pumped to each mesocosm through piping and manifolds. When water is flowing, throttling valves regulate flow and paddlewheel flow meters record flow. Chemical stock solutions are pumped from carboys into water lines. Inline mixer provides high energy mixing for short duration (1-1.5 minutes). Campbell CR10X records operational data and controls pumping and dosing schedules. Shaded slow mixing tanks and second inline mixer installed for the June 1999 mesocosm study.

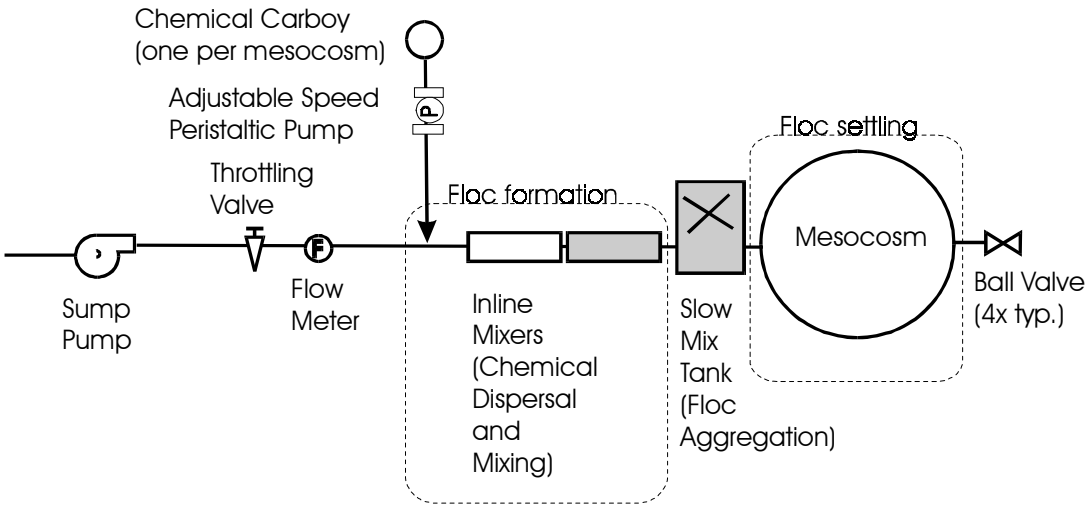

Figure 5. Mesocosm Design.
Mesocosm was buried 12 to 18 inches into the peat sediments. Wooden staves installed at 90° prevented bowing and bending during installation. Water flowed into the mesocosms via an inflow pipe above the water column. Water exited the mesocosms through four gate valves offset by 90°. Surrounding marsh water elevations controlled water elevations within the mesocosms. Water flow to mesocosms was controlled by Campbell CR10X.

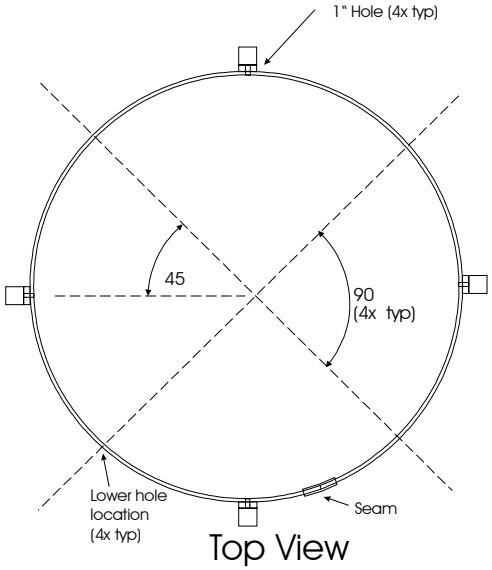

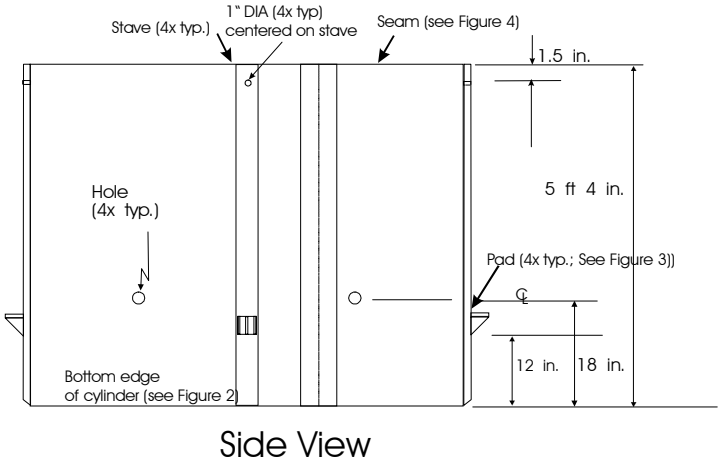

Please construct or modify an existing chamber as follows:
1. Cut out existing seam and reseam to reduce diameter to 70" (5' 10")
2. Trim 6" off bottom so that bottom of staves and cylinder line up. Rebevel bottom edge.
3. Trim 8" off top.
4. Put 1" holes through staves so that hole center is 1.5" from top of cylinder.
Changes are shown on sketch. Final dimensions should match those shown in sketch.

Note:
1. All joints and connections are to be glued. No welding shall be used. Adhesive used should be specifically designed for joining and gluing polycarbonate.
2. Not too scale

12/18/97

Figure 6. Mesocosm Installation
Mesocosms were installed with a portable crane. Mesocosms were constructed of polycarbonate and approximately 6 ft tall with 6 ft diameters. Wooden staves along the sides of the mesocosms stiffened the cylinders for installation into the ENR sediments. Four outlet valves offset at 90° allowed water flow into and out from the mesocosms to equilibrate water levels between the mesocosms and the surrounding marsh.

2.2.2. Operation and Modifications

Each site was designed with seven mesocosms as shown in the Site Layout (Figure 2). Sites were designed so that both water and chemicals could be pumped independently to each chamber to allow for varying water flow, chemical flow and chemical concentrations to each mesocosms (Figure 4). An eighth location at each site in which no mesocosm was installed was defined as the unwalled control. This location provided background water quality information.

Water was pumped from a central location and distributed through a manifold to each mesocosm (Figure 7) while chemicals were supplied from a pre-mixed chemical stock solution and metered into the water lines with a peristaltic pump. Chemicals were immediately dispersed into the water lines with inline rapid mixers. Water flow was controlled with manual throttling valves and flow was measured into each mesocosm with paddlewheel flow sensors.

Figure 7. Manifold Piping.
Water was delivered to mesocosm through a distribution manifold. Flow to each mesocosm was individually throttled and monitored. All lines could be isolated and purged for cleaning or calibration. Chemicals were injected into water lines with peristaltic pump.

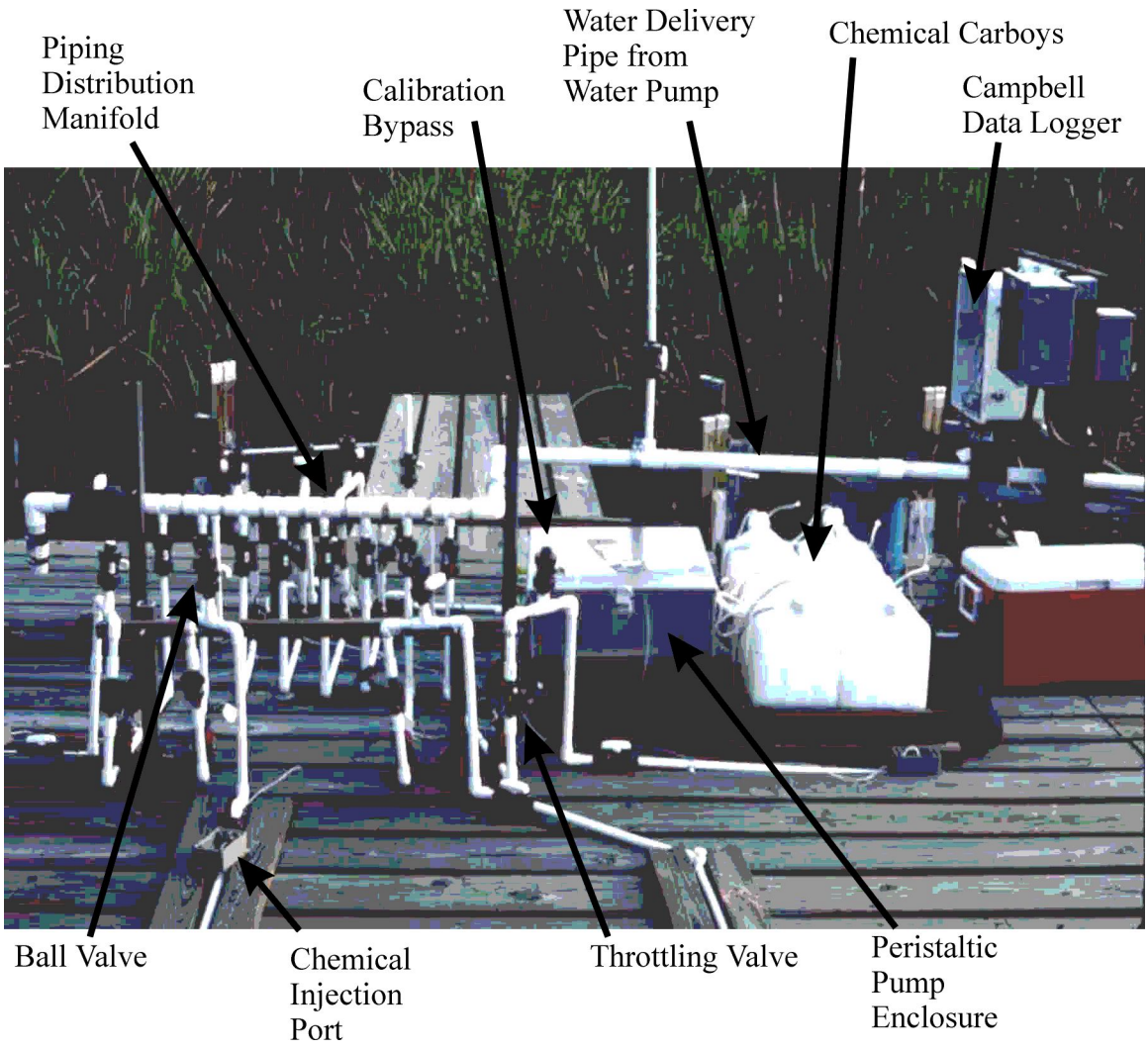

Two modifications resulted from jar test findings that are discussed in later sections. During Phase I, one inline mixer was used in each line for chemical mixing. During Phase II, an additional inline mixer was added based upon jar test findings that are discussed later. This increased the energy and detention time for rapid mixing.

A second modification was the installation of a slow mixing tank added immediately upstream of each mesocosm receiving chemical dosing. This

modification was made during June 1999 to improve floc aggregation (Figure 8a,b). The decision to install mixing tanks was based upon jar test results and conversations with industry specialists. Mixing tanks were 15 gallon 15-inch diameter polyethylene tanks with a 6.5-inch diameter Lightnin™ propeller located halfway up the water column (Figure 8a, b). Water flowed through the mixing tank in an upward direction against the downward current created by the impellers. The impellers were driven at 102 rpms by a gearmotor located at the top of the mixing tank. The design was developed from conversations with industry specialists on chemical flocculation technologies (Zimmerman, 1999; Sims, 1999). Flows through the system averaged about 1.4 gpm and a volume of 14 gallons was utilized for each mixing tank. Thus, the HRT for water flowing through the mixing tank was approximately 10 minutes. This was a reasonable slow mixing HRT based upon the jar test findings.

Mixing tanks were considered necessary at this scale to provide the slow agitation necessary for effective floc aggregation. At this scale, flows are so low that they do not provide much mixing energy when discharged into quiescent waters and this is associated with problems of scale (White, 1979). At a larger-scale natural flows exiting from pumps and gates may be enough to provide the necessary mixing needed for floc aggregation.

Figure 8. Slow mixing tanks for LICD.
Slow mixing tanks were installed during June 1999 to help with floc aggregation and improve P removal rates.

A. Photograph

B. Sketch of mixing tank in relation to mesocosms. Not drawn to scale.

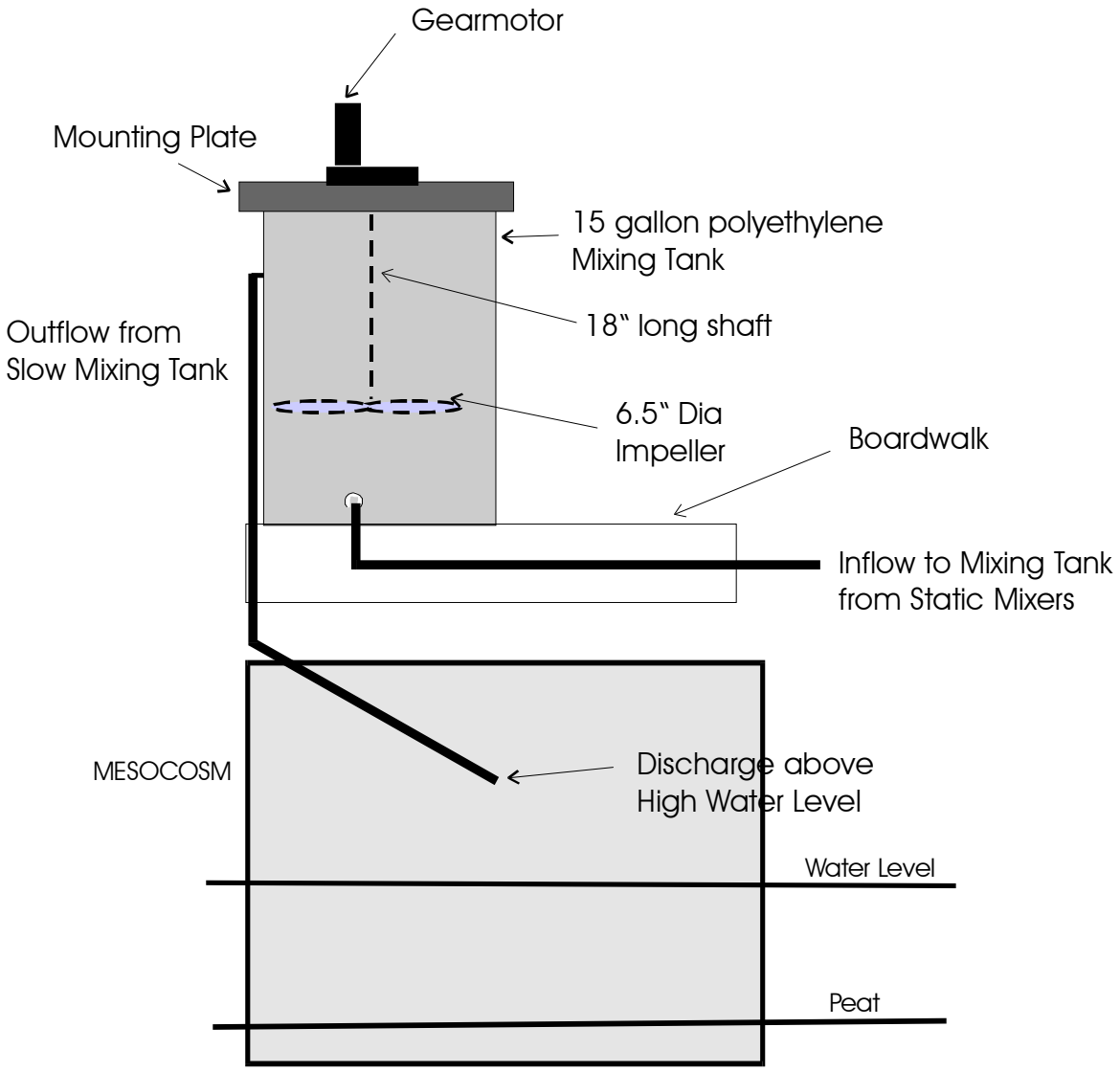

A weather station which recorded precipitation, solar radiation, air temperature, wind direction, wind speed and humidity was installed during Phase I at Site A in order to determine rain fall and estimate evapotranspiration. At all sites, a Campbell CR10X controlled pumping time and frequency, and recorded water flow rates to each mesocosm. At Site A, the CR10X also recorded climate data and water elevation.

Mesocosms were operated under two different configurations during this study: batch flow and continuous flow. Batch flow studies were implemented in June

and October 1999. Continuous flow studies were implemented in February 2000. The experimental designs for the different mesocosm studies are presented in the Process Development Section. General operational and sampling methodologies are presented in this section.

2.2.3. Batch-Flow Studies Methodologies

Two batch-flow studies were conducted during this study. One batch study was conducted in June 1999 and a second was conducted in October 1999. During Batch Flow studies, three volumes of mesocosm water were pumped into each mesocosm at the initiation of the experiment. Pumping was conducted to flush each mesocosm with chemically-dosed water. Inflow water flowed through the static mixers for the necessary rapid mixing and through the slow mixing tank to aid with floc aggregation. During pumping, mesocosm outlet valves were open to allow water to be displaced from the mesocosm into the surrounding marsh (Figure 6). After pumping ceased, mesocosm outlet valves were closed and process variables (e.g. P species, dissolved and total aluminum and iron, bromide, DOC) monitored several times per week over a two-week period. Sampling frequency for the various process variables are shown in Table 5. On the day of pumping, water samples were taken at the inflows and at one location (mesocosm center, 6 inches from water surface) of each mesocosm (Figure 9). On subsequent sampling days, two samples were taken from each mesocosm (mesocosm center, 6 inches from the water surface; mesocosm center, 6 inches from the water/sediment interface). All laboratory methods and parameters sampled are detailed in the QAPP for this project (DUWC, 1999; Appendix C). The June 1999 study was conducted at Site C which was a site that had not previously had chemical dosing during Phase I (Bachand et al., 1999). The September 1999 study was conducted at all three mesocosm sites in a replicated study.

Table 5. Sampling frequencies of mesocosm process variables.

Subtasks	2.3	2.2
Experimental enclosure[1]	Batch	Cont.
Estimated length of each experimental run (wk.)	2	26
Number of Enclosures	8	8
Parameters		
Surface Water		
Grab samples		
Dissolved reactive phosphate (PO4-P)	60-100/wk	35/wk
Total dissolved P (TDP)	60-100/wk	35/wk
Total P in water (TP)	60-100/wk	35/wk
Dissolved organic phosphorus (DOP)	60-100/wk	35/wk
Particulate phosphorus in water (PP; calculated)	60-100/wk	35/wk
Dissolved Fe and Al	60-100/wk	35/wk
Total Fe and Al.	60-100/wk	35/wk
Particulate FE and Al. (calculated)	60-100/wk	35/wk
Br	60-100/wk	
DOC	60-100/wk	35/wk
Sondes[4]		
pH		6/hr
Temperature		6/hr
Conductivity		6/hr
Turbidity		6/hr
DO		6/hr
Process Data (CR10X)[5]		
Flow rates[6]	96/hr	96/hr
Air Temperature	1/hr	1/hr
Solar Radiation	1/hr	1/hr
Water Depth	1/hr	1/hr
Precipitation	1/hr	1/hr
Wind Speed	1/hr	1/hr
Wind Direction	1/hr	1/hr
Evapotranspiration (calculated)	1/hr	1/hr
Sediment/Soil[2]		
Total Phosphorus (TP)		40/25
Total C, N		40/25
Al and Fe		40/25
Ca, Cu, Mg, Zn		40/25
Extractable forms of Phosphorus		40/25
Extractable forms of Fe and Al		40/25

Notes:
1. For mesocosm studies, enclosures include unwalled control locations
2. Sediment sampling for the continuous study will be done at the initiation and conclusion of the run. Values shown are for number of samples at beginning and conclusion of run.
3. Final Batch Run is replicated across all 3 sites.
4. Sondes will be deployed approximately half time during Continuous Run Study at the frequency shown. Each sonde collects data hourly.
5. A Campbell CR10X will control and monitor the process equipment at each Mesocosm Site (e.g. A, B, C).
6. Flow rates are only measured during pumping periods at frequency given.

Figure 9. Water grab sampling locations during Batch Flow Studies.
Grab sample locations for water sampling are marked with an "X". Samples were collected over a 2-week period for each Batch Flow Study. Studies were conducted during March/April 1999 and October 1999. March/April study was conducted at all mesocosm locations at Site A. October 1999 study was at four mesocosm locations and one unwalled control location at each of Sites A, B and C.

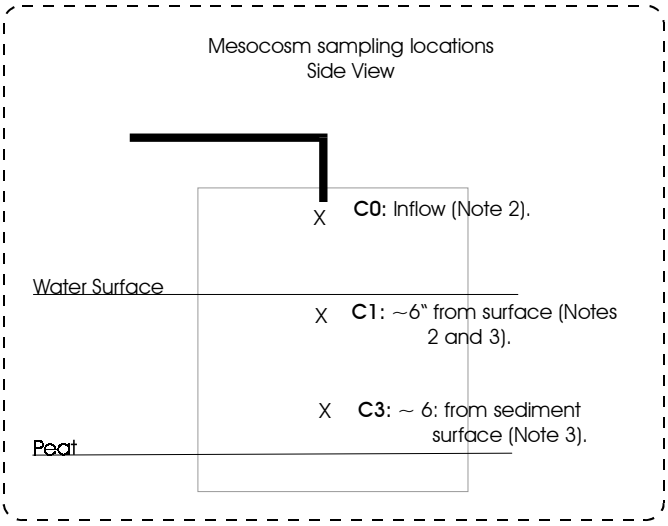

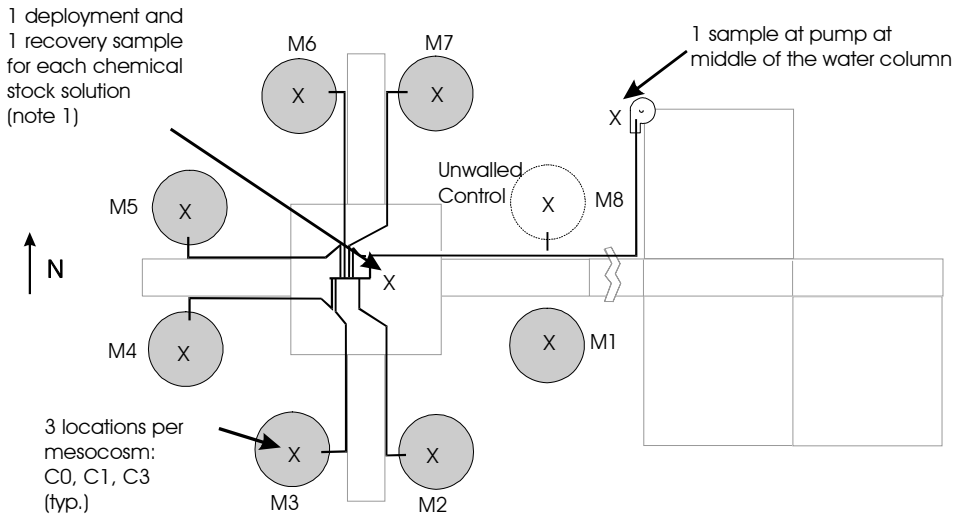

Notes:
1. Each chemical carboy was sampled before and after deployment. Each carboy was deployed once at beginning of the Batch experiment.
2. Samples were taken on day of pumping.
3. Samples were taken 2 to 4 days per week after pumping ceased. Sampling occurred over a fourteen day period.

2.2.4. Continuous-Flow Mesocosm Studies

One Continuous Flow Study was initiated during February 2000 as the final study in this First Year Phase II study. This study was conducted at Sites A and C and occurred over a one-month period. This study was the final experiment for this SOW with the goal of field testing results and conclusions from all previous studies. Additionally, variables specifically required for marsh readiness were collected during this study (FDEP, 1997). For this study, approximately three volumes of water were initially pumped into each mesocosm to flush the mesocosms with chemically dosed waters and establish an initial condition. This initial pumping occurred over a two-day period and was conducted with all mesocosm outlet valves open. After this initial flushing period, the mesocosms were pumped once a day to simulate continuous-flow pumping.

During periods of pumping, rapid mixing occurred after chemical addition in the static mixers. One rapid mixer was located after the injection port for metal addition and one rapid mixer was located after the injection port for PAM dosing. After rapid mixing, the water flowed into a slow mixing tank for an approximate 10 minute period of slow mixing, after which it flowed directly to the mesocosms. Because water was pumped once per day, the mixing tanks would be quiescent for one day. Grab samples were collected from the mixing tanks approximately at their midpoint in the water column. Samples were collected between 9:00 AM and 1:00 PM. As water pumping started at 1:30 and continued till around 4:00 PM, mixing tank samples were collected a minimum of 19 hours after the pumping discontinued. Therefore, the samples from the mixing tank represent samples taken at a 18 – 24 HRT. Daily pumping volumes were based upon a desired 2.5 day HRTs for the mesocosms. Thus, samples collected from the mesocosms represent samples collected from a system operated on a 2.5 day HRT.

Water samples were collected twice per week from each mesocosm at multiple locations (Figure 10). Water exited the mesocosms through four outflow pipes located near the sediment layer and offset from each other at 90° (Figures 6). Water levels in the surrounding marsh controlled mesocosm water elevations. Sampling frequencies are shown in Table 5. All laboratory methods and parameters sampled are detailed in the QAPP for this project (DUWC, 1999; Appendix C).

Variables specific to marsh readiness and not required as process variables (Table 1; e.g. total nitrogen, dissolved nitrogen, ammonia, nitrate, color, sulfate, silica, chloride, magnesium, sodium, potassium, manganese, alkalinity and total suspended solids) were collected twice during this study.

Figure 10. Water grab sample locations during Continuous-Flow Studies
Grab sample locations for water sampling are marked with an "X". Samples were collected in mesocosms, in mixing tanks and after static mixers.

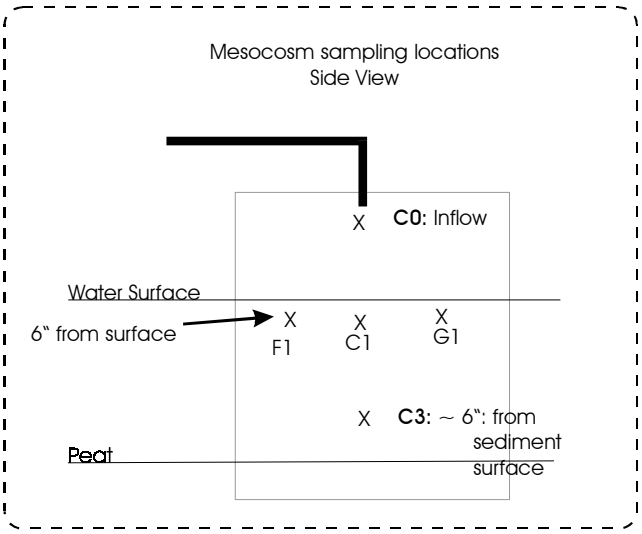

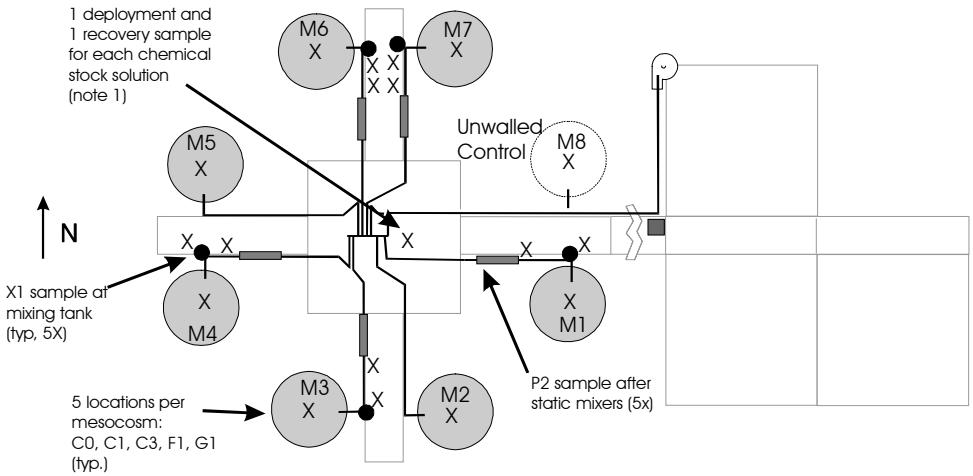

Notes:
1. Each chemical carboy was sampled before and after deployment.

2.2.5. Sediment Data

Sediment data was collected in two steps. The first set of data was collected in coordination with Phase I studies. During Phase I, a long-term eight month dosing study was conducted at Site A between August 1998 and February 1999. This was the longest term dosing study conducted so far. To capture long-term sediment changes soil cores were collected from the sediments at the initiation and completion of that study. Sediment samples were collected at the initiation and completion of the long-term run. Cores were partitioned by depth (top layer, 0-1 cm, 1-2.5 cm, 2.5- 5 cm., 5-10 cm.) and analyzed for phosphorus, iron, aluminum, calcium, copper, magnesium and zinc (Table 2). At the initiation of the study, one sediment core was collected at the center of each mesocosm. At the completion of the study, three sediment cores were collected at random locations within each mesocosm. The three sediment cores were composited by depth. All laboratory methods and parameters sampled are detailed in the QAPP for this project (DUWC, 1999; Appendix C).

Chapter 3. Jar Test No. 1, April 1999

Jar Test No. 1 was conducted as the first step to address challenges presented in the Phase I findings (Bachand et al., 1999). Bachand et al. (1999) determined that LICD required process development to have more robust and reliable phosphorus removal. Floc aggregation and subsequent settling repeatedly showed itself as needing improvement and the investigation of metal/polymer blends was recommended as a water and wastewater industry practice to meet this need.

3.1. Goals and Hypotheses.

The specific goals for this study were to:

- Establish total phosphorus/turbidity relationships
- Identify jar test settling and sampling times
- Identify most promising metal/polymer blends
- Recommend appropriate metal dosing levels
- Identify percent cationic polymers for aluminum and ferric iron chemical blends (Table 3).

3.2. Methods

Eleven chemical blends at varying dosing levels were tested (Tables 4 and 6). In all eight ferric iron blends and three aluminum blends were analyzed. Treatments were generally not replicated but instead the experiment was designed to quickly screen and assess chemical treatments. Ferric iron blends consisted of ferric chloride, ferric sulfate polymer blends and ferric polysulfate polymer blends. Aluminum blends consisted of alum and alum polymer blends.

Table 6. Chemical coagulants screened during Jar Test No. 1

Metal	Code	Definition
Ferric Iron[1]	FeCl	Ferric chloride
	FeSO4	Ferric sulfate
	FPA	Ferric sulfate + 5% cationic polymer
	FPB	Ferric sulfate + 10% cationic polymer
	FPC	Ferric sulfate + 15% cationic polymer
	FPD	Ferric sulfate + 20% cationic polymer
	PFS	Polyferric sulfate
	PFS-A	Polyferric sulfate + 5% cationic polymer
Aluminum	Alum	Aluminum sulfate
	Cl4100	Clarion 4100 (Aluminum sulfate + 10% cationic polymer)
	ClA410P	Clarion A410P (Aluminum sulfate + 10% cationic polymer, acidified)

Notes

1. All ferric iron blends were supplied by Kemiron.
2. All aluminum blends were supplied by General Chemical.

Because floc aggregation and settling was considered during Phase I as an area needing improvement (Bachand et. al, 1999), turbidity was measured as an indicator of such. Turbidity was routinely sampled at 2 hours, 4 hours, 1 day and 3 days. pH was measured at 0 minutes immediately after mixing ceased to identify pH changes resulting from dosing. Total phosphorus concentrations were measured at 2 hours to determine phosphorus removal at that time. For these studies, a 20 second rapid mix at 300 rpms was followed by a 20 min slow mix at 30 rpms (Table 4).

3.3. Results and Discussion

Turbidity was measured as a water quality indicator of total phosphorus to expedite analyses. Turbidity weakly predicted total phosphorus concentrations when both iron and aluminum results were combined (Figure 11). However, when iron and aluminum dosed jars were separated the correlation between turbidity and water column total phosphorus concentrations improved greatly (Figure 12). Thus, turbidity was considered an excellent indicator of water column phosphorus concentrations under chemical dosing when ferric iron and aluminum results were considered separately. Turbidity was fairly constant with time for all chemical coagulants (Figure 13) showing that:

- sampling time intervals used did not provide sufficient resolution to determine floc settling rates for the different coagulants
- floc generally did not re-suspend into the water column for the three day sampling period, and
- particle settling occurred generally within the first two hours after chemical dosing (as shown by relatively constant turbidity at time equal to and greater than 120 minutes).

Figure 11. Turbidity as a predictor of total phosphorus.
Jar Test No. 1. Turbidity did not provide a good predictor of total phosphorus in jar tests when data from aluminum and iron coagulants were combined.

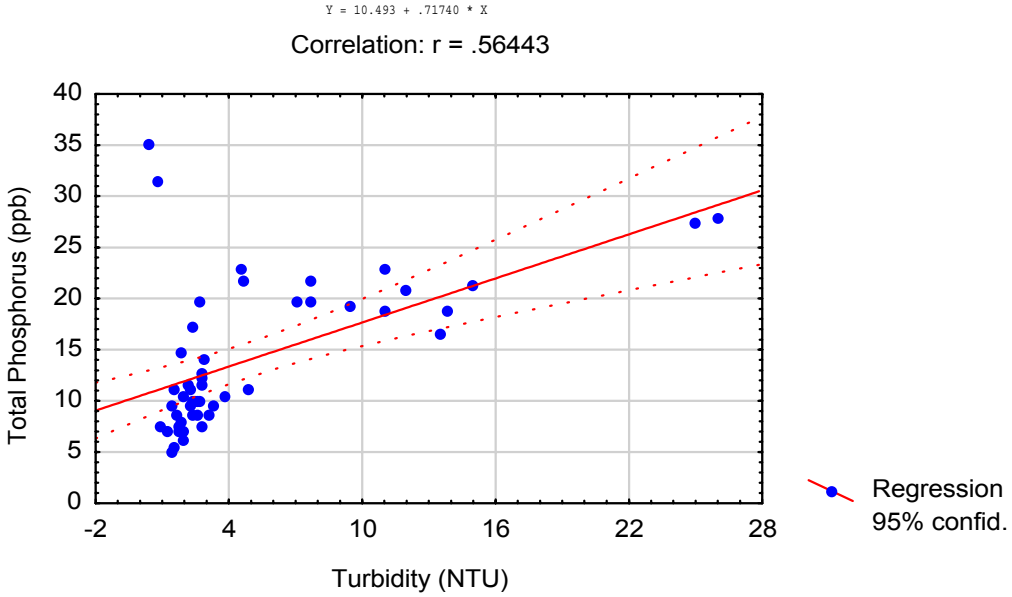

Figure 12. Turbidity/phosphorus relationships when iron and aluminum treatments are separated.
Jar Test No. 1. Turbidity was found to be a reasonable predictor of total phosphorus concentrations for the purpose of screening chemical coagulants. Total phosphorus removed depended upon the chemical effectiveness for settling formed floc.

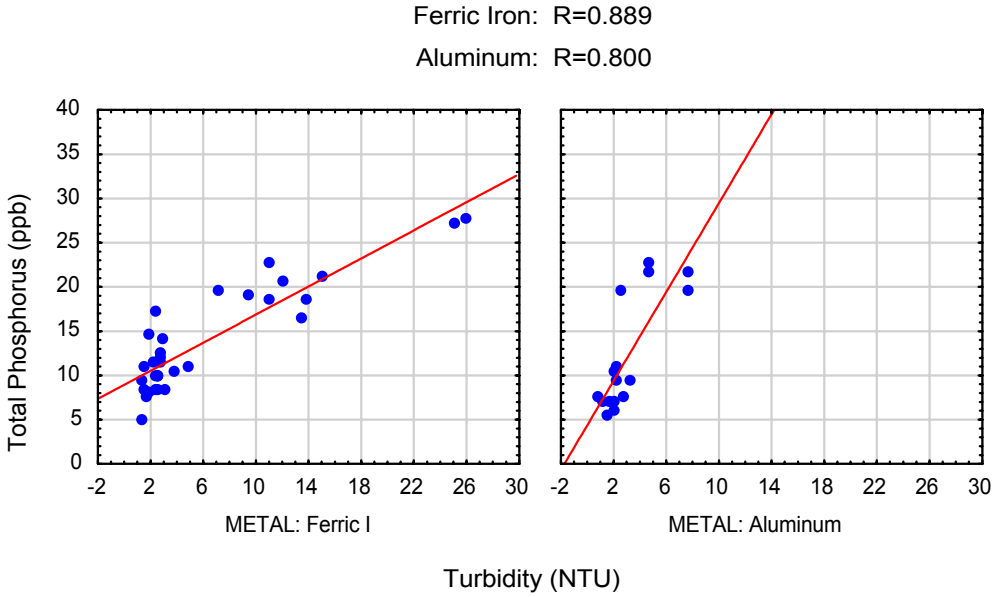

Figure 13. Time dependence of turbidity for different chemical coagulants.
Jar Test No. 1.

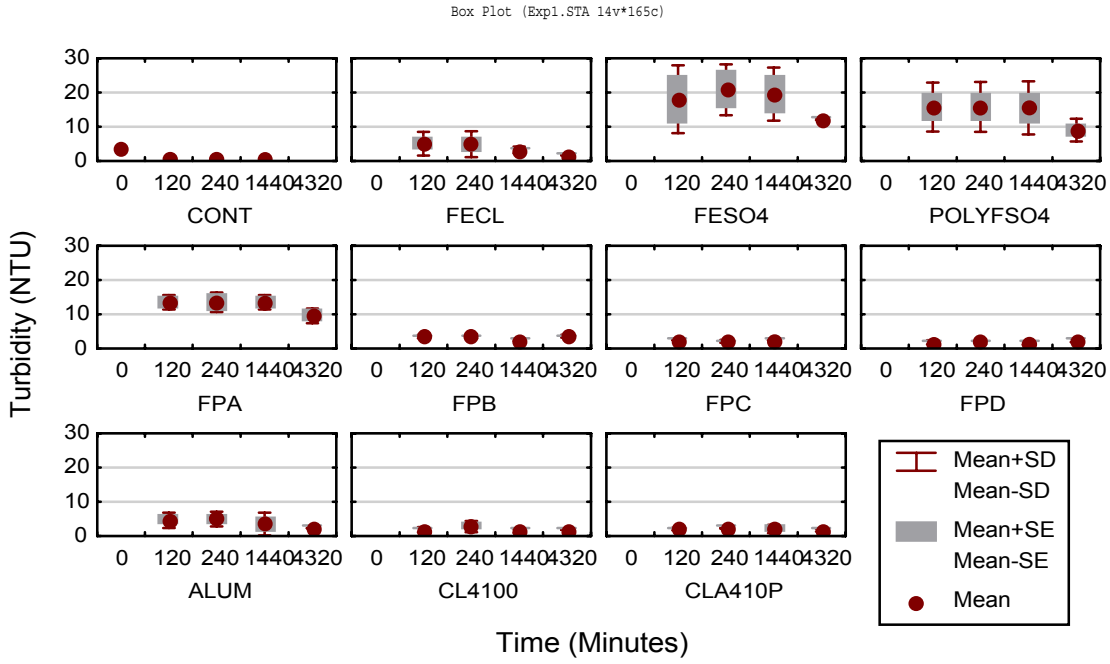

Notes:
1. Table 6 lists abbreviations for different coagulants.

For the ferric iron, turbidity differed statistically ($p<0.0001$) between coagulant treatments. Figure 14 shows turbidity at ferric iron and aluminum doses of 100 and 200 μM. Ferric chloride and ferric sulfate plus 10, 15 and 20% polymers (e.g. FPB, FPC and FPD) provided the lowest turbidity values. When just those treatments were considered, turbidity differed statistically between those four treatments ($p=0.0063$). In general, increased polymer doses up to 20% resulted in lower turbidity. This trend was the same when considering total phosphorus at the same metal dosing concentrations (Figure 15). All ferric iron treatments lowered total phosphorus concentrations below background levels (31.4 μg L^{-1}). Ferric chloride reduced total phosphorus the least to 13 μg L^{-1} and FPD the most to approximately 7 μg L^{-1}. The latter represented decreased total phosphorus concentrations by more than 75%.

Figure 14. Turbidity values for different chemical coagulants.
Jar Test No. 1. Chemical coagulant dosing levels used were 100 and 200 µM of iron or aluminum. Turbidity values shown are mean values for measurements taken at 2 hours, 4 hours, 1 day and 3 days.

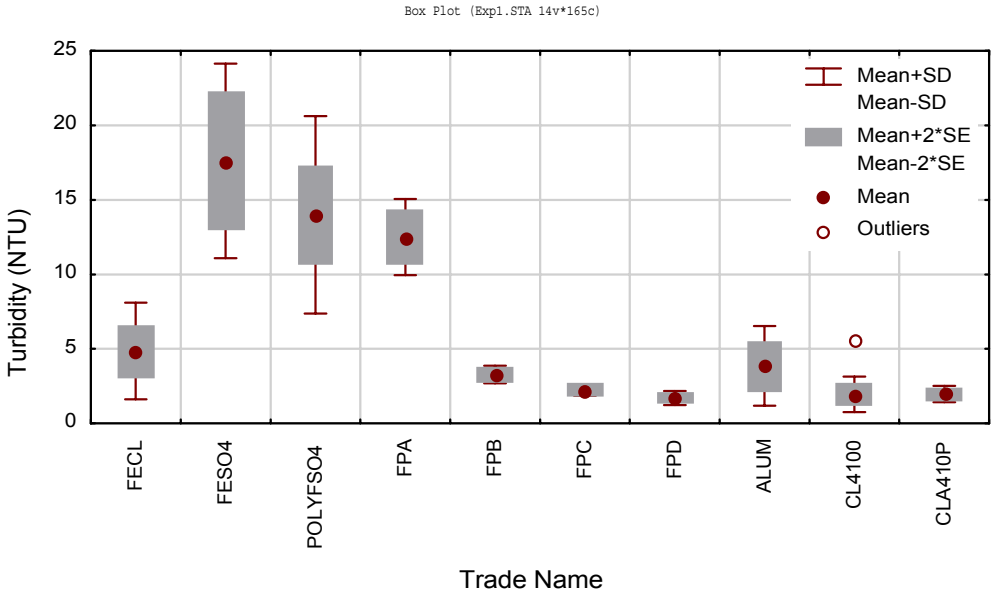

Notes.
1. See Table 6 for abbreviation definitions of chemical coagulants.

Figure 15. Resultant total P concentrations for different coagulants tested.
Jar Test No. 1. Chemical dosing levels of 100 and 200 µM of iron or aluminum were used. Background phosphorus concentration for ENRP waters used was 31.4 µg L^{-1}.

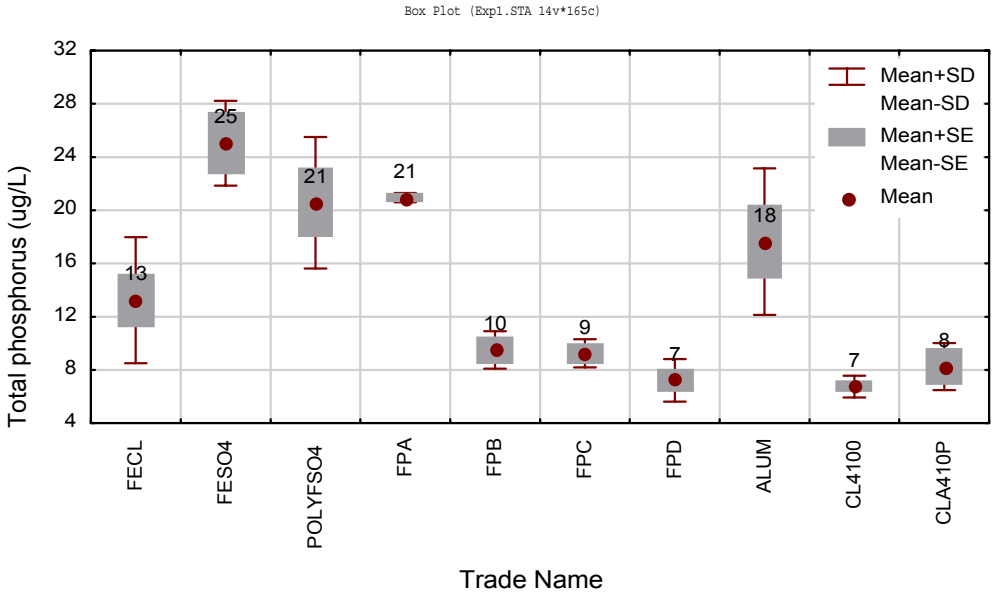

Notes:
1. Table 6 lists abbreviations for different coagulants.

Turbidity also differed significantly between aluminum treatments though the difference was less pronounced (p=0.0219). Both aluminum polymer blends achieved similar mean phosphorus concentrations of just under 2 μg L^{-1} and both resulted in lower total phosphorus concentrations than found in the alum treatment (3.9 μg L^{-1}). Alum and alum polymer blends resulted in over a 90% removal of total phosphorus from background levels of 31.4 μg L^{-1}.

FPD and Clarion 4100 were the most promising treatments for iron and aluminum respectively. FPB was also considered an important possible choice because 10% polymer appeared to be a breakpoint at and above which significant improvements in phosphorus removal capabilities occurred for iron blends.

Dosing levels of 50, 100 and 200 μM were tested on Ferric chloride, FPD, alum and Clarion 4100 (Figure 16). Though ferric chloride and alum were less effective coagulants, testing continued as these had been the primary coagulants studied during Phase I. Except for ferric chloride, increased metal dose resulted in lower total turbidity concentrations (Figure 16). These improved reductions in turbidity were generally small. Figure 17 presents total phosphorus concentrations for different doses of the above four metal/polymer blends. When total phosphorus is considered, higher metal doses decreased total phosphorus concentrations except for ferric chloride.

Figure 16. Resultant turbidity values for coagulants at metal dosing levels of 50, 100 and 200 μM.
Jar Test No. 1. Polymer blends were more effective at reducing turbidity values at all dosing concentrations. All the coagulants except for ferric chloride resulted in slightly lower turbidity values at higher dosing levels.

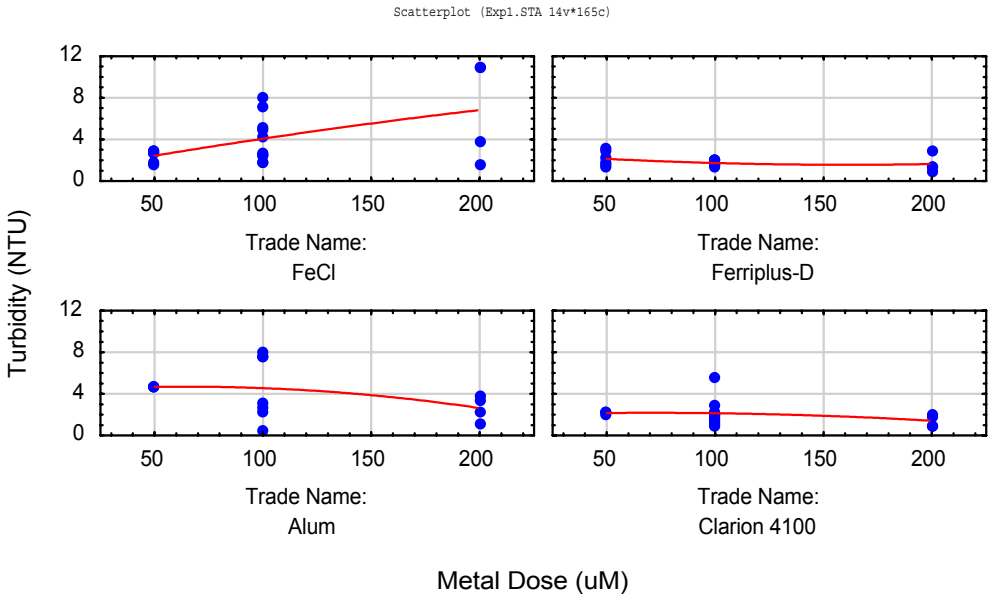

Figure 17. Resultant total P concentrations for selected coagulants at metal dosing levels of 50, 100 and 200 µM.

Jar Test No. 1. Polymer blends resulted in lower total P concentrations for all dosing levels. Except for ferric chloride, higher metal dosing levels resulted in lower total P concentrations. These trends were earlier predicted by turbidity measurements. ENRP water used for this jar test had background concentrations of 31.4 µg L^{-1}. Lines are shown to identify trends.

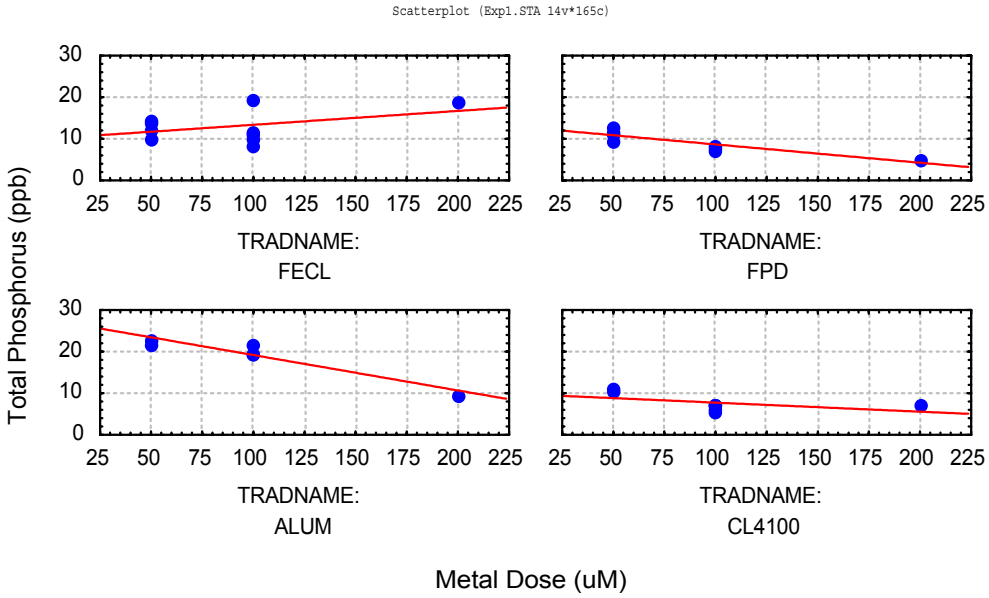

Notes:

1. Table 6 lists abbreviations for different coagulants.

3.4. Conclusion

- Turbidity is a good indicator of total phosphorus concentrations when ferric iron and aluminum blends are considered separately
- Floc settling in the jar test occurred in less than 2 hours
- Of the ferric iron treatments, FPD is the most promising treatment though a very noticeable breakpoint in performance for ferric iron blends occurs at 10% cationic polymer (FPB)
- Of the aluminum treatments, a 10% aluminum/polymer blend will outperform alum alone.
- Total phosphorus concentrations under 8 µg L^{-1} appear possible for both aluminum and ferric iron based chemical treatments if the process is optimized
- Dosing concentrations of 100 and 200 µM of either aluminum or ferric iron should suffice for total phosphorus removal

Chapter 4. Jar Test No. 2, April 1999

This test primarily assessed rapid and slow mixing effects on phosphorus removal (Table 3). Bachand et al. (1999) recommended improved mixing protocols as a mean to improve phosphorus removal. Rapid and slow mixings are both considered very important in the Water Treatment industry for optimizing chemical additions though this had not been a focus of earlier LICD studies. Bachand et al (1999) initially addressed rapid mixing concerns in the mesocosm studies by implementing a rapid mix stage in the LICD Phase I study. This was conducted to improve chemical dispersion. This test addressed recommendations of Bachand et al. (1999) regarding using improved mixing regimes to enhance chemical dispersal and improve precipitation, floc aggregation and floc settling.

4.1. Methods

Slow mixing times of 0 and 30 minutes were used in these studies. During Phase I LICD, no *in situ* slow mixing step occurred in the mesocosm studies. Slow mixing at 0 minutes was tested to simulate that operational mode. Slow mixing at 30 minutes was tested to determine if the addition of slow mixing facilities would likely improve floc aggregation and settling. Rapid mixing times of 15 and 30 seconds were also used in this study (Table 4). Ferric chloride, FBP, FPD, alum and Clarion 4100 were tested and replicated (N=2). Water was sampled and analyzed for total and dissolved phosphorus, iron and aluminum as well as for dissolved organic carbon. Samples were collected at 2 hours and 1 day (Table 4). Metal was dosed at 100 μM.

4.2. Results and Discussion

Rapid mixing caused significant differences in total phosphorus reductions, dissolved phosphorus and dissolved organic carbon concentrations (Table 7, $p<0.05$). Total and dissolved ferric iron and aluminum concentrations did not differ significantly for the different rapid mixing scenarios. Except for alum, longer rapid mixing time led to lower total phosphorus concentrations (Figure 18). For ferric iron treatments, FPD at 30 seconds rapid mix was the most effective chemical blend and resulted in mean total phosphorus concentrations of less than 4 μg L^{-1}. For the alum, Clarion 4100 at 30 seconds rapid mix was the best treatment and resulted in total phosphorus concentrations less than 2.5 μg L^{-1}. These concentrations compared to background total phosphorus concentrations of 10.1 μg L^{-1} for the ENRP water used in this study (Table 8).

Table 7. Effects of rapid mix on phosphorus concentrations.
Jar Test No. 2. Samples were collected at 2 hours and 1 day after mixing ceased. Mean values use data from samples collected at both sampling times. Aluminum and ferric iron blends are combined. Calculation of the p-value uses data from samples collected at 2 hours and 1 day. 2 hour and 1 day samples were considered independent samples given the long period between sampling.

Analyte		Unit	15 seconds	30 s	p-value
UTP	Mean	$\mu g\ L^{-1}$	**7.4**	**5.8**	**0.0423**
	SD	$\mu g\ L^{-1}$	3.5	3.4	
	N	#	44	36	
FTP	Mean	$\mu g\ L^{-1}$	**2.8**	**1.5**	**0.0282**
	SD	$\mu g\ L^{-1}$	3.0	2.1	
	N	#	44	36	
FOC	Mean	$Mg\ L^{-1}$	**12.1**	**12.8**	**0.0438**
	SD	$Mg\ L^{-1}$	1.2	2.1	
	N	#	44	36	
FFE[1]	Mean	$Mg\ L^{-1}$	0.07	0.05	0.6639
	SD	$Mg\ L^{-1}$	0.17	0.08	
	N	#	20	16	
UFE[1]	Mean	$Mg\ L^{-1}$	1.71	1.70	0.9867
	SD	$Mg\ L^{-1}$	1.56	2.05	
	N	#	20	16	
FAL[2]	Mean	$Mg\ L^{-1}$	0.10	0.09	0.7118
	SD	$Mg\ L^{-1}$	0.06	0.05	
	N	#	16	16	
UAL[2]	Mean	$Mg\ L^{-1}$	1.5	1.43	0.8639
	SD	$Mg\ L^{-1}$	1.13	1.12	
	N	#	16	16	

Notes:
1. Ferric iron blends only
2. Aluminum blends only

Table 8. Background water conditions for Jar Test 2

Analyte	Units	Mean	SD	N
FTP	$\mu g\ L^{-1}$	4.7	3.2	14
UTP	$\mu g\ L^{-1}$	10.1	2.5	14
DOC	$Mg\ L^{-1}$	14.2	1.6	14
FFE	$Mg\ L^{-1}$	0.00	0.00	6
UFE	$Mg\ L^{-1}$	0.16	0.08	6
FAL	$Mg\ L^{-1}$	0.06	0.04	8
UAL	$Mg\ L^{-1}$	-0.01	0.35	8

Figure 18. Rapid mixing effects on enhancing phosphorus removal.
Jar Test No. 2. Metal dosing concentrations used were 100 µM. Samples were collected at 2 and 24 hours. Each treatment had two replicates. Values represents mean values of those collected at 2 and 24 hours. Background phosphorus concentrations in ENRP waters used for jar test were 10.1 µg L^{-1}.

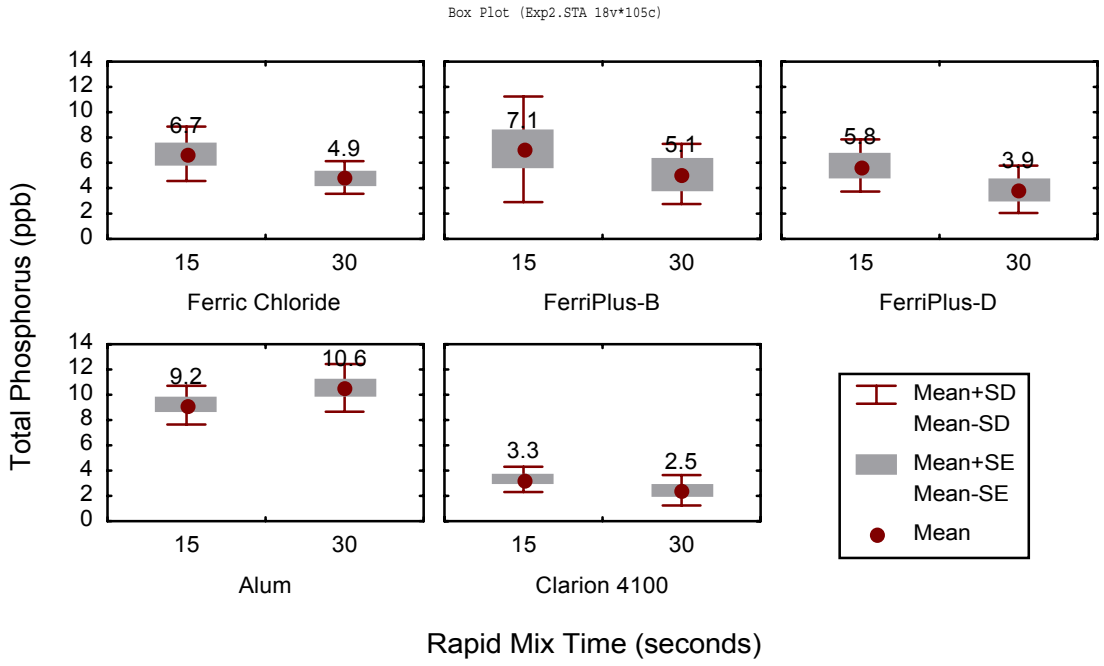

Total phosphorus concentration was the only parameter that differed significantly for different slow mixing scenarios (Table 9, $p<0.05$). Particulate species were more affected by the different slow mixing scenarios than dissolved species. Thus, floc aggregation may be improved by slow mixing though initial floc formation and precipitation is probably not. Figure 19 shows the different total phosphorus concentrations for dosed waters after 0 and 30 minutes of slow mixing. For all chemical blends, longer mixing resulted in lower total phosphorus concentrations and better floc settling.

Table 9. Effects of slow mix on phosphorus concentrations.
For samples at time 2 hr and 1 day. Aluminum and ferric iron blends are combined. Mean values represents data for both samples time. Two hour and 1 day samples were considered independent given the long time between sampling.

Analyte		Unit	0 m	30 m	p-value
UTP	Mean	$\mu g\ L^{-1}$	**7.6**	**5.9**	**0.0352**
	SD	$\mu g\ L^{-1}$	4.0	2.9	
	N	#	38	42	
FTP	Mean	$\mu g\ L^{-1}$	2.2	2.1	0.8400
	SD	$\mu g\ L^{-1}$	2.7	2.7	
	N	#	38	42	
FOC	Mean	$Mg\ L^{-1}$	12.41	12.40	0.9803
	SD	$Mg\ L^{-1}$	1.69	1.73	
	N	#	38	42	
FFE[1]	Mean	$Mg\ L^{-1}$	0.07	0.05	0.6359
	SD	$Mg\ L^{-1}$	0.16	0.10	
	N	#	18	22	
UFE[1]	Mean	$Mg\ L^{-1}$	2.00	1.18	0.1416
	SD	$Mg\ L^{-1}$	1.78	1.66	
	N	#	18	22	
FAL[2]	Mean	$Mg\ L^{-1}$	0.08	0.09	0.5107
	SD	$Mg\ L^{-1}$	0.06	0.05	
	N	#	20	20	
UAL[2]	Mean	$Mg\ L^{-1}$		0.88	0.1069
	SD	$Mg\ L^{-1}$		0.91	
	N	#		20	

Notes:
1. Ferric iron blends only
2. Aluminum blends only

Figure 19. Slow mixing effects on enhancing floc aggregation and subsequent P removal.
Jar Test No. 2. Metal dosing levels used were 100 µM. Water samples were taken at 2 and 24 hours. Each treatment had two replicates.

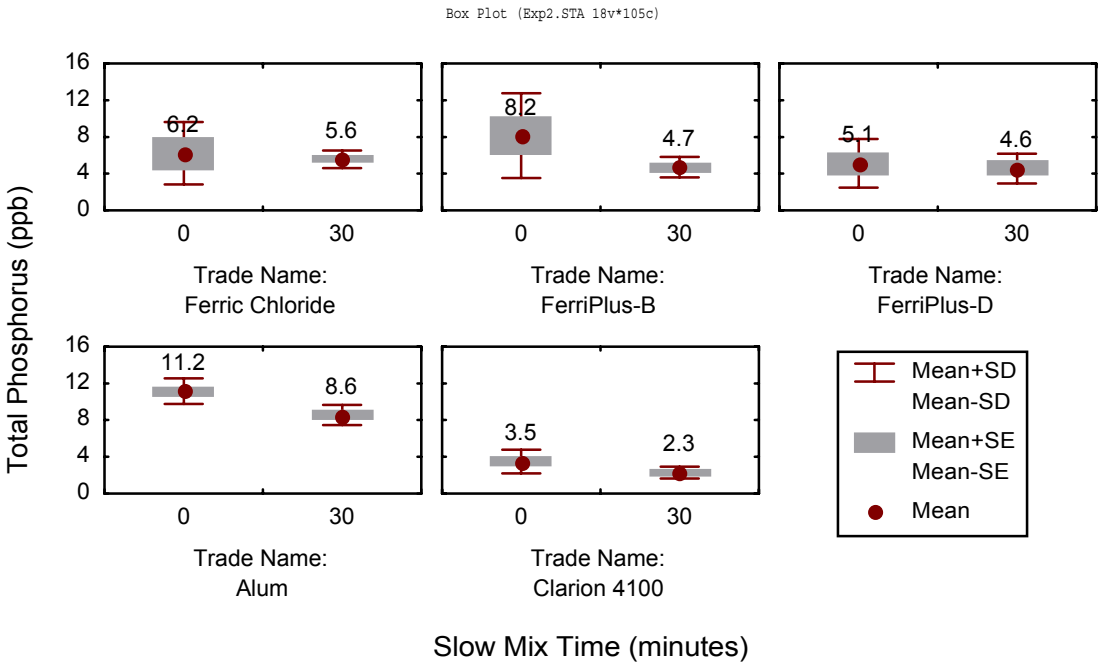

4.3. Conclusion

Both rapid and slow mixing improved total phosphorus removal ($p<0.05$). Rapid mixing improved floc precipitation and slow mixing improved total P removal. These results suggest that total phosphorus removal at the mesocosms could be improved by:

- The addition of a slow mixing chamber immediately upstream of the mesocosms for improved floc aggregation
- The installation of an additional inline mixer to increase the rapid mix time would improve the metal/phosphorus reactions and aid with floc aggregation and settling.

Metal dosing levels of 100 µM with the optimal chemical/polymer blends and improved mixing appeared to provide sufficient phosphorus removal

Chapter 5. Batch Flow Mesocosm Study, June 1999

June 1999 Batch Flow Study was conducted to field verify jar test findings and had the following goals:

- Determine changes in dissolved and total phosphorus over time.
- Field test the feasibility of 100 μM dosing with a metal/polymer blend with regard to total and dissolved phosphorus removal. This study was conducted under improved mixing regimes.
- Assess water quality effects (DOC, iron, aluminum)

5.1. Methods

Table 10 shows the experimental design for the June 1999 Batch Flow Study. All metals were dosed at 100 μM. Non-Dosed, Clarion 4100 and FPB treatments were replicated. FPD treatment was not. FPD and Clarion 4100 were selected as optimal metal/polymer blends. FPB was considered as10% cationic polymer appeared to be the breakpoint above which phosphorus removal improved for ferric iron blends.

Table 10. Experimental Design for June 1999 Batch Flow Study. Study was conducted at Site C. This study was the first dosing study conducted at Site C. All metals were dosed at 100 μM.

Mesocosm	Blend	Metal	Metal Coagulant	Cationic polymer (%)
1	FPB	Fe	Ferric sulfate	10
2	Clarion 4100	Al	Aluminum sulfate	10
3	Non-Dosed	---	---	---
4	FPD	Fe	Ferric sulfate	20
5	Clarion 4100	Al	Aluminum sulfate	10
6	FPB	Fe	Ferric sulfate	10
7	Non-Dosed	---	---	---
8	UnWalled Control (Background)	---	---	---

Rapid mixing was improved for this field study by increasing the number of inline static mixers from one to two for each mesocosm receiving chemical dosing. Jar Test No. 2 results suggested that phosphorus removal could be improved by better rapid mixing. LICD Phase I results also supported this with regard to ferric iron dosing. For iron dosing, approximately one third of the dosed iron remained

in the water column as dissolved iron (Bachand et al. 1999). This suggested either inadequate mixing energy or mixing time for effective iron precipitation. By doubling the number of inline mixers, both the energy and detention time of rapid mixing were doubled.

Slow mixing tanks were also installed in these studies. Jar Test No. 2 suggested that slow mixing would improve floc aggregation as statistically different phosphorus concentrations resulted after mixing when a slow mixing step was used. This is not a surprise as a common industry practice is to have such a step for floc aggregation. Thus for this batch flow study, the mesocosm sites were modified to have a slow mixing tank with a 10 minute detention time installed immediately upstream of the mesocosms (Figure 8). Water was mixed with an impeller. The design for this modification is discussed in more detail in Chapter 2.

Mesocosms were initially dosed with three volumes of water and then during the following weeks water was sampled at multiple locations several times per week. A schedule summary with actions taken and parameters sampled is shown in Table 11. This study focused only on process variables considered critical for assessing this technology. These variables were total phosphorus, dissolved phosphorus, total and dissolved aluminum and iron, bromide and dissolved organic carbon. Sampling locations are shown in Figure 9.

5.2. Results and Discussion

Figures 20 and 21 show changes in total and dissolved phosphorus concentrations in the mesocosms after dosing ceased as represented by Day 0. Total and dissolved phosphorus concentrations were constant up through Day 8. On Day 8, a sharp increase in both dissolved and total phosphorus concentrations occurred in some treatments. Most noticeable was in the Non-Dosed mesocosms where dissolved phosphorus concentrations increased from 12 to 24 $\mu g\ L^{-1}$ and total phosphorus concentrations increased from 40 to 70 $\mu g\ L^{-1}$. These concentrations exceeded background concentrations (e.g. unwalled control) of approximately 18 $\mu g\ L^{-1}$ for dissolved phosphorus and approximately 40 $\mu g\ L^{-1}$ for total phosphorus.

Table 11. Schedule for June 1999 Batch Flow Mesocosm Study

Date	Day	Action	Sampling Locations	Parameters Sampled.
7	Mon.			
8	Tues.			
9	Wed.	Background sampling.	Mesocosms	FTP, UTP, FOP, DOC.
10	Thurs.			
11	Fri.	Sample chemical stock solutions.	Chemical carboys	UTP, UFE, FFE, UAL, FAL, FBr
12	Sat.			
13	Sun.			
14	Mon.	Deploy stock solutions. Begin pumping.		
15	Tues.	Sample. End pumping.	Piping, mesocosms.	FTP, UTP, FOP, UFE, FFe, UAL, FAl, DOC, FBr
16	Wed.	Sample. Recover stock solutions.	Mesocosms.	FTP, UTP, FOP, UFE, FFe, UAL, FAl, DOC, FBr
17	Thurs.	Sample.	Mesocosms, chemical carboys	FTP[1], UTP, DOC[1], FBr, UFe[2], FFe[2], Ual[2], Fal[2]
18	Fri.	Sample	Mesocosms.	FTP, UTP, DOC, FBr
19	Sat.			
20	Sun.			
21	Mon.	Sample	Mesocosms.	FTP, UTP, FOP, UFE, FFe, UAL, FAl, DOC, FBr
22	Tues.			
23	Wed.	Sample	Mesocosms.	FTP, UTP, DOC, FBr
24	Thurs.			
25	Fri.	Sample	Mesocosms.	FTP, UTP, DOC, FBr
26	Sat.			
27	Sun.			
28	Mon.	Sample	Mesocosms.	FTP, UTP, FOP, UFE, FFe, UAL, FAl, DOC, FBr

Notes.
1. Samples at mesocosms only.
2. Sample at chemical carboys only.

Figure 20. Changes in mesocosm dissolved phosphorus concentrations over time for selected coagulants, June 1999 Batch Flow Study.
Samples were taken at two locations within each mesocosm after pumping had ceased. Clarion 4100, FPD and Non-dosed treatments were replicated (N=2). Study was conducted at Site C.

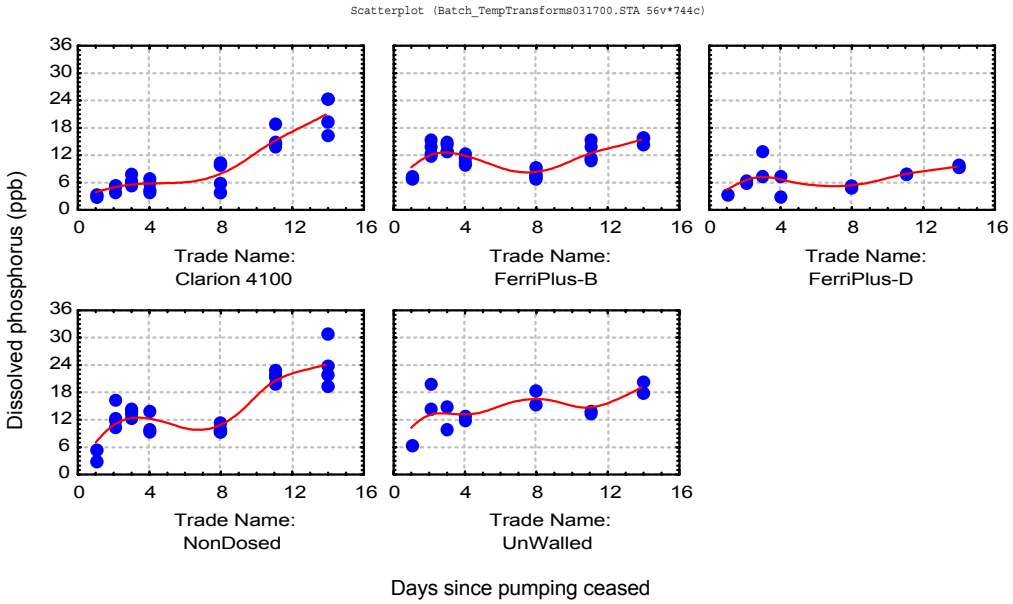

Figure 21. Changes in mesocosm total P concentrations over time for selected coagulants, June 1999 Batch Flow Study.
Samples were taken at two locations within each mesocosm after pumping had ceased. Clarion 4100, FPD and Non-dosed treatments were replicated (N=2). Study was conducted at Site C.

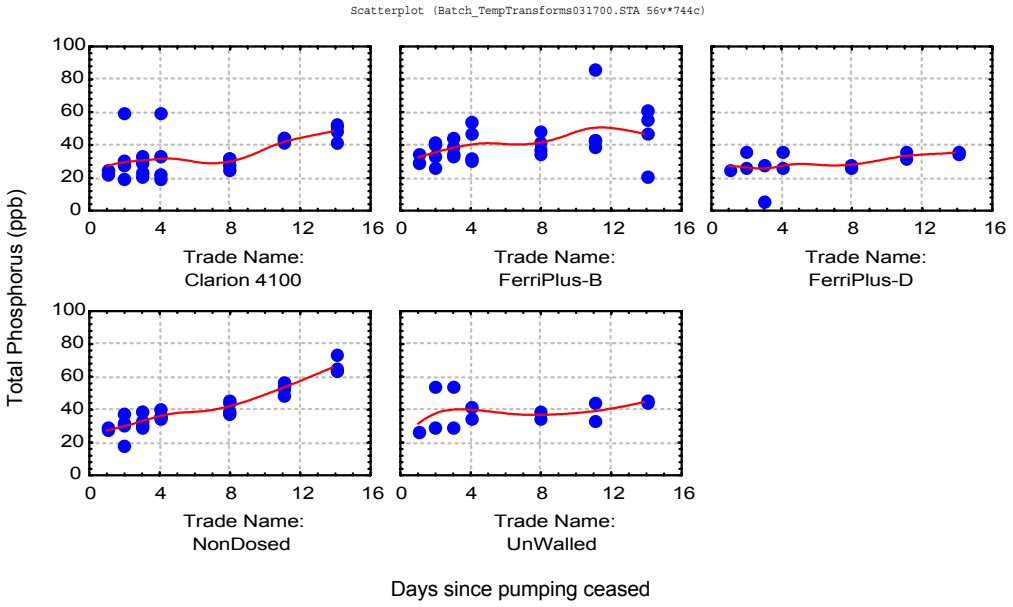

Mesocosm outflow valves (Figures 5 and 6) remained closed during this experiment. In this configuration, any water entering or exiting the mesocosms in response to water elevation changes in the surrounding marsh occur through the peat (Figure 5). The mesocosm studies were installed in ENRP Cell 2. Water level data for Cell 2 taken by South Florida Water Management District (SFWMD) presents hydrologic data that explains the sudden rise in both dissolved and total phosphorus concentrations in the mesocosms (Figure 22). From Day 0 through Day 8, water levels dropped 0.3 feet. During this time, water levels in the mesocosms equilibrated with those in the surrounding marsh by with water exiting the mesocosms through the underlying peat. This direction of flow could not affect water mesocosm phosphorus concentrations. On Day 8 with the surrounding marsh water elevation rising, water began entering the mesocosms through the peat. This direction of flow could increase phosphorus concentrations by forcing phosphorus-enriched pore water into surface waters. This apparently occurred as shown by the phosphorus data from the Non-Dosed Treatments.

Figure 22. ENRP Cell 2 Water elevation changes during June 1999 Batch Flow Study.

Water elevation decreased from 12 to 11.65 feet from Day 0 to Day 8, representing a 4 inch (10.7 cm) drop. From Day 8 to Day 16, water elevations rose to 12.15 feet, representing a increase in water elevation of 6 inches (15 cm). Data from SFWMD gauging stations located in the ENRP Cell 2.

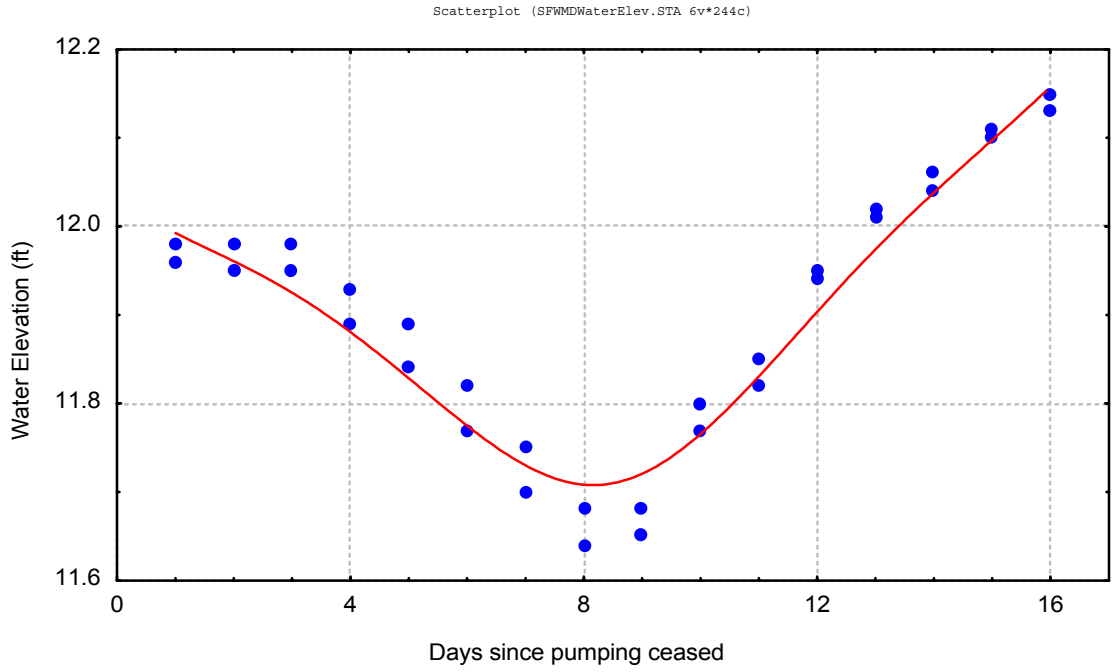

Thus, both dissolved and total phosphorus mesocosm concentrations were relatively constant up to the time when water levels began to rise in the marsh. Interestingly, the resulting concentrations from this event differed between treatments. The Clarion 4100 treatment experienced sharp increases in dissolved and total concentrations during this period of rising water levels. The ferric iron treatments experienced less of a concentration increase with almost no increase for the FPD treatment (ferric iron + 20% polymer). These results strongly support the hypothesis that the application of low concentrations of metals, especially iron, forms a metal blanket that helps prevent the export of phosphorus from wetland sediments into the overlying water.

Water column phosphorus concentrations were considered from Day 0 through Day 8 to separate chemical from hydrologic effects on phosphorus concentrations. Both total and dissolved phosphorus concentrations differed significantly with treatment as shown in Figure 23 ($p<0.01$). Clarion 4100 treatment and the FPD treatment decreased total and dissolved phosphorus concentrations below those in both background waters and those in the Non-Dosed treatment. Both treatments resulted in dissolved phosphorus concentrations near 5 $\mu g\ L^{-1}$. The Clarion 4100 treatment decreased mean total phosphorus concentrations to 30 $\mu g\ L^{-1}$. This was 79% of background levels and 87% of Non-dosed levels. The FPD treatment decreased mean total phosphorus concentrations to 27 $\mu g\ L^{-1}$ which was 71% of background levels and 78% of Non-dosed levels. The FPB treatment was ineffective at decreasing either total or dissolved phosphorus concentrations adequately.

Notably, the *in situ* decreases in total and dissolved phosphorus occurred at ferric iron and aluminum dosing levels of only 100 μM. This corresponds to a ferric iron dosing level of 5.6 mg L^{-1} and an aluminum dosing level of 2.7 mg L^{-1}.

Dosing of both aluminum and ferric iron affected water quality. Aluminum dosing raised aluminum concentrations from near 0 mg L^{-1} to around 1 mg L^{-1}, with most the aluminum as particulate (Figure 24). Thus, approximately one third of the dosed aluminum remained in the water column. Ferric iron dosing raised iron concentrations from near 0 mg L^{-1} to 1 to 2 mg L^{-1} depending upon the ferric iron/polymer blend used (Figure 24). The blend with the higher polymer decreased residual iron concentrations in the water column by half. All dosing treatments decreased dissolved organic carbon levels below both background and Non-Dosed chamber levels (Figure 25).

Figure 23. Mean total and dissolved phosphorus concentrations in mesocosms during June 1999 Batch Flow Study.
Data represents time period of Day 0 through Day 8 before rising water elevations caused phosphorus concentrations to increase.

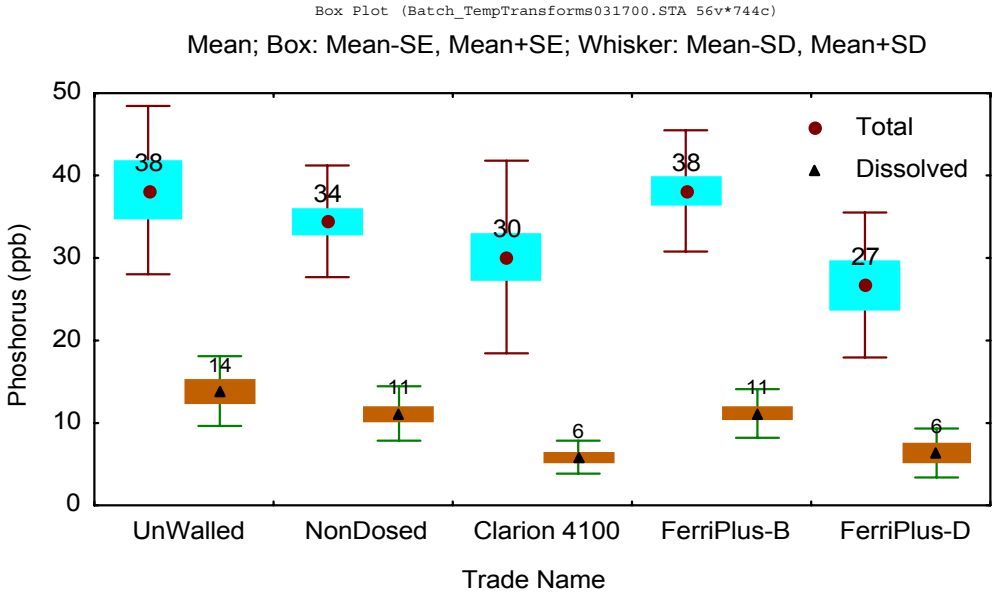

Figure 24. Mean dissolved and total iron and aluminum concentrations, June 1999 Batch Flow Study.
Data represents time period from Day 0 through Day 8 before water elevations began to rise.

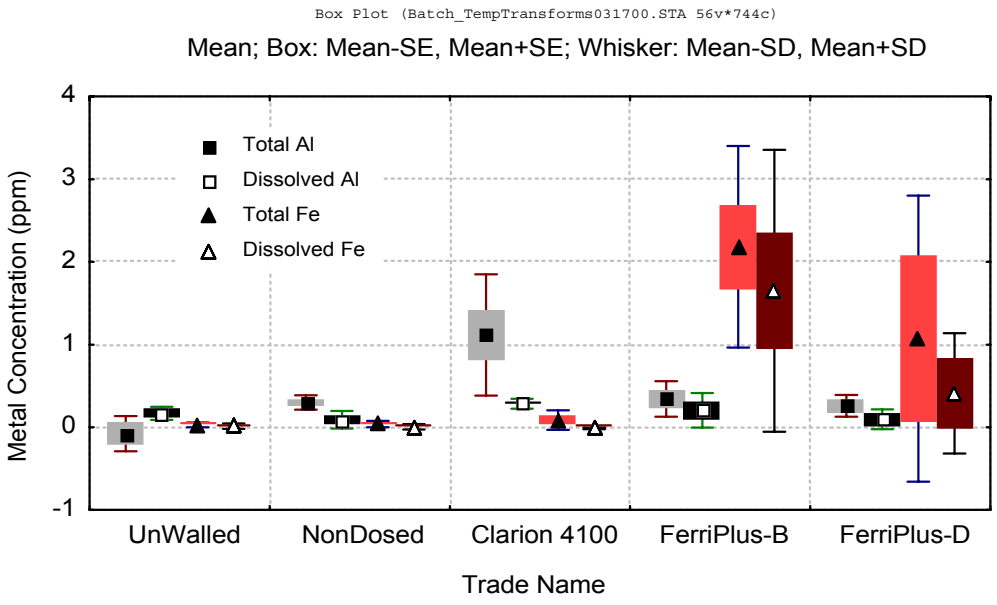

Figure 25. Mean dissolved organic carbon concentrations, June 1999 Batch Flow Study.
Data represents time period from Day 0 through Day 8 before water elevations began to rise.

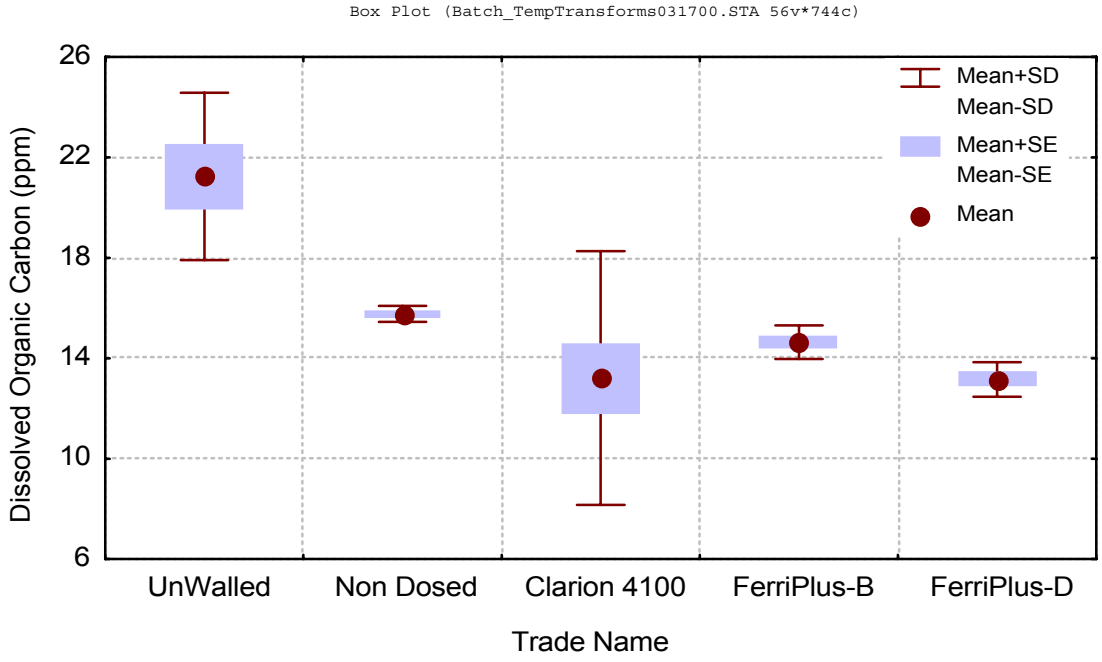

5.3. Conclusion

- Ferric iron provides a sediment cap or blanket. This cap interferes with phosphorus export from the sediments to the water column. This may be especially important during periods of rising groundwater water and exfiltration.
- At times of stable or falling water levels, resulting phosphorus concentrations in the water column were constant for up to eight days.
- When used in combination with cationic polymers, aluminum and ferric iron dosing levels of 100 µM decreased total phosphorus concentrations to or below 30 µg L^{-1} and dissolved phosphorus concentrations to near 5 µg L^{-1}.
- Cationic polymer concentrations of 20% more effectively improved total and dissolved phosphorus removal by ferric iron blends than lower polymer concentrations. 10% cationic polymers sufficed for aluminum treatments.
- Aluminum and ferric iron dosing increased concentrations of the respective metals in the water column. Both decreased dissolved organic carbon concentrations.
- Metal/cationic polymer blends used in this study were inadequate for reducing total phosphorus concentrations below 20 µg L^{-1}.

Chapter 6. Jar Test No. 3, July 1999

Jar Test No. 3 was implemented to determine if these laboratory studies could effectively predict phosphorus concentrations achieved at the mesocosm studies under *in situ* chemical dosing (Table 3).

6.1. Methods

The chemical blends chosen were the same used for the June Batch Study (Table 10). Water used for this study was collected from Site C during the June Batch Flow Study. Total phosphorus concentrations were measured at 0 minutes, 30 minutes, 2 hours and 1 day after mixing ceased. Dissolved phosphorus, aluminum, iron and carbon was measured 0 minutes, 2 hours and 1 day after mixing ceased (Table 4). Each treatment was replicated 3 times.

6.2. Results and Discussion

At the initiation of each study, total phosphorus concentrations for each treatment was approximately 60 µg L^{-1} (Figure 26). This exceeded concentrations for the concurrent field study of 40 µg L^{-1}.

Figure 26. Changes in total P over time for jar test study replicating June 1999 Batch Flow Study.

Jar Test No. 3. Source water and coagulants used were the same as those used during the June 1999 Batch Flow Study. Jar test was conducted to determine whether jar tests could effectively predict final P concentrations achieved in the field with *in situ* dosing. Each treatment was replicated (N=3).

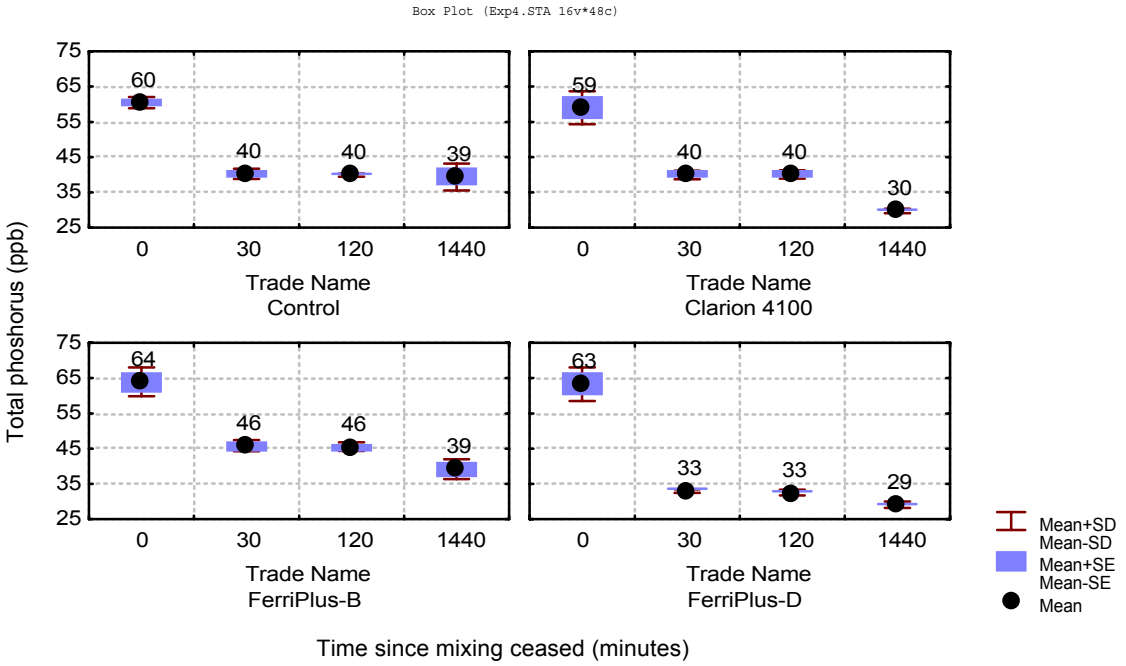

Thirty minutes after the mixing ceased, the control samples had total phosphorus concentrations of 40 μg L^{-1}. This decrease represents the removal of phosphorus as settleable solids. Under normal relatively quiescent conditions, these solids would not be expected in the water column. As with the June field study, FPB ineffectively removed total phosphorus (Figure 27). Both the Clarion 4100 and the FPD resulted in lower total phosphorus than the background and control levels. Average total phosphorus concentrations from 30 minute, 2 hour and one day samples were 32 μg L^{-1} for FPD and 37 μg L^{-1} for Clarion 4100 (Figure 27). The 24-hour sample had the lowest total phosphorus concentrations for both the Clarion 4100 and the FPD demonstrating that longer settling times improved phosphorus removal. For that sample, Clarion 4100 decreased total phosphorus concentrations to 30 μg L^{-1} as it did in the field. FPD decreased total phosphorus concentrations to 29 μg L^{-1} as opposed to 27 μg L^{-1} in the field. Dissolved phosphorus concentrations were higher in the jar test studies as opposed to those in the field.

These results showed that the jar test reasonably predicted field results for total phosphorus. Resultant total phosphorus concentrations at 24 hours for the different chemical blends were equivalent to those achieved in the field. Dissolved phosphorus concentrations were not well predicted in this study.

6.3. Conclusion

- Jar test reasonably predicts field trends under similar dosing regimes.

Figure 27. Mean total and dissolved P concentrations achieved during jar test replicating June 1999 Batch Flow Study.
Jar Test No. 3. Data are from water samples collected at 30 minutes, 2 hours and one day. Each treatment was replicated (N=3).

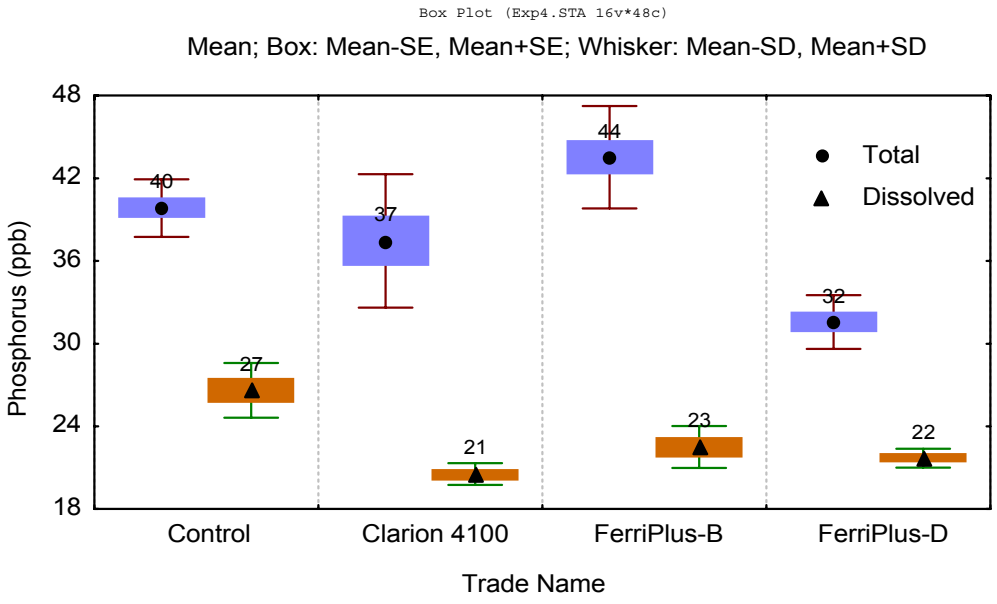

Chapter 7. Jar Test No. 4, July 1999

Jar Test No. 4 was implemented to further refine LICD methods (Table 3).

7.1. Methods

To expedite the research, turbidity was used as an indicator of floc aggregation and settling. Higher dosing concentrations were investigated (e.g. 100, 200, 400 µM) and iron/aluminum blends were investigated at dosing concentrations of 100 µM. All treatments were replicated (N=3). Measurements were taken at 0, 30, 60, 120 and 240 minutes after mixing ceased (Table 4).

7.2. Results and Discussion

FPB, FPD and Clarion 4100 were tested at dosing concentrations of 100, 200 and 400 µM. Each treatment reached steady state turbidity levels at 30 minutes (Figure 28). FPD and Clarion 4100 resulted in equivalent turbidity levels. Both differed significantly with FPB (2-Way ANOVA: coagulant vs. dose, p=0.05). Turbidity values slightly achieved under FPD and Clarion 4100 dosing slightly increased with the higher dosing level of 400 µM. With the FPB treatment, the increase was more pronounced.

Figure 28. Changes in turbidity over time for metal/cationic polymer blends.
Jar Test 4. Metal dosing levels of 100, 200 and 400 µM were used for this study. Steady state was generally achieved by 30 minutes after mixing ceased.

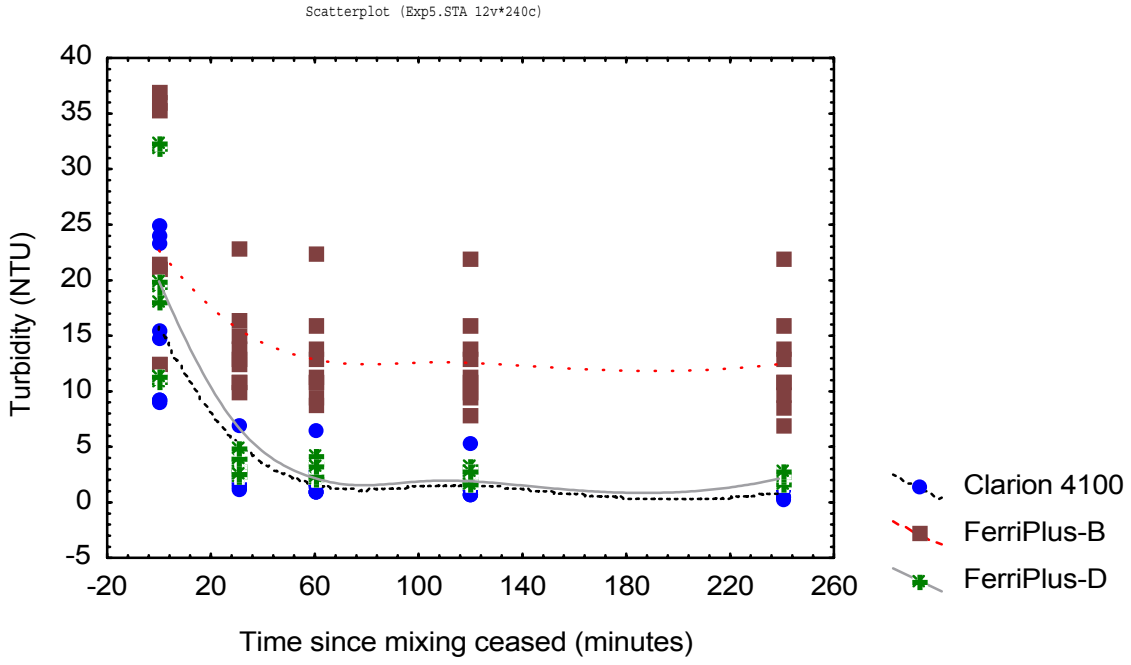

Aluminum and iron blends were investigated to determine if there would be synergistic effects improving phosphorus removal. Earlier results suggested that both metals may have slightly different phosphorus removal mechanisms. Aluminum blends typically resulted in higher decreases in dissolved organic carbon than ferric iron blends suggesting aluminum blends more likely formed metal-organic complexes whereas iron blends more likely formed metal hydroxides. Thus, blending aluminum and ferric iron was considered a means to possibly broaden the phosphorus removal mechanisms during chemical dosing.

For aluminum, various blends were investigated. These combinations were conducted at metal dosing levels of 100 µM. Clarion 4100 in combination with FPD achieved the lowest turbidity values though these values were not significantly different than those achieved by Clarion 4100 alone (Figure 29). Both Clarion treatments were better and differed significantly with the alum treatments. For ferric iron, FPD in combination with ferric iron achieved the lowest turbidity values though these differences were not statistically significant (Figure 29). Adding alum decreased the effectiveness of ferric iron in reducing turbidity.

Figure 29. Testing iron/aluminum blends.
Jar Test No. 4. Data represents samples taken for a subset of metal dosing levels of 100 µM. Mixing iron and aluminum did not improve floc settling characteristics as measured by turbidity.

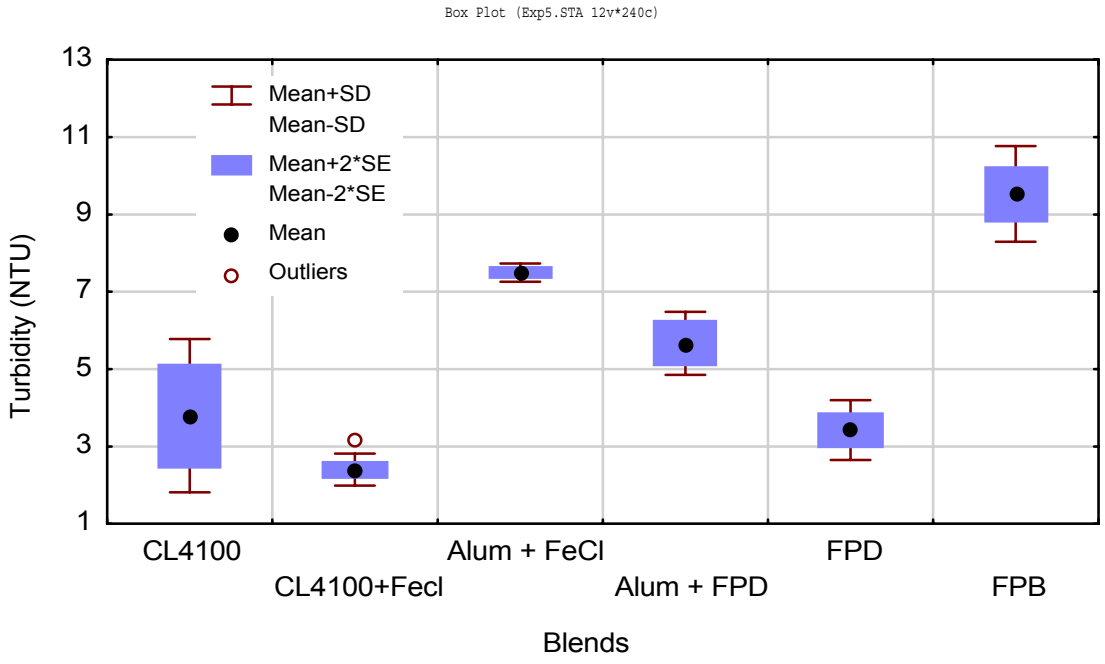

Notes:
1. Table 6 lists abbreviations for different coagulants.

7.3. Conclusion

- Metal dosing concentrations greater than 200 μM in the jar tests did not reduce turbidity significantly. In some cases, increasing dose raised turbidity.
- FPD and Clarion 4100 performed similarly and outperformed FPB.
- Ferric iron/aluminum blends do not improve performance over ferric iron or aluminum alone.

Chapter 8. Jar Test No. 5, August 1999

This study focused on using calcium or anionic polyacrylamides (PAMs) to improve phosphorus removal by the formation of larger and more rapidly settling flocs (Table 3). The goals for this study were to:

- Determine if calcium could be added alone for phosphorus removal,
- Determine if calcium when used in combination with ferric iron or aluminum would improve floc settling rates,
- Determine if anionic polyacrylamides (PAMs) could be used in combination with ferric iron or aluminum to improve floc settling rates, and
- Determine the most promising PAM.

8.1. Methods

Jar tests were conducted with a 15-second rapid mix after chemical addition to aid with chemical dispersions and reactions, followed by a 5-minute slow mix for floc aggregation. When combinations of calcium and iron or aluminum were used, a 15-second rapid mix followed the addition of each chemical. Each chemical was added individually. Calcium was added as calcium hydroxide (slaked lime). Calcium was added at dosing concentrations of 25, 50, 100 and 150 mg L^{-1} which corresponds with dosing concentrations of 625, 1250, 2500 and 3750 μM. Anionic polyacrylamides were investigated in this study and these are defined in Table 12. When PAMs were added, PAM addition always followed metal addition and included a 15-second rapid mix after the addition. Upon completion of all chemical addition and rapid mixing, a 5-minute slow mix followed. Rapid mixing occurred at 300 rpms and slow mixing occurred at 30 rpms. Turbidity was measured at 0, 5, 10, 30 and 60 minutes after mixing ceased (Table 4).

Table 12. PAM descriptions, Jar Test No. 5.

Cytec Trade Name	Molecular Weight	Charge density (%)
SuperFloc A 110	High	18
SuperFlow A130	High	35
A1849[1]	Medium	3

Notes:
1. Tested previously by CH2Mhill (1999).

8.2. Results and Discussion

Calcium additions were ineffective at reducing turbidity. In fact, as calcium concentrations increased from 25 to 100 mg L^{-1}, average turbidity values calculated from averaging samples taken at 5, 10 and 30 minutes increased (Figure 30). Turbidity was not measured at 60 minutes for these samples. At the calcium concentration dose of 25 mg L^{-1}, turbidity declined slightly during the

sampling period (Figure 31). These data suggest that calcium additions alone will not effectively reduce water column phosphorus concentrations. Calcium additions at concentrations of 25, 50, 100 and 150 mg L^{-1} were also conducted in combination with ferric iron and aluminum doses of 200 µM. Again, these blends generally increased turbidity (Figure 32).

PAM doses at 0, 0.25 and 0.75 mg L^{-1} were conducted in combination with FPD and Clarion 4100 at metal doses of 100 and 200 µM. A 2-Way ANOVA with the independent variables as metal dose and PAM dose showed that turbidity differed significantly with PAM doses (p=0.0015). A post-hoc analyses showed that this was due to statistical differences between turbidity values at 0 and 0.25 mg L^{-1} (p=0.0012; Figure 33).

Figure 30. Calcium additions leading to increases in turbidity.
Jar Test No. 5. Data represents water samples collected at 5, 10 and 30 minutes.

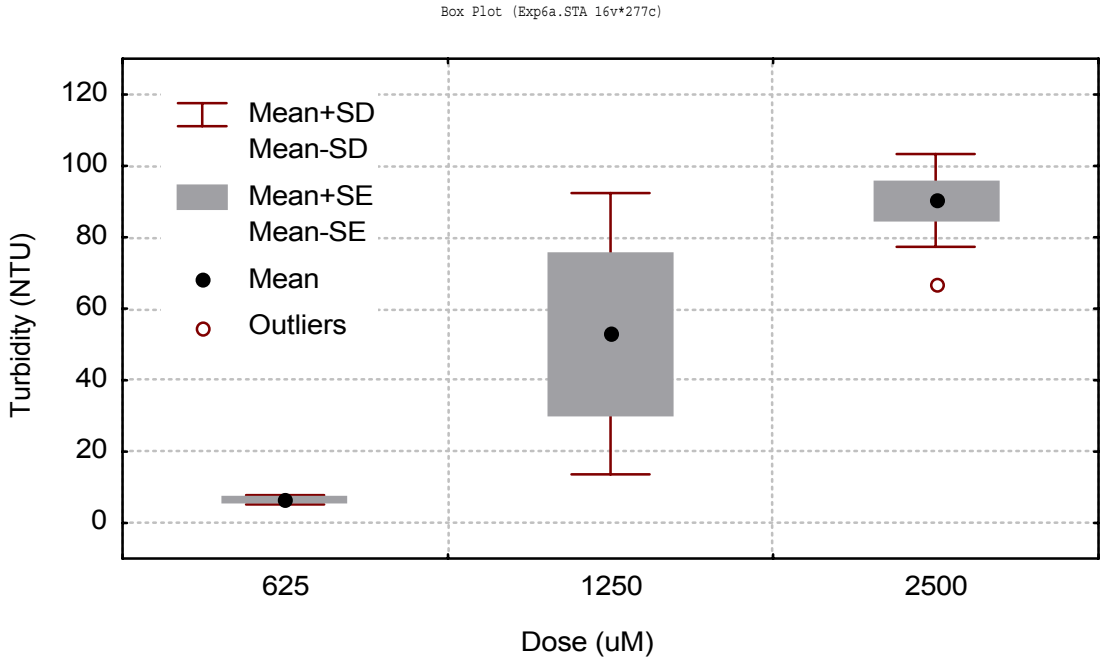

PAM dosing improved floc settling. Mean turbidity values of samples collected at 5, 10, 30 and 60 minutes after mixing ceased showed that at higher PAM dosing levels lowered turbidity and narrowed the variance (Figure 33). For aluminum blends, PAM dosing only slightly lowered turbidity though it decreased the standard deviation by over half (Figure 34). For iron, the effect of PAMs were more noticeable and statistically significant (p<0.5, Figure 34). Aside from

lowering mean turbidity for the sampled time period, PAM addition increased the rate at which flocs initially settled. When PAMs were used in the iron treatments, turbidity decreased immediately after mixing ceased as can be seen from a comparison of turbidity at time zero for iron treatments at different PAM dosing levels. When PAMs were not used, turbidity averaged around 20 NTU for iron treatments at time zero. However, at PAM dosing concentrations of 0.25 and 0.75 mg L^{-1}, turbidity was about half that at time zero. Moreover, turbidity achieved baseline values within five minutes of mixing ceased when PAMs were used as opposed to twice that long when PAMs were not used (Figure 35). Baseline turbidity values were more stable for iron blends when PAMs were incorporated into the process. When PAMs were not used, turbidity decreased more slowly, achieving baseline after 10 minutes and it was not as stable over the sample time period. However, even with the aluminum blend, the curve describing floc settling was steeper when PAMs were used as opposed to when they were not used (Figure 35), resulting in a lower standard deviation (Figure 34).

Three different polymers were tested during this study. These PAMs represented a range of charge densities and molecular weights (Table 12). Each polymer was tested identically during this study. Turbidity values achieved with the different polymers differed significantly during this study ($p=0.0078$). A130 outperformed the other two polymers (Figure 36).

Based on these analyses, the most promising treatments were FPD and Clarion 4100 at 200 μM using 0.25 mg L^{-1} SuperFloc A130. These combinations decreased turbidity to less than 3.4 (Figure 37). These values did not differ statistically ($p=0.7158$). For the aluminum treatment, floc settled within 5 minutes of mixing and for the FPD treatment, floc settled immediately after mixing ceased (time = 0 minutes, Figure 38).

Figure 31. Turbidity changes over time for different calcium dosing levels.
Jar Test No. 5. Calcium dosing generally led to increases in turbidity during the first 30 minutes after mixing ceased. Longer-term measurements showed no reliable settling of floc.

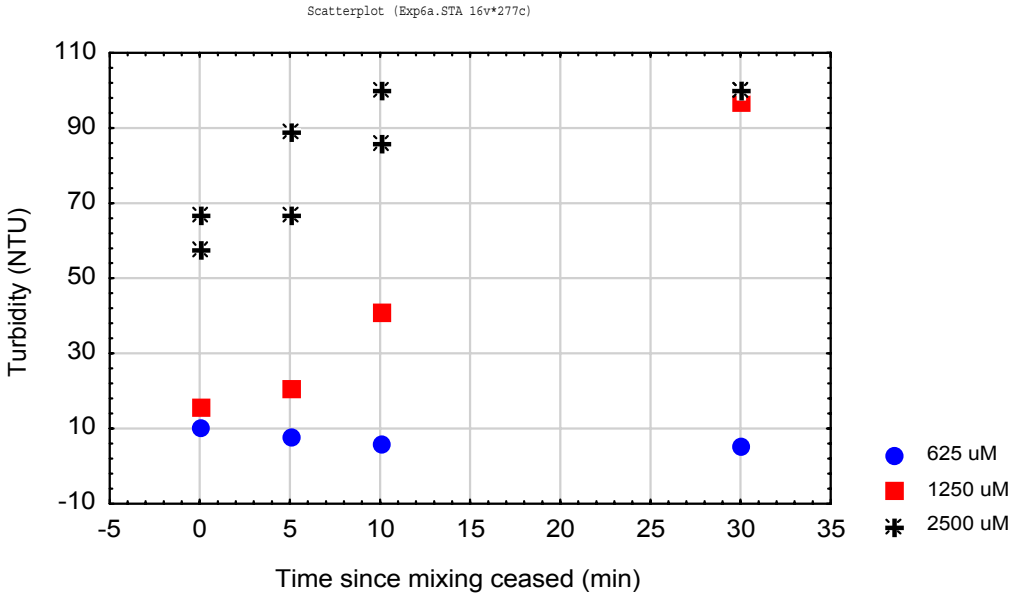

Figure 32. Effects on turbidity of adding calcium in combination with iron or aluminum.
Jar Test No. 5. Data represent water samples collected at 5, 10, 30 and 60 minutes. Using calcium in combination with either iron or aluminum generally led to higher turbidity values than achieved when the metal coagulants were used alone. Iron and aluminum were dosed at 200 µM.

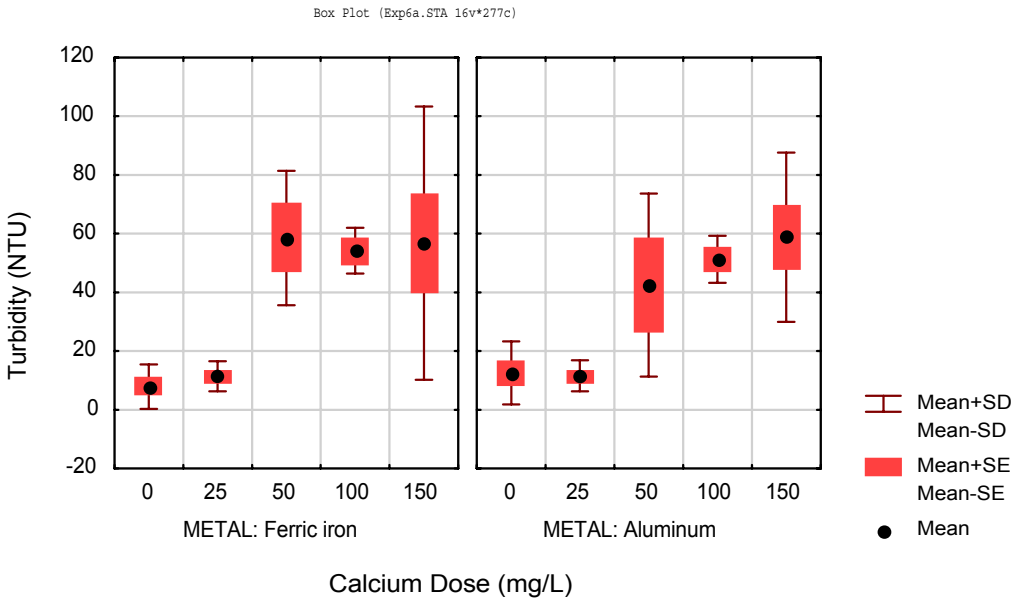

Figure 33. Using anionic polyacrylamides (PAMs) following iron and aluminum dosing to decrease turbidity.

Jar Test No. 5. Data represent water samples taken at 5, 10, 30 and 60 minutes. Metal blends used were FPD and Clarion 4100 at metal dosing levels of 100 and 200 µM. PAM dosing levels of 0.25 mg L^{-1} were statistically different from other treatments (p=0.0015). Two standard error approximate statistical difference (p=0.05) between

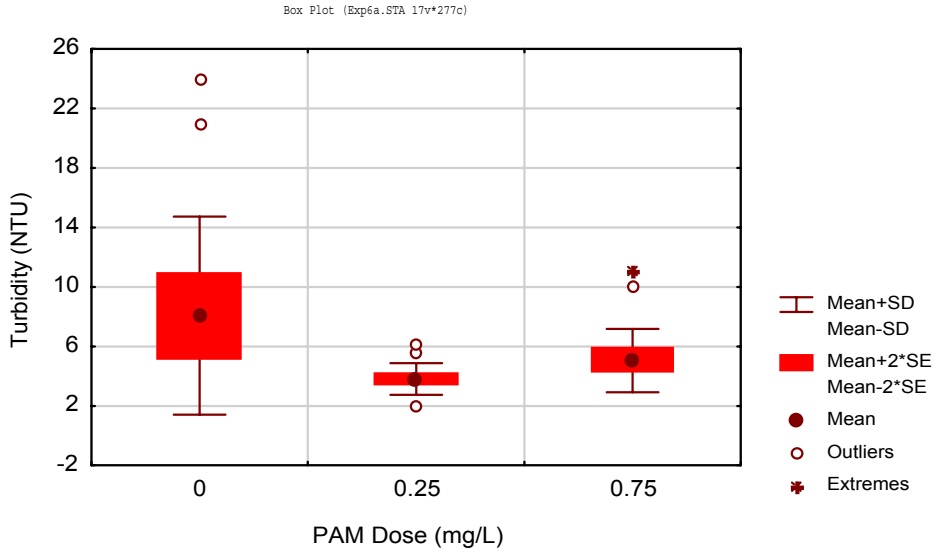

treatments.

Figure 34. PAM effects on turbidity for FPD and Clarion 4100 at dosing levels of 100 and 200 µM metal.

Jar Test No. 5. Data represents mean value of water samples collected at 5, 10, 30 and 60 minutes. PAM effects on reducing turbidity were much greater and more statistically significant with ferric iron as opposed to aluminum blends. PAMs resulted in smaller standard deviations for turbidity for both iron and aluminum blends.

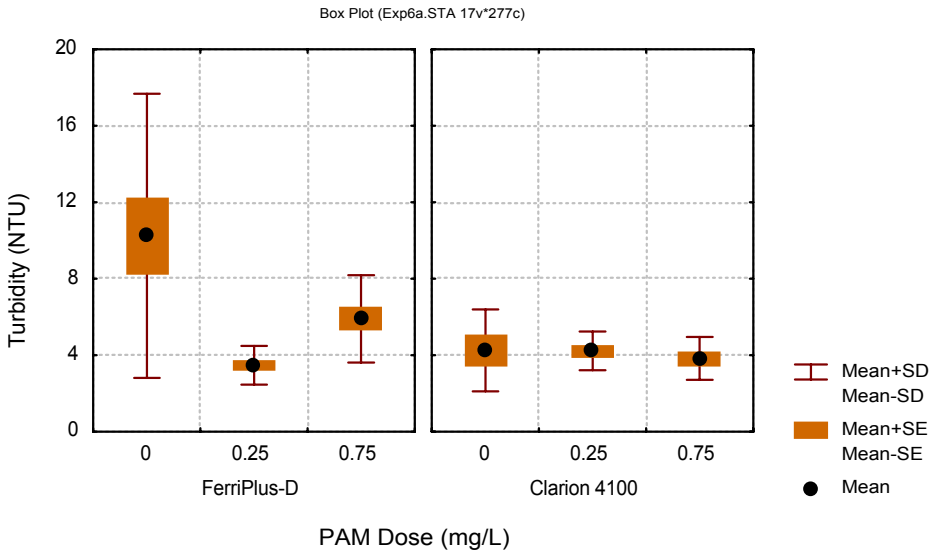

Figure 35. PAM effects on floc settling rates for FPD and Clarion 4100 as indicated by turbidity measurements.
Jar Test No. 5. Dosing of 0.25 and 0.75 mg L^{-1} PAM increased floc settling rates for both FPD and Clarion 4100 when compared to no PAM additions.

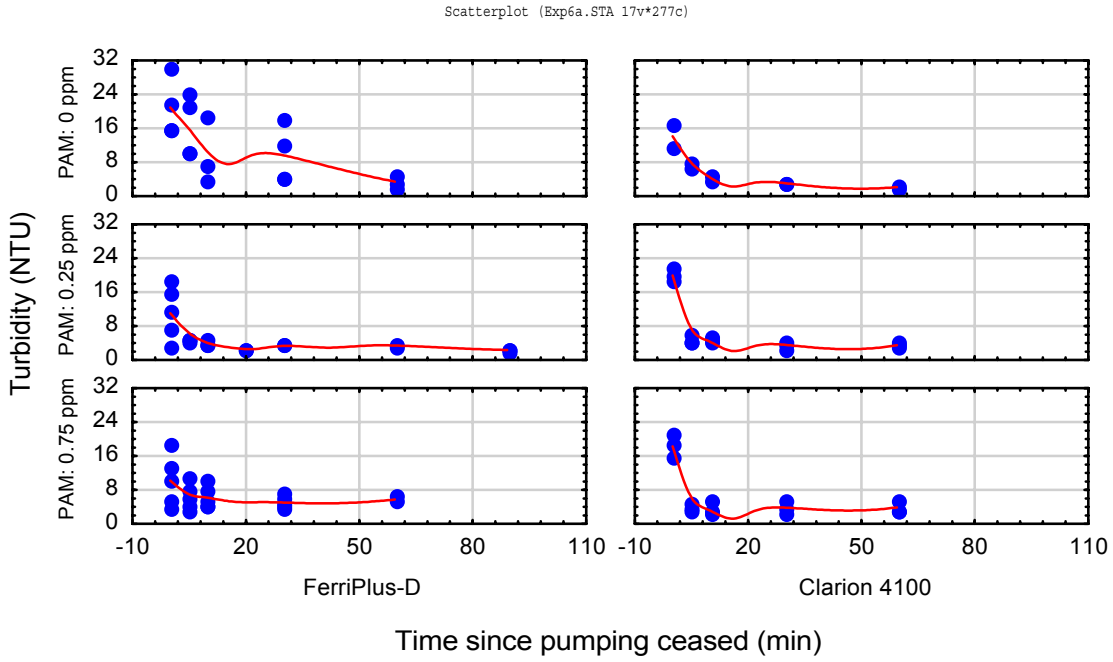

Figure 36. Turbidity values achieved for PAMs of different charge densities and molecular weights.
Jar test No. 5. Data represent water samples collected at 5, 10, 30 and 60 minutes.

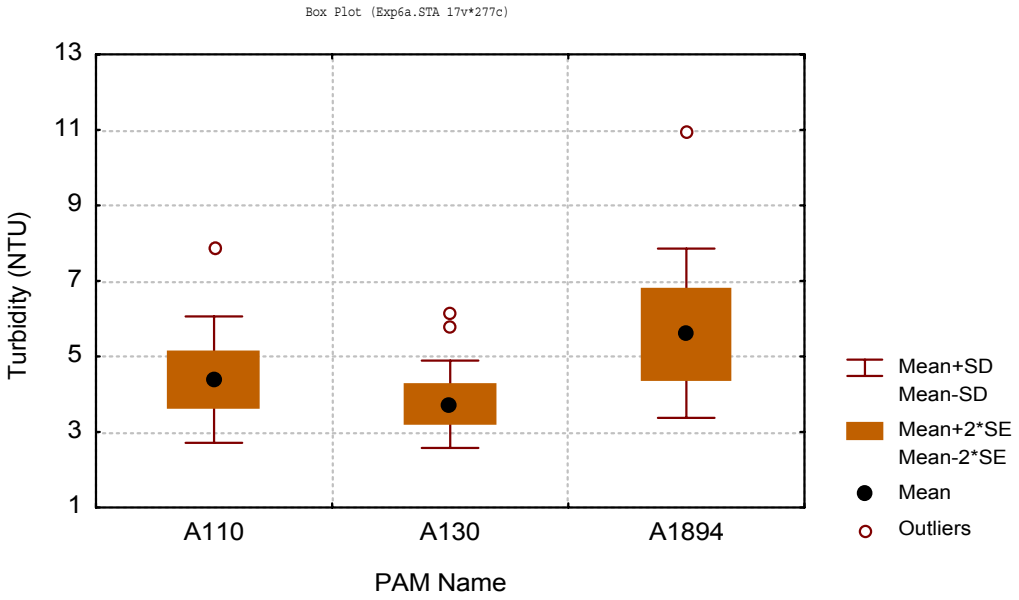

Figure 37. Turbidity values achieved for optimal metal blends, Jar Test No. 5.
Jar Test No. 5. FPD and Clarion 4100 were determined to be the most effective coagulants at metal dosing levels of 200 µM. Each metal/cationic polymer blend was followed by 0.25 mg L^{-1} dosing of PAM Superfloc A130. Data represents water samples taken at 5, 10, 30 and 60 minutes.

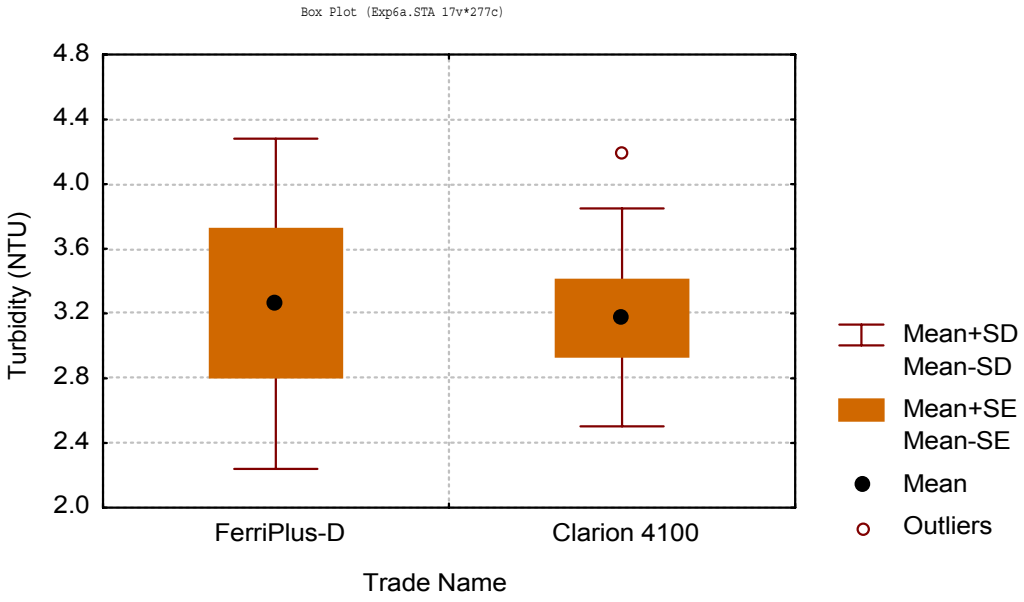

Figure 38. Floc settling as indicated by turbidity measurements for optimal metal/polymer blends, Jar Test No. 5.
Jar Test No. 5. FPD and Clarion 4100 were determined to be the most effective coagulants at metal dosing levels of 200 µM. Each metal/cationic polymer blend was followed by 0.25 mg L^{-1} dosing of PAM Superfloc A130. For FPD, floc settled immediately after mixing ceased (time 0). For Clarion 4100, floc settled within 5 minutes after mixing ceased.

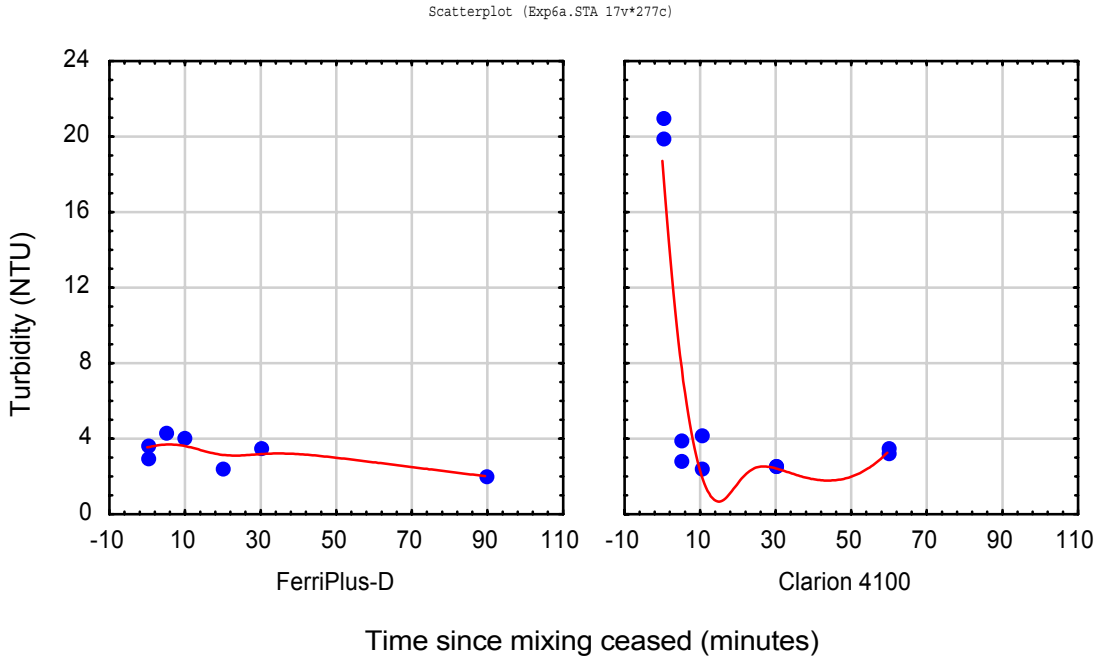

8.3. Conclusion

- Calcium either alone or in combination with iron and aluminum is ineffective at improving floc settling rates.
- PAMs dramatically improve floc aggregation and floc settling rates when used with ferric iron blends.
- PAMs slightly improved floc settling rates when used with aluminum blends.
- A130 was the best performing floc
- The optimum treatments tested here were Clarion 4100 and FPD at 200 µM followed by 0.25 mg L^{-1} SuperFloc A130.

Chapter 9. Jar Test No. 6, August 1999

Jar Test No. 6 was conducted to validate the turbidity tests used in Jar Test 5 with measurements of total and dissolved phosphorus. The goals for this study were:

- to reassess relationships between total phosphorus removal and turbidity,
- to assess each blend for its potential to decrease dissolved and total phosphorus, and
- to characterize water quality changes from dosing.

9.1. Methods

Ten different dosing treatments were selected:

- 100 μM Fe as FeCl,
- 200 μM Fe as FeCl,
- 200 μM Fe as FeCl + 25 mg L^{-1} Ca as CaOH,
- 100 μM Fe as FPD,
- 200 μM Fe as FPD,
- 100 μM Al as alum,
- 200 μM Al as alum,
- 200 μM Al + 25 mg L^{-1} Ca as CaOH, and
- 200 μM Al as Clarion 4100.

Each of these treatments included dosing with 0.25 mg L^{-1} Superfloc A130.

Dosing was conducted as follows:

1. Metal coagulant added.
2. 15 second rapid mix.
3. Superfloc A130 added.
4. 15 second rapid mix.
5. 5 minute slow mix.

Each treatment was replicated (N=3).

Samples were taken at 0 minutes, 10 minutes, 30 minutes and 24 hours after mixing ceased. Turbidity, dissolved phosphorus and total phosphorus were analyzed in all samples taken. On a subset, one sample was taken from each treatment (N=1) at 0 minutes and 24 hours and analyzed for dissolved organic carbon, dissolved aluminum and dissolved iron.

9.2. Results and Discussion

Jar Test No. 1 showed that turbidity is a reasonable indicator of total phosphorus concentrations when aluminum and iron are considered separately. Figure 39 confirms this assumption for the purpose of screening coagulants. Turbidity

predicted nearly 50% of the variance associated with total phosphorus for aluminum coagulants and two thirds the variance for iron coagulants.

Figure 39. Turbidity and total phosphorus relationships, Jar Test No. 6.
Jar Test No. 6. Turbidity predicted over 60% of the variance for ferric iron coagulants and 42% for aluminum coagulants. Turbidity measurements were considered a reasonable coagulant screening measurement.

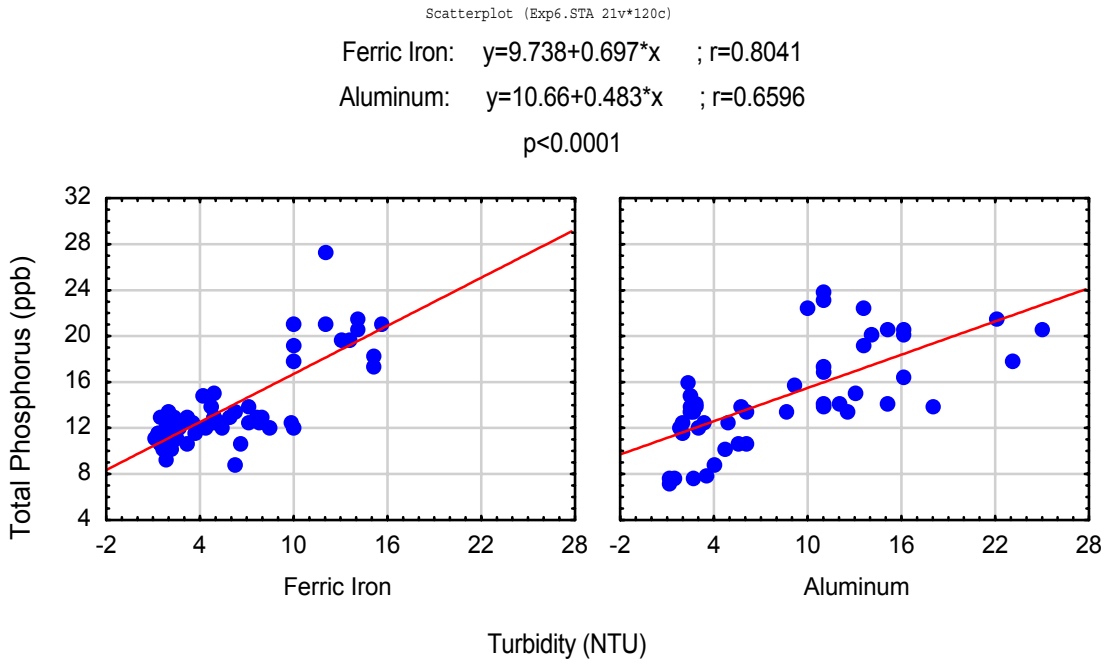

Both iron and aluminum reached steady state conditions for total phosphorus concentrations at 10 minutes. Figure 40a shows total phosphorus for the four metal treatments (e.g. FeCl, Ferriplus-D, Alum, Clarion 4100) dosed at a concentration of 200 μM. For all treatments, total phosphorus concentrations decrease very quickly over the first 10 minutes and then remained relatively unchanged thereafter for the next 24 hours. Iron Chloride at doses of 200 μM experienced the most rapid removal and this is shown by the large standard deviation associated with total phosphorus at time zero. Dissolved phosphorus concentrations for all treatments at time zero were greatly decreased below background levels of 16 μg L^{-1} (Figure 40b). Initial dissolved phosphorus concentrations were lower when cationic polymers were used (e.g. FPD, Clarion 4100). All treatments except for alum saw an increase in dissolved phosphorus over the 24 hour period though only under ferric chloride dosing was that

increase greater than 2 μg L^{-1}. This increase in dissolved phosphorus did not correspond to an increase in total phosphorus.

Ferric chloride, FPD and alum treatments were implemented at 100 and 200 μM. A 2-way ANOVA was conducted with total phosphorus concentrations as the dependent variable and dose and treatment as the independent variables. Total phosphorus concentrations differed significantly with both coagulant ($p<<0.0001$) and dose ($p=0.0059$). For individual coagulants treatments, total phosphorus concentrations were only slightly lower at higher dosing levels (Figure 41).

Total phosphorus concentrations achieved under ferric chloride and FPD dosing were nearly identical for both metal dosing levels (Figure 41). This suggested that when ferric iron chemical blends were used in combination with anionic polymers the presence of cationic polymers in the initial iron blend did not greatly affect total phosphorus removal. Total phosphorus concentrations for aluminum blends were very different showing that when aluminum was used, the presence of cationic polymers in the initial aluminum blend greatly improved total phosphorus removal. For iron blends at 200 μM, total phosphorus concentrations were decreased by 40% from 20 to 12 μg L^{-1}. For the Clarion 4100 treatment, total phosphorus concentrations were decreased by 55% to around 9 μg L^{-1}.

Dissolved phosphorus concentrations did not show great difference between the two different dosing concentrations of 100 and 200 μM (Figure 42). These data support Phase I findings (Bachand et al., 1999) and earlier jar test findings showing that even at low metal dosing concentrations, dissolved phosphorus has been effectively transformed to particulate phosphorus.

Calcium dosing at 25 mg L^{-1} was tested in combination with ferric iron and aluminum dosing at 200 μM. For aluminum treatments, calcium dosing (Alum + CaOH) hindered dissolved phosphorus removal and had no effect on total phosphorus removal (Figure 43). Alum blended with a cationic polymer provided superior total and dissolved phosphorus removal. For iron treatments, neither calcium or the cationic polymer improved dissolved phosphorus removal. However, both improved total phosphorus removal. Calcium at these doses had the greatest effect on total phosphorus with steady state phosphorus concentrations achieved immediately after mixing ceased.

Figure 40. Phosphorus changes over time for different metal/cationic polymer blends, Jar Test No. 6.

Both aluminum and iron blends were dosed at 200 µM followed by a PAM Superfloc A130 dose of 0.25 mg L^{-1}. Each treatment was replicated (N=3)

A. Total phosphorus

All treatments lowered total P after 10 minutes. Background total P concentrations were 20 µg L^{-1}.

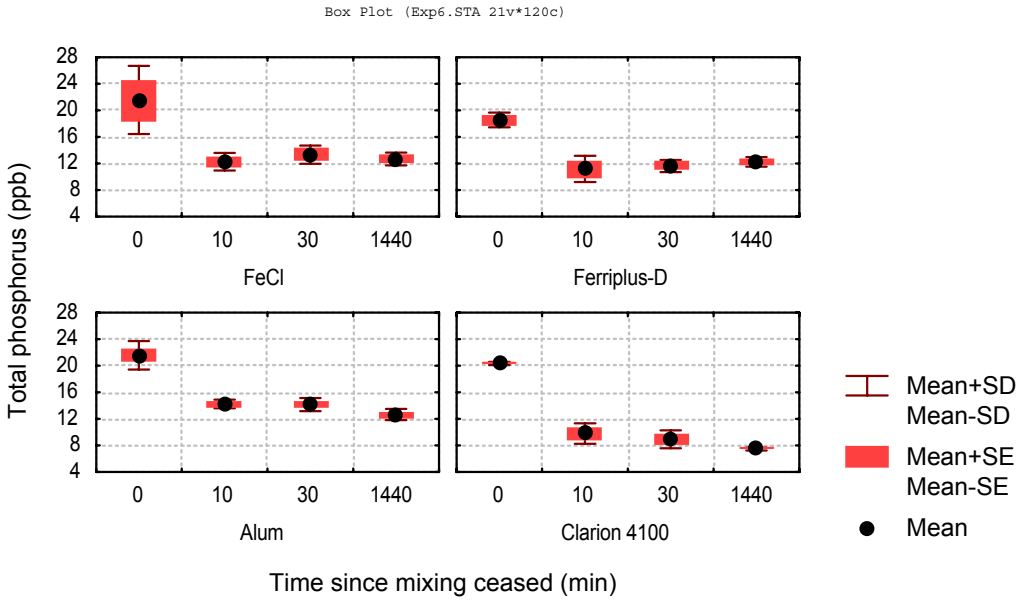

B. Dissolved phosphorus

Background concentrations of dissolved phosphorus for source water was 16 µg L^{-1}.

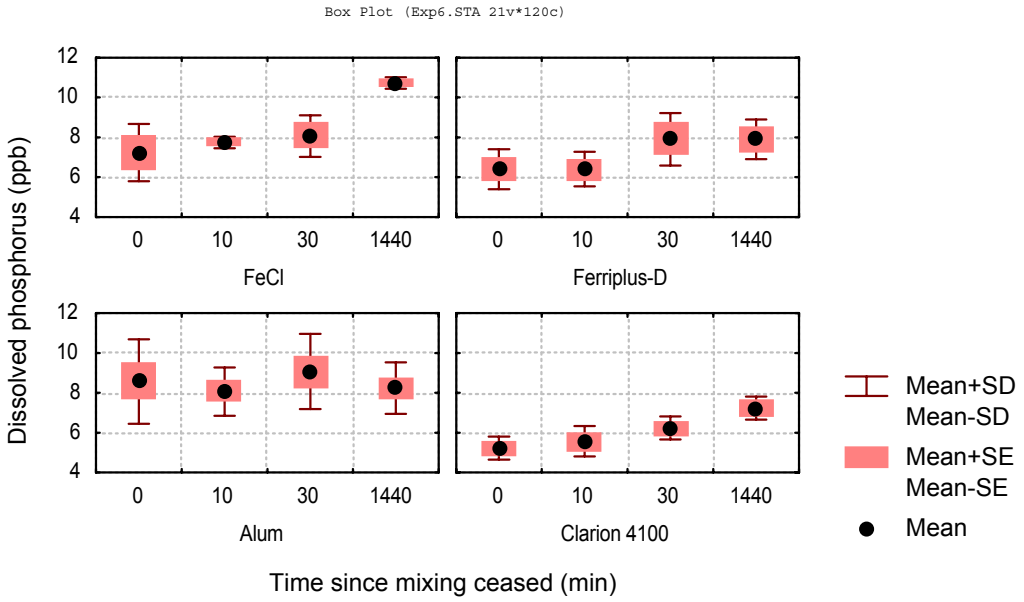

Figure 41. Total P concentrations achieved for different metal/cationic polymer/PAM blends at different dosing levels.
Jar Test No. 6. Data represent samples taken at 10 minutes, 30 minutes and 24 hours (N=3 for each treatment). Background concentrations of total phosphorus for source water was 20 µg L^{-1}.

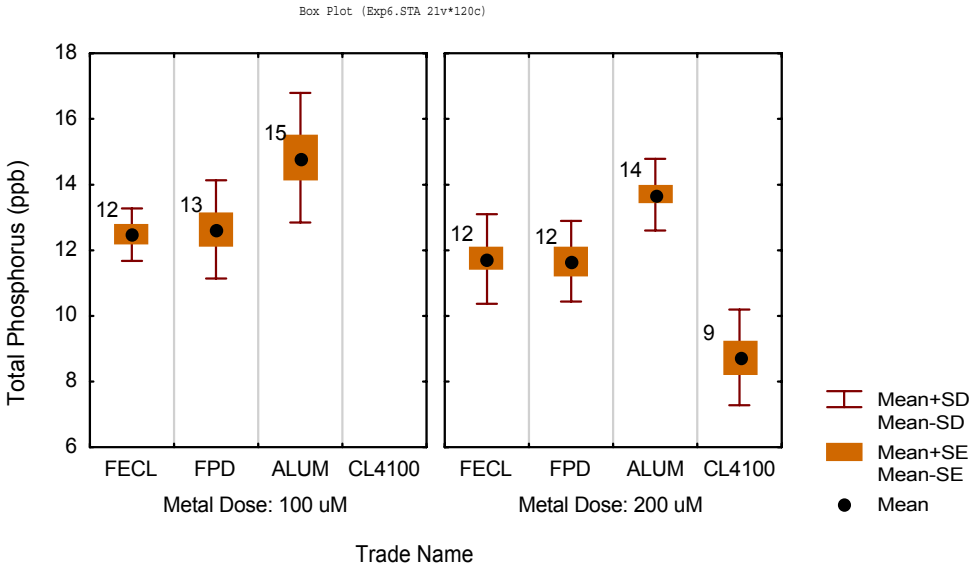

Figure 42. Dissolved P concentrations achieved for different metal/cationic polymer/PAM blends at different dosing levels.
Jar Test No. 6. Data represent samples taken at 10 minutes, 30 minutes and 24 hours (N=3 for each treatment). Background concentrations of total phosphorus for source water was 20 µg L^{-1}.

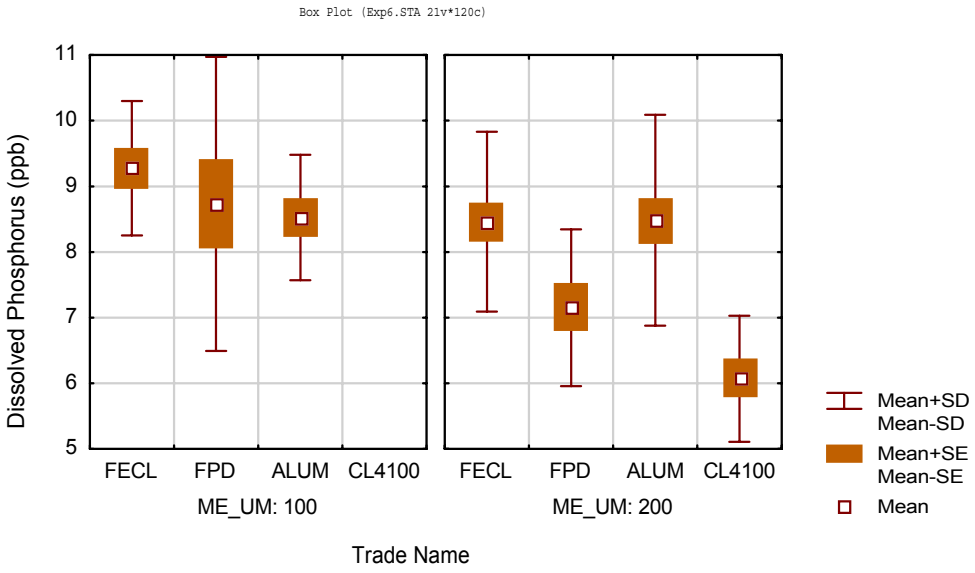

Figure 43. A comparison of the effects of Calcium vs. cationic polymers on total phosphorus precipitation.

All metals were dosed at 200 µM and all treatments replicated (N=3). Calcium was dosed at 25 mg L^{-1}. All treatments were followed by PAM dosing at 0.25 mg L^{-1}.

A. Dissolved phosphorus

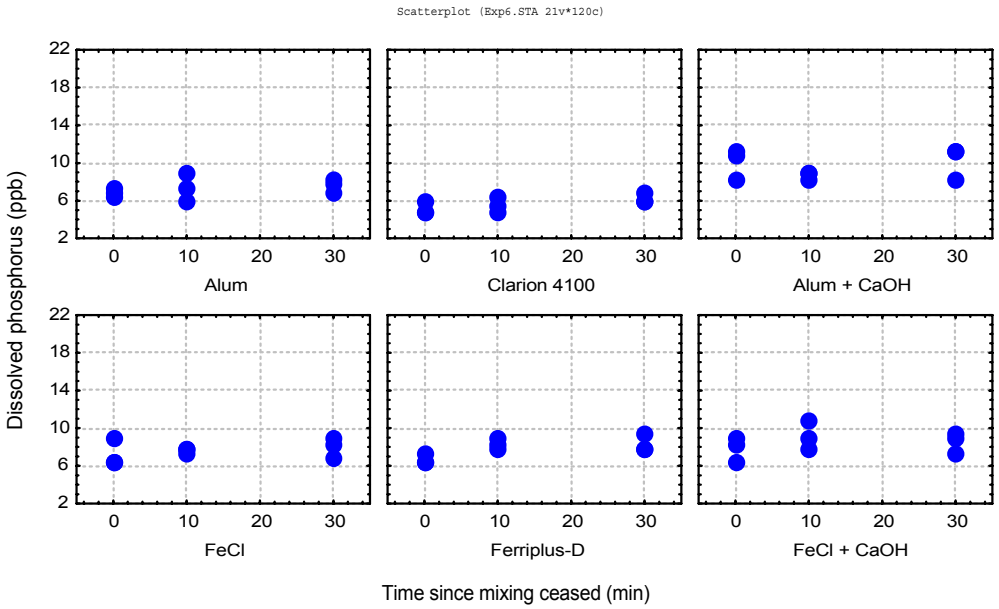

B. Total Phosphorus

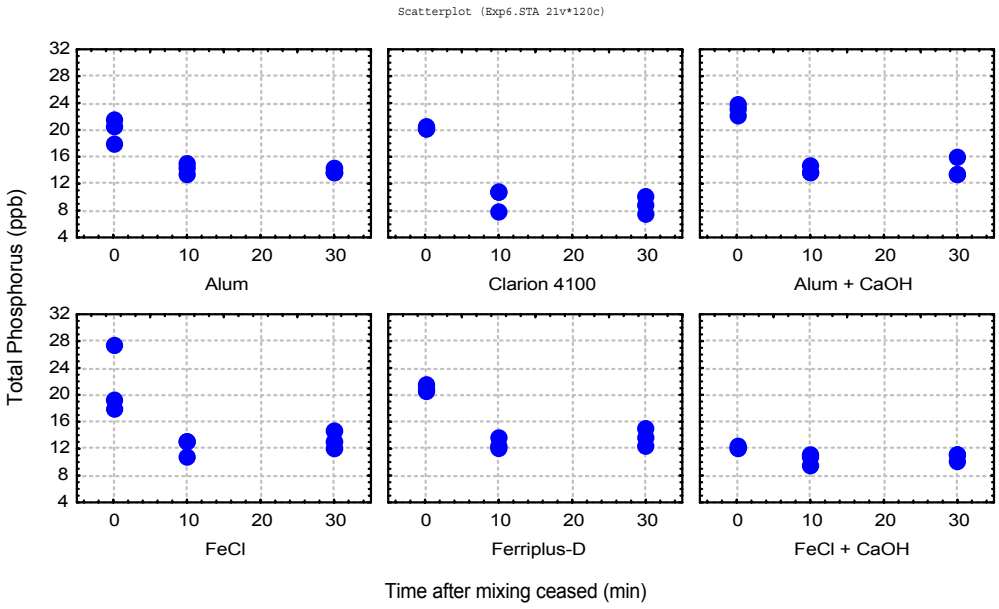

The different dosing treatments affected other water quality characteristics. Organic carbon was significantly reduced in all treatments ($p<0$) and was lowered to mean concentrations as low as 33 $\mu g\ L^{-1}$ for the Clarion 4100 treatments (Figure 44). Both metal blends increased metal concentrations above background levels though that effect was less pronounced with iron as compared to aluminum (Figure 45).

9.3. Conclusion

- Turbidity is a reasonable predictor of total phosphorus concentrations during screening runs though results need to be verified with direct measurements
- Total phosphorus removal is more rapid at higher metal doses
- For background total phosphorus concentrations of 20 $\mu g\ L^{-1}$, ferric iron decreased total phosphorus concentrations 40% to 12 $\mu g\ L^{-1}$ and Clarion 4100 decreased total phosphorus concentrations 55% to 9 $\mu g\ L^{-1}$.
- Cationic polymers led to greater initial precipitation of dissolved phosphorus though some of the phosphorus re-dissolved into the water column. This did not lead to an increase in total phosphorus in the water column.
- Total phosphorus was removed from the water column within 10 minutes after mixing
- Calcium addition at 25 mg L^{-1} improved total phosphorus removal by iron but not by aluminum. All chemical blends led to decreases in dissolved organic carbon
- Chemical dosing led to slight increases in iron or aluminum concentrations in the water column, depending upon the metal used during dosing.

Figure 44. Dissolved organic carbon concentrations achieved for different metal/cationic polymer/PAM blends.
Jar Test No. 6. Data represent mean values of samples taken at 0 minutes and 24 hours (N=1). Includes data from dosing levels of 100 and 200 µM.

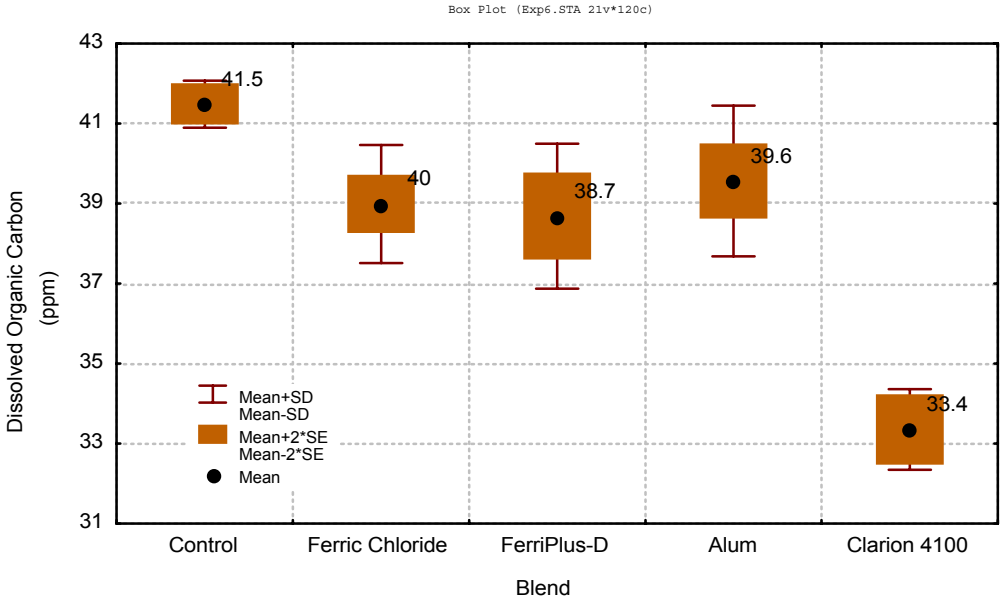

Figure 45. Dissolved iron and aluminum concentrations after dosing of different metal/cationic polymer/PAM blends.
Jar Test No. 6. Data represent mean values of samples taken at 0 minutes and 24 hours (N=1). Includes data from dosing levels of 100 and 200 µM. Same control was used for both iron and aluminum treatments.

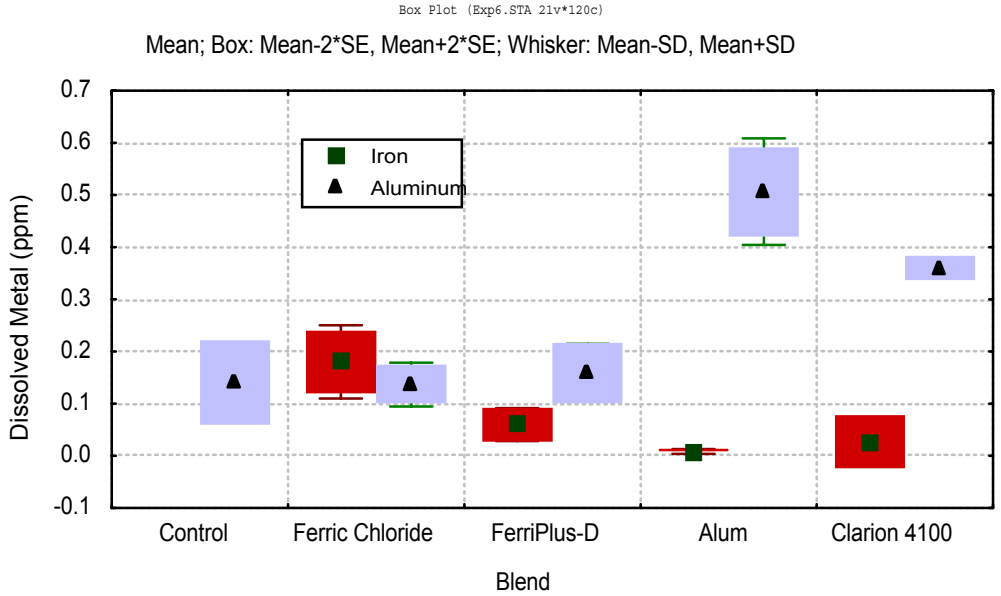

Chapter 10. Jar Test No. 7, August 1999

Jar Test No. 7 was conducted to determine if low calcium concentrations would aid with floc settling (Table 3). Higher concentrations had proved ineffective in earlier jar test studies. Lower concentrations were considered on the theory that the added slurry may provide "seeds" for the formation of floc.

10.1. Methods

Calcium was dosed at 0, 2.5, 5 and 10 mg L^{-1} in combination with ferric iron dosing at 100 and 200 μM. Turbidity was measured at 0, 10 and 30 minutes (Table 4). PAM was not used in these studies.

10.2. Results and Discussion

Figure 46 shows that calcium additions increased turbidity at time zero. Baseline turbidity values were achieved for all treatments at about 10 minutes after mixing ceased.

10.3. Conclusion

- Calcium will not aid with floc settling.

Figure 46. Negligible effects from dosing with low calcium concentration of turbidity achieved under ferric chloride and FPD treatments..

Jar Test No. 7. All metal dosing followed by PAM dosing at 0.25 mg L^{-1}.

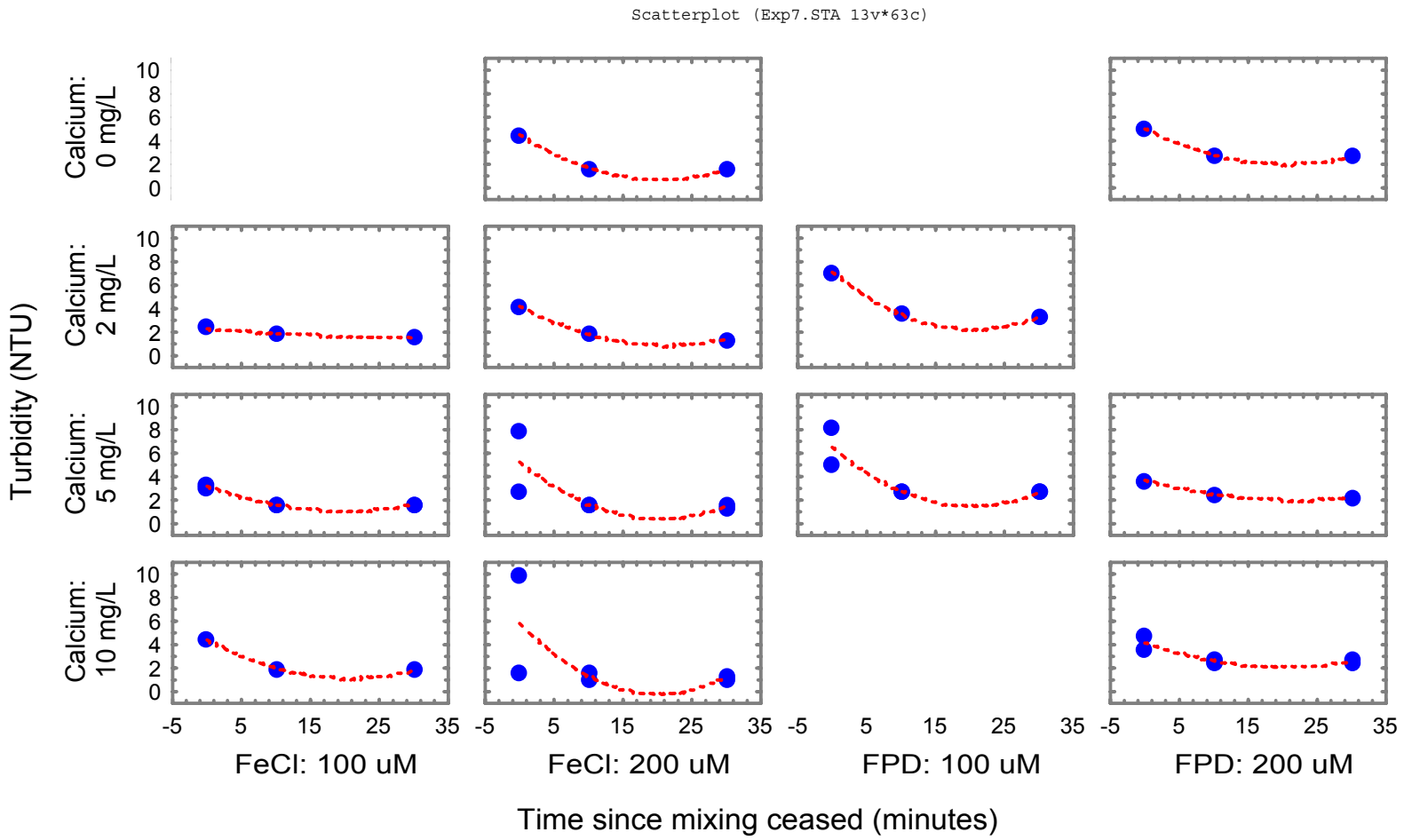

Chapter 11. Jar Test No. 8, August 1999

Jar Test No. 8 was conducted to verify calcium would not improve phosphorus removal (Table 3).

11.1. Methods

Water was dosed with 200 µM ferric iron in the form of ferric chloride followed by calcium dosing of 0, 2.5, 5 and 10 mg L^{-1}. Chemical blends were than followed by the addition of 0.25 mg SuperFloc A130. Water samples were taken at 0, 10, 30 and 1440 minutes and analyzed for total phosphorus (Table 4).

11.2. Results and Discussion

Calcium did not improve total phosphorus removal rates. Calcium dosing generally increased the variance in total phosphorus concentrations at time 0 (Figure 47).

11.3. Conclusion

- Low level calcium additions (<25 mg L^{-1}) used in combination with metal/polymer blends will not improve phosphorus removal.

Figure 47. Negligible effects of dosing with low calcium concentrations on total phosphorus concentrations achieved in ferric iron treatments.
Jar Test No. 8. 200 µM ferric iron was applied with ferric chloride followed by PAM dosing of 0.25 mg L^{-1}.

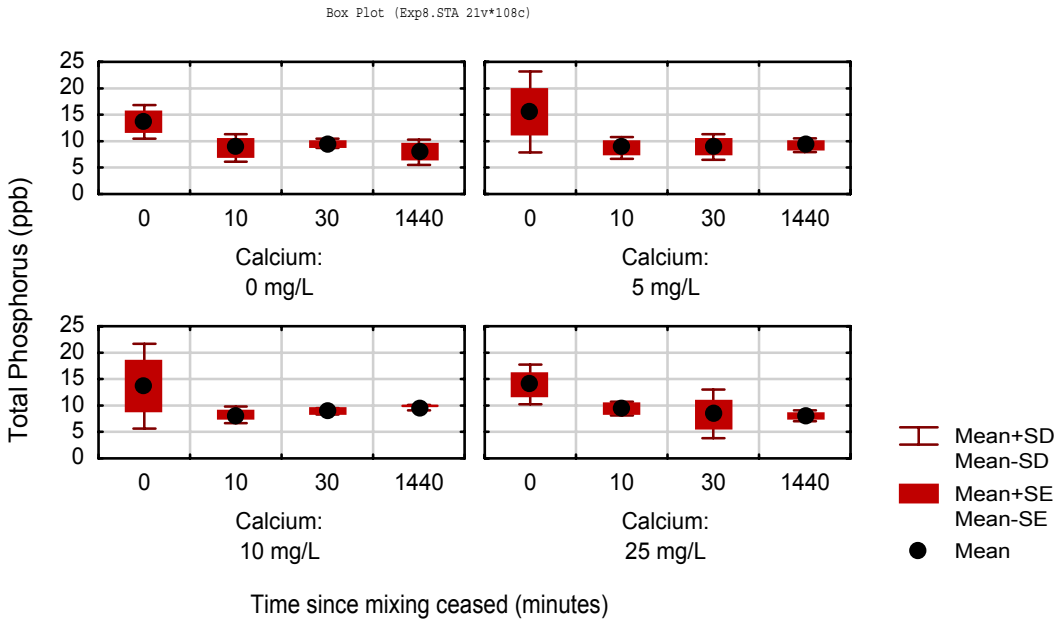

Chapter 12. Summary of Jar Test Results

In this study, a series of eight jar tests were conducted following the principles of process development and adaptive management. The goals of the jar tests were to investigate several different variables. These included:

- different chemical blends
- different chemical dosing levels,
- cationic polymers,
- different PAMs,
- PAM dosing levels,
- dosing with both ferric iron and aluminum,
- calcium dosing amendments, and
- different mixing regimes.

In some cases turbidity was used as an indicator during early stages of assessments. Total and dissolved phosphorus concentrations were determined for more promising treatments and methods.

Jar tests initially indicated that slow and rapid mixing improved phosphorus removal and the field sites were modified for the June 1999 study for that purpose.

More recently, jar test findings suggested that both anionic and cationic polymers would improve the dissolved and total phosphorus removal from the water column during LICD. Cationic polymer blends generally outperformed pure metal coagulants. Ferric iron with 20% cationic polymers was the most promising iron blend and alum with 10% polymer was the most promising aluminum blend. Metal/cationic polymer blends generally resulted in lower turbidity, lower dissolved phosphorus and lower total phosphorus concentrations.

Anionic polyacrylamides (PAMs) were investigated to determine if they would aid with floc aggregation and phosphorus removal. When metal/cationic polymer blends were followed by PAMs, floc aggregation and settling rates improved for both aluminum and iron treatments. This was very dramatic for iron blends and only slightly so for aluminum blends. For ferric iron blends, PAMs may have minimized the need to use the cationic polymers. Thus, ferric iron blends were most improved by the addition of PAMs and only slightly so by the use of cationic polymers. Aluminum blends were most improved by the use of cationic polymers and only slightly so by the use of PAMs. Several different PAMs were tested and SuperFloc A130 was found to be the most effective.

Adding calcium into the dosing regime at low and high concentrations was tested. High calcium concentrations dramatically increased turbidity and thus did not aid with floc aggregation or settling. Low calcium concentrations (< 25 mg L^{-1}) did not hinder or improve total or dissolved phosphorus removal. Thus, calcium was eliminated from consideration.

In jar tests, using metal/cationic polymer /anionic polymer combinations led to total phosphorus concentrations near or under 10 μg L^{-1} for both ferric iron and aluminum for metal dosing concentrations of 200 μM. The optimum treatments tested in this field study were Clarion 4100 (Alum + 10% anionic polymer) and FPD (Ferric sulfate + 20% polymer) at 200 μM followed by 0.25 mg L^{-1} SuperFloc A130.

Chapter 13. Batch Flow Mesocosm Study, October 1999

The October 1999 Batch Flow Study was conducted after the completion of all jar tests. The general goal of the study was to field verify jar test findings. The strategy for this Batch study was to investigate some of these treatments using Sites A, B and C. The specific goals for this study were to:

- Assess site effects on phosphorus levels
- Determine if mesocosms varied between and within sites with regard to phosphorus removal rates
- Determine stability of total and dissolved phosphorus concentrations over time during this run
- Assess effects of cationic polymers on phosphorus levels and water quality
- Assess anionic polyacrylamide effects on phosphorus levels and water quality
- Determine optimum chemical blend
- Estimate phosphorus levels that can be achieved.

13.1. Methods

The selected metal polymer blends chosen based upon the jar test screening were:

- 200 μM ferric iron as ferric chloride + 0.25 mg SuperFloc A130 (N=2),
- 100 μM ferric iron as FPD + 0.25 mg SuperFloc A130 (N=2),
- 200 μM ferric iron as FPD + 0.25 mg SuperFloc A130 (N=2),
- 200 μM aluminum as alum + 0.25 mg L^{-1} SuperFloc A130 (N=1),
- 100 μM aluminum as Clarion 4100 + 0.25 mg L^{-1} SuperFloc A130 (N=1), and
- 200 μM aluminum as Clarion 4100 + 0.25 mg L^{-1} SuperFloc A130 (N=1).

Additionally, both alum and ferric chloride without polymers were tested during this study. 200 μM aluminum as alum and 200 μM ferric iron as ferric chloride were replicated across all three sites. This was designed to provide information on site effects and benchmark removal information to compare the metal/polymer blends. At each site, 2 mesocosms remained non-dosed. These were to provide information on mesocosm effects on and biotic uptake of phosphorus. Finally, at each site, an UnWalled Control was operated and sampled to provide background marsh data. The Experimental Design for this study is shown in Table 13.

Table 13. Experimental Design form October 1999 Mesocosm Batch Flow Study

Mesocosm	Site A	Site B	Site C
1 Treatment	**Alum 200**	**FeCl 200**	**NonDosed**
Metal	Al	Fe	WC
Metal Dose	200	200	0
PAM			
Cat. Poly			
2 Treatment	**NonDosed**	**Alum 200**	**FeCl 200**
Metal	WC	Al	Fe
Metal Dose	0	200	200
PAM			
Cat. Poly			
3 Treatment	**FeCl 200**	**FPD 100 + PAM**	**Alum 200**
Metal	Fe	Fe	AL
Metal Dose	200	100	200
PAM		X	
Cat. Poly		X	
4 Treatment	**FeCl 200 + PAM**	**Walled Control**	**FPD 200 + PAM**
Metal	FE	WC	FE
Metal Dose	200	0	200
PAM	X		X
Cat. Poly			X
5 Treatment	**NonDosed**	**Clarion 200 + PAM**	**NonDosed**
Metal	WC	Al	WC
Metal Dose	0	200	0
PAM		X	
Cat. Poly		X	
6 Treatment	**FeCl 200 + PAM**	**NonDosed**	**Clarion 100 + PAM**
Metal	Fe	WC	Al
Metal Dose	200	0	100
PAM	X		X
Cat. Poly			X
7 Treatment	**Alum 200 + PAM**	**FPD 100 + PAM**	**FPD 200 + PAM**
Metal	Al	Fe	Fe
Metal Dose	200	100	200
PAM	X	X	X
Cat. Poly		X	X
8 Treatment	**UnWall Control**	**UnWall Control**	**UnWall Control**

As in the earlier June mesocosm study, mesocosms were initially dosed with three volumes of water and then during the following weeks water was sampled at multiple locations several times per week. A schedule summary with actions taken and parameters sampled is shown in Table 14. Because this study was replicated across all three sites, manpower and resource limitations required staggering the schedules. All tasks at Site C were done one day after the same task had been completed at Sites A and B.

This study focused only on process variables considered critical for assessing this technology. These variables were total phosphorus, dissolved phosphorus, total and dissolved aluminum and iron, bromide and dissolved organic carbon. Sampling locations are shown in Figure 9.

Table 14. Schedule for October 1999 Mesocosm Study

Site A		Site B		Site C				
Date	Day	Date	Day	Date	Day	Action	Sampling Locations	Parameters Sampled.
9/29.	Wed	9/29.	Wed	9/30	Thurs	Background Sampling	Mesocosms	FTP, UTP, DOC
9/30	Thurs	9/30	Thurs	10/1	Fri	Sample and deploy chemical stock solutions (Site C)	Carboys	UTP, UFE, FFe, UAl, FAl
10/1	Fri	10/1	Fri	10/2	Sat	Sample and deploy chemical stock solutions (Sites A and B)	Carboys	UTP, UFE, FFe, UAl, FAl
10/2	Sat	10/2	Sat	10/3	Sun			
10/3	Sun	10/3	Sun	10/4	Mon	Pumping and dosing begins		
10/4	Mon	10/4	Mon	10/5	Tues	Pumping and dosing ends Sampling	Mesocosm, Piping	FTP, UTP, UFE, FFe, UAL, FAl, DOC, FBr
10/5	Tues	10/5	Tues	10/6	Wed	Sampling	Mesocosms	FTP, UTP, UFE, FFe, UAL, FAl, DOC, FBr
10/6	Wed	10/6	Wed	10/7	Thurs	Sampling	Mesocosms	FTP, UTP, FBr
10/7	Thurs	10/7	Thurs	10/8	Fri	Sampling Sample and recover Site C chemical stock solutions	Mesocosms Carboys	UTP, UFE, FFe, UAl, FAl
10/8	Fri	10/8	Fri	10/9	Sat	Sample and recover Sites A and B chemicals stock solutions	Carboys	UTP, UFE, FFe, UAl, FAl
10/9	Sat	10/9	Sat	10/10	Sun			
10/10	Sun	10/10	Sun	10/11	Mon			
10/11	Mon	10/11	Mon	10/12	Tues	Sample	Mesocosms	FTP, UTP, FBr
10/12	Tues	10/12	Tues	10/13	Wed			
10/13	Wed	10/13	Wed	10/14	Thurs			
10/14	Thurs	10/14	Thurs	10/15	Fri	Sample	Mesocosms	FTP, UTP, UFE, FFe, UAL, FAl, DOC, FBr

13.2. Results and Discussion

13.2.1. Site effects

The first step in the analyses was to consider site differences with respect to background water conditions and water treatment of phosphorus. Background waters were compared between sites by considering the UnWalled Control Treatments. Total and dissolved phosphorus concentrations and dissolved organic carbon concentrations were compared between sites. In an ANOVA comparison where the site was the independent variable, dissolved phosphorus ($p<0.0001$) and total phosphorus ($p=0.0010$) differed significantly between sites. Post-hoc analyses showed that dissolved phosphorus at Site B differed significantly with that at Sites A and C, and that total phosphorus at Site A differed significantly with that at Sites B and C (Figure 48). Dissolved organic carbon concentrations were similar between sites. Thus, background marsh water dissolved and total phosphorus concentrations differed between sites.

Figure 48. Background water quality variations at the three mesocosm sites, October 1999 Batch Flow Study.
Data represents water samples collected at UnWalled Control.

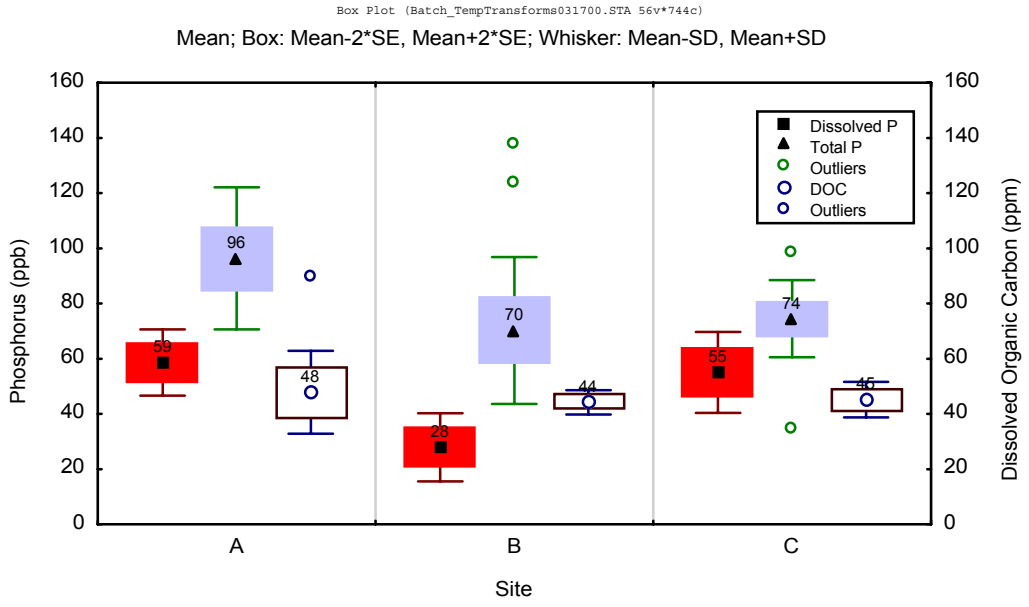

Water treatment in terms of total and dissolved phosphorus removal was also assessed. Three chemical treatments were replicated between sites:

- 200 μM ferric iron dosing as ferric chloride,
- 200 μM aluminum dosing as alum, and
- Non-dosing.

For each of these three treatments, total phosphorus, total phosphorus removed, dissolved phosphorus, and dissolved phosphorus removed were considered. Total phosphorus removed was defined as the phosphorus difference between that entering each mesocosm during pumping and the long-term average concentration of total phosphorus in the mesocosms during the batch study. Dissolved phosphorus removed was defined as the dissolved phosphorus concentrations measured at the pumps minus the long-term average concentration of dissolved phosphorus in the mesocosms during the batch study.

Table 15 shows the statistical analyses of site effects and differences in performance between the sites. For each of the three treatments, dissolved phosphorus concentrations did not differ statistically between sites ($p>0.05$) though dissolved phosphorus removal did. This result infers that for each treatment, there is a dissolved phosphorus concentration that can be achieved independent of initial dissolved phosphorus concentrations. For ferric chloride that concentration is approximately 15 $\mu g\ L^{-1}$ and for alum that concentration is 10 $\mu g\ L^{-1}$. That compares to17 $\mu g\ L^{-1}$ in the Non-Dosed mesocosms in which dissolved phosphorus removal is only by biotic uptake.

Total phosphorus concentrations did not differ statistically between sites for ferric chloride nor for the Non-Dosed treatments. Under ferric chloride dosing, total phosphorus concentrations of 63 $\mu g\ L^{-1}$ were achieved which were higher than the concentrations of 54 $\mu g\ L^{-1}$ which were measured in the Non-Dosed mesocosms. These data infers that at each site, similar steady state total phosphorus concentrations will be achieved when no chemical dosing is implemented. For iron, dosing led to higher total phosphorus levels. This is apparently due to an accumulation in the water column of buoyant floc-bound particulate phosphorus during the initial pumping event. Total phosphorus concentrations did differ significantly for alum though total phosphorus removal rates did not.

These analyses present several findings

- Dissolved phosphorus concentrations between sites after dosing should be similar and this appears to be due to a lower limit that can be achieved for dissolved phosphorus under dosing of individual coagulants.
- Total phosphorus concentrations between sites did not statistically differ for the Non-Dosed treatments suggesting that for this study a steady state level in the range of 50 – 55 $\mu g\ L^{-1}$ would be expected. This relationship held for ferric iron dosing but not for aluminum dosing.

13.2.2. Mesocosm effects

Differences in mesocosm total and dissolved phosphorus concentrations within sites were also considered. For these analyses, the Non-Dosed mesocosm treatment was considered as that treatment was replicated at each site. Figure 49 shows total and dissolved phosphorus concentrations for each Non-Dosed treatment at the different sites. Significant difference can be approximated by considering if the means differ by two standard errors. Total phosphorus differed significantly within sites for Sites A and C though not for Site B. Dissolved phosphorus did not differ significantly within sites.

Figure 49. Total and dissolved phosphorus concentration variations in the Non-dosed mesocosms, Sites A, B and C.

Data represents water samples collected at Non-dosed treatments. Total P concentrations above 150 µg L^{-1} were considered outliers and not included in the analyses.

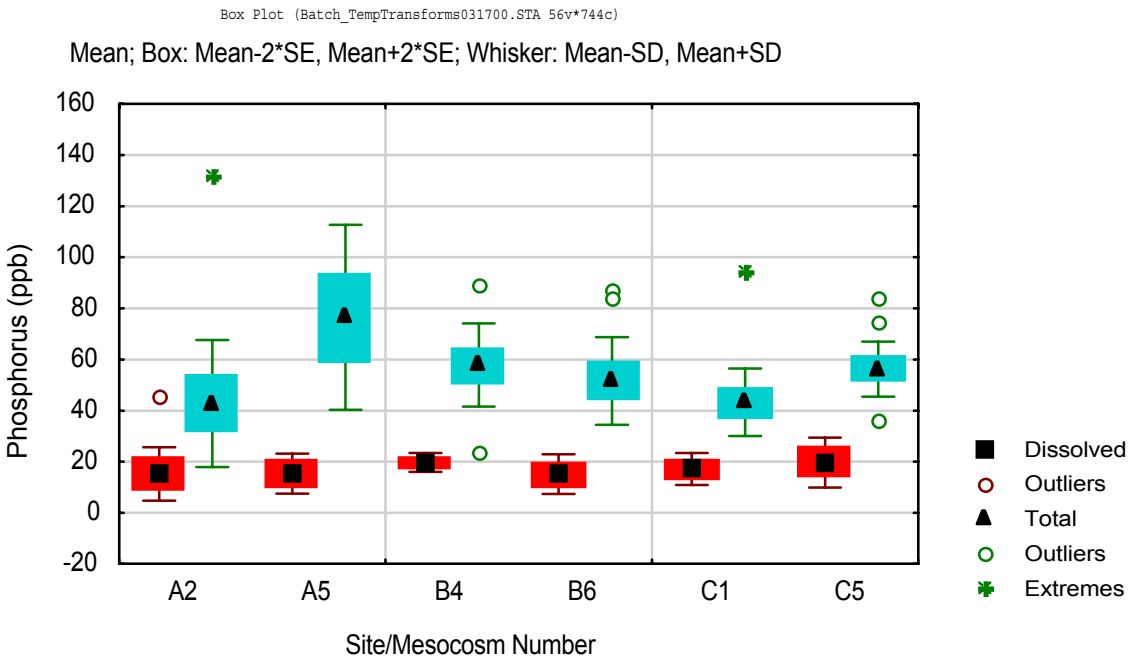

Thus, when considering comparing the performance of different treatments, considering final dissolved phosphorus concentrations is valid. Considering total phosphorus concentrations is more problematic. Achievable total phosphorus concentrations may vary between sites depending upon the chemical treatment and may also vary statistically within sites. Thus, to assess the effectiveness of different treatments for removing total phosphorus will require consideration of the strength of the trends and not just a simple statistical analyses.

13.2.3. Hydrology

A second step in conducting these analyses was considering the hydrologic pressures that might affect total and dissolved phosphorus as occurred during the June mesocosm study. Figure 50 shows that during this run, water levels were relatively stable increasing by an average of only about two centimeters during the two week period though some daily variation greater than that was experienced. This was reflected by relatively stable bromide concentrations with some slight dilution leading to a slight decline in bromide concentrations over the study period (Figure 51). Note that mesocosm 3 experienced clogging during this run and was excluded from the analyses. This mesocosm received aluminum dosing at 200 μM without any polymers. The relatively stable water levels suggests that hydrology was not expected to affect phosphorus concentrations greatly.

Figure 50. Water elevations measured at Site A during October 1999 Batch Flow Study.

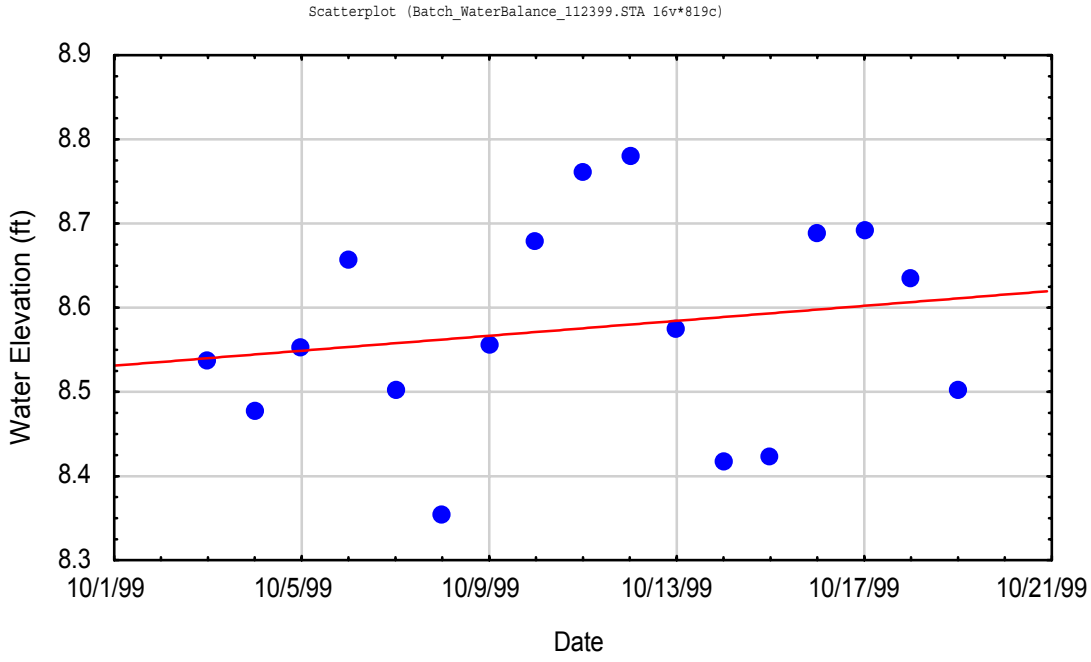

Figure 51. Bromide concentrations at each mesocosm during October 1999 Batch Flow Study.
Samples taken per schedule shown in Table 9 and at locations shown in Figure 9. Mesocosm 3 at Site C experienced clogging and was excluded from the analyses.

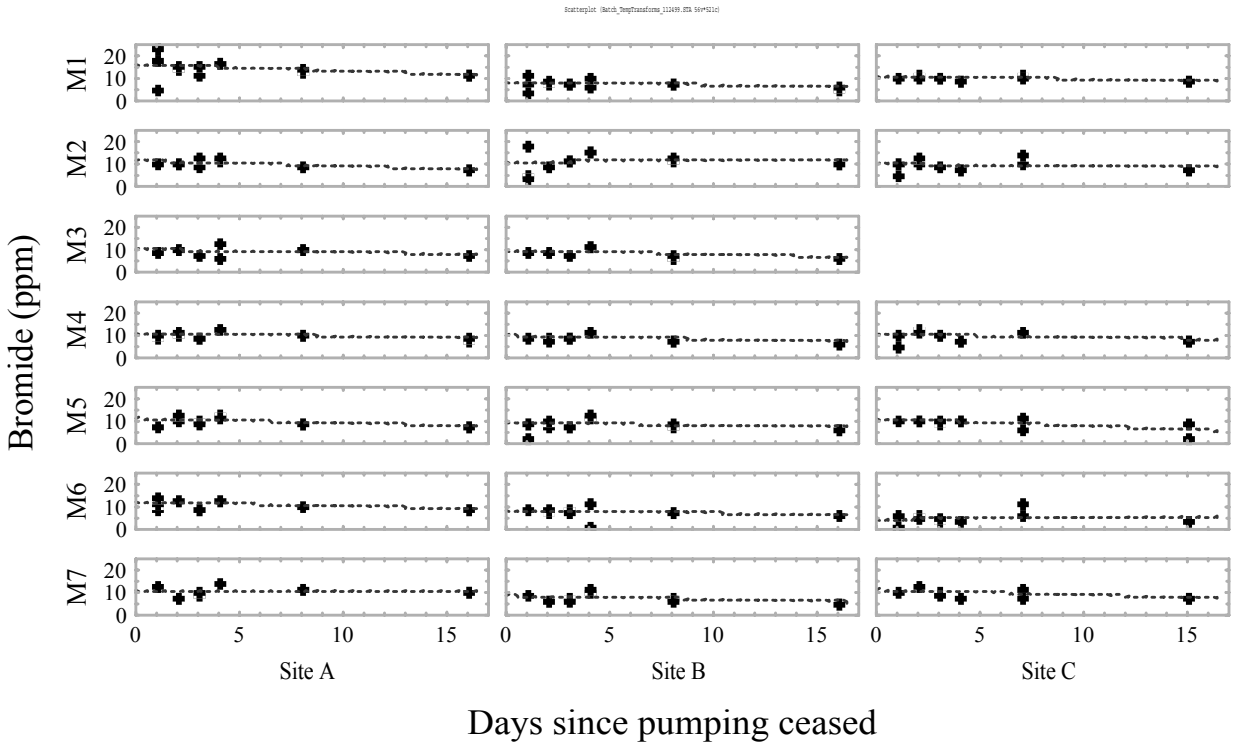

13.2.4. Experimental Design

The experimental design in this study allowed multiple analyses

- PAMs effects on phosphorus removal
- Cationic polymers effects on phosphorus removal
- Differences in metal doses for iron/polymer blends

These analyses were completed for both iron and aluminum.

13.2.5. Analyses of iron and polymer dosing combinations

For iron treatments, comparisons were made between the 200 µM ferric chloride treatment and the 200 µM ferric chloride treatment plus PAM. Final concentrations of total and dissolved phosphorus were compared between the different mesocosms and treatments (Figure 52). Dissolved phosphorus concentrations achieved with PAMs were 11 µg L^{-1} as opposed to 14 µg L^{-1} when PAMs were not used though these concentrations did not differ significantly (p=0.1690). Total phosphorus concentrations achieved when using PAMs were 68 µg L^{-1}, higher than those achieved without PAMs where concentrations were 63 µg L^{-1}. These concentrations also did not differ significantly (p=0.1885).

Figure 52. *In situ* PAM application effects (0.25 mg L^{-1}) on total and dissolved P concentrations achieved within mesocosms using ferric chloride dosing.
Samples were collected using the sampling schedule shown in Table 14 after pumping ceased and at the mesocosm locations shown in Figure 9. Data are from Sites A, B and C. Ferric iron was dosed at 200 µM. Total phosphorus concentrations greater than 150 µg L^{-1} were considered outliers and not included in the analyses.

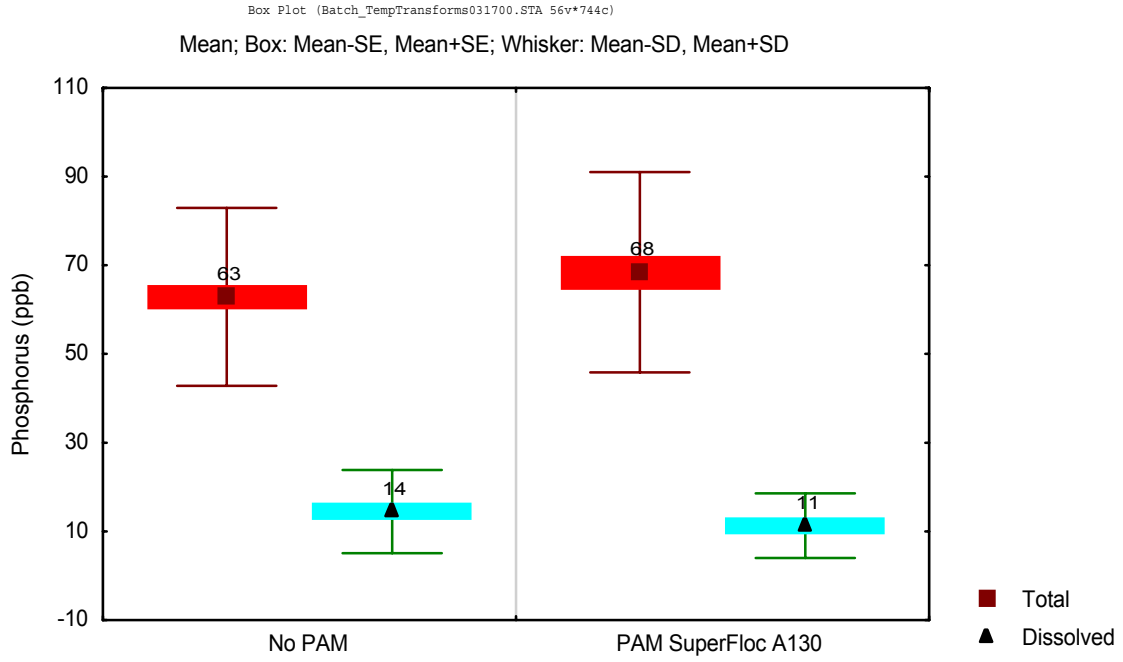

The removal of total and dissolved phosphorus was also considered for ferric chloride dosing with and without PAMs. Both treatments increased total phosphorus concentrations slightly and the concentrations did not differ significantly (p=0.5276; Figure 53). However, the PAM treatment removed much more dissolved phosphorus than the treatment without PAM and these resulting concentrations differed significantly (p=0.00713). The addition of PAM to ferric chloride dosing did not improve total phosphorus removal. There may have been some improvement in dissolved phosphorus removal as more dissolved phosphorus was removed in the PAM treatments. However, earlier site analyses suggests that this improvement was more likely due to the higher inflow concentrations in the treatments receiving PAMs than the use of PAMs themselves.

Figure 53. Improvements in total phosphorus removed in ferric chloride treatments by applying PAM *in situ* at 0.25 mg L^{-1}.
Samples were collected using the sampling schedule shown in Table 14 after the cessation of pumping and at the mesocosm locations shown in Figure 9. Data are from Sites A, B and C. Ferric iron was dosed at 200 µM. Total phosphorus concentrations greater than 150 µg L^{-1} were considered outliers and not included in the analyses. Total phosphorus removal is across the mesocosm. Dissolved phosphorus removal is across the entire system.

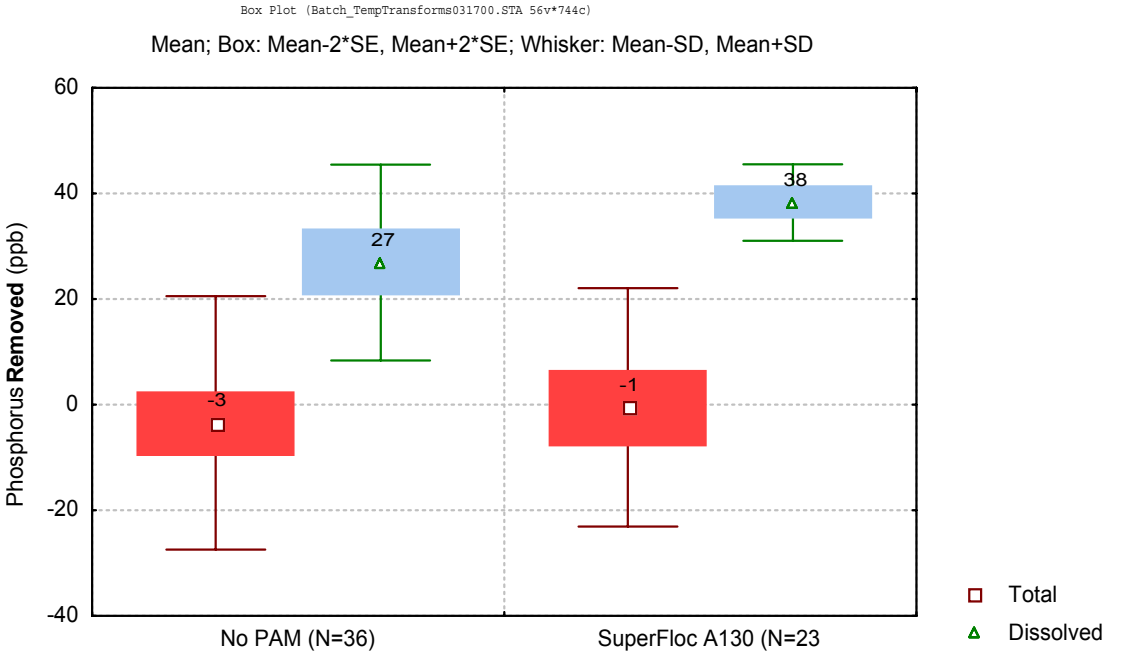

The use of cationic polymers was assessed by comparing the 200 μM ferric chloride dosing plus PAMs at Site A with the 200 μM FPD dosing plus PAMs at Site C (Table 16). Dissolved phosphorus inflow concentrations (at pump) to both treatments were similar at 50 – 51 μg L^{-1}. Total phosphorus inflow concentrations of 78 μg L^{-1} (at pipe) at Site C were approximately 10 μg L^{-1} higher than the inflow concentrations of 68 μg L^{-1} at Site A. When comparing the two treatments, total phosphorus, total phosphorus removed and dissolved phosphorus removed differed significantly between the two treatments (Table 16). Both treatments were effective at decreasing dissolved phosphorus though the FPD treatment decreased dissolved phosphorus over 85% from a mean of 50.9 μg L^{-1} to a mean of 8.6 μg L^{-1} (Table 16, Figure 54). FPD treatments much more effectively decreased total phosphorus concentrations than the ferric chloride treatment. Ferric chloride typically provided poor removal of total phosphorus because of poor settling characteristics (Bachand et al. 1999). This was apparent in this mesocosm study as well. However, where the ferric chloride treatment led to a slight increase in total phosphorus above inflow levels, the FPD treatment decreased concentrations by 30% (Figure 55, Table 16). For an inflow concentration of 78.4 μg L^{-1}, mean mesocosm concentrations of 55 μg L^{-1} were achieved. This performance was better than results from the June mesocosm study and appears to represent a synergistic effect of cationic and anionic polymers on floc aggregation, floc settling and resultant total phosphorus removal.

Both treatments were considered over time. Both iron dosing treatments reduced total phosphorus the greatest by days 2 through 4 (Figure 56). Ferric chloride achieved total phosphorus concentrations near 60 μg L^{-1}. FPD treatments achieved total phosphorus concentrations of approximately 40 μg L^{-1}. Both treatments also appeared to have a return of total phosphorus back into the water column with the total phosphorus concentrations near 80 μg L^{-1} at the end of the run. Both treatments rapidly removed dissolved phosphorus and dissolved phosphorus did not return back into the water column (Figure 57).

Figure 54. Achieving lower total phosphorus concentrations in ferric iron treatments by *in situ* use of cationic polymers, October 1999 Batch Flow Study. All treatments were followed by PAM applications of 0.25 mg L^{-1}. Samples were collected on the schedule shown in Table 14 after pumping ceased and at the locations shown in Figure 9. Ferric iron was dosed at 200 µM for all treatments. FerriPlus-D is ferric sulfate plus 20% cationic polymer.

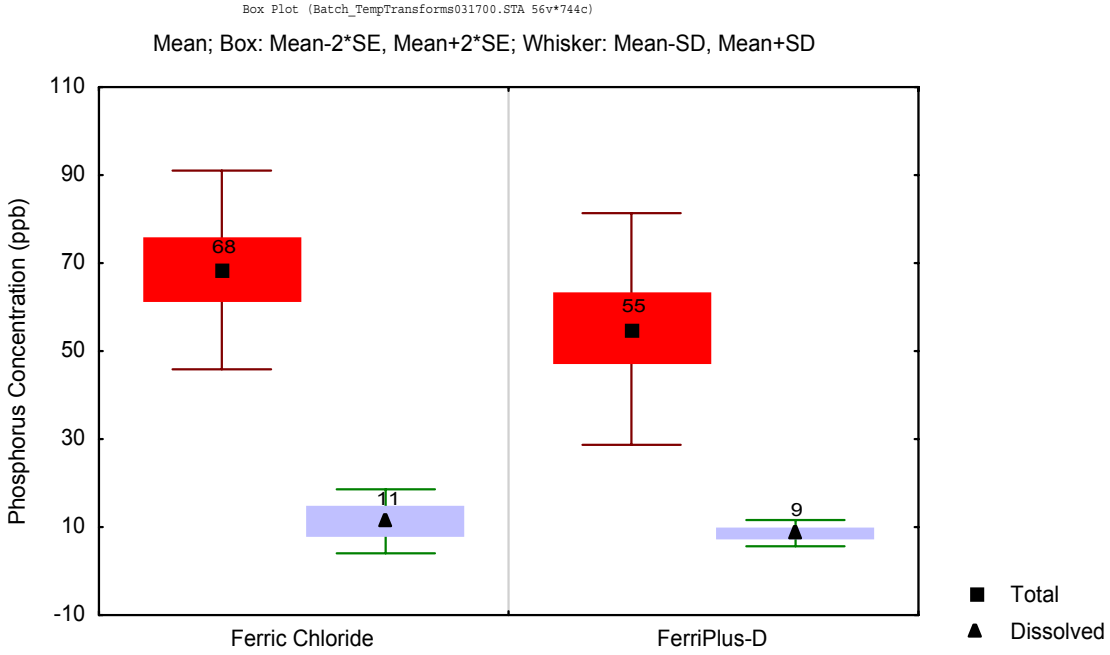

Finally, dose comparisons of 100 µM vs. 200 µM were considered for the FPD treatments. Both dosing levels resulted in similar mesocosm concentrations of total and dissolved phosphorus (Table 17). The higher dosing level had higher removal of both dissolved and total phosphorus though that may have been a function of the higher initial concentrations of each as opposed to the higher dosing level.

Figure 55. Greater *in situ* total and dissolved phosphorus removal in ferric iron treatments with the use of 20% cationic polymers, October 1999 Batch Flow Study. All treatments were followed by PAM applications of 0.25 mg L^{-1}. Samples were collected on the schedule shown in Table 14 after pumping ceased and at the locations shown in Figure 9. Ferric iron was dosed at 200 µM for all treatments. FerriPlus-D contains 20% cationic polymers.

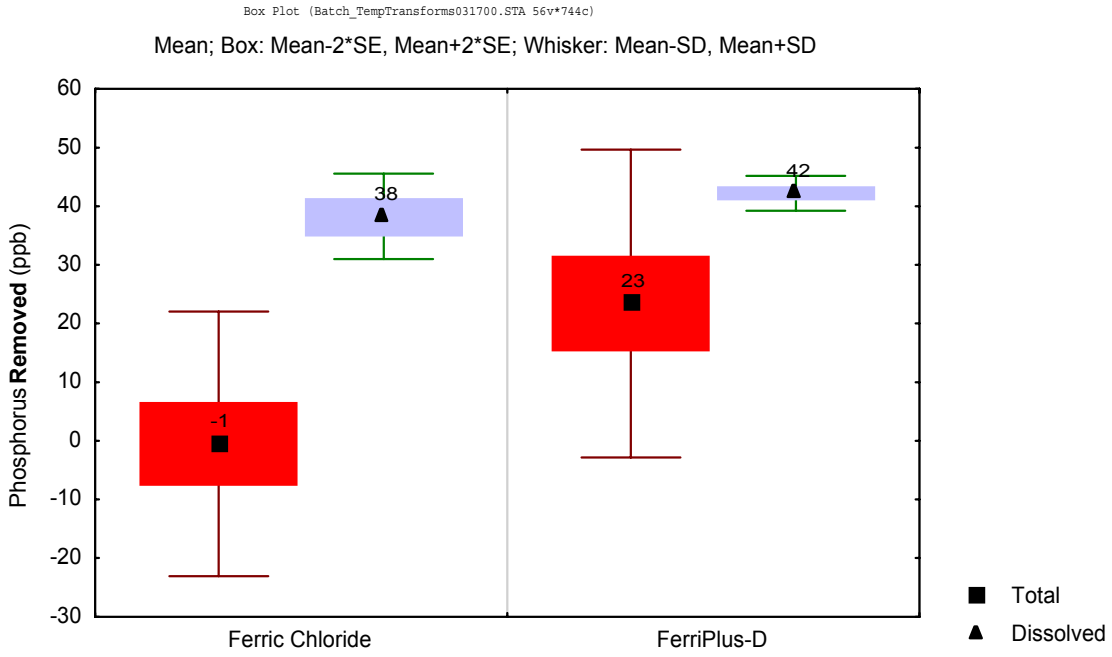

Figure 56. Temporal changes in mesocosm total phosphorus concentrations following *in situ* ferric iron dosing, October 1999 Batch Flow Study.
Ferric iron was dosed at 200 µM and followed by PAM applications of 0.25 mg L^{-1}. Samples were collected within the mesocosms at the locations shown in Figure 9.

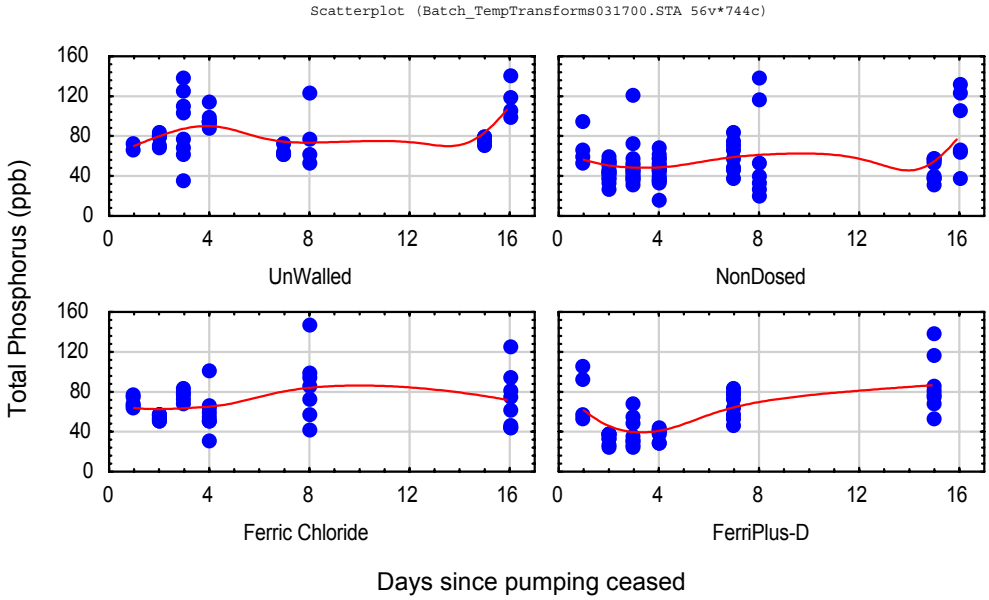

Figure 57. Temporal changes in mesocosm dissolved phosphorus concentrations following *in situ* ferric iron dosing, October 1999 Batch Flow Study.
Ferric iron was dosed at 200 µM and followed by PAM applications of 0.25 mg L^{-1}. Samples were collected within the mesocosms at the locations shown in Figure 9.

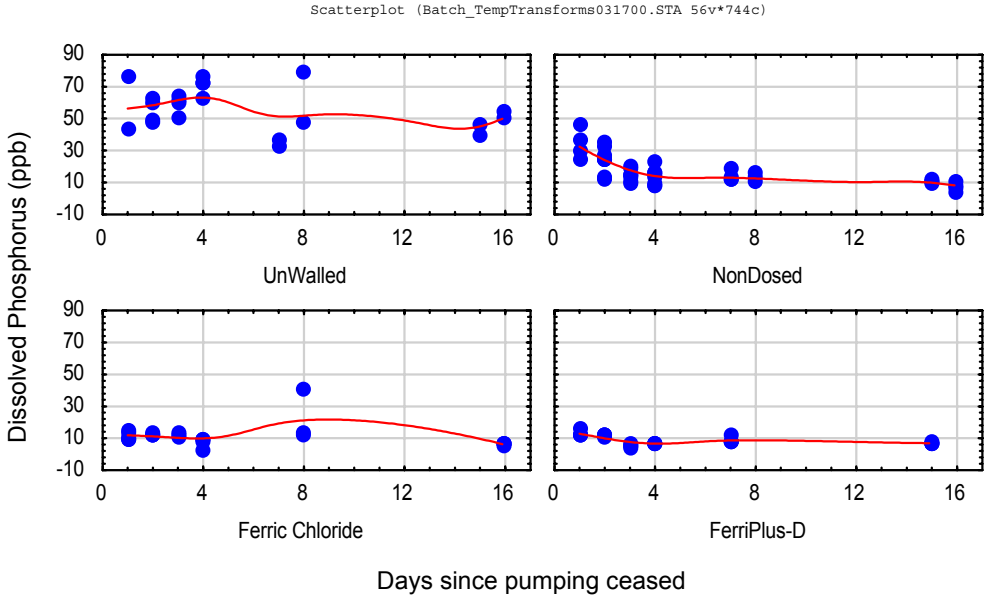

Table 15. Statistical differences in total and dissolved phosphorus concentrations and removal between sites, October 1999. Includes only treatments in which no PAM was added. Total phosphorus concentrations above 150 µg L^{-1} is excluded as outliers. Data are only from days after dosing was completed.

		Inflow FTP At site	FTP				FTP rem[1]				Inflow UTP Into Meso	UTP				UTP rem[1]			
			mean	SD	N	p	mean	SD	N	p		mean	SD	N	p	mean	SD	N	p
Treat[2]	Site																		
200 µM	A	49.6	11.3	6.4	11		38.3	6.4	11		64.4	69.2	24.3	20		-4.8	24.3	20	
Fe as	B	23.7	19.8	9.5	12		4.0	9.5	12		44.1	64.4	15.2	22		-20.3	15.2	22	
FeCl	C	50.9	12.4	9.9	13		38.5	9.9	13		69.7	56.0	18.8	23		13.8	18.8	23	
	All	41.4	14.5	9.4	36	0.0512	**26.9**	**18.6**	**36**	**0.0000**	59.4	62.9	20.1	65	0.0882	**-3.5**	**24.0**	**65**	**0.0000**
200 µM	A	49.6	10.7	8.9	13		38.8	8.9	13		64.9	61.8	19.6	21		3.0	19.6	21	
Al as	B	23.7	8.9	4.7	13		14.8	4.7	13		36.1	37.4	11.3	23		-1.3	11.3	23	
Alum	C	50.9																	
	All	41.4	9.8	7.1	26	0.5262	**26.8**	**14.1**	**26**	**0.0000**	50.5	**49.1**	**19.9**	**44**	**0.0000**	0.7	15.8	44	0.3683
Non-	A	49.6	14.9	9.5	20		34.7	9.5	20		65.4	57.7	32.6	36		7.8	33.1	36	
Dosed	B	23.7	17.1	6.6	22		6.7	6.6	22		46.4	55.2	17.1	42		-8.9	16.8	42	
	C	50.9	18.6	8.5	22		32.3	8.5	22		68.3	50.6	13.3	42		17.7	16.0	42	
	All	41.4	16.9	8.2	64	0.3535	**24.2**	**15.2**	**64**	**0.0000**	60.0	54.3	22.0	120	0.3492	**5.4**	**25.2**	**120**	**0.0000**

Notes:

1. Dissolved phosphorus (FTP) removed is calculated from the difference between pumped water and mesocosm water. Total phosphorus removed (UTP) is calculated from the difference between inflow water at each mesocosm and mesocosm water.
2. Phosphorus values are in µg L^{-1}.

Table 16 Statistical differences in total and dissolved phosphorus concentrations and removal for iron dosing with and without cationic polymers, October 1999.

		Inflow FTP At site	FTP				FTP rem[1]				Inflow UTP Into Meso	UTP				UTP rem[1]			
			mean	SD	N	p	mean	SD	N	p		mean	SD	N	p	mean	SD	N	p
Treat[2]	Site																		
200 µM Fe as FeCL	A	50.0	11.3	7.3	23		38.3	7.3	23		67.9	68.4	22.6	41		-0.5	22.6	41	
200 µM Fe as FPD	C	50.9	8.6	3.0	24		42.2	3.0	24		78.4	55.0	26.3	44		23.4	26.3	44	
All			9.9	5.6	47	0.1066	**40.3**	**5.8**	**47**	**0.0182**		**61.5**	**25.4**	**85**	**0.0139**	**11.9**	**27.2**	**85**	**0.0000**

Notes:

1. Dissolved phosphorus (FTP) removed is calculated from the difference between pumped water and mesocosm water. Total phosphorus removed (UTP) is calculated from the difference between inflow water at each mesocosm and mesocosm water.
2. Phosphorus values are in µg L^{-1}.

Table 17 Statistical differences in total and dissolved phosphorus concentrations and removal for different iron dosing levels, October 1999.

Includes only treatments in which no PAM was added. Total phosphorus concentrations above 150 µg L^{-1} is excluded as outliers. Data are only from days after dosing was completed.

		FTP	FTP				FTP rem[1]				UTP	UTP				UTP rem[1]			
		At site	mean	SD	N	p	mean	SD	N	p	Into Meso	mean	SD	N	p	mean	SD	N	p
Treat[2]	Site																		
100 µM Fe as FPD	B	23.7	8.1	2.4	22		15.6	2.4	22		40.6	54.8	19.6	40		-14.2	19.6	40	
200 µM Fe as FPD	C	50.9	8.6	3.0	24		42.2	3.0	24		78.4	55.0	26.3	44		23.4	26.3	44	
All			8.4	2.7	46	0.5175	**29.5**	**13.7**	**46**	**0.0000**		54.9	23.2	84	0.9613	**2.0**	**28.0**	**84**	**0.0000**

Notes:

1. Dissolved phosphorus (FTP) removed is calculated from the difference between pumped water and mesocosm water. Total phosphorus removed (UTP) is calculated from the difference between inflow water at each mesocosm and mesocosm water.
2. Phosphorus values are in µg L^{-1}.

13.2.6. Analyses of aluminum and polymer dosing combinations

Similar analyses were conducted for aluminum blends. Figure 58 shows total phosphorus into each mesocosm during pumping, mesocosm phosphorus concentrations during the run and the amount of phosphorus removed. Dosing of aluminum at 200 μM without PAM was not successfully conducted at Site C because of clogging. This mesocosm was excluded from the analyses.

Dosing with 200 μM aluminum without PAM resulted in near zero total phosphorus removal during this run. Inflow phosphorus concentrations at Site A were approximately 65 $\mu g\ L^{-1}$ while inflow concentrations to Site C were approximately 40 $\mu g\ L^{-1}$. Mean total phosphorus concentrations within the mesocosms were relatively unchanged. However when PAMs were used during 200 μM aluminum dosing with alum, 20 $\mu g\ L^{-1}$ of total phosphorus was removed representing a 30% decrease in total phosphorus. The use of PAMs did not appear to improve dissolved phosphorus removal as can be best shown by comparing the two mesocosms at Site A receiving aluminum dosing at 200 μM as alum. Both treatments resulted in dissolved phosphorus concentrations near 10 $\mu g\ L^{-1}$, representing an approximate 80% decrease below inflow values near 50 $\mu g\ L^{-1}$ (Figure 59).

Comparing mesocosms A7 and B5 in Figure 58 can be used to assess the effects of cationic polymers. Mesocosm A7 which did not use cationic polymers achieved total phosphorus concentrations of 46 $\mu g\ L^{-1}$ for a 29% reduction below inflow levels of 65 $\mu g\ L^{-1}$. Mesocosm B5 which did receive cationic polymers achieved total phosphorus concentrations of 32 $\mu g\ L^{-1}$ for a 33% reduction below inflow levels of 48 $\mu g\ L^{-1}$ (Figure 58). Using cationic polymers achieved lower total phosphorus concentrations in the mesocosms though inflow concentrations were also lower. However, a greater percent reduction was also achieved for aluminum treatments using cationic polymers.

The effects of cationic polymers on dissolved phosphorus are more clear. No aluminum treatment except for the one using cationic polymers achieved dissolved phosphorus concentrations near 5 $\mu g\ L^{-1}$ (Figure 59). This result agrees with earlier Jar test findings showing that aluminum blends with cationic polymers lead to dissolved phosphorus concentrations near 5 $\mu g\ L^{-1}$ and these levels are below those achievable by aluminum blends without cationic polymers.

Thus, cationic polymers further decreased dissolved phosphorus concentrations and anionic polymers improved settling to aid with lowering total phosphorus concentrations. In all treatments, dissolved and total phosphorus concentrations were stable over the course of the run (Figures 60 and 61).

Figure 58. Greater total phosphorus removal and lower residual concentrations achieved in aluminum treatments with the incorporation of cationic polymers and PAMs, October 1999 mesocosm study.
Total phosphorus concentrations greater than 150 µg L^{-1} were outliers and excluded from the analyses. Data was collected at the locations shown in Figure 9 on the sampling schedule in Table 14 after pumping ceased. Clarion 4100 is defined as alum with 10% cationic polymer.

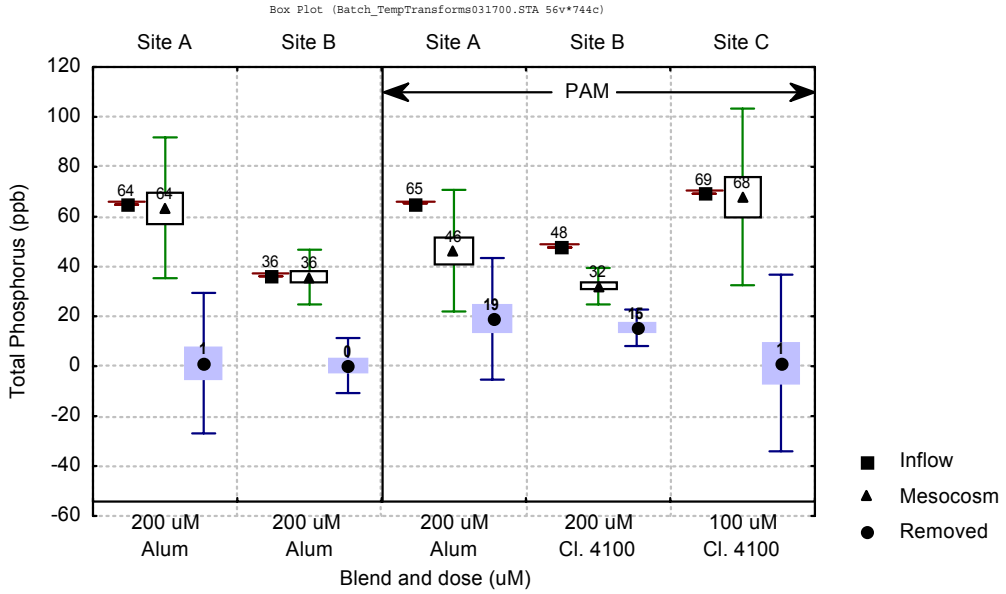

Figure 59. Dissolved phosphorus concentrations achieved during October 1999 mesocosm study for different aluminum treatments.
Data was collected at the locations shown in Figure 9 on the sampling schedule in Table 14 after pumping ceased.

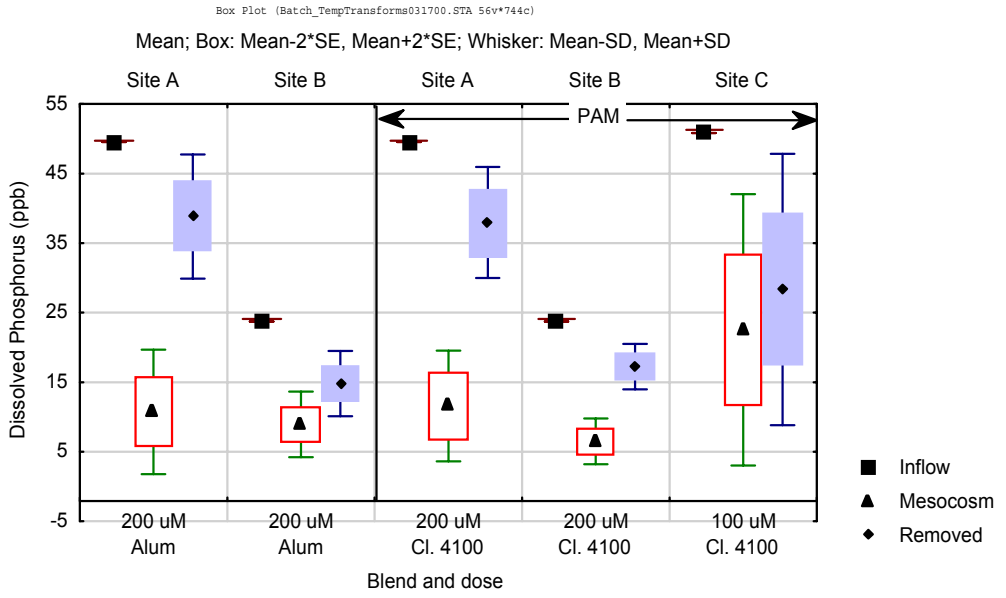

Figure 60. Temporal changes in total phosphorus concentrations for mesocosms undergoing aluminum dosing at 200 µM.
Data from October 1999 Batch Flow Study.

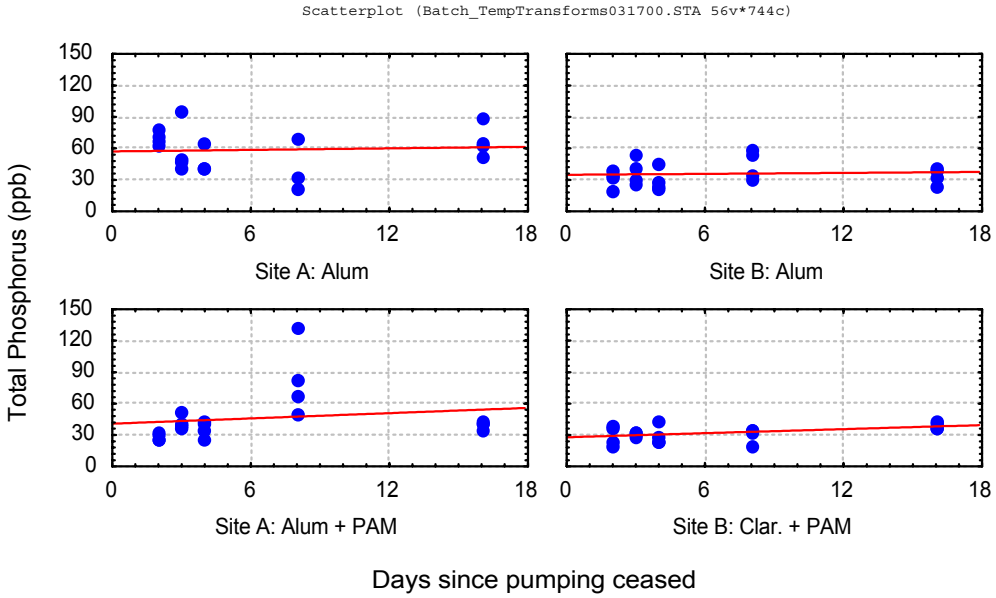

Figure 61. Temporal changes in dissolved phosphorus for mesocosms undergoing aluminum dosing at 200 µM.
Data is from October 1999 Batch Flow Study.

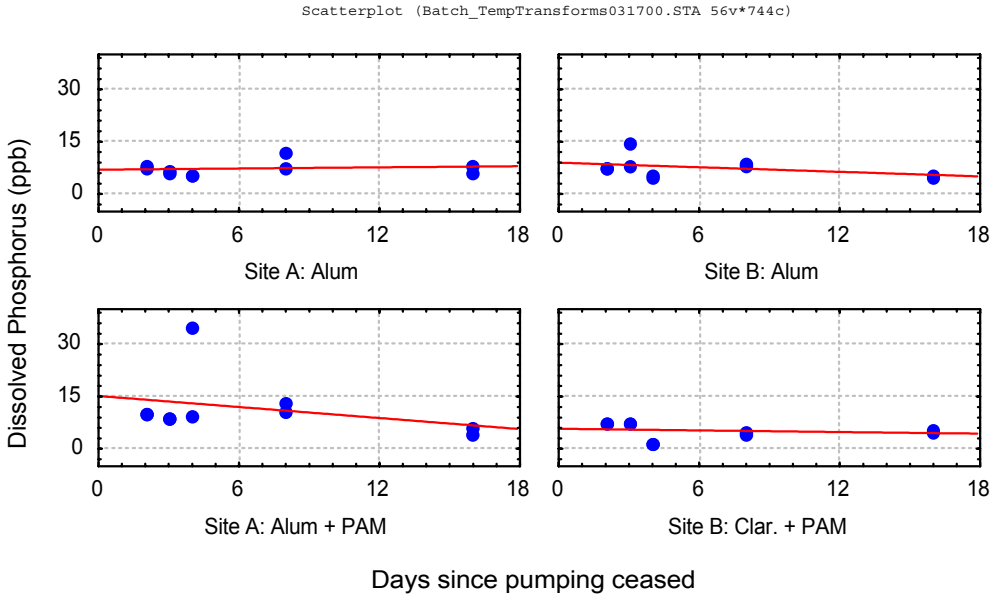

Finally, the effects of aluminum dosing levels were considered when Clarion 4100 was used. Dosing at 200 μM aluminum as Clarion 4100 was clearly more effective than dosing at 100 μM. At the lower dosing concentration, nearly no total phosphorus removal occurred and higher dissolved phosphorus concentrations resulted (Figures 58 and 59).

Based on these analyses, the optimal blends for aluminum is very clear. The use of both cationic polymers and PAMs for aluminum dosing improved the removal of total and dissolved phosphorus. Dosing levels for aluminum of 200 μM were better than lower dosing concentrations. Thus, for this mesocosm study, the optimal aluminum blend was dosing aluminum at 200 μM with the Clarion 4100 followed by the addition of PAM (Superfloc A130). These results were predicted by the jar test and were not surprising. For iron blends, the optimal blend is less clear. Using cationic polymers clearly aided with total phosphorus removal initially though there appeared to be a return of total phosphorus back into the water column over time. PAMs did not show any effect on total phosphorus concentrations nor did different dosing levels. These results are very surprising given strong evidence from the jar tests showing that both cationic and anionic polymers improved performance and that the greatest effects was from the PAMs. Using both polymer types did lower dissolved phosphorus concentrations. Thus no clear optimal iron blend was determined for this study though the use of polymers likely improves the removal of bio-available phosphorus.

13.2.7. Total phosphorus concentrations and PAMs

Total phosphorus concentrations achieved during this study for the optimal chemical blends were much higher than was expected based upon results from the jar test series. PAM dosing at 0.25 mg L^{-1} did not improve total phosphorus removal by iron blends though there was a slight improvement with aluminum blends. This result is counter intuitive as jar test results had shown that PAMs dramatically improved phosphorus removal by iron blends. For iron dosing of 200 μM ferric iron as FPD followed by PAM dosing at 0.25 mg L^{-1}, a total phosphorus concentration of 55 μg L^{-1} from a background concentration of 78 μg L^{-1}, representing a decrease in total phosphorus by 30% (Figures 54 and 55). For aluminum dosing of 200 μM as Clarion 4100 followed by PAM dosing at 0.25 mg L^{-1}, a total phosphorus concentration of 32 μg L^{-1} from a background concentration of 48 μg L^{-1}, representing a decrease in total phosphorus by 33% (Figure 58). Neither of these optimal blends provided the level of treatment anticipated from the jar tests. The slight improvement with PAMs for aluminum treatments was encouraging. However, that and the lack of improvement with iron blends suggested that insufficient PAM was being utilized for the field studies.

13.2.8. Conclusion

- Site effects and mesocosms effects were apparent for total phosphorus concentrations in the mesocosms, for total phosphorus removed from the mesocosms, and total dissolved P removed. There was no apparent site or mesocosm effect on mesocosm dissolved phosphorus concentrations suggesting a lower limit that can be achieved by chemical dosing.
- Anionic polymers had no clear beneficial effect on phosphorus removal by iron dosing.
- Cationic polymers improved the dissolved phosphorus removal by iron dosing.
- Under iron dosing total phosphorus returned to the water column whereas dissolved phosphorus did not.
- Both cationic and anionic polymers improved total and dissolved P removal by aluminum. The optimum aluminum dose was 200 μM.
- Total phosphorus removal of about 30 – 33% was achieved for the optimal blends. The final phosphorus concentration depended upon initial background concentrations. The lowest total phosphorus concentration achieved for all blends in this study was 32 $\mu g\ L^{-1}$.

Chapter 14. Continuous Flow Mesocosm Study, February/March 2000

The February/March 2000 Continuous Flow Mesocosm Study was the final study for this contract. The previous batch study suggested that anionic polymers did not improve *in situ* total phosphorus removal when ferric iron coagulants were used. This strongly contradicted earlier jar test studies. Qualitative visual studies conducted during December 1999 at the mesocosms sites confirmed this suspicion. PAM dosing levels of 0.25 mg L^{-1} as had been used in the jar tests did not appear to improve floc aggregation over systems in which no PAM was used. However, with higher PAM exceeding 0.5 mg L^{-1}, much larger floc formed and settling was more rapid. Thus, this study was conducted to further investigate the use of PAMs as a method to improve floc aggregation and settling during LICD.

14.1. Methods

The experimental design for this study is shown in Table 18. For this study, Sites A and C were used. This approach allowed us to optimize the data collected given our manpower and resources. The October 1999 Batch Flow Study had been operated at all three experimental sites (Sites A, B and C; Table 13) to establish site variance as required in the SOW. However, that approach was found to have limited utility given the time and resource commitments required to operate and sample the three sites simultaneously. The decision to use two sites for this final study evolved from our experience and was considered the best method to most efficiently use our resources and manpower towards our efforts to optimize LICD. The two main questions addressed were:

- Can higher anionic polymer doses improve total phosphorus removal and
- Can higher metal dosing levels of either iron or aluminum improve *in situ* total phosphorus removal?

The experimental design uses a regression approach with regard to both metal dose and anionic polymer dose. Iron and aluminum dosing levels of 200, 400 and 600 μM were used in combination with anionic polymer dosing levels of 0.5 and 1.0 mg L^{-1}. No individual treatment combination (metal vs. metal dose vs. anionic polymer dose) was replicated. Replication of each combination may have provided more robust results. However, interpreting even replicated treatment combinations can be problematic. Our earlier mesocosm studies showed mesocosm and site effects confounded data from these studies. Thus, as an alternative, a regression approach was used in which we believed that by using regression and correlation analyses, we could distinguish site, mesocosm, metal type, metal dosing level and anionic polymer dosing effects and their associated variance. Under this design, individual operational parameters (e.g. ferric iron dosing at 200 μM) were replicated between mesocosms. This overall approach

was taken to optimize the findings from the study given the manpower, logistical and costs limitations associated with mesocosm studies.

Table 18. Experimental Design for February/March 2000 Continuous Flow Mesocosm Study.

Mesocosm	Site A	Site C
1 Treatment	**Clarion 4100**	**NonDosed**
Metal	Al	WC
Metal Dose	200	0
PAM	0.5	0
YSI	**YES**	Na
2 Treatment	**NonDosed**	**FerriPlus D**
Metal	WC	Fe
Metal Dose	0	200
PAM	0	1
YSI	Na	Na
3 Treatment	**FerriPlus D**	**Clarion 4100**
Metal	Fe	Al
Metal Dose	200	200
PAM	0.5	1
YSI	**YES**	Na
4 Treatment	**FerriPlus D**	**Clarion 4100**
Metal	Fe	Fe
Metal Dose	400	600
PAM	1	1
YSI	**Yes**	Na
5 Treatment	**NonDosed**	**NonDosed**
Metal	WC	WC
Metal Dose	0	0
PAM	0	0
YSI	**YES**	Na
6 Treatment	**FerriPlus D**	**Clarion 4100**
Metal	Fe	Al
Metal Dose	600	400
PAM	1	0.5
YSI	Na	Na
7 Treatment	**Clarion 4100**	**FerriPlus D**
Metal	Al	Fe
Metal Dose	400	400
PAM	1	0.5
YSI	**YES**	Na
8 Treatment	**UnWalled Control**	**UnWalled Control**
YSI	**YES**	Na

Notes:

1. Metal doses are in μM.
2. PAM additions require individual carboys. PAM doses are in mg L^{-1}. Cationic polymers are mixed directly with metals.
3. Bromide is mixed into every chamber with the metal if metal is added. Otherwise, a separate carboy is required.
4. YSI represent multi-parameter sonde (YSI 6000). Yes represents deployed at mesocosm location.

The design specifications and scheduling are summarized in Table 19. During this study, the pumps were operated under two scenarios, flushing and continuous flow. The flushing mode was conducted at the beginning of the studies. Initially, all mesocosms were flushed with three volumes of dosed water to establish within the mesocosms the desired chemical and polymer concentrations, and thus accelerate the establishments of steady state conditions. After this initial flushing period, the systems were then operated under continuous mode. In this mode, water was pumped daily for approximately two hours with the necessary water volume necessary for the design HRT of 3 days. Pumping began at 1:30 PM and ceased approximately 2 hours later. Specific pump times depended upon the flow rates achieved during pumping at the two different sites.

Table 19. Operational specifications for February/March 2000 Continuous Flow Study.

System Characteristics	Units	Specification
Initial Water Depth	Ft	2.5
Data Loggers Deployment and Recovery		
Deploy YSIs/Hydrolabs		February 15
Recover YSIs/Hydrolabs		March 17
Flushing Cycle		
Dates of mesocosm flushing		February 17 - 18
Mesocosm volumes flushed	Volume	3
Mesocosm volume	gallons	500
Total water pumped	gallons	1500
Pump time	Hrs	~20
Normal Operation		
Date normal operation begins		February 19
Design HRT	Days	3
Water pumped	GPD	167
Flow rate	Gpm	~1.4
Pumping frequency		Daily
Pumping begins		13:30
Pumping ends		~15:30
Sampling frequency		Twice weekly
Sampling begins		~9:00
Chemical stock solution deployment		Weekly
PAM stock solution deployment		Twice weekly

Sampling was conducted twice per week at each site (Tables 19 and 20). Sampling within the mesocosms and mixing tanks began in the morning and was

completed before water pumping began. Thus, water sampled from the mesocosms had been undisturbed and quiescent for at least 18 hours. Once pumping began, water was sampled from the outlet pipes. These samples represented dynamic water quality changes occurring during chemical dosing.

Table 20. February/March 2000 mesocosm study sampling schedule.

Water Sampling	Sampling Frequency	Locations	Site
Grab			
FOP	Weekly	C1, P2	A,C
UTP	Twice weekly	C1, C3, F1, G1, X1, P2	A,C
FTP	Twice weekly	C1, C3, X1, P2	A,C
UFE, UAL	Weekly	C1, C3, X1, P2	A,C
FFe, FAl	Weekly	C1, C3, X1, P2	A,C
NH4	Twice total[1]	C1, C3, X1, P2	A,C
NOX	Twice total[1]	C1, C3, X1, P2	A,C
Total dissolved-N (TDN)	Twice total[1]	C1, C3, X1, P2	A,C
Total N (TN)	Twice total[1]	C1, C3, X1, P2	A,C
DOC	Twice weekly	C1, C3, X1, P2	A,C
Alkalinity	Twice total[1]	C1	A,C
Color	Twice total[1]	C1, P2	A,C
Ca, Na, Mg, Mn, K, Zn, Cu	Twice total[1]	C1, X1, P2	A,C
Si	Twice total[1]	C1	A,C
Cl-, SO_4^{-2},	Twice total[1]	C1, P2	A,C
Br-	Twice weekly	C1, P2	A,C
TSS	Twice total[1]	C1	A,C
Unattended			
DO	Hourly	C2	A
Temperature	Hourly	C2	A
pH	Hourly	C2	A
Turbidity	Hourly	C2	A
Specific conductivity	Hourly	C2	A

Notes:
1. Sampling conducted once steady state conditions had been achieved

For addressing the process questions adequately, phosphorus, dissolved organic carbon, iron, aluminum, bromide, dissolved oxygen, conductivity, turbidity and pH were measured intensely. Phosphorus, bromide, dissolved organic carbon, iron and aluminum grab samples were collected weekly to twice weekly at multiple locations within the mesocosms (Table 20). Dissolved oxygen, turbidity, conductivity and pH were monitored at selected mesocosms at Site A with data

sondes. Additionally, other parameters noted in Table 20 were collected less frequently at fewer locations to address other water quality changes that might occur during chemical dosing. These samples were analyzed to partially address the question of LICD effects on the marsh readiness of treated waters.

14.2. Results and Discussion

14.2.1. Mesocosm Hydrology

The design HRT for this study was 3 days. Average flow into the mesocosms during this study was 160 gpd and the average water depth was 2 feet. Thus, the calculated HRT for this study was 2.5 days (Table 21).

Table 21. Estimated HRT for February/March 2000 mesocosm study.

Flow in	160	gpd
Water depth	2	ft
Mesocosm water volume	400	Gallons
Estimated HRT	2.5	Days
Design HRT	3	Days

The hydraulic loading rate (HLR) was based upon the pumped loading of treated water to each mesocosm and was calculated from the period beginning on February 19, 2000 and continuing through the duration of the study. The HLR was compared to evapotranspiration calculations and measured precipitation. Mean HLR to the mesocosms was two orders of magnitude greater than contributions from evapotranspiration and precipitation (Table 22). At Site A, HLR averaged 9.887 in d^{-1} and at Site C HLR averaged 9.002 in d^{-1}. The standard deviation for HLR at Site C was over 40% greater than that at Site A. A closer examination of Site C shows that during the study, Mesocosm 4 experienced median flows of less than half of any other mesocosm and had much greater variation (Figure 62). This was apparently due to clogging. Thus, Mesocosm 4 data from Site C was eliminated from the analyses. When that data was eliminated, both sites had near identical HLR (Table 22).

Table 22: Water Budget for February/March 2000 Mesocosm Study.
Hydrologic loading are daily averages to all mesocosms at each site.

Parameter	Site	Mean (in d^{-1})	SD (in d^{-1})
HLR	A	9.89	2.25
	C	9.00	3.22
	C (w/o Meso 4)	9.87	2.17
ET		0.115	0.021
Rain		0.026	0.119
Marsh Water		0.101	1.012

Notes
1. Represents the absolute value for marsh water.

Figure 62. Calculated hydraulic loading rates (HLRs) for Site C mesocosms, February/March 2000 Continuous Flow Study.
HLR represents daily water loads pumped into each mesocosm during continuous dosing period beginning on February 19, 2000 through the entire study. Mesocosm C4 experienced frequent clogging and was excluded from subsequent data analyses.

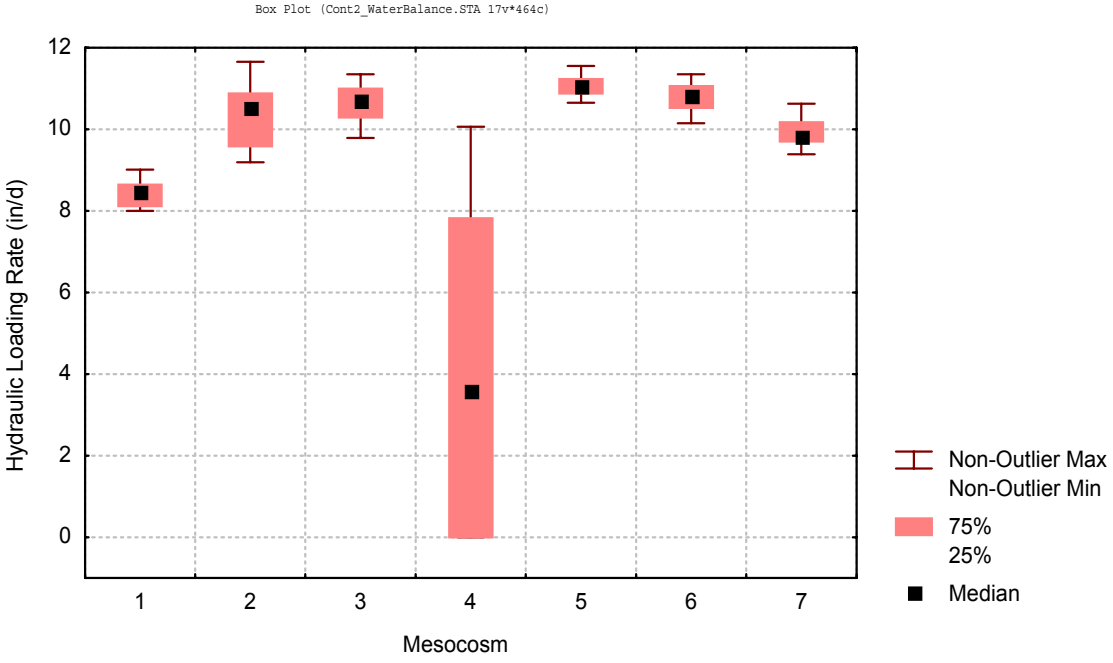

Standard deviation on evapotranspiration and rain was at least one order of magnitude lower than for either HLR or for marsh inflows. As a percent of the mean, the standard deviation for marsh inflows was much greater than for any

other hydrologic input (Table 22). Mesocosm 1 at Site A was chosen as representative of daily inputs to the mesocosm during the study (Figure 63). Pumped inflow into the mesocosm was very constant from day to day except on March 1st and 2nd which likely represent sampling and maintenance disturbances. Marsh inputs to the mesocosms generally hovered near zero representing slight daily variations in marsh water elevation during the study. This did not represent water level variations and mixing effects that could occur more frequently.

Figure 63. Hydrologic balance for mesocosms during February/March 2000 Mesocosm study.

Data includes HLR and calculated hydrologic contribution from the marsh into the mesocosms. Calculations are based upon daily hydrologic data. Water entering from the marsh would be driven by variations in marsh water elevations. Graph is for Mesocosm 1 at Site A and is considered typical of all mesocosms operated in this study.

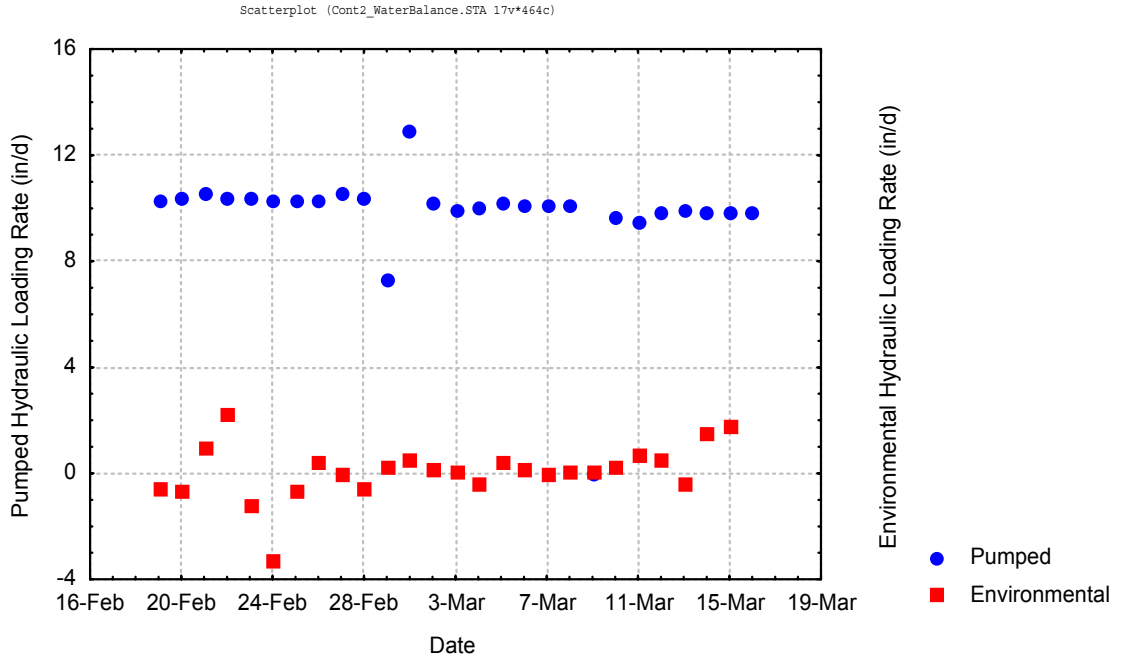

14.2.2. Determination of Steady State Conditions

Bromide tracer studies were conducted to assess steady state conditions for the dosed mesocosms. Mesocosms had been initially pumped with three volumes of dosed mesocosm water on February 17 and 18 to hasten the attainment of steady state conditions. Mesocosms were then operated at the desired HRT for the remainder of the study. This is described in the Chapter 2.

Bromide concentrations were determined for both inflow and water column samples for each treated mesocosm on each day grab samples were collected. Water column samples were collected six inches below the water surface. A dependent t-test was conducted to determine if bromide concentrations were different (Table 23). Bromide concentrations in the inflow and mesocosm water differed significantly ($p<<0.0001$). Dosing water averaged 9.05 mg L^{-1} as compared to mesocosm water which averaged 2 mg L^{-1} less at 7.08 mg L^{-1}. Overall, bromide concentrations in the mesocosms were slowly approaching those in the inflows (Figure 64) though mesocosm concentrations would always be expected to be slightly less due to marsh water inflows into the mesocosms during marsh water fluctuations. Thus, the mesocosms had not attained steady state conditions at the initiation of the study. A comparison of the bromide concentrations on the first and last sampling day show that on average, mesocosm bromide concentrations were approximately 74% of inflow concentrations on the first sampling day and improved slightly to 83% by the last sampling day (Table 24). The last sampling day represented over 8 HRT cycles since the initiation of the experiment and over 11 flushes of the mesocosms. By the final sampling day, steady state conditions were achieved and some dilution apparently occurred naturally due to water entering the mesocosms during marsh water level fluctuations. Thus, though steady state conditions had not quite been achieved by the first sampling day, the system was very near steady state considering natural dilution affects.

Table 23. Analyzing inflow and mesocosm bromide concentrations with a T-test for dependent samples.
Mean values are for the entire time period for this continuous flow experiment.

Variable	Mean	SD	Difference Mean	Difference SD	N	p-value
	mg L^{-1}	mg L^{-1}	mg L^{-1}	mg L^{-1}		
Bromide concentration in dosed inflows	9.05	2.23	1.97	2.60	55	0.0000
Bromide concentration in mesocosm water	7.08	1.60				

Notes:
1. Samples with bromide concentrations above 20 mg L-1 were excluded from the analyses as these were either contaminated or represented malfunctions. Bromide data less than 2 mg L^{-1} in the dosed inflows was also excluded as one mesocosm had the sampling inflow sampling location upstream of the bromide dosing location. Finally Mesocosm 4 at site C was excluded because of consistent clogging in that line during the study as shown by the hydrologic budget analyses.

Table 24. Comparison of inflow and mesocosm bromide concentrations on first and last day of sampling.

Sampling day	Inflow bromide concentration	Mesocosm bromide concentration	
	mg L^{-1}	mg L^{-1}	% of inflow
First	7.96	5.89	74
Last	8.55	7.12	83

Figure 64. Trends in inflow and mesocosm water bromide concentrations, February/March 2000.
Data represents bromide concentrations recorded at all mesocosms at Sites A and C during the continuous flow mesocosm study.

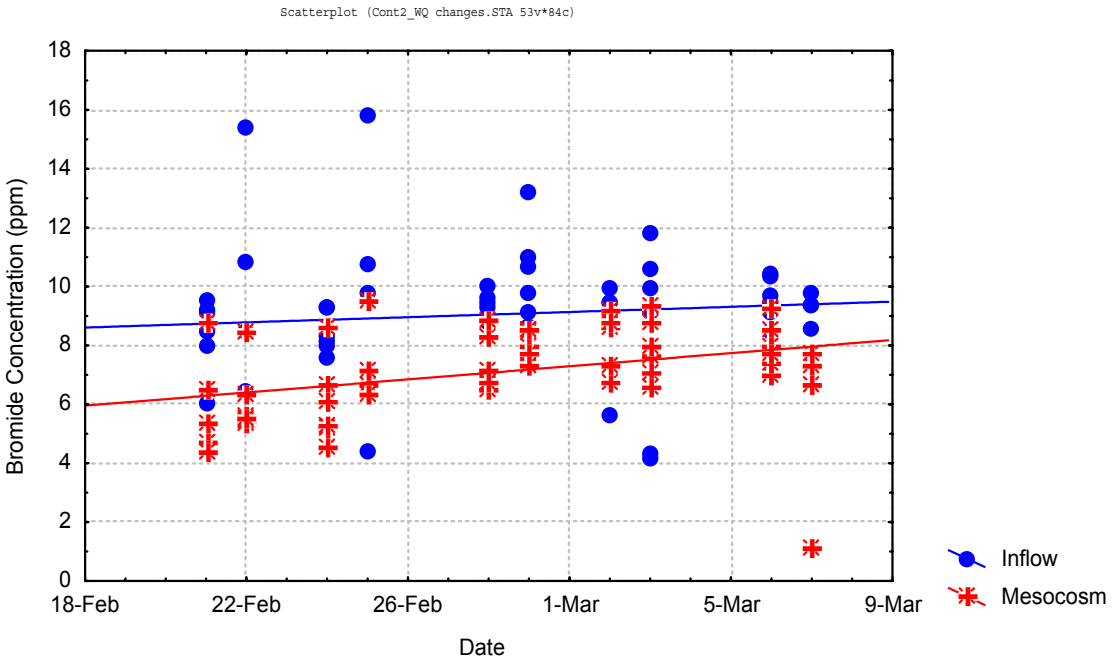

Assuming steady state conditions, bromide concentrations could be used to calculate typical dilution caused from daily fluctuations in the marsh water column. Water depth averaged approximately 2 ft during this study corresponding to a measured water elevation of 7.28 ft. However, that water elevation varied between 7.08 and 7.60 ft during this study, corresponding to a standard deviation of 0.135 ft and a total swing in water depth of 0.5 ft during this study. These variations caused daily dilution of bromide concentrations within the mesocosms. From steady state mass balance analyses, the dilution flow Q_{dil} can be estimated as:

$$Q_{dil} = \frac{[Br]_{in} - [Br]_{out}}{[Br]_{in}} Q_{in} \qquad \textbf{Equation 1}$$

where:
Q_{in} = flow into the mesocosms,
Br_{in} = bromide concentrations in the mesocosm inflow, and
Br_{out} = bromide concentration within the mesocosms which is also equal to concentration from the mesocosm under CFSTR conditions.

From that calculation, Q_{dil} for steady state conditions is approximately 14% of the inflows. This is based upon bromide data from the final day of the study in which steady state conditions were most likely achieved.

14.2.3. Phosphorus Analyses

Phosphorus analyses was conducted in two phases. The first phase was conducted using raw data with the goal of identifying factors affecting phosphorus concentrations and phosphorus removal. The second phase used created a matrix of process data and was used to develop input-output mass balance models for this study.

14.2.3.1. Raw Data Analyses

Grab samples were collected throughout this study using the experimental design shown in Table 18, the schedule shown in Table 19 and the sample frequency shown in Table 20. Sampling efforts focused manpower and efforts on the parameters of greatest interest. Thus, greater effort was used on sampling total and dissolved phosphorus than other parameters. Moreover, sampling frequencies for a given parameter were also based upon the anticipated relative variance of the sample parameters. For instance, dissolved organic carbon is measured in the ppm (mg L^{-1}) range and generally has low relative variance. Total phosphorus is measured in the $\mu g\ L^{-1}$ range, can be contaminated during sampling by collection of algal particulates or other biotic material, and is analyzed in a range near the MDL. The variance of total phosphorus is therefore relatively high. Thus, fewer samples are required to reasonably characterize DOC then to reasonably characterize total phosphorus. This approach was used for all sampled parameters in order to maximize our efforts. The resulting raw data has varied sampling locations and frequencies based upon the sampled parameters. From this heterogeneous data set, phosphorus trends were identified and characterized.

14.2.3.1.1. Background water characteristic

As a first step in understanding the system and the resulting effects of chemical dosing, background phosphorus concentration concentrations and trends were analyzed.

Site effects

Background total and dissolved phosphorus concentrations differed significantly at the two sites (Figure 65; $p<0.05$). At Site A, mean total phosphorus concentrations were 128 $\mu g\ L^{-1}$ and dissolved phosphorus concentrations were 98 $\mu g\ L^{-1}$. At Site C, total phosphorus concentrations were 105 $\mu g\ L^{-1}$ and dissolved phosphorus concentrations were 63 $\mu g\ L^{-1}$. At Site A, dissolved and total phosphorus concentrations were increasing during the study and at Site C, those parameters were decreasing (Figures 66 and 67).

Figure 65. Differences in background Total and Dissolved Phosphorus Concentrations between sites, February/March 2000.
Plots are of mean values. Median values were the same for total phosphorus and nearly the same for dissolved phosphorus.

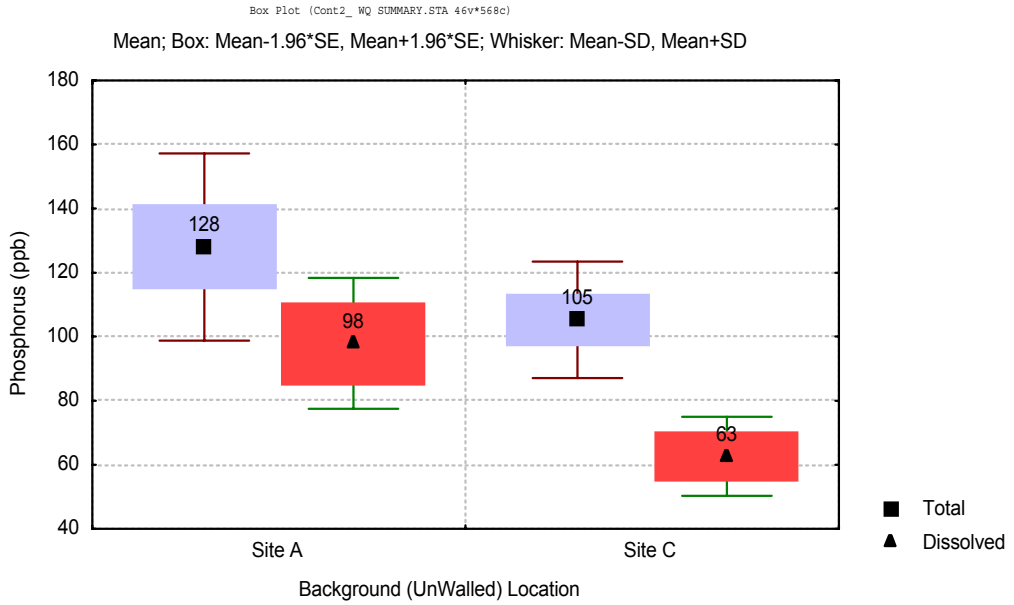

Figure 66. Temporal changes in total and dissolved phosphorus concentrations at Site A during February/March 2000 mesocosm study.
Total and dissolved phosphorus increased at Site A during the three week study.

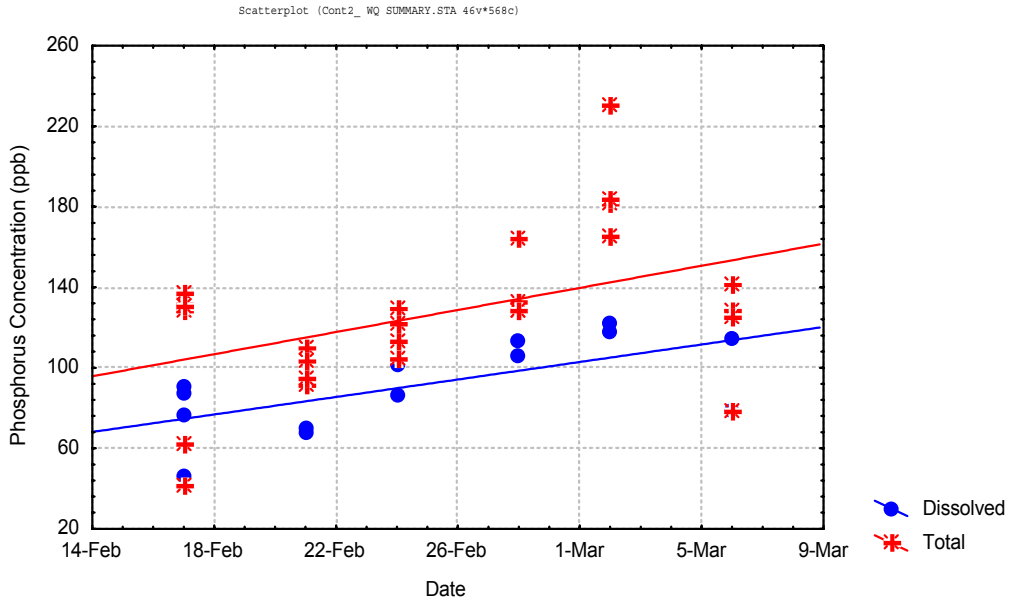

Figure 67. Temporal changes in total and dissolved phosphorus concentrations at Site C during February/March 2000 mesocosm study.
Phosphorus concentrations decreased slightly at Site C during the three week study.

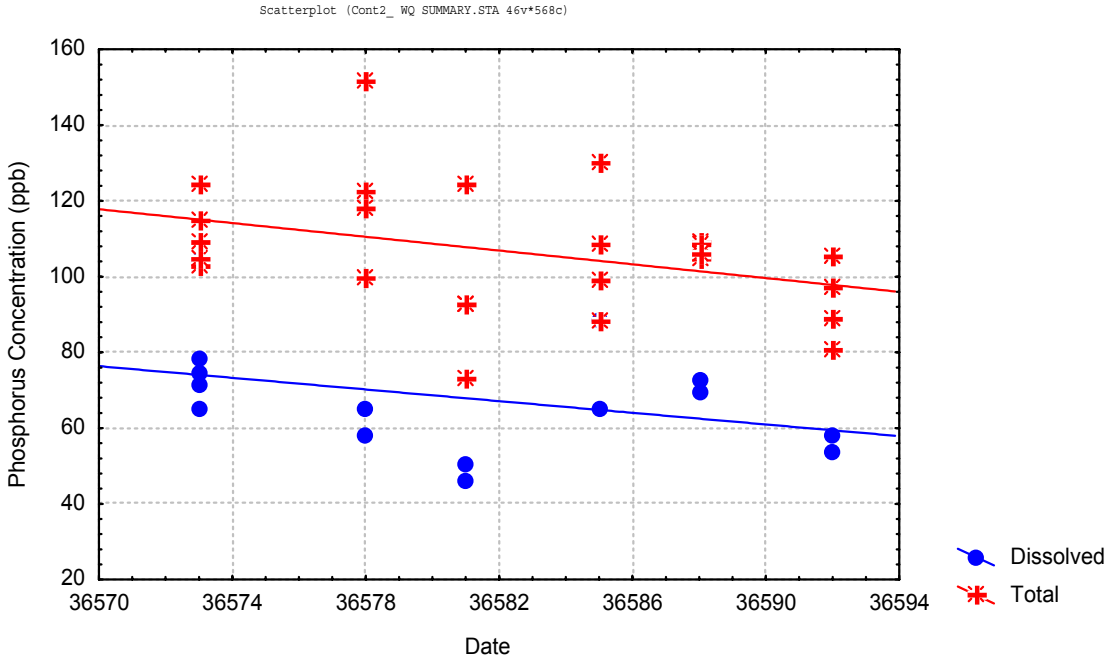

Mesocosm effects

Mesocosms exhibited differences with regard to total and dissolved phosphorus concentrations and uptake. In general, total and dissolved phosphorus concentrations differed significantly between the different mesocosms as shown by the error bars in Figure 68. In general, total phosphorus temporal trends in the Non-Dosed mesocosms mirrored those in the water column except for mesocosm C1 at Site C in which total phosphorus concentrations of approximately 50 μg L^{-1} were maintained regardless of background and inflow concentrations (Figure 69).

Figure 68. Total and dissolved phosphorus concentrations varied between sites and mesocosms, February/March 2000 Study.

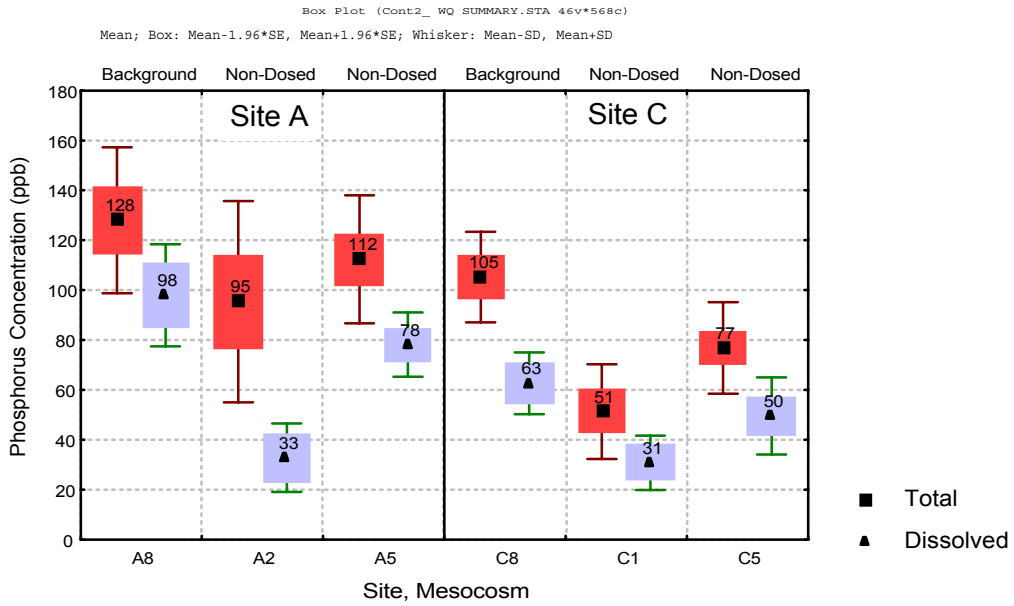

Figure 69. Temporal trends for total phosphorus concentrations in the Non-Dosed Mesocosms, February/March 2000 mesocosm study.
At Site A, phosphorus generally increased during the study whereas at Site C concentrations were relatively flat.

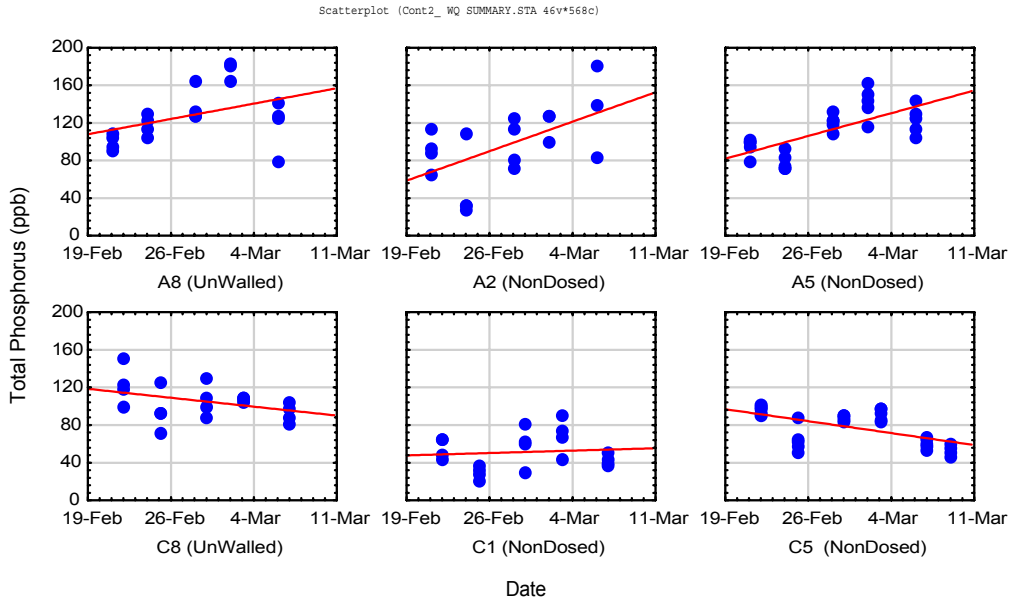

At Site A, dissolved phosphorus concentration trends in the Non-Dosed mesocosms generally mirrored background concentrations. Higher concentrations in the Non-Dosed mesocosms occurred as background concentrations rose (Figure 70). However, at Site C, the trends were less predictable with Mesocosm C5 experiencing continual declines in dissolved phosphorus despite constant background concentrations. Table 25 summarizes total and dissolved phosphorus uptake by the different Non-Dosed mesocosms. Both total and dissolved phosphorus uptake varied greatly between the four different mesocosms. The greatest reduction in total phosphorus concentrations occurred at mesocosm C1 with a decrease of 54 μg L^{-1}. The lowest reduction occurred at mesocosm A5 with a total phosphorus reduction of 16 μg L^{-1} occurring. The greatest reduction in dissolved phosphorus concentrations occurred in mesocosm A2 with a dissolved phosphorus reduction of 65 μg L^{-1}. The lowest reduction in dissolved phosphorus concentrations occurred in mesocosm C5 with a dissolved phosphorus reduction of 13 μg L^{-1} occurring.

Figure 70. Dissolved phosphorus temporal trends in the Non-Dosed Mesocosms during the February/March 2000 mesocosm study.

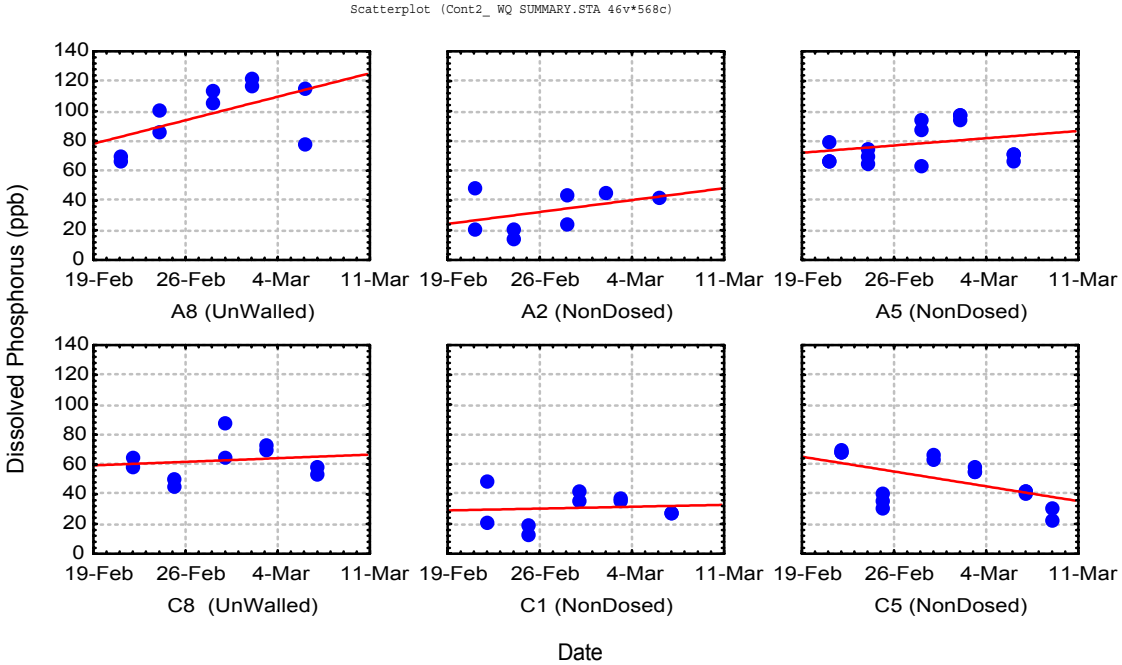

Table 25. Phosphorus uptake in Non-Dosed mesocosms during February/March 2000 study.

Values are in μg L-1

Site		Mesocosm:		
		A2	**A5**	**Average**
Site A	Total P	33	16	24
	Dissolved P	65	20	42
		C1	**C5**	**Average**
Site C	Total P	54	28	41
	Dissolved P	32	13	22

14.2.3.1.2. Inflow Analyses

Inflow analyses is defined as a comparison of phosphorus speciation before and after chemical addition (Figure 4). This analyses allows assessment of the first step in phosphorus removal by LICD, the effective formation of precipitates (Figure 1). This analyses was conducted to answer four fundamental questions:

- Are dosed waters lower in dissolved P than non-dosed waters?
- Are those effects greater for aluminum or iron?
- Are those effects PAM dependent?
- Are those effects dose dependent?

Dosed waters were clearly lower in dissolved phosphorus than non-dosed waters. After *in situ* dosing with both iron and aluminum blends, median dissolved phosphorus concentrations in the inflows were near 7 μg L^{-1} as opposed to 70 μg L^{-1} in the non-dosed waters (Figure 71). Thus, metal dosing reduced dissolved phosphorus concentrations by 90%. For seventy five percent of the samples, dissolved phosphorus concentrations were under 10 μg L^{-1} for aluminum dosing and were under 15 μg L^{-1} for iron dosing (Figure 71).

Figure 71. Nearly eliminating dissolved phosphorus in inflow waters with metal dosing.
Data included for iron and aluminum coagulants at dosing levels of 200 and 400 µM.

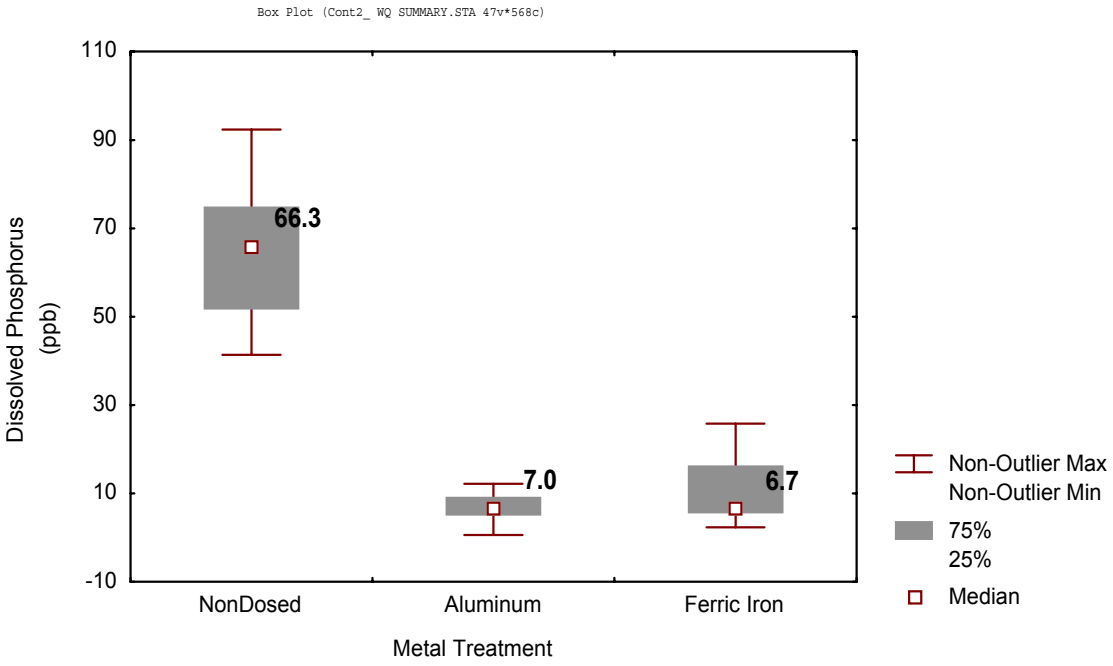

Dissolved phosphorus concentrations were generally lower for aluminum dosed treatments and these differences were statistically significant when assuming that each treatment had different variance (Table 26). This result needs to be understood in the context that dissolved phosphorus data was not normally distributed and that characteristic may affect the validity of the t-test result.

Table 26. T-test comparing dissolved phosphorus concentrations in inflow water to that in mesocosm water after aluminum and iron dosing treatments.
T-test for sample populations with different variances (StatSoft, 1998)

Treatment	Mean (µg L^{-1})	SD (µg L^{-1})	N	p-variance
Clarion 4100	10.5	2.9	20	0.000134
Ferriplus-D	6.8	7.6	19	

PAM dosing did not affect the dissolved phosphorus concentration. Median concentrations were all near 8 μg L^{-1} regardless of metal dosing level for both iron and aluminum blends (Figure 72). These data were normally distributed allowing comparison of means. Figure 72 shows that though there is greater difference between the means, dissolved phosphorus concentrations did not differ significantly ($p<0.05$) for either iron or aluminum dosing. This result is not surprising as PAM addition was not expected to improve precipitation of dissolved phosphorus but instead floc aggregation of precipitates formed after the addition of ferric iron or aluminum.

Metal dosing concentration effects on dissolved phosphorus reduction was considered. For aluminum, median dissolved phosphorus concentrations after metal dosing were 8.1 μg L^{-1} at 200 μM dosing and 6.4 μg L^{-1} at 400 μM dosing (Figure 73). Resulting dissolved phosphorus concentrations did not differ significantly for the different dosing levels using a T-test for populations with different variances ($p=0.734$;Table 27). As data was not normally distributed, the non-parametric Mann-Whitney U Test was also considered. Under that test, populations were not significantly different ($p=0.131$, Table 27). For ferric iron blends, median dissolved phosphorus concentrations were 12.6 μg L^{-1} at 200 μM, 6.5 μg L^{-1} at 400 μM and 6.3 μg L^{-1} at 600 μM. These values were very similar to their mean concentrations (Figure 74). Assuming a normal distribution of the data, dosing levels for iron significantly affected the resulting dissolved phosphorus concentrations as shown by the standard errors in Figure 74. T-test for populations with different variances show that dissolved phosphorus concentrations achieved with ferric iron dosing at 200 μM differed significantly with those achieved with ferric iron dosing at 400 μM ($p=0.023$; Table 28). If non-parametric tests were used, dissolved phosphorus concentrations for the different dosing levels did not differ significantly ($p=0.060$; Table 28). Thus, these differences may or may not differ significantly. However, at the higher metal dosing levels, variance in the data did decrease.

Figure 72. Dissolved phosphorus concentrations in treated inflow waters were generally unaffected by PAM dosing levels.

Metal dosing treatments of 200 and 400 µM were used in this data set. Median dissolved phosphorus concentration in background waters was 67 µg L^{-1} (Figure 71).

A. Median Values

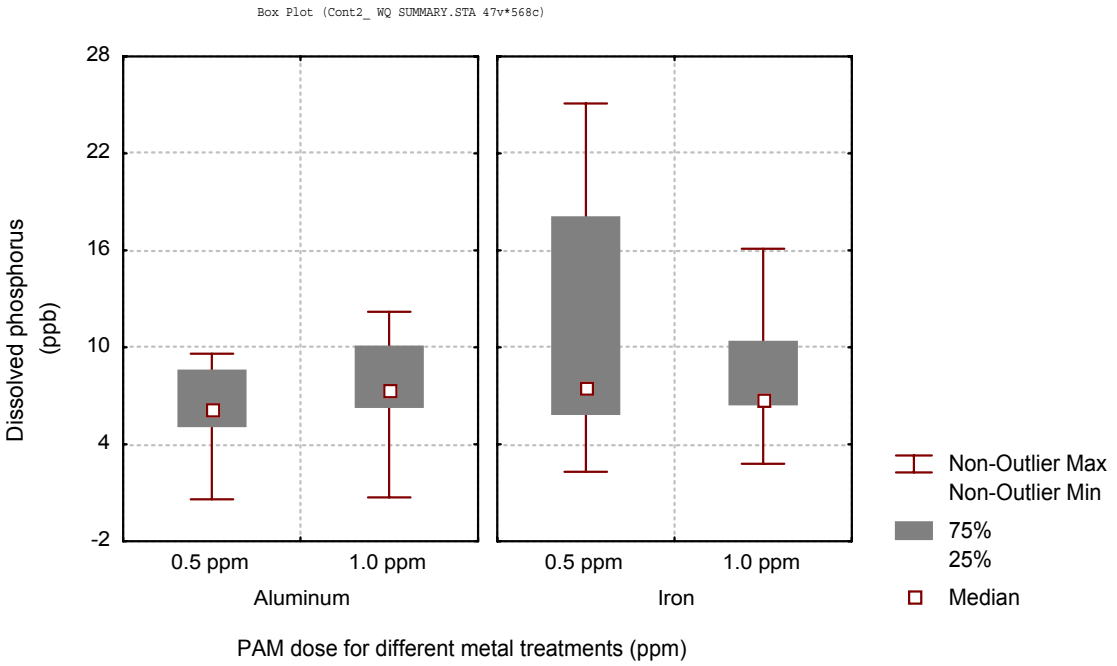

B. Mean Values

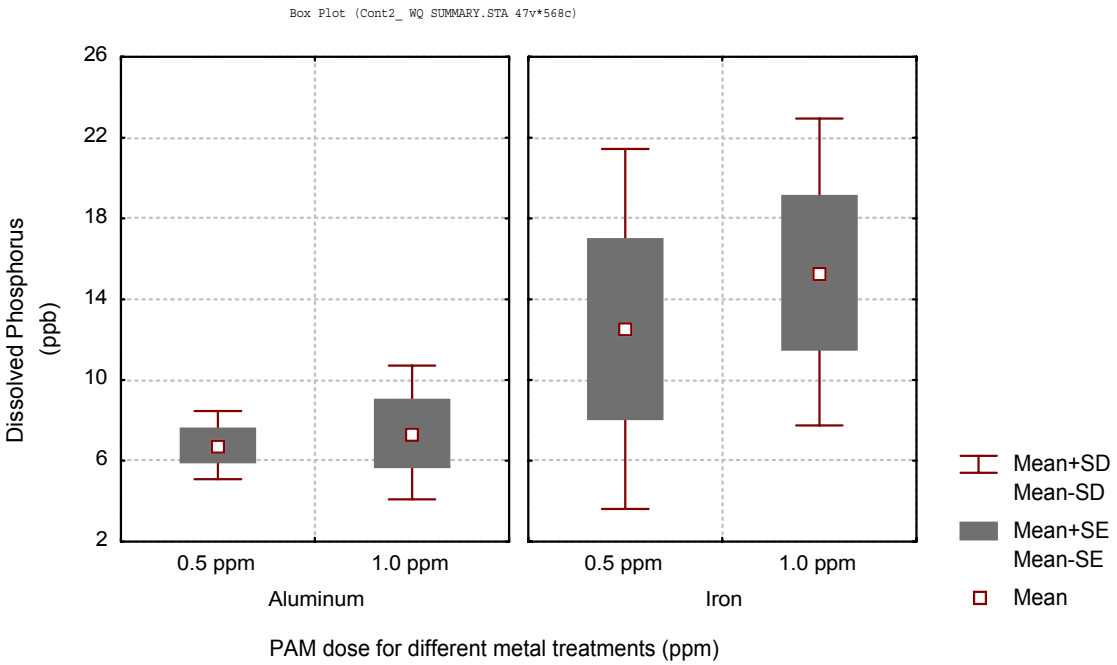

Figure 73. Higher aluminum dosing concentrations marginally decreased dissolved phosphorus concentrations in inflow waters.
Median dissolved phosphorus concentrations were 67 µg L^{-1}. Dissolved phosphorus did not show a normal distribution.

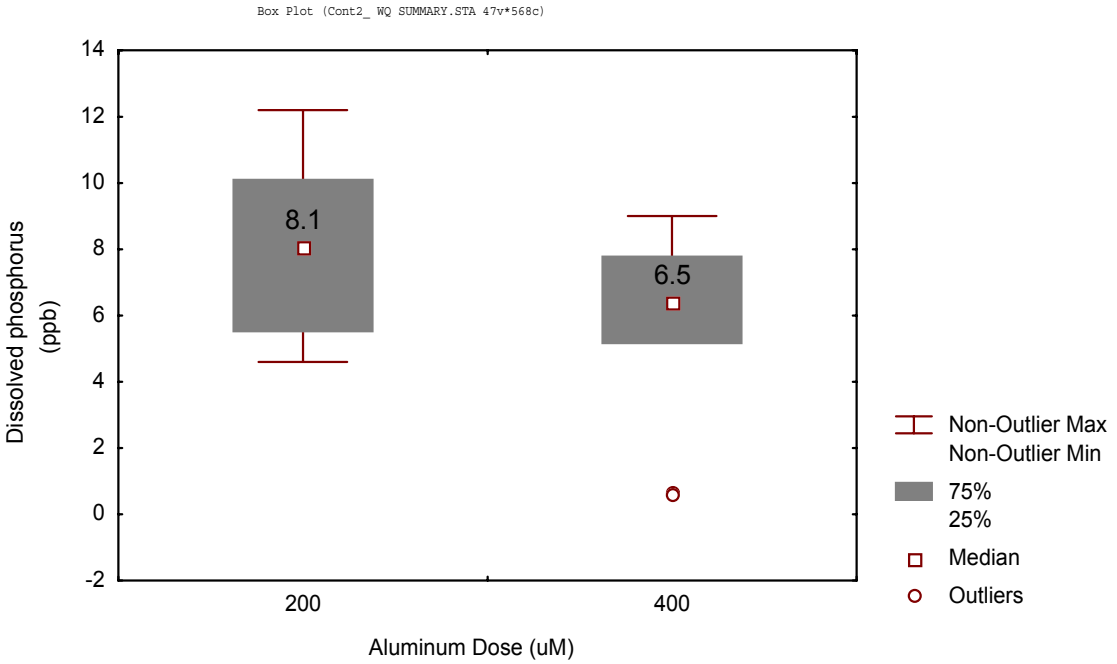

Table 27. T-test comparing dissolved phosphorus concentrations in inflow water to that in mesocosm water after aluminum dosing at different concentrations
T-test for sample populations with different variances (StatSoft, 1998)

Parametric w/different population variances				
Treatment	Mean (µg L^{-1})	SD (µg L^{-1})	N	p-value
200 µM	8.0	2.6	10	0.7340
400 µM	5.6	2.9	10	
Mann-Whitney U Test				
200 µM	---	---	10	0.1306
400 µM	---	---	10	

Figure 74. Dissolved phosphorus concentrations in inflow waters were slightly higher and more variable at lower dosing concentrations.
Median dissolved phosphorus concentrations were 67 µg L^{-1}.

A. Median values

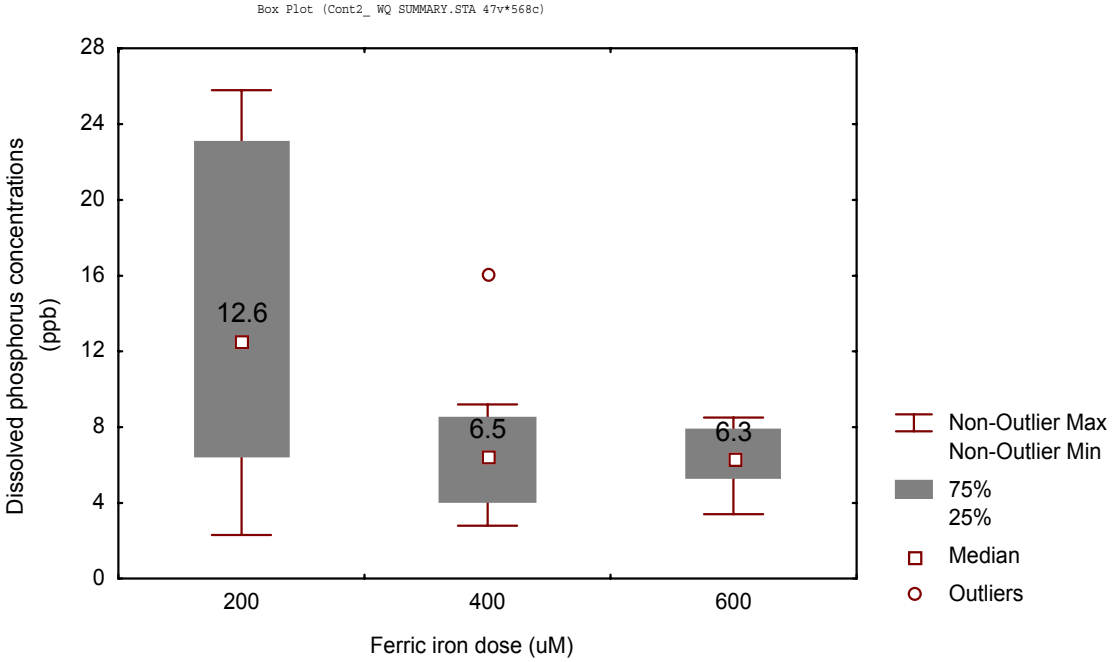

B. Mean Values

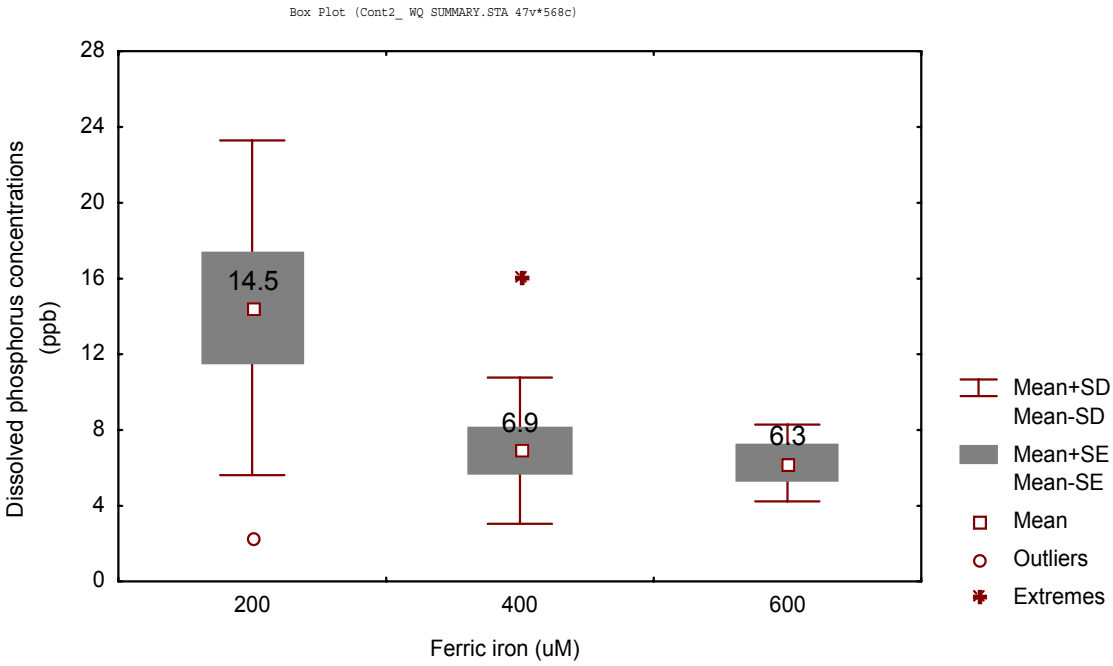

Table 28. T-test comparing dissolved phosphorus concentrations in inflow water to that in mesocosm water after ferric iron dosing at 200 and 400 µM.

T-test for sample populations with different variances (StatSoft, 1998)

Parametric w/different population variances Treatment	Mean (µg L^{-1})	SD (µg L^{-1})	N	p-value
200 µM	14.5	8.9	9	0.02313
400 µM	6.9	3.9	10	
Whitney U Test Mann-				
200 µM	---	---	9	0.06040
400 µM	---	---	10	

14.2.3.1.3. Mixing Tank

Mixing tank data was next considered to investigate phosphorus removal without macrophyte effects. Grab samples were collected from the mixing tanks approximately at their midpoint in the water column. Samples were collected between 9:00 AM and 1:00 PM. As water pumping started at 1:30 and continued till around 4:00 PM, mixing tank samples were collected a minimum of 19 hours after the pumping discontinued and therefore represented samples collected with an approximate one day detention time. Mixing tanks were cleaned before the beginning of the study and were free of attached algal at the initiation of the study. For aluminum and iron treatments, water sampled from the mixing tanks had been dosed with both metals and polymers, and undergone rapid and slow mixing.

Mixing tank data was collected to determine several questions with regard to water column phosphorus concentrations after one day HRT:

- Did dosed waters continue to be lower in dissolved phosphorus concentrations than non-dosed waters?
- Are dosed waters lower in total phosphorus than non-dosed waters?
- Is aluminum or iron more effective with regard to creating settleable particulate phosphorus?
- Are total phosphorus concentrations dependent upon metal dosing levels?
- Do PAMs affect the resulting total phosphorus concentrations?
- Which blends were most effective at creating settleable particulate phosphorus?

Dosed waters were lower in both dissolved phosphorus and total phosphorus concentrations (Figure 75). Median dissolved phosphorus concentration in the non-dosed tanks was 30 μg L^{-1}. This was lower than dissolved phosphorus concentrations in the inflow of 67 μg L^{-1} (Figure 71) and suggests that biotic uptake occurred in the mixing tanks leading to a reduction in dissolved phosphorus. In both the iron and aluminum treatments, median dissolved phosphorus concentrations of near 5 μg L^{-1} were achieved. This was only 8% of background levels and 17% of non-dosed levels. Assuming a normal distribution and different population variances, resulting dissolved phosphorus concentration differed significantly for aluminum and iron (Table 29; p = 0.00008). However, there was some deviation from the assumption of normal distribution. Thus, for the non-parametric Mann U Test, dissolved phosphorus concentrations did not differ significantly (Table 29, p=0.0653).

Median total phosphorus concentrations in the NonDosed mixing tanks were approximately 60 μg L^{-1} (Figure 75) which were lower than inflow background concentrations of 116 μg L^{-1}. Thus, in the mixing tanks, approximately 50% of total phosphorus was removed through uptake and settling. Median total phosphorus concentrations were 18 μg L^{-1} for aluminum dosing and 25 μg L^{-1} for iron dosing. For aluminum dosing, resulting total phosphorus concentrations in the mixing tanks were 31% of those for the non-dosed treatments and 16% of background levels. For ferric iron dosing, resulting total phosphorus concentrations in the mixing tanks were 43% of non-dosed treatment levels and only 28% of background levels. Thus, in the mixing tanks receiving aluminum dosing, 84% removal of total phosphorus was achieved and in the mixing tanks receiving ferric iron dosing, 72% of total phosphorus was removed.

Table 29. T-test comparing dissolved phosphorus concentrations in mixing tank waters for aluminum and iron blend dosing treatments.

T-test for sample populations with different variances (StatSoft, 1998)

Parametric w/different population variances Treatment	Mean (μg L^{-1})	SD (μg L^{-1})	N	p-value
Aluminum	5.5	2.4	20	0.00008
Ferric Iron	8.5	6.3	19	
Mann-Whitney U Test				
Aluminum	---	---	9	0.06528
Ferric Iron	---	---	10	

Figure 75. Total and dissolved phosphorus concentrations in mixing tanks after one day period of quiescent water.
Data does not include metal dosing data at 600 µM as that data was invalid for aluminum.

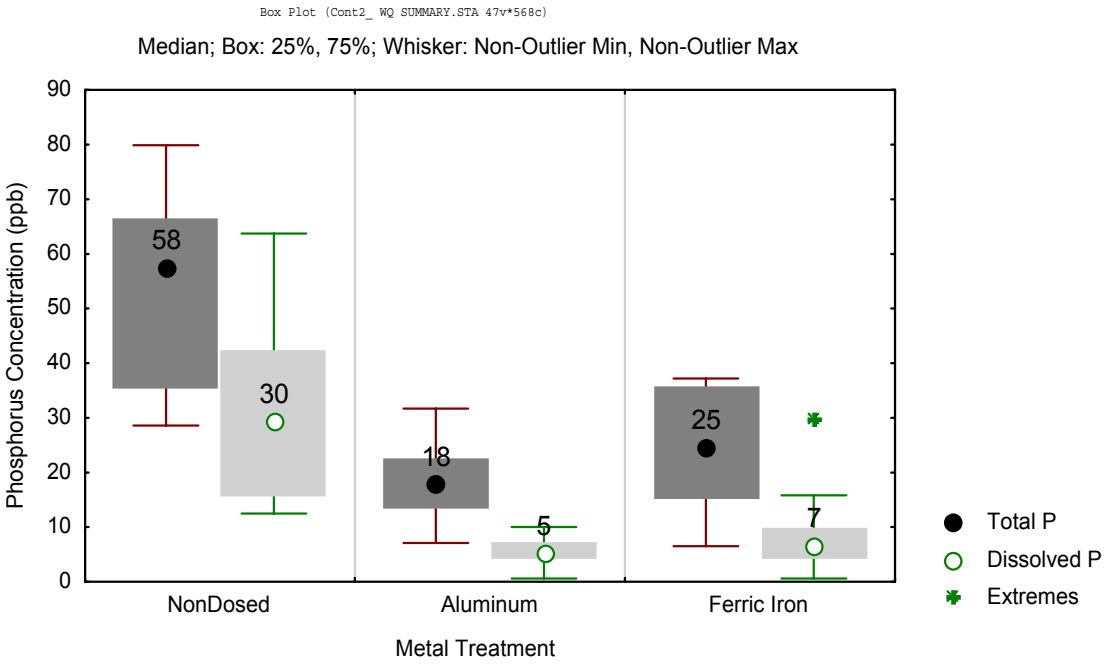

Total phosphorus concentrations achieved from chemical dosing did not differ statistically for the different PAM concentrations shown (p=0.3768). For aluminum dosing, higher PAM concentrations appeared to lead to higher total phosphorus concentrations (Figure 76). For iron dosing, total phosphorus was fairly similar for the different PAM dosing levels.

Total phosphorus concentrations were lower for higher metal dosing levels for both aluminum and iron (Figures 77 and 78). These differences did not differ statistically for aluminum (T-test: p=0.486). They also did not differ statistically for iron dosing at the 200 and 400 µM. Higher iron dosing levels decreased variability in the data.

Figure 76. Total phosphorus concentrations achieved in mixing tanks after one day HRT for different PAM dosing levels.

Data do not include 600 µM metal dosing data as data was not available for aluminum. Thus, data are from metal dosing levels of 200 and 400 µM.

A. Mean Values

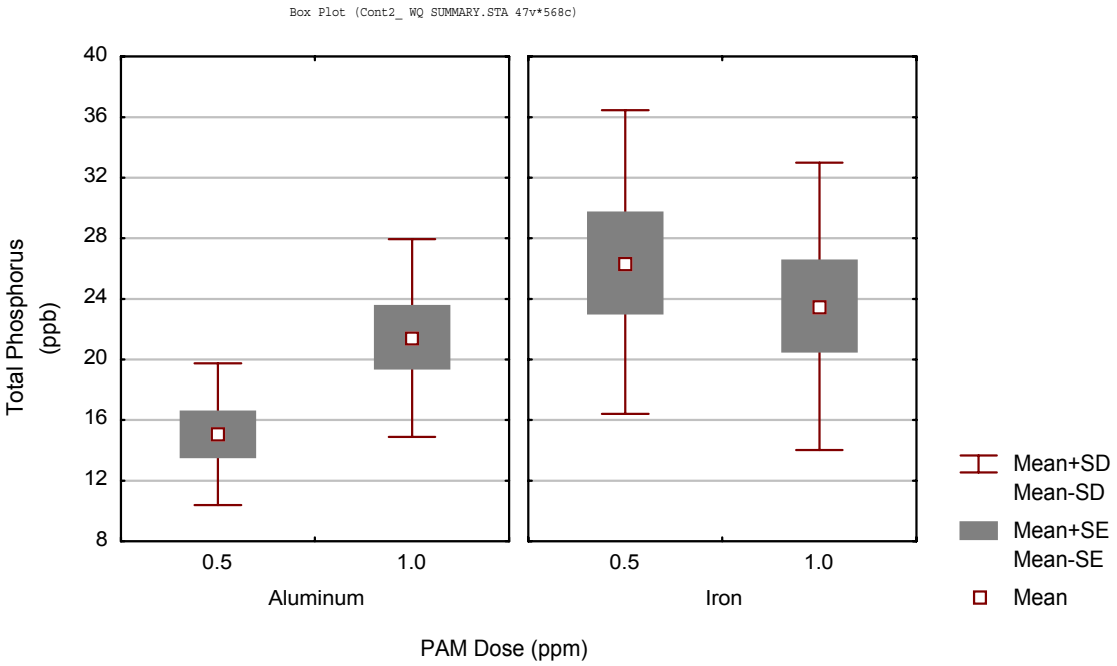

B. Median Values

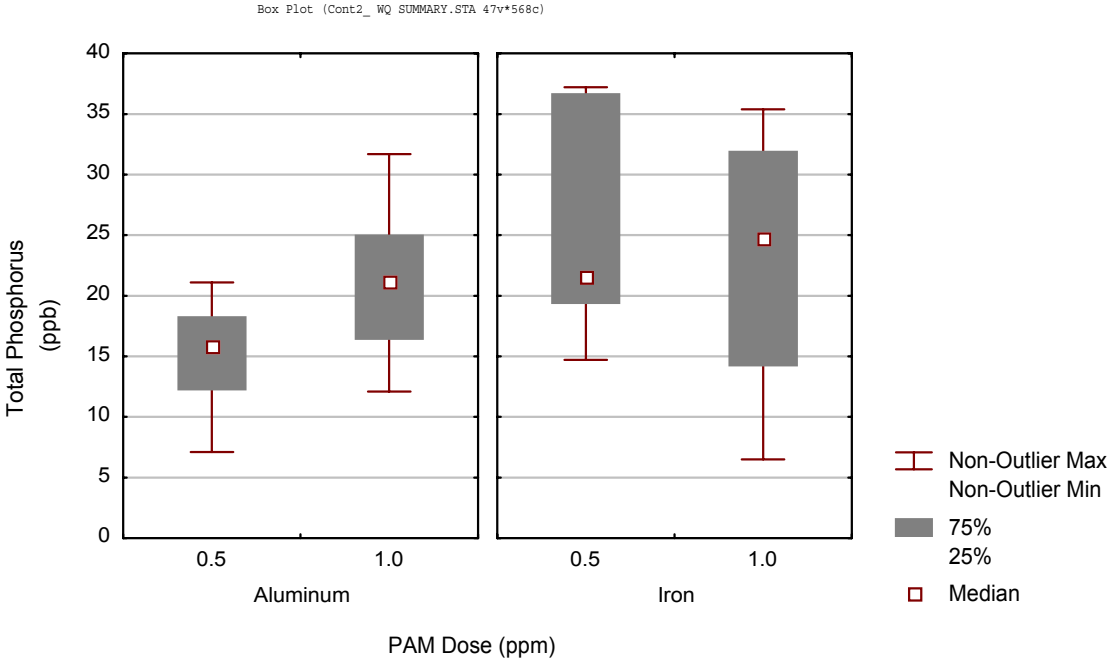

Figure 77. Metal dosing effects on mixing tank total and dissolved phosphorus concentrations after one day HRT under Aluminum dosing.

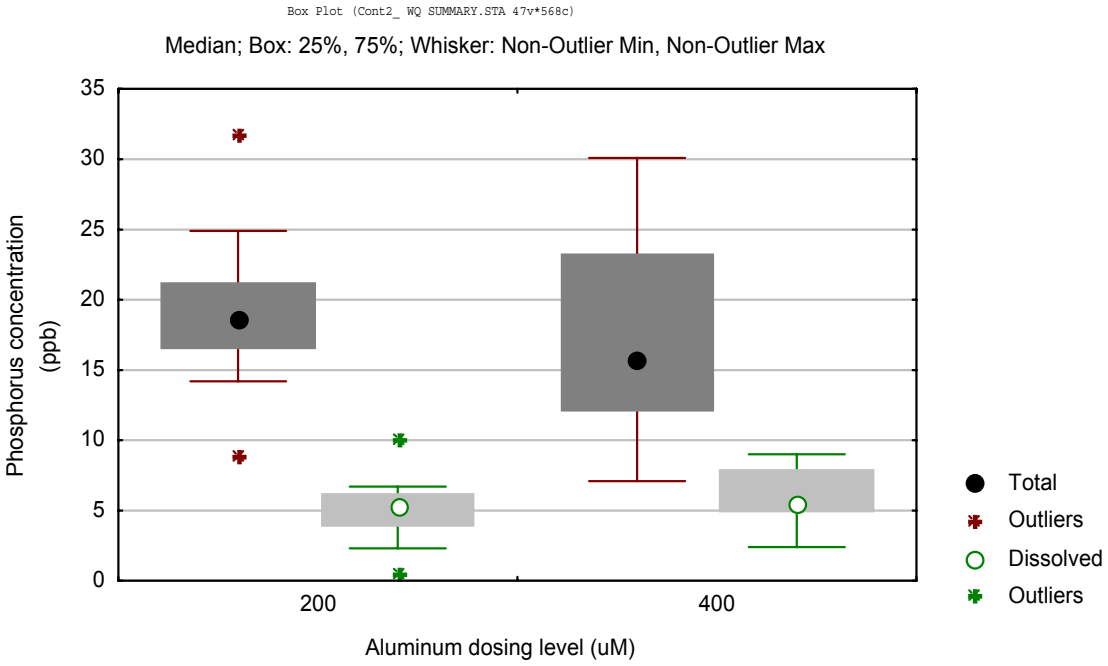

Figure 78. Metal dosing effects on mixing tank total and dissolved phosphorus concentrations after one day HRT under iron dosing.

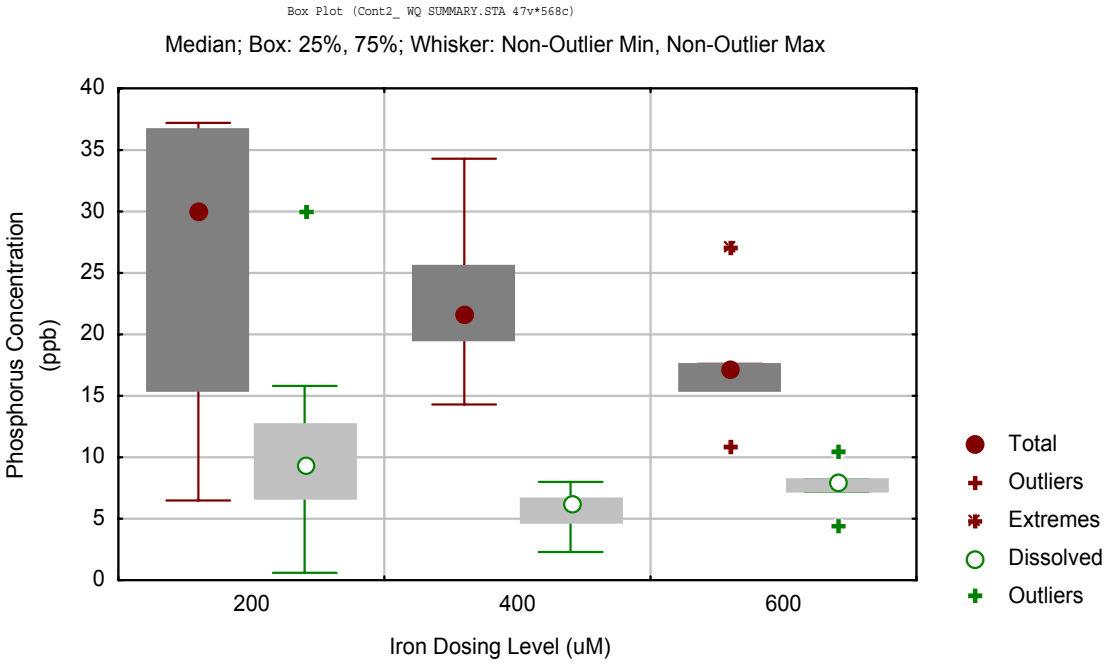

As a final step in the analyses, individual mixing tank data was reviewed. For ferric iron dosing, higher metal dosing levels achieved slightly lower total phosphorus concentrations and slightly higher percent removal (Figure 79). PAMs appeared to effect phosphorus removal slightly. At 400 μM Fe dosing, resulting total phosphorus concentrations were similar. However, at the lower dosing level of 200 μM, a PAM dose of 0.5 mg L^{-1} only achieved median total phosphorus concentrations of 37 mg L^{-1} as opposed to 24 mg $^{-1}$ for PAM dosing at 1.0 mg L^{-1}. Total phosphorus removal ranged from 71% to 87%.

For aluminum dosing, dosing concentration did not improve total phosphorus removal and PAM dosing also had no noticeable affect (Figure 80). Total phosphorus removal ranged from 82% to 88%.

Removal rates under both iron and aluminum dosing were higher than has been typical in the field studies. Previous field studies (in which metal was dosed at 200 μM during Phase I and Phase II) achieved total phosphorus removal of 21% to 48% (Table 30). The minimum mean total phosphorus concentration achieved for any of those examples was 22 μg L^{-1}. In the mixing tanks, metal dosing concentrations of 200 μM achieved removal rates of 71% to 86%. The minimum mean total phosphorus concentration for any of these treatments (e.g. iron and aluminum at 200 μM) was 18 μg L^{-1} (Figures 79 and 80; Table 30).

Figure 79. Total and dissolved phosphorus concentrations achieved in the mixing tanks for iron dosing treatments from 0 – 600 µM.

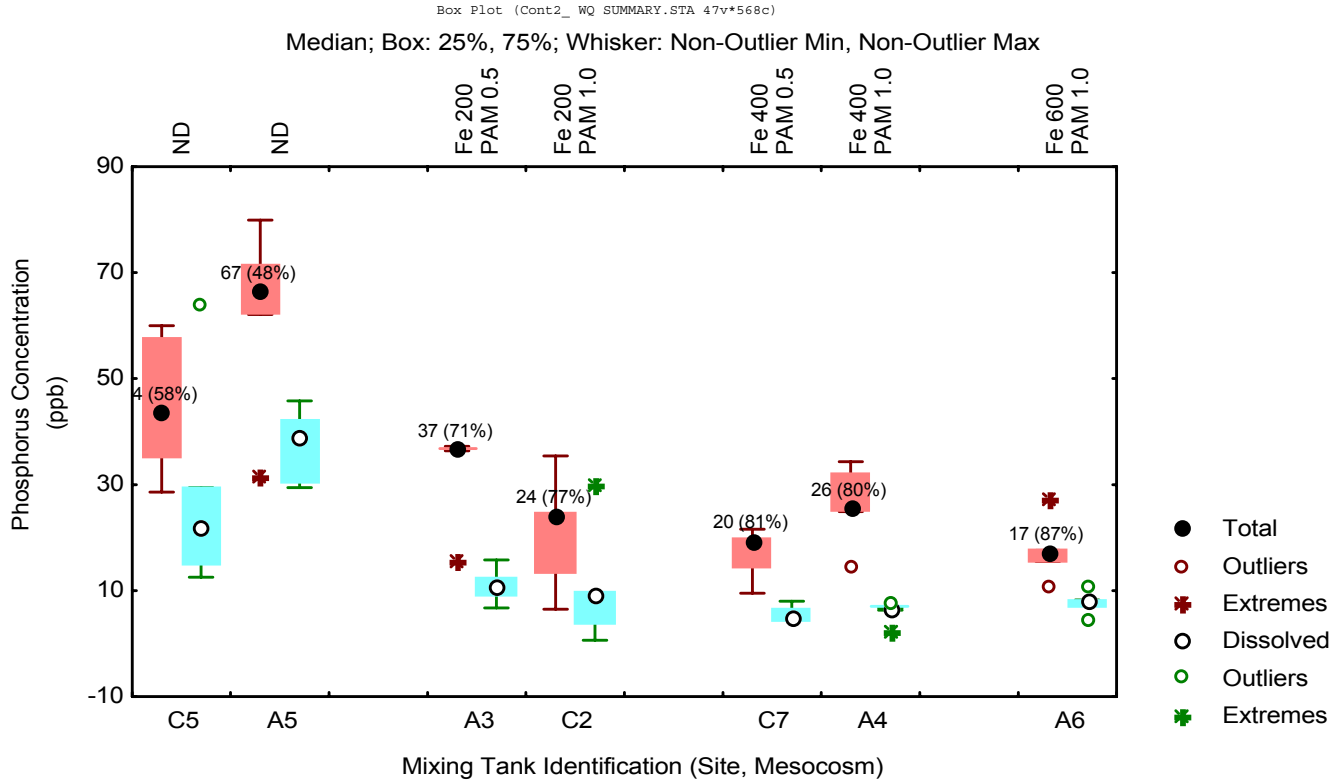

In summary, the mixing tank data show the following findings.

- Less than one day HRT in the mixing tanks provided large reductions in total phosphorus
- Total and dissolved phosphorus concentrations were much lower in mixing tanks receiving metal treatments
- Median total phosphorus concentrations were 18 $\mu g\ L^{-1}$ for aluminum dosing and 25 $\mu g\ L^{-1}$ for ferric iron dosing. This represented a 72% and 84% reduction in total phosphorus below background levels for the respective treatments.
- Under aluminum dosing, median total phosphorus concentrations achieved were generally equivalent for different PAM doses. For iron dosing, PAM dosing levels did affect total phosphorus concentrations at iron dosing levels of 200 μM.
- Different metal dosing levels did not statistically improve total phosphorus removal for either aluminum or iron.
- Percent total phosphorus removal was much higher than measured previously in the mesocosms and lower total phosphorus concentrations were achieved.
- For iron dosing, all metal dosing levels have provided equivalent results (200, 400 and 600 μM). A PAM dosing level of 1 $mg\ L^{-1}$ is recommended, especially at lower iron dosing levels. For aluminum dosing, all metal/PAM dosing combinations provided similar results. These dosing recommendations may differ from recommendations in larger-scale systems or more biologically active systems.

Figure 80. Total and dissolved phosphorus concentrations achieved in the mixing tanks for aluminum dosing treatments from 0 – 400 µM.

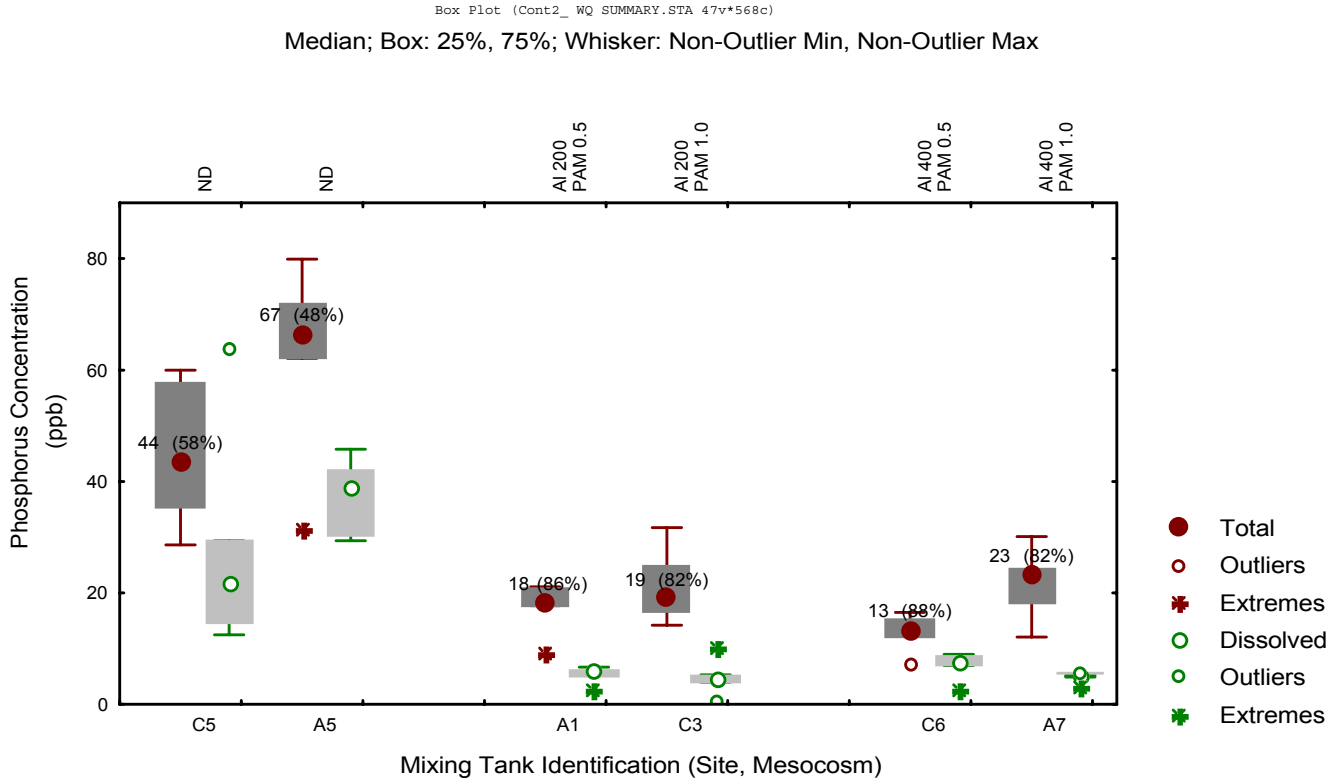

Table 30. Summary of PAM effects on total phosphorus concentrations for all LICD field studies.
Data summary is for metal dosing at 200 μM for Phase I and Phase II LICD.

Period	Configuration	Site	Metal Blend	PAM Dose (ppm)	Background Total P Concentrations (ppb)	Resulting Total P Concentration (ppb)	Removal %	References
Ferric Iron dosing at 200 uM								
Dec 98 - Feb 99	Continuous	A	FeCl	0.00	42	31	26	Bachand et al., 1999
Mar - April 99	Batch	A	FeCl	0.00	42	22	48	Bachand et al., 1999
Oct 99	Batch	A, B, C	FeCl	0.00	80	63	21	Figs 48, 52
		A	FeCl	0.25	96	68	29	Figs 48, 52, 54
		C	FPD	0.25	75	55	27	Figs 48, 54
Feb - Mar 00	Continuous	A (Mix)	FPD	0.50	128	36	72	Fig 79
		C (Mix)	FPD	1.00	105	24	77	Fig 79
		A	FPD	0.50	128	102	20	Fig 85
		C	FPD	1.00	105	29	72	Fig 85
Aluminum dosing at 200 uM								
Dec 98 - Feb 99	Continuous	A	Alum	0.00	42	27	36	Bachand et al., 1999
Oct 99	Batch	A, B	Alum	0.00	83	50	40	Figs 48, 52
		A	Alum	0.25	96	65	32	Figs 48, 58
		B	Clarion	0.25	70	48	31	Figs 48, 58
Feb - Mar 00	Continuous	C (Mix)	Clarion	0.50	105	18	83	Fig 80
		A (Mix)	Clarion	1.00	128	19	85	Fig 80
		C	Clarion	0.50	105	77	27	Fig 85
		A	Clarion	1.00	128	39	70	Fig 85

14.2.3.1.4. Mesocosm

Figure 81 shows total phosphorus concentrations achieved from the different metal blends treatments during this study. Figure 82 shows dissolved phosphorus concentrations achieved for the different metal blends during this study.

Dissolved phosphorus was effectively removed from the water column for all treatments. Median background dissolved phosphorus concentrations were 98 $\mu g\ L^{-1}$ at Site A and 63 $\mu g\ L^{-1}$ at Site C (Figure 82). Median dissolved phosphorus concentrations in the Non-Dosed treatments ranged from 31 $\mu g\ L^{-1}$ to 78 $\mu g\ L^{-1}$. Samples in the middle quartiles (25% to 75%) generally covered a range of around 20 $\mu g\ L^{-1}$ for both background and Non-Dosed treatments. Metal treatments decreased dissolved phosphorus concentrations dramatically with median dissolved phosphorus concentrations ranging from 7 to 14 $\mu g\ L^{-1}$. Sample variance was also decreased with phosphorus concentrations in the 25% to 75% quartiles covering from 5 to 10 $\mu g\ L^{-1}$. Dissolved phosphorus concentrations for the different metal polymer blends did not show any apparent relationship with metal coagulant (e.g. iron, aluminum), metal dose or PAM dose.

Figure 81. Total phosphorus concentrations achieved in mesocosms for various coagulant blends and dosing levels, February/March 2000 mesocosm study.

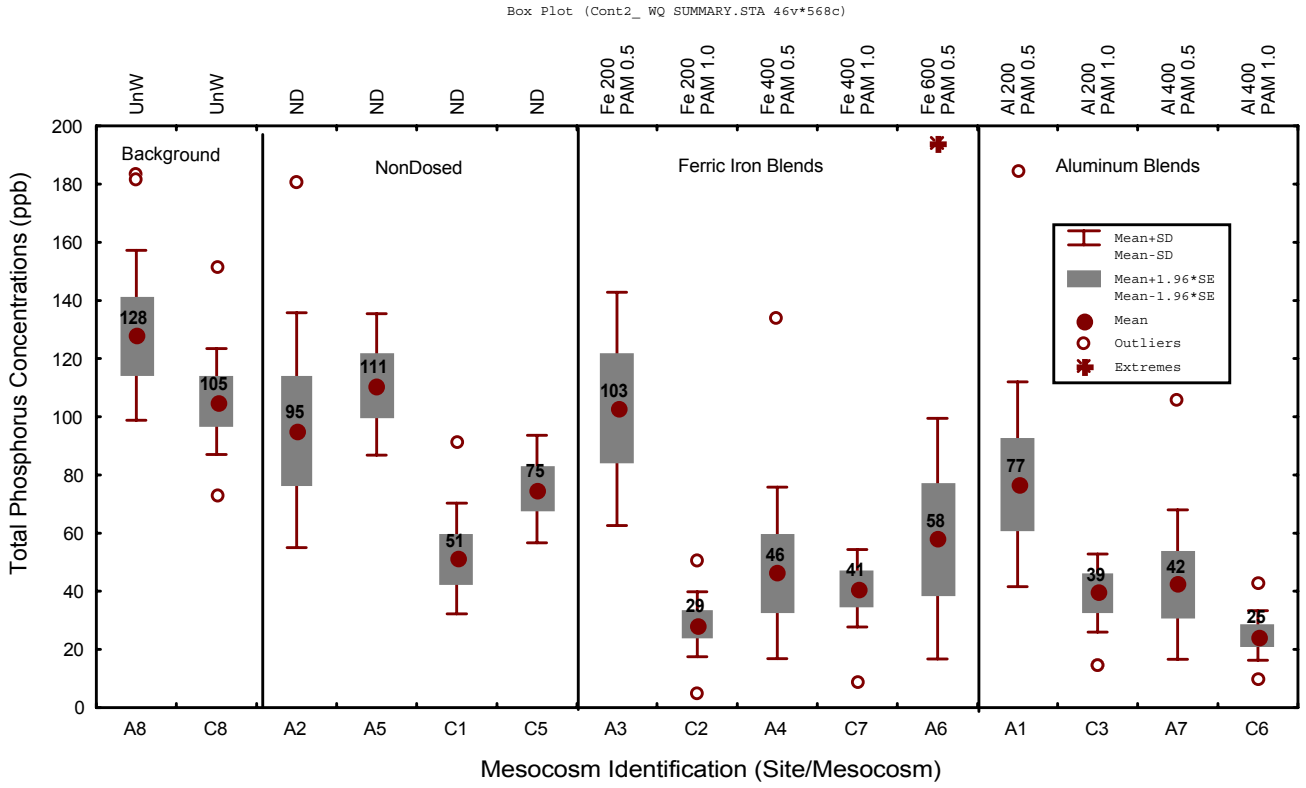

Figure 82. Dissolved phosphorus concentrations achieved in mesocosms for various coagulant blends and dosing levels, February/March 2000 mesocosm study.

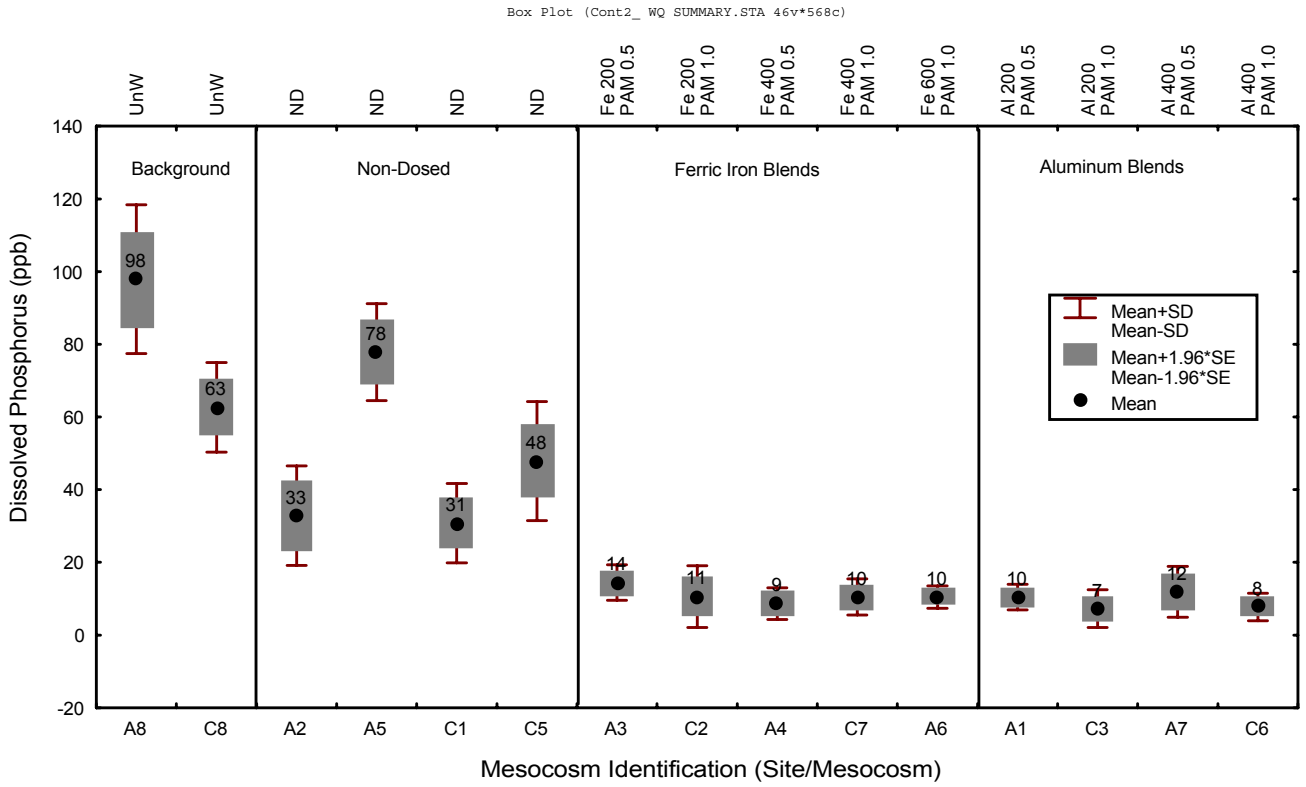

Median total phosphorus concentrations ranged from 105 to 128 μg L^{-1} depending upon the Site (Figure 81). In the Non-Dosed treatments, median total phosphorus concentrations ranged from 51 to 111 μg L^{-1} and were higher in the Non-Dosed treatments at Site A. The two middle quartiles for total phosphorus generally covered a range of approximately 20 μg L^{-1}.

Median total phosphorus concentrations for mesocosms receiving iron dosing ranged from 29 to 103 μg L^{-1} (Figure 81). The poorest treatment was iron dosing at 200 μM with a PAM dose of 0.5 mg L^{-1}. That treatment resulted in median total phosphorus concentrations of 103 μg L^{-1} for a percent removal of 24%. The best treatment also received iron dosing of 200 μM but had a PAM dose of 1.0 mg L^{-1}. That treatment achieved median total phosphorus concentrations of 29 μg L^{-1} for a percent removal of 72%. This treatment had much better performance than previous mesocosm studies receiving iron treatment. Previously, a maximum of 48% total phosphorus removal had been achieved for iron dosing at 200 μM (Table 30). These results demonstrate that PAM dosing greatly improves particulate phosphorus removal in Everglades waters.

The data also suggests that for treatments in which phosphorus effectively settles, higher metal doses lead to poorer phosphorus removal. This conclusion needs to be considered in light of site effects. Site A had higher inflow total phosphorus concentrations than Site C. Total phosphorus concentrations resulting from iron dosing were higher at Site A than Site C and this suggests site effects and a dependence upon initial phosphorus concentrations (Figure 83).

Median total phosphorus concentrations for mesocosms receiving aluminum dosing ranged from 25 to 77 μg L^{-1}. The poorest treatment was aluminum dosing at 200 μM and PAM dosing at 0.5 mg L^{-1}. As with iron, these results suggest that PAM addition improves particulate precipitation and aggregation under metal dosing. For aluminum dosing of 200 μM and PAM dosing of 0.5 mg L^{-1}, median total phosphorus concentrations were 77 μg L^{-1} for a removal rate of 40%. For the same aluminum dosing concentration but with PAM dosing of 1.0 mg L^{-1}, median total phosphorus concentrations were 39 μg L^{-1} for a removal rate of 70%. As with iron, removal rates in this study exceeded those in previous Phase I and Phase II LICD studies. Total phosphorus removal rates ranged from 31 to 40% for the previous mesocosm batch-flow and continuous-flow studies. In this study, removal rates were consistently higher and generally above 70% (Table 30). For both metals, metal dosing concentrations seemed to minimally effect the resultant mesocosm total phosphorus concentrations (Figure 81).

Figure 83. Total phosphorus concentrations achieved in dosed mesocosms varied between sites.
Each site had aluminum and iron treatments of 200 and 400 µM..

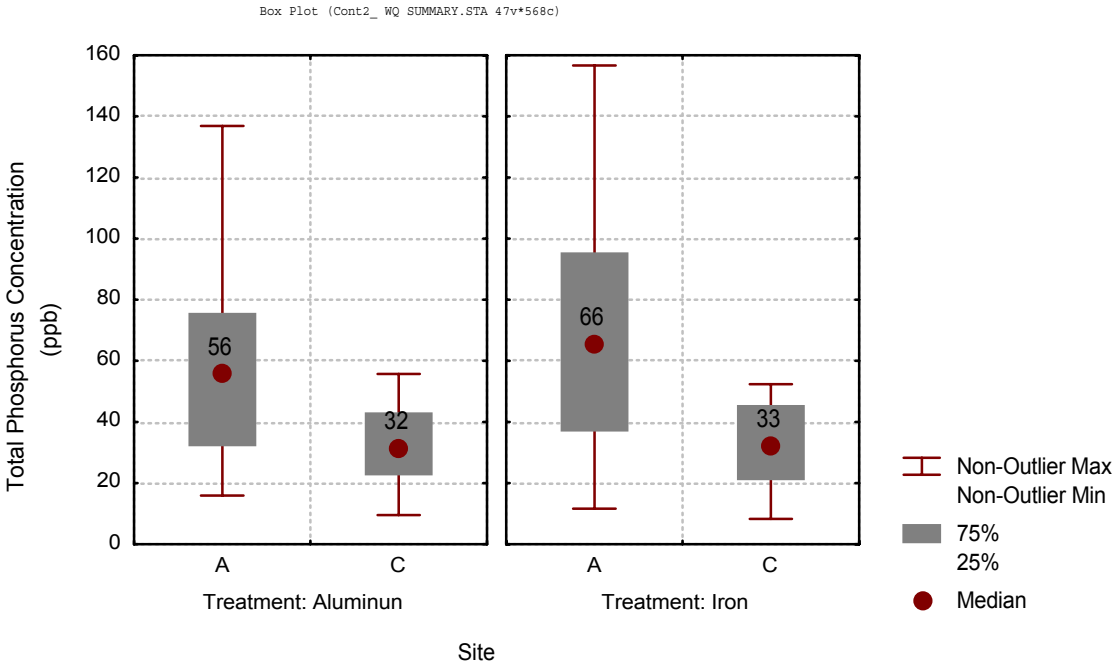

Based upon the results we further investigated several factors that may affect final phosphorus concentrations using a variety of statistical tests. These factors included:

- Site effects
- Initial phosphorus concentrations
- Metal dosing levels
- PAM concentrations

Site effects were investigated by comparing the resultant phosphorus concentrations achieved after chemical dosing at each site with parametric and nonparametric statistical tests. At each site, aluminum and iron were dosed at 200 and 400 µM and PAM doses of 0.5 and 1.0 mg L^{-1} (Table 18). Thus, each site received similar though not exact treatments.

Figure 83 shows resulting total phosphorus concentrations for iron and aluminum treatments. Median total phosphorus concentrations for Site A mesocosms under iron dosing were 66 µg L^{-1} at Site A as opposed to 33 µg L^{-1} at Site C. For aluminum dosing, medium concentrations are 56 µg L^{-1} at Site A and 32 µg L^{-1} at Site C. Parametric and non-parametric statistical tests were conducted. Both

tests showed that resultant total phosphorus concentrations from chemical dosing differed for the different sites for both aluminum and iron dosing at 200 and 400 μM (Table 31). Thus, there is a site effect which is likely in part do to background phosphorus concentrations.

Table 31. T-test comparing resultant total phosphorus concentrations at different sites after iron and aluminum dosing of 200 and 400 μM, February/March 2000.
T-test for sample populations with different variances (StatSoft, 1998)

Aluminum				
Parametric w/different population variances				
Site	Mean (μg L^{-1})	SD (μg L^{-1})	N	p-value
A	55.7	29.8	22	0.0010
C	33.1	13.8	20	
Mann-Whitney U Test				
A	---	---	22	0.0050
C	---	---	20	
Ferric Iron				
Parametric w/different population variances				
A	71.0	42.0	20	0.0000
C	32.5	13.2	18	
Mann-Whitney U Test				
A	---	---	20	0.0024
C	---	---	18	

The effects of different metal dosing levels were tested for both aluminum and iron coagulants using parametric and nonparametric statistical tests. Total phosphorus concentrations did not differ statistically for different aluminum dosing concentrations under a T-test assuming different variances for each dosing level (Table 32). This assumed a normal distribution for the sample populations. Under the Mann U Whitney non-parametric alternative which has no distribution assumptions, total phosphorus concentrations differed significantly for the different aluminum dosing levels. Median total phosphorus concentrations were 28 μg L^{-1} for 200 μM dosing and 40 μg L^{-1} for 400 μM dosing (Figure 84). For iron dosing, total phosphorus concentrations did not differ significantly with either test (Table 32). Both dosing levels achieved median total phosphorus concentrations near 40 μg L^{-1} (Figure 84). Thus, different iron dosing levels did not significantly affect resultant phosphorus concentrations. Different aluminum dosing levels may have significantly affected resultant total phosphorus

concentrations though that result depends upon the statistical assumptions and analyses used.

Figure 84. The effects of metal dosing levels on phosphorus levels achieved in mesocosms.
Data are for aluminum and iron dosing levels of 200 and 400 µM at Sites A and C during February/March 2000 mesocosm study.

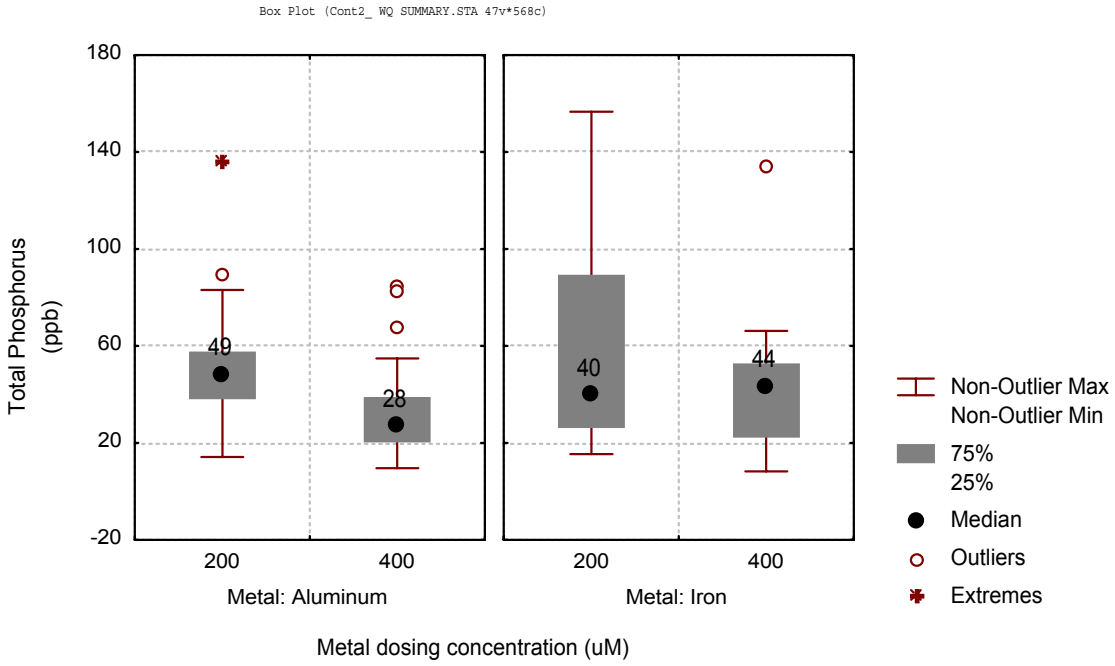

Table 32. T-test comparing total phosphorus concentrations achieved for different metal dosing concentrations, February/March 2000.

T-test for sample populations with different variances (StatSoft, 1998)

Aluminum				
Parametric w/different population variances				
Dose	Mean ($\mu g\ L^{-1}$)	SD ($\mu g\ L^{-1}$)	N	p-value
200 µM	52.5	25.6	22	0.4748
400 µM	34.3	21.7	20	
Mann-Whitney U Test				
200 µM	---	---	22	0.0039
400 µM	---	---	20	
Ferric Iron				
Parametric w/different population variances				
Dose	Mean ($\mu g\ L^{-1}$)	SD ($\mu g\ L^{-1}$)	N	p-value
200 µM	57.3	40.8	20	0.1425
400 µM	43.4	28.5	18	
Mann-Whitney U Test				
200 µM	---	---	20	0.4829
400 µM	---	---	18	

For aluminum dosing, total phosphorus concentrations did not differ statistically for different PAM dosing levels used in this study (Table 33). For iron dosing, total phosphorus concentrations were not statistically different when using a T-test for populations with different variances (p=0.1349). However, as typical of the data, total phosphorus concentrations do not follow a normal distribution. Thus, the Mann-Whitney U Test which is a non-parametric alternative gave conflicting results showing the total phosphorus concentrations differed significantly for different dosing concentrations (p=0.0130; Mann-Whitney U Test). Figure 85 shows total phosphorus concentrations achieved under the different PAM dosing levels for both aluminum and ferric iron. Total phosphorus concentrations were generally lower for higher PAM dosing levels when using ferric iron blends.

Table 33. T-test comparing total phosphorus concentrations achieved for different PAM dosing levels, February/March 2000.

T-test for sample populations with different variances (StatSoft, 1998)

Aluminum				
Parametric w/different population variances				
Dose	Mean ($\mu g\ L^{-1}$)	SD ($\mu g\ L^{-1}$)	N	p-value
0.5 mg L^{-1}	45.7	30.7	22	0.0509
1.0 mg L^{-1}	42.2	20.0	20	
Mann-Whitney U Test				
0.5 mg L^{-1}	---	---	22	0.0504
1.0 mg L^{-1}	---	---	20	
Ferric Iron				
Parametric w/different population variances				
0.5 mg L^{-1}	64.4	39.4	20	0.1349
1.0 mg L^{-1}	38.4	27.6	18	
Mann-Whitney U Test				
0.5 mg L^{-1}	---	---	20	0.0130
1.0 mg L^{-1}	---	---	18	

The mesocosm data suggest several conclusions:

- Both aluminum and ferric iron blends can reduce dissolved phosphorus concentrations to less than 10 $\mu g\ L^{-1}$. This level of dissolved phosphorus removal can be achieved under a broad range of metal treatments for both iron and aluminum.
- Total phosphorus removal improves greatly with the use of adequate dosing levels of PAMs. The data suggest that improved floc aggregation occurs at a threshold dosing level. When PAM dosing levels exceed the threshold, total phosphorus removal of 70 to 85% can be achieved in CFSTR conditions. Total phosphorus concentrations did not differ for PAM concentrations of 0.5 and 1.0 mg L^{-1} for mesocosms receiving aluminum dosing whereas they did differ for mesocosms receiving iron dosing. This suggests that for aluminum blends the PAM threshold is below 0.5 mg L^{-1} and for iron blends the PAM threshold is above 0.5 mg L^{-1}.
- Total phosphorus concentrations achieved in the mesocosms differed between sites. Sites with higher background phosphorus concentrations had higher mesocosm phosphorus concentrations. This result suggests that final phosphorus concentrations achieved under metal dosing depend upon the initial phosphorus concentrations. Higher mesocosm concentrations may have also been in part to dilution of mesocosm water with background marsh

water during periods in which marsh water levels are changing. This conclusion is supported by the bromide data which suggests that approximately 15% of the water in the mesocosms under steady state conditions is untreated marsh water.

- Higher aluminum dosing levels improved total phosphorus removal although that was not the case with ferric iron dosing.
- Under iron dosing, the resultant total phosphorus concentrations did not statistically depend upon metal dosing level. For aluminum, the relationship was less clear.

Figure 85. The effects of different PAM dosing levels on total phosphorus concentrations achieved in mesocosms undergoing metal treatments.
Data is for aluminum and iron dosing of 200 and 400 µM at Sites A and C during February/March 2000 mesocosm study.

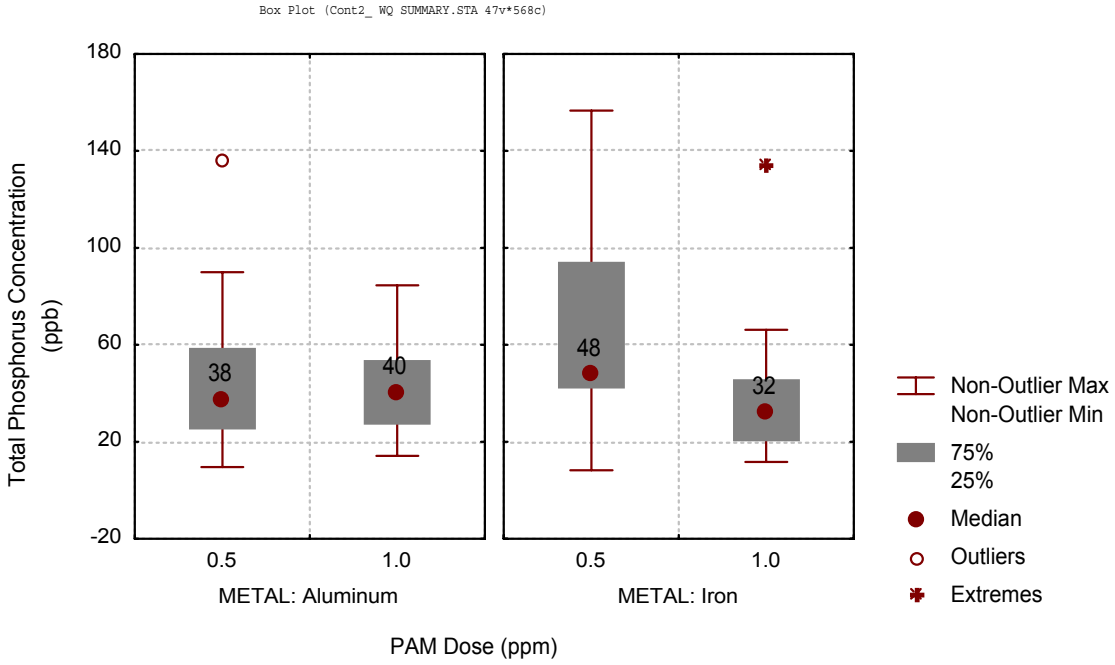

14.2.3.1.5. Raw data analyses summary

From the raw data analyses, several generalizations could be made with regard to both iron and aluminum metal treatments.

For iron dosing:

- Phosphorus changes from dissolved to particulate species occurred in the mesocosm piping and rapid mixers. Near total removal of dissolved phosphorus occurred in the mixing tanks. In the mesocosms, higher iron dosing levels resulted in the formation of more particulate phosphorus. Higher PAM dosing levels did not improve dissolved phosphorus removal and therefore had no effect on phosphorus speciation changes. Phosphorus speciation changes appear to be controlled by both kinetics and chemicals used.
- PAM improved total phosphorus removal. This appears through improved floc aggregation and settling in this study as opposed to earlier study. Total phosphorus removal in the mixing tanks and the mesocosms exceeded total phosphorus removal in earlier studies. The threshold for *in situ* marsh dosing of PAMs above which total phosphorus removal is much improved appears to be between 0.5 and 1.0 mg L^{-1}. Iron dosing levels of 200 μM achieved total phosphorus concentrations of 24 $\mu g\ L^{-1}$ for an HRT of less than 1 day. In the mesocosms, the same iron dosing treatment achieved total phosphorus concentrations of 29 $\mu g\ L^{-1}$ for an HRT of 2.5 days.
- Total phosphorus removal generally improved at higher dosing levels though these differences were frequently not statistically significant.
- Final total phosphorus concentrations in the mesocosms receiving iron treatments depended upon background total phosphorus concentrations. Higher background concentrations led to higher mesocosm concentrations. This was likely due to both a metal dosing dependence upon phosphorus concentrations as well as dilution of mesocosm water with surrounding marsh water. Under steady state conditions, approximately 15% of the water in the mesocosms appears to be non-treated marsh water. During the time period of this study, approximately 20% of water was non-treated marsh water.

For aluminum dosing:

- Phosphorus changes from dissolved to particulate species also occurred in the mesocosm piping and rapid mixers. Like with iron, near total removal of dissolved phosphorus occurred in the mixing tanks. Higher PAM dosing levels did not improve dissolved phosphorus removal and therefore had no effect on phosphorus speciation changes. Phosphorus speciation changes appear to be controlled by both kinetics and chemicals used.
- Total phosphorus concentrations achieved in the mixing tanks were generally lower under aluminum dosing than under iron dosing. PAM dosing apparently

improved total phosphorus removal as total phosphorus removal in the mixing tanks and the mesocosms exceeded total phosphorus removal in earlier studies. However, no differences in total phosphorus removal appeared for the PAM doses used in this study. Thus, the threshold for *in situ* marsh dosing of PAMs above which total phosphorus removal is much improved under aluminum dosing appears to be less than 0.5 mg L^{-1}. Aluminum dosing at 200 μM in the mixing tanks achieved total phosphorus concentrations of 18 μg L^{-1} for an HRT of less than 1 day. At dosing levels of 400 μM, total phosphorus concentrations in the mixing tanks were even lower at 13 μg L^{-1}. In the mesocosms, that treatment achieved total phosphorus concentrations of 25 μg L^{-1} for an HRT of 2.5 days.

- Total phosphorus removal in the mesocosms did not significantly improve at higher aluminum dosing levels.
- Final total phosphorus concentrations in the mesocosms receiving aluminum treatments depended upon background total phosphorus concentrations. Higher background concentrations led to higher mesocosm concentrations. As with iron, this was likely due to a metal dosing dependence upon phosphorus concentrations as well as dilution of mesocosm water with surrounding marsh water.

14.2.3.2. Process Data Analyses

Process analyses created a matrix of process data with the goal of establishing water quality trends as water passed through the LICD system and allow the necessary information to develop mass balance and statistical models for this study. For this analysis, data were reorganized. Mesocosm data was collected from four locations when sampling for total phosphorus and this data is presented as such in the raw data. However, several factors led to high variance with that data. Mesocosm sampling requires sampling from quiescent waters. Under that scenario, the sampling apparatus can possibly lead to unusually high total phosphorus concentrations from disturbing the water column. Macrophytes and algae dominate these waters and the particles suspended from sampling are likely biotic and high in total phosphorus as compared to typical water concentrations in the μg L^{-1} range. Additionally, the sampled water is not well mixed as it would be when sampling from a stream or pipe. These factors increase variance. Thus, for this analysis, total phosphorus concentrations from the mesocosm grab samples were averaged for each mesocosm on each sampling day. This likely more accurately represents total phosphorus samples from well-mixed waters and allows a 1:1:1 comparison of inflow, mixing tank and mesocosm data for each sampling day at each mesocosm.

The goals of this analysis were to:

- Characterize changes in total and dissolved phosphorus through the LICD process.
- Develop a model describing the formation of particulate phosphorus during LICD as dependent upon factors such as metal dose, inflow phosphorus concentrations and PAM dosing levels.
- Assess background water dilution effects and integrate that into the data.
- Fit a regression model to the data to show the factors controlling dissolved, particulate and total phosphorus concentrations in the mesocosms.
- Develop mass balance model describing dilution effects on mesocosm phosphorus concentrations.

14.2.3.2.1. Changes in total and dissolved P through the LICD process

Chemical dosing at low metal concentrations decreased total phosphorus concentrations in the mixing tanks to levels generally between 13 and 30 $\mu g\ L^{-1}$ after less than one day HRT (Figures 79, 80). In the mesocosms the same treatments resulted in total phosphorus concentrations between 25 and 103 $\mu g\ L^{-1}$. Excluding the low aluminum and iron doses in combination with the low PAM doses which were the treatments experiencing the poorest settling, total phosphorus concentrations achieved after dosing were in the range of 25 to 58 $\mu g\ L^{-1}$ (Figure 81). These levels were higher than in the accompanying mixing tanks.

Mixing tanks were installed with one non-dosed treatment and all metal treatments at each site. The one non-dosed treatment was to provide background phosphorus changes in the mixing tanks as compared to those treatments receiving dosing. For all treatments at both Sites A and C, total phosphorus concentrations in the mixing tank after an approximate one day HRT were lower than total phosphorus concentrations achieved in the mesocosms after an approximate 2.5 day HRT (Figure 86). Two factors likely contributed to this result.

One possible factor is that phosphorus settling was hindered in some and perhaps all mesocosms. The mesocosms can be modeled as continuously mixed systems or Continuous-Flow Stirred Tank Reactors (CFSTR). They are subject to temporal and diel mixing as well as possible resuspension of phosphorus from biotic activity. Both the iron and aluminum 200 μM treatments with PAM doses of 0.5 mg L^{-1} had the poorest settling for the respective metal treatments and apparently had developed floc that experienced hindered settling in the mesocosm environment. Unlike the full-scale STAs which operate as non-ideal Plug-Flow Reactors (PFRs) and in which the flow path is perpendicular to the vegetation, the mesocosms cannot demonstrate spatial settling effects.

A second reason for the higher total phosphorus concentrations in the mesocosms than in the mixing tanks is dilution of the low-phosphorus mesocosm water with high-phosphorus background marsh water. Figure 87 shows mean

mesocosm total phosphorus concentrations as a function of inflow phosphorus concentrations. Figure 87 clearly shows that LICD treatments decreased total phosphorus concentrations. Figure 87 also shows that for all treatments, mesocosm phosphorus concentrations increased as inflow phosphorus concentrations increased. This happened regardless of treatment, occurring in the unwalled controls, nondosed and metal dosed treatments. Changes in pumped inflow concentrations are caused by changes in background concentrations. In theory, inflow and background phosphorus concentrations are identical.

The relationship between background or inflow total phosphorus concentrations and mesocosm concentrations could be due to either a dependence of metal dosing effectiveness on inflow total phosphorus concentrations, dilution of mesocosm water with high phosphorus background water or both. From the phosphorus data, these two possibilities cannot be distinguished. However, bromide tracer data provides insight into this result. Mesocosm bromide concentrations averaged approximately 78% of inflow bromide concentrations during the period phosphorus sampled were collected (Table 23). With mass balance analyses, the differences in bromide concentration can be explained through a dilution effect of mesocosm water with background marsh water. The concentration gap narrowed during the study (Figure 64). However, even under steady state conditions, mesocosm concentrations of bromide averaged only 83% of background concentrations (Table 24). The mechanism for dilution can be through water level variations in the surrounding marsh forcing surface water in and out of the mesocosms as water levels in the mesocosms respond.

14.2.3.2.2. Modeling particulate phosphorus formation

Figure 88 shows phosphorus speciation changes through the LICD process for both aluminum and iron dosing. Speciation of dissolved and particulate phosphorus for both metals are very similar. Inflow concentrations of dissolved phosphorus are high and particulate phosphorus is low. Once metal dosing has occurred, dissolved phosphorus concentrations are reduced to means of less than 10 $\mu g\ L^{-1}$. Those levels are maintained in the mixing tanks and then slightly increase in the mesocosms suggesting dilution of mesocosm water with marsh water. Particulate phosphorus concentrations increase greatly after metal dosing suggesting that metal dosing levels are effective at causing precipitation. Particulate phosphorus concentrations are around 90 $\mu g\ L^{-1}$ after chemical dosing. Within one day in the mixing tanks, particulate phosphorus concentrations decrease dramatically by about 85% for the two metals used.

Figure 86. Changes in total phosphorus concentrations from inflow through mesocosms.
Data includes mesocosms receiving iron and aluminum dosing at 200 and 400 µM.

A) Site A:

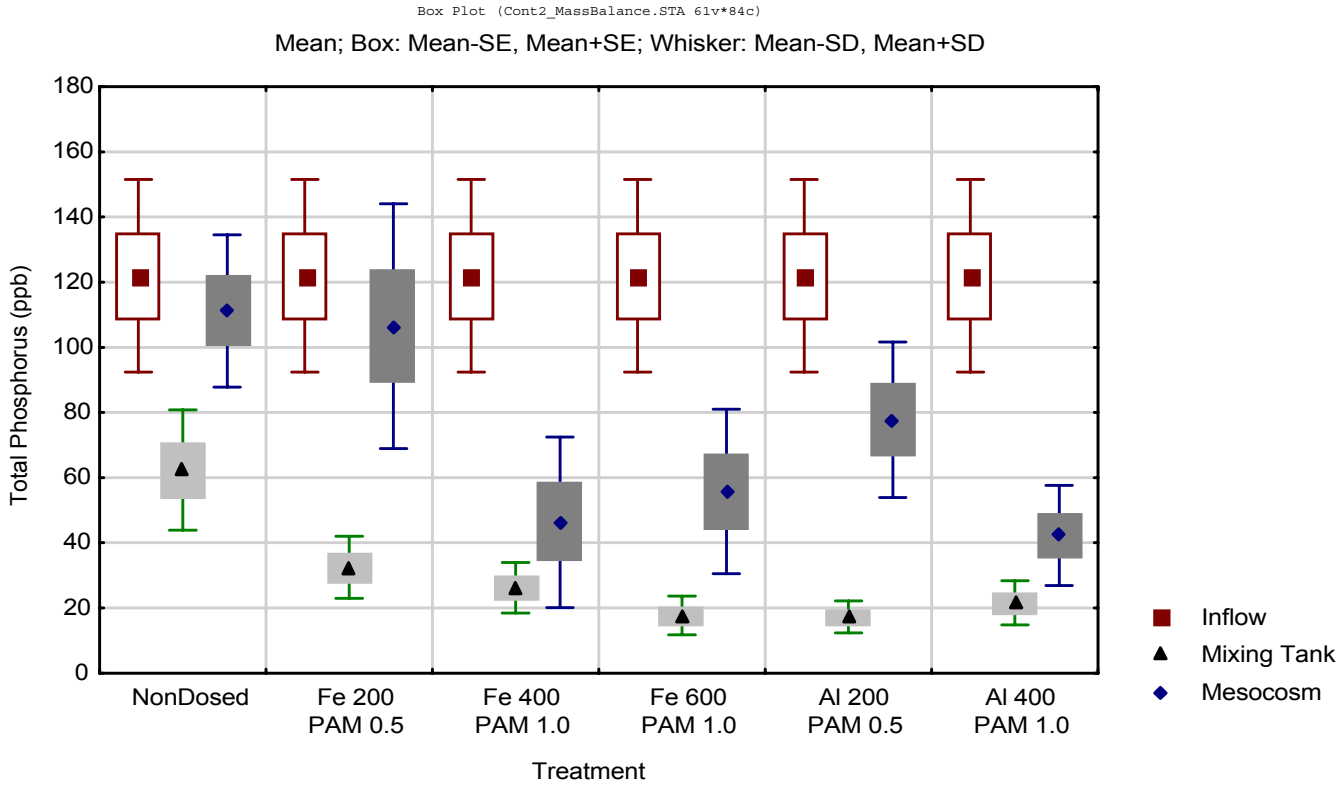

B) Site C:

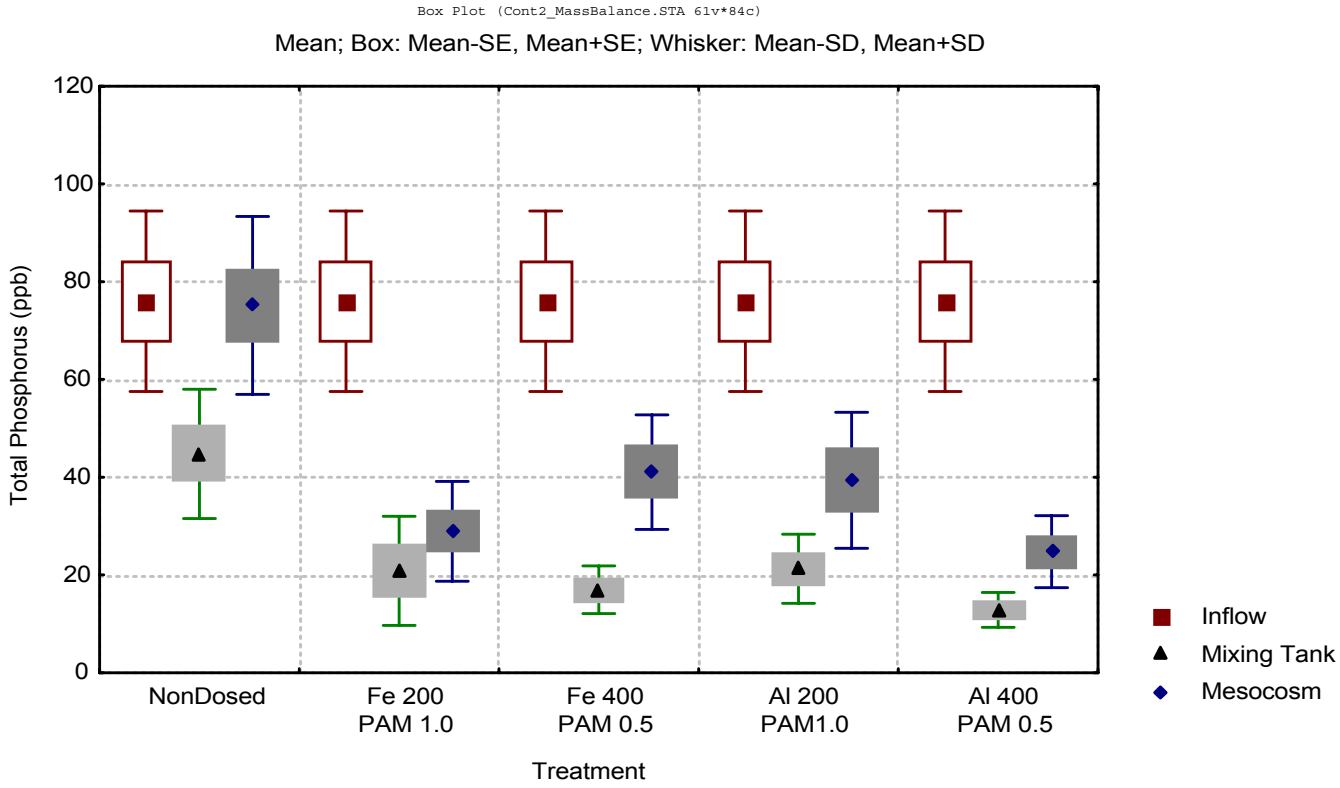
Box Plot (Cont2_MassBalance.STA 61v*84c)
Mean; Box: Mean-SE, Mean+SE; Whisker: Mean-SD, Mean+SD
Total Phosphorus (ppb)
120
100
80
60
40
20
0
NonDosed
Fe 200 PAM 1.0
Fe 400 PAM 0.5
Al 200 PAM1.0
Al 400 PAM 0.5
Treatment
Inflow
Mixing Tank
Mesocosm

Figure 87. Mesocosm phosphorus concentrations increased as background and inflow phosphorus concentrations increased. The relationship between mesocosm and background phosphorus concentrations were less linear and flatter for mesocosms receiving effective metal polymer combinations.

A) Site A:

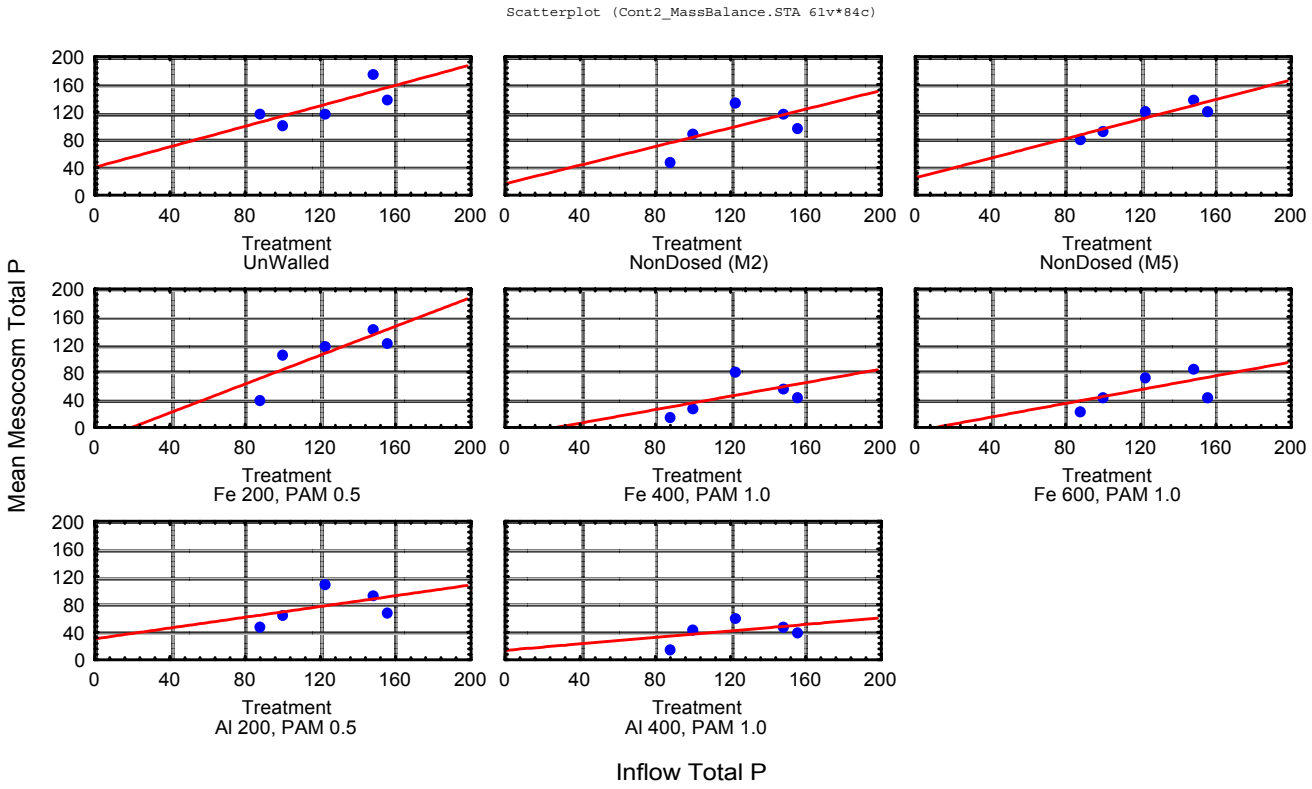

B) Site C:

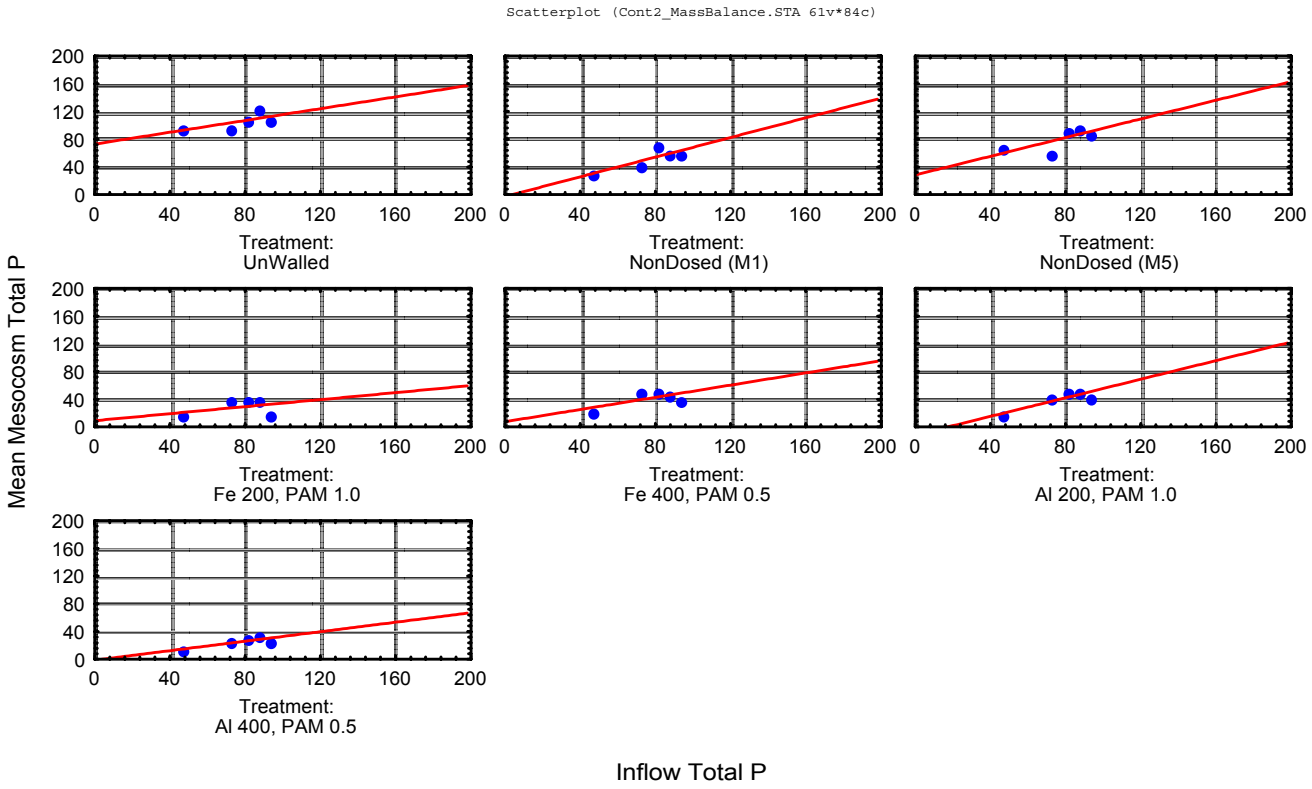
Scatterplot (Cont2_MassBalance.STA 61v*84c)
Mean Mesocosm Total P
Inflow Total P
Treatment: UnWalled
Treatment: NonDosed (M1)
Treatment: NonDosed (M5)
Treatment: Fe 200, PAM 1.0
Treatment: Fe 400, PAM 0.5
Treatment: Al 200, PAM 1.0
Treatment: Al 400, PAM 0.5
0
40
80
120
160
200

Figure 88. Changes in dissolved and particulate phosphorus from inflow through mesocosms.

Includes data from iron and aluminum dosing at 200 and 400 µM. Particulate phosphorus concentration greater than 80 µg L^{-1} were considered outliers and excluded from the analyses.

A) Dissolved Phosphorus

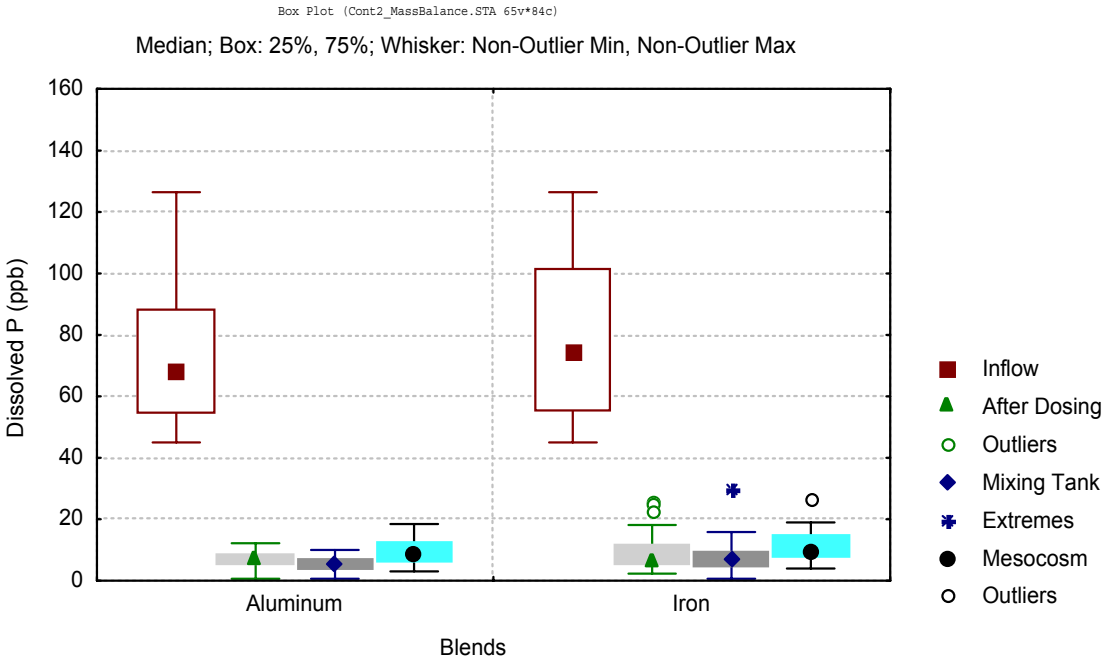

B) Particulate Phosphorus

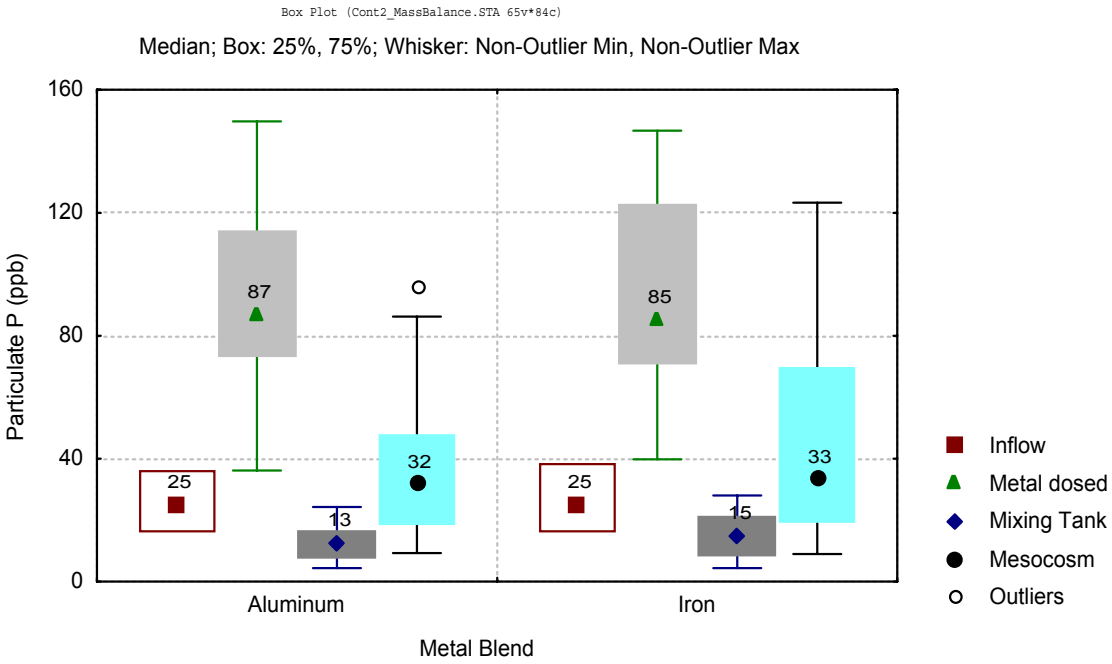

Figure 89 presents a conceptual model of the processes occurring during the various LICD steps. The first step is the formation of particulate phosphorus resulting from chemical dosing. Figure 90 presents measured particulate phosphorus concentrations resulting from design (target) chemical dosing concentrations. This rudimentary analysis suggests that an empirical exponential relationship exists for the conversion of dissolved phosphorus to particulate phosphorus with regard to metal dosing. The formation of precipitates occurs very rapidly from fractions of a second to seconds and thus the particulates formed after rapid mixing are likely in or near an equilibrium condition. Thus, the reaction we are interested in describing is likely one of equilibrium chemistry as opposed to kinetics. The exact mechanisms occurring during this process with regard to the formation of hydroxides and metal organic complexes, and the adsorption and incorporation of the various dissolved phosphorus species are not defined. Thus an empirical relationship is a reasonable approach to aid in describing the system and aiding in future design. We described dissolved concentrations following chemical dosing as follows:

$$\frac{\partial(FTP)}{\partial(Me_{In})} = K_{Me} \times FTP \qquad \textbf{Equation 2}$$

where

FTP = Dissolved phosphorus concentration
Me_{In} = iron or aluminum dosing concentration and
K_{Me} = Metal dosing constant.
Upon integration, this becomes:

$$FTP_{Me} = FTP_{Marsh} \exp(-K_{Me} Me_{In}) \qquad \textbf{Equation 3}$$

where

FTP_{Marsh} = dissolved phosphorus concentration in the marsh and
FTP_{Me} = dissolved phosphorus concentration following metal dosing of either iron or aluminum.

Figure 89. LICD Phosphorus Removal Model

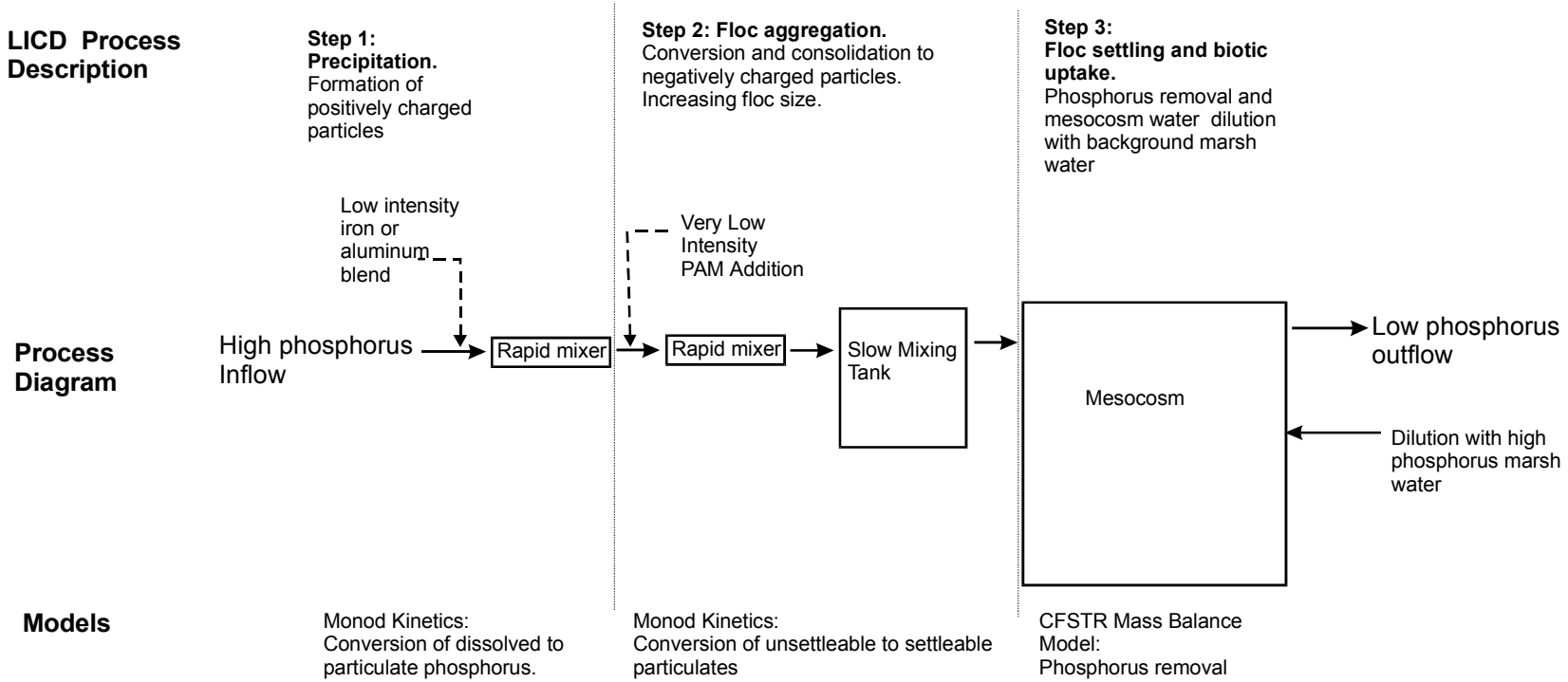

Figure 90. Particulate phosphorus concentrations entering mesocosms after dosing with aluminum and iron blends.
Data from aluminum dosing at 600 µM was excluded from the analyses. Metal dosing concentrations are target not measured concentrations. Fitted line is an approximation shown to characterize relationship.

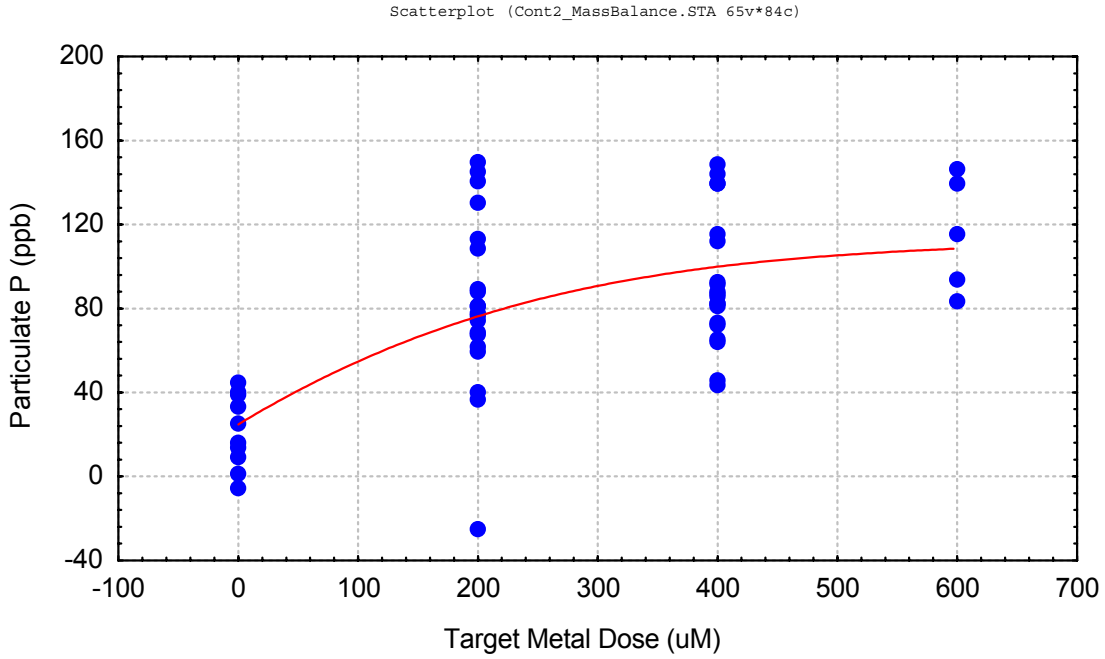

Formation of particulate phosphorus after chemical dosing can be determined by:

$$PP_{Me} = (FTP_{Marsh} - FTP_{Me}) + PP_{Marsh}$$ **Equation 4**

where

PP = particulate phosphorus.

Combining Equations (2) and (4) leads to:

$$PP_{Me} = FTP_{Marsh}(1 - \exp(-K_{Me} Me_{In})) + PP_{Marsh}$$ **Equation 5**

Figure 91 shows the changes in dissolved phosphorus following iron dosing. K_{Me} was determined by fitting a line to these data. Figure 92 shows the differences

between predicted and observed values using the above exponential relationship. Figure 93 shows the differences between predicted and observed particulate phosphorus concentrations following iron dosing. Table 34 provides regression data for the decrease in dissolved phosphorus and the increase in particulate phosphorus following metal dosing. These models explain approximately 98% of the variance in the data for iron dosing (Table 34). Figure 94 shows the changes in dissolved phosphorus following aluminum dosing and Figure 95 shows the differences between predicted and observed values using Equation (2) for aluminum dosing. Figure 96 shows the differences between predicted and observed values of particulate P using Equation (4) for aluminum dosing. Again, the regression fit is very good with the regression models of Equations (3) and (5) explaining approximately 82% of the variance associated with the decrease in dissolved phosphorus and increase in particulate phosphorus following dosing (Table 34).

Figure 91. Dissolved phosphorus concentrations following iron dosing.
Fitted line is an approximation shown to characterize relationship.

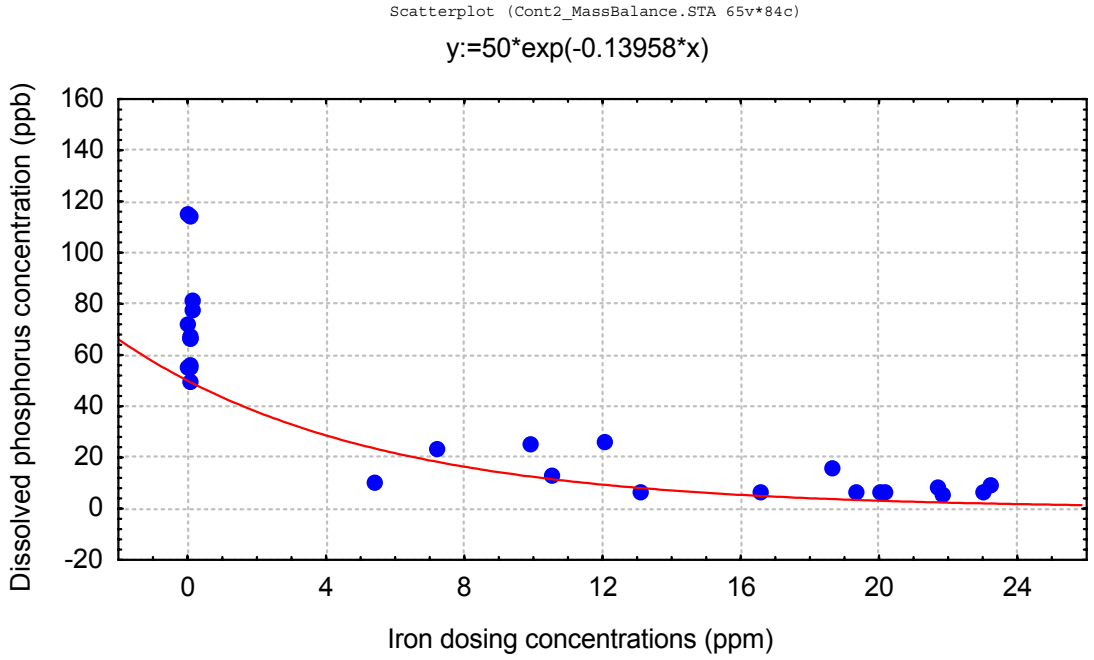

Figure 92. Predicted vs. Observed dissolved phosphorus concentrations for iron dosed waters.

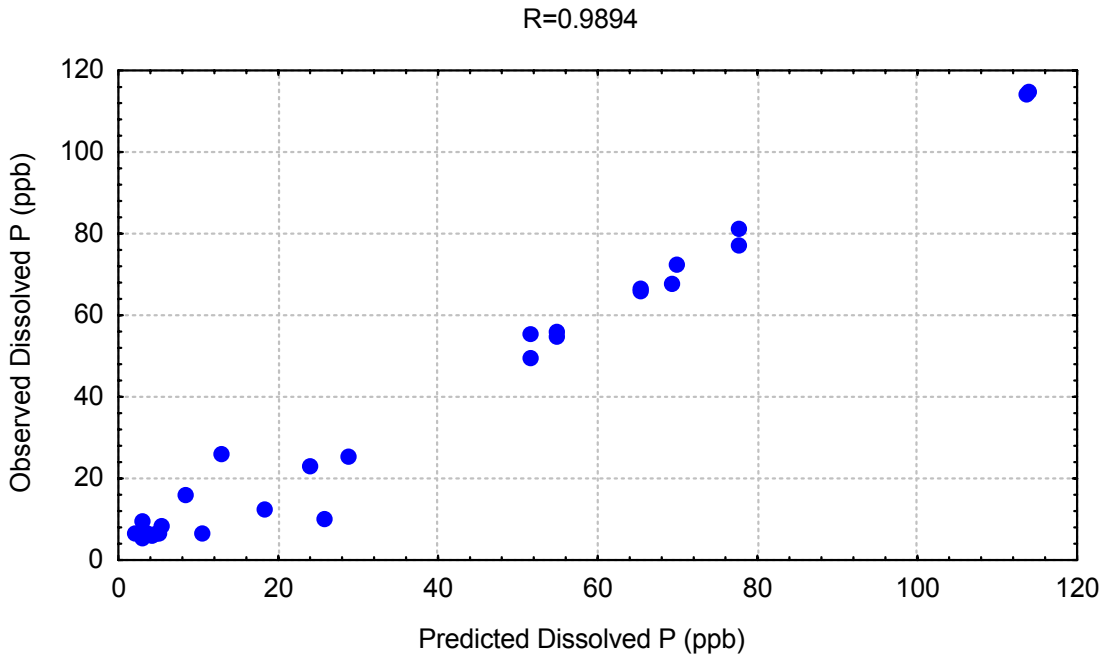

Figure 93. Predicted vs. Observed particulate phosphorus concentrations for iron dosed waters.

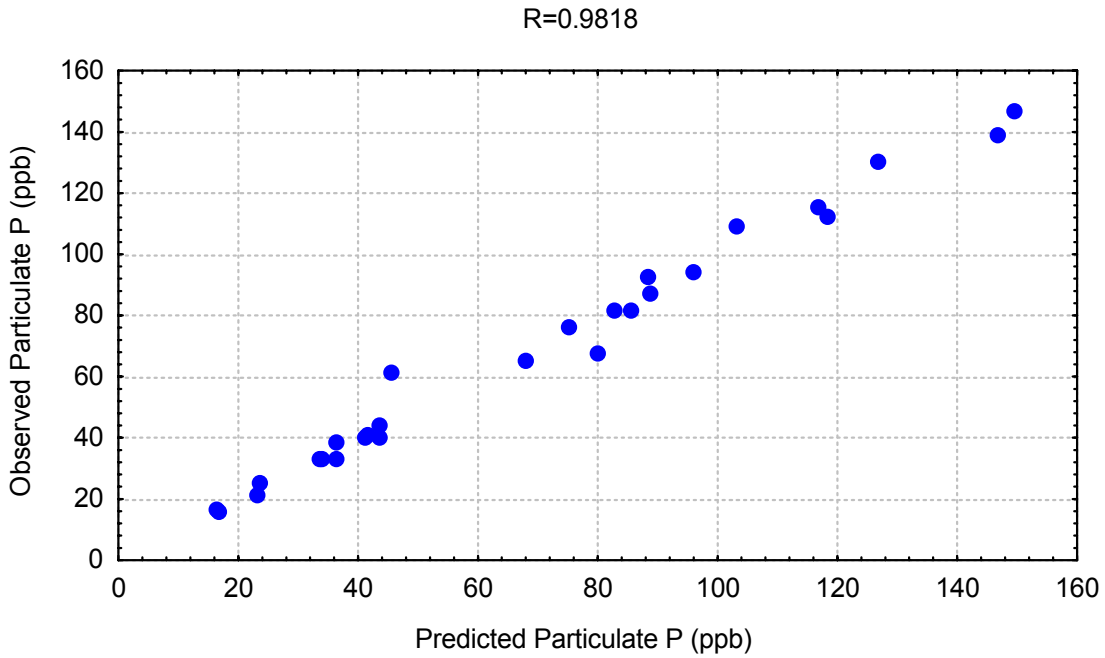

Figure 94. Dissolved phosphorus concentrations following aluminum dosing. Fitted line is an approximation shown to characterize relationship.

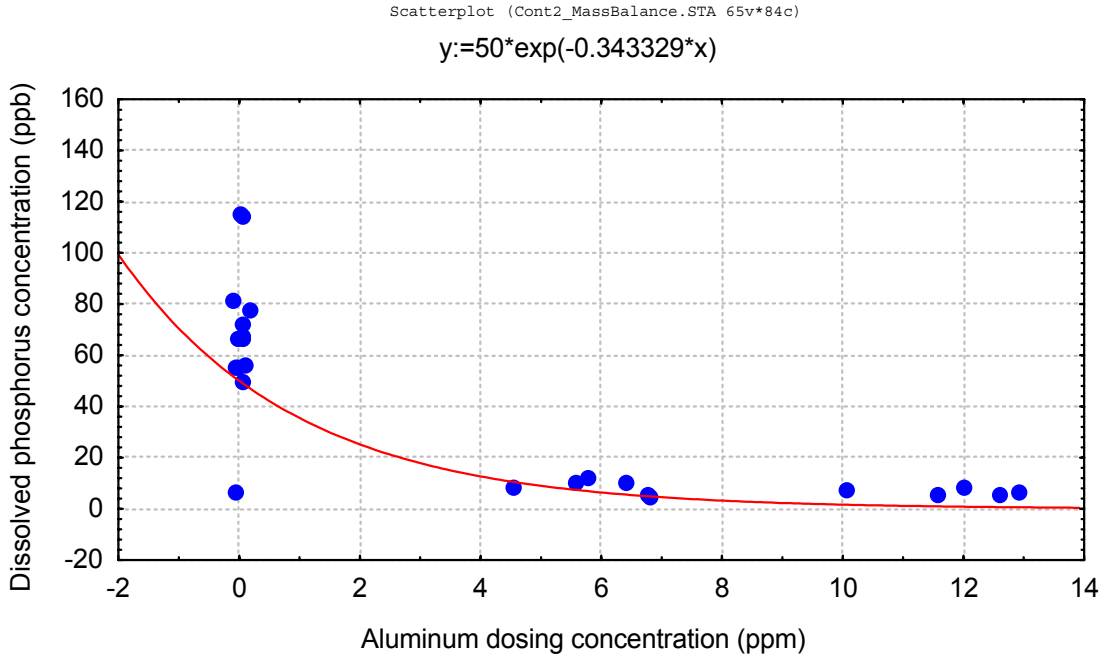

Figure 95. Predicted vs. Observed dissolved phosphorus concentrations for aluminum dosed waters.

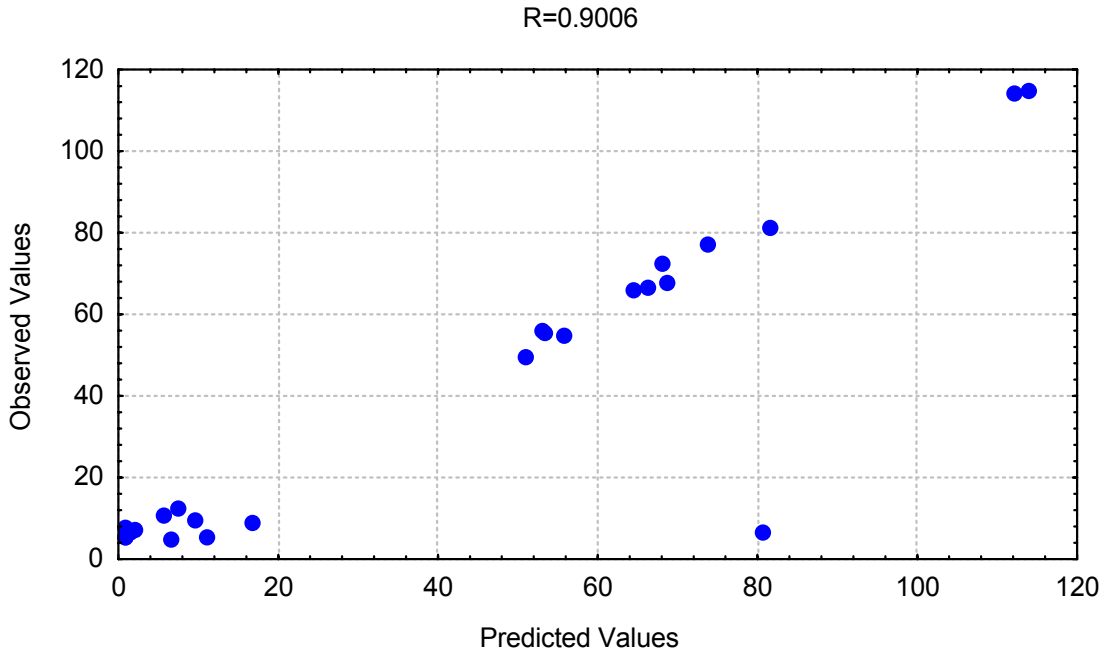

Figure 96. Predicted vs. Observed particulate phosphorus concentrations for aluminum dosed waters.

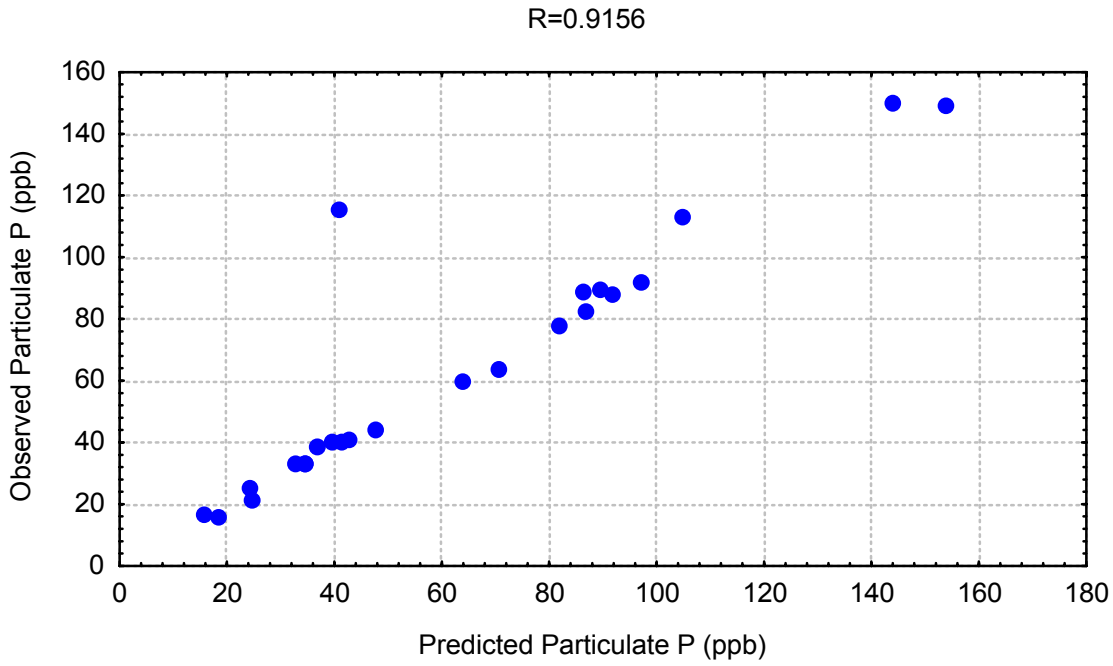

Table 34. Phosphorus speciation model following metal dosing, February/March 2000.

Marsh phosphorus concentrations were assumed to be equivalent to pumped (inflow) concentrations. Mesocosm C4 was excluded from the analyses.

Metal dosing model	Metal	K_{Me}	R^2	$Me_{In,\ 1/2}$
Dissolved P reduction	Iron	0.139580	0.9790	4.96
	Aluminum	0.343329	0.8111	2.02
Particulate P increase	Iron	0.139580	0.9837	4.96
	Aluminum	0.343329	0.8384	2.02

From examination of Equation (3), we can determine the metal dose for which half the dissolved phosphorus is precipitated by:

$$Me_{In,1/2} = \frac{0.693}{K_{Me}}. \qquad \textbf{Equation 6}$$

Where $Me_{In,\ ½}$ is the metal dose to convert half the dissolved phosphorus to particulate phosphorus. For iron, this model predicts a half-dose of approximately 5 mg L^{-1} or 100 μM and for aluminum a half-dose of approximately 2 mg L^{-1} or 100 μM (Table 34).

14.2.3.2.3. Floc aggregation

As with formation of precipitates, the aggregation of precipitates is a complex process. Fundamentally, the addition of anionic polyacrylamides will convert positively charged precipitates to negatively charged precipitates and lead to an aggregation of particles. The effectiveness of the PAM addition depends upon initial mixing energy for rapid chemical dispersal, slow mixing for floc aggregation and PAM dose. The exact interactions of these three processes are not well defined and again an empirical relationship describing floc aggregation is sought.

Earlier jar test studies had determined several findings that were important in developing the empirical relationships. First, PAM effects differed for the different metal blends being more effective for iron than aluminum. Bachand et al. (1999) showed in the Phase I study for LICD that aluminum and iron additions affected DOC concentrations differently and these findings are supported during Phase 2. This suggests that the solid precipitates formed by LICD differ for the different chemical blends. Thus, PAM effects would also likely differ given the different chemistries of the metal precipitates. These findings from Phase I and Phase 2 led to us developing floc aggregation models that differentiated between aluminum and iron. Second, jar test studies had shown with proper mixing and PAM doses, resulting settling occurred very rapidly in the range of seconds to minutes. This system was operated at HRTs on the order of days. Thus, floc aggregation was considered an equilibrium relationship and not a kinetic relationship because the time scale of this study was several orders of magnitude greater than the mixing and settling times of formed floc.

To develop the floc aggregation model, mixing tank data was considered. PAM only affected particulate phosphorus and this model only addresses that phosphorus specie. From Figure 89, a mass balance relationship for settleable particulate phosphorus can be described by:

$$PP_{Me} \Rightarrow PP_{PAM} \Rightarrow PP_{Settleable} + PP_{Mix} \qquad \textbf{Equation 7}$$

where

PP_{PAM} = particulate phosphorus after PAM addition and mixing
PP_{Mix} = the resulting non-settleable particulate phosphorus and
$PP_{Settleable}$ = the resulting settleable particulate phosphorus that has formed and settled in the mixing tank in less than one day.

Field studies tested PAM dosing at only two dosing levels, 0.5 and 1.0 mg L^{-1}. Two points were considered too few to use for developing the relationship. Jar Test Number 5 during August 1999 considered SuperFloc A130 at three dosing levels (0, 0.25 and 0.75 mg L^{-1}) in combination with both iron and aluminum dosing at 100 and 200 µM. In the jar test, turbidity was considered an indicator of particulate phosphorus settling. Both iron and aluminum showed an empirical exponential relationship for turbidity as a function of PAM dosing level (Figures 97 and 98).

Figure 97. Jar Test Relationships between PAM A130 dose and turbidity for iron dosed marsh water.
Data is from Jar Test No. 5. Includes ferric chloride and FPD data for 100 and 200 µM collected over several sampling times from 5 to 60 minutes. Because different PAMs tested during the Jar Tests gave significantly different results, and because SuperFloc A130 was used in these field studies, this data only includes A130 PAM additions. N=31. Fitted line is an approximation shown to characterize relationship.

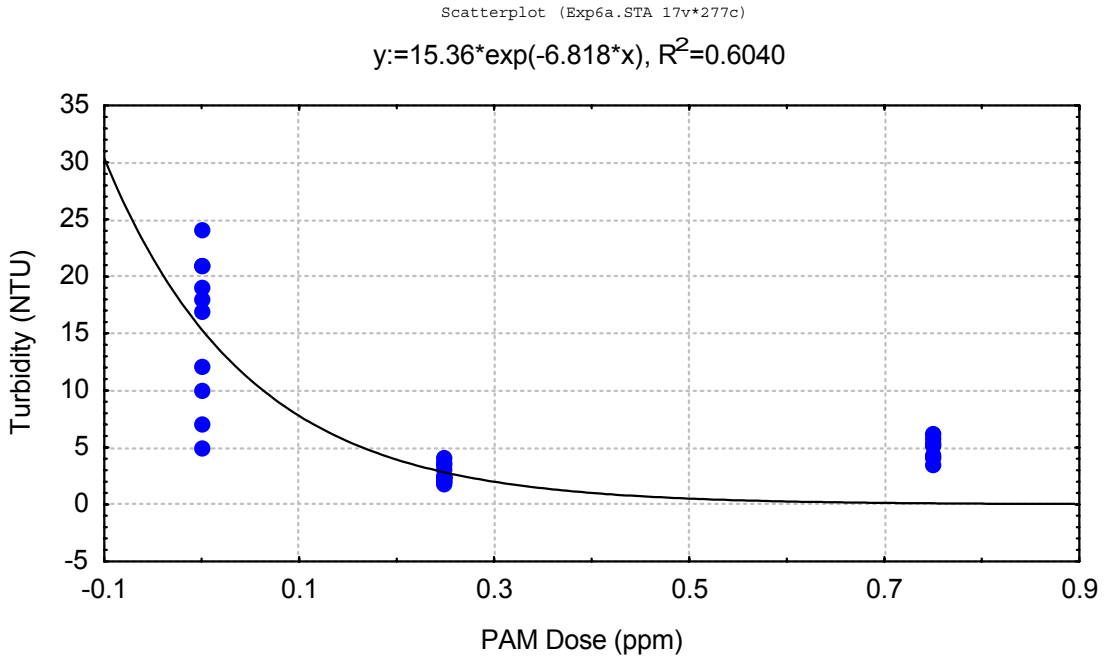

Figure 98. Jar Test Relationships between PAM A130 dose and total phosphorus for aluminum dosed marsh water.
Data is from Jar Test No. 5. Includes alum and Clarion 4100 data for 100 and 200 µM collected over several sampling times from 5 to 60 minutes. Because different PAMs tested during the Jar Tests gave significantly different results, and because a130 was used in these field studies, this data only includes A130 PAM additions. N=19. Fitted line is an approximation shown to characterize relationship.

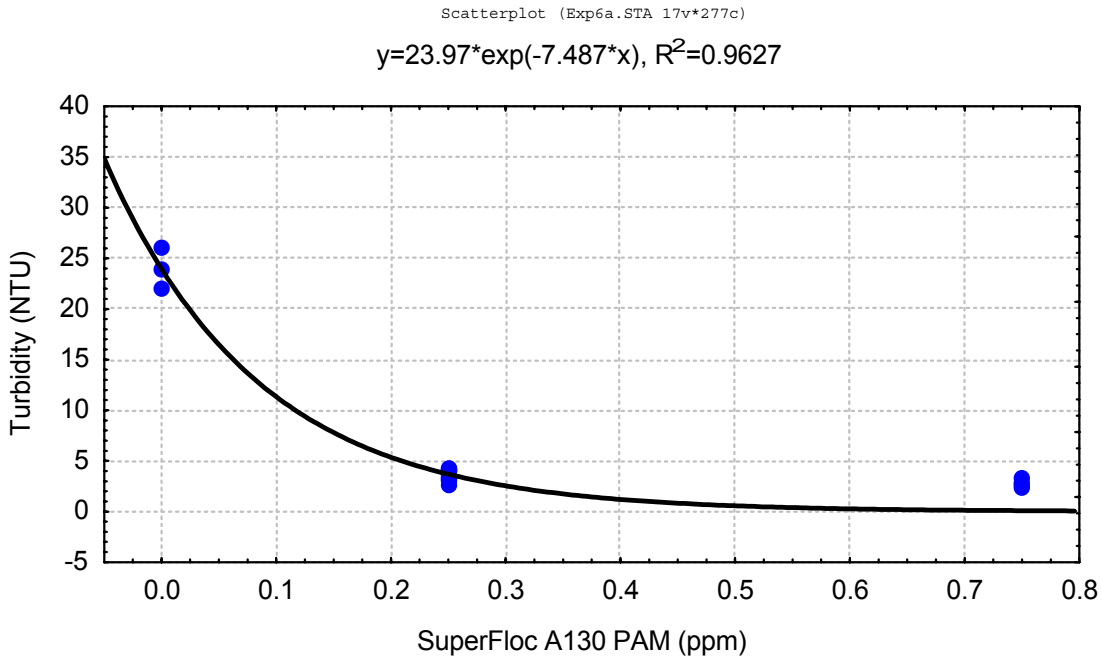

This relationship could be described by:

$$Turbidity = Turbidity_{Max} \exp(K_{PAM,Turb} PAM_{In}) \qquad \textbf{Equation 8}$$

where

K_{PAM} = PAM dosing constant and
PAM_{In} = the dose of PAM into the system in mg L^{-1}.

For the mixing tanks, Equation (8) would be modified to:

$$PP_{settleable} = PP_{PAM}(1 - \exp(K_{PAM} PAM_{In})). \qquad \textbf{Equation 9}$$

Equation (9) was applied to the mixing tank field data to develop the PAM dosing constant (Figure 99; Table 35). For ferric iron, K_{PAM} was determined to be 2.730

for a PAM half dose of 0.26 mg L^{-1}. This model explained 90% of the variance associated with the data. For aluminum, K_{PAM} was determined to be 4.000 for a PAM half dose of 0.17 mg L^{-1}. For aluminum, the model explained 86% of the variance. For iron, PAM dosing levels in the field of over 0.5 mg L^{-1} are necessary for effective settling given the PAM half dose constant. For aluminum, the effective dosing level need be over 0.34 mg L^{-1}. The lower K_{PAM} values achieved in the field as opposed to the jar tests suggests that PAM was less effectively dosed in the field than in the jar test and this is likely do poorer mixing.

Table 35. Phosphorus settling model following PAM dosing, February/March 2000.

Metal	K_{PAM}	R^2	$PAM_{In,\ 1/2}$
Iron	2.730	0.9010	0.26
Aluminum	4.000	0.8614	0.17

14.2.3.2.4. Dilution of marsh water raising mesocosm phosphorus concentrations

Figure 86 shows that lower total phosphorus levels were reached in the mixing tanks after a less than one day HRT than in the mesocosms after the 2.5 day HRT. It can be concluded that the marsh hindered the settling of particulate phosphorus though this effect can also be explained in part by considering dilution effects of background water on water treated with LICD. In this study, the mixing tanks were hydrologically isolated and the mesocosms were not. Bromide tracer studies demonstrated that mesocosm bromide concentrations averaged 78% of inflow concentrations during this study. Mass balance for bromide can be written as:

$$Br_{In}Q_{In} = Br_{Out}Q_{Out} \qquad \textbf{Equation 10}$$

where:

Br_{In} = bromide concentrations in the inflow,
Br_{Out} = bromide concentrations in the outflow
Q_{in} = Water flow rates in the inflow, and
Q_{out} = Water flow rates in the outflow.

The water balance follows:

$$Q_{In} + Q_{Dilution} = Q_{Out} \qquad \textbf{Equation 11}$$

where:

Figure 99. Predicted vs. Observed settleable particulate phosphorus concentrations for PAM dosed marsh water.
Settleable particulate phosphorus was determined from mixing tank data. All water had been previously treated with metal coagulants.

A) FerriPlus-D treatments (ferric iron):

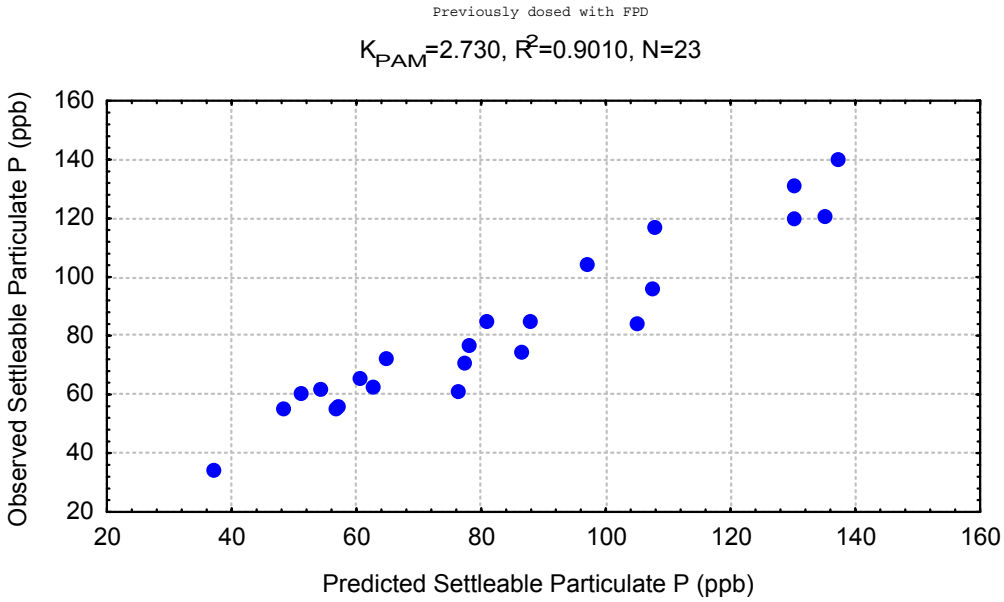

B) Clarion 4100 treatments (aluminum):

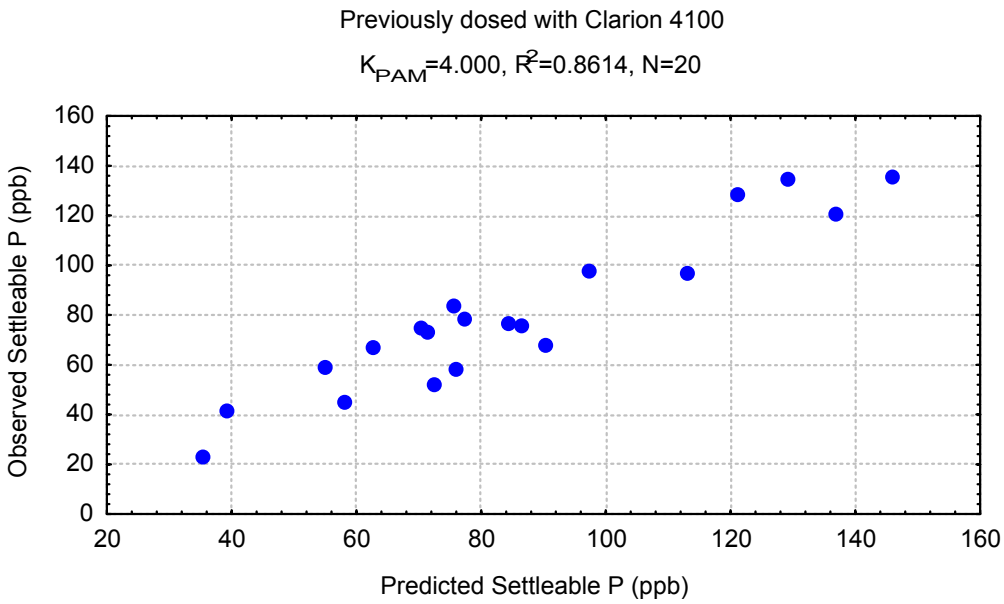

$Q_{dilution}$ = dilution water from varying water concentrations in the marsh in relation to mesocosm water and the resulting water level corrections.

Combining Equations (10) and (11) leads to:

$$Q_{Dilution} = \frac{(Br_{In} - Br_{Out})}{Br_{Out}} Q_{In} \qquad \textbf{Equation 12}$$

and

$$Q_{Out} = \frac{Br_{In}}{Br_{Out}} Q_{in} \qquad \textbf{Equation 13}$$

Phosphorus mass from the mesocosms can be separated into that which has been chemically treated and that which is from dilution water and is now being expelled:

$$P_{Meso} Q_{Out} = P_{LICD*} Q_{In} + P_{Marsh} Q_{Dilution} \qquad \textbf{Equation 14}$$

where

P_{meso} = total phosphorus measured at the mesocosm
P_{LICD*} = total phosphorus concentration resulting from LICD treatment and
P_{marsh} = background marsh concentrations of total phosphorus.

Essentially, treated low phosphorus water from the LICD process mixes with higher concentration marsh water and leads to higher phosphorus concentrations in the mesocosm outflows. Thus, P_{LICD*} is the predicted phosphorus concentration achievable under low intensity chemical dosing when the system is hydrologically isolated. Using bromide tracer studies, Equation (14) can be rewritten as:

$$P_{Meso} \frac{Br_{In}}{Br_{Out}} = P_{LICD*} + P_{Marsh} \frac{Br_{In} - Br_{Out}}{Br_{Out}} \qquad \textbf{Equation 15}$$

and when solved for P_{LICD*} shown as:

$$P_{LICD*} = \left(P_{Meso} Br_{In} - P_{Marsh} (Br_{In} - Br_{Out})\right) \Big/ Br_{Out} . \qquad \textbf{Equation 16}$$

Because of variation in the bromide data, average concentrations for bromide during the entire run were used:

$$P_{LICD*} = \left(P_{Meso}\,\overline{Br}_{In} - P_{Marsh}\left(\overline{Br}_{In} - \overline{Br}_{Out}\right)\right) \Big/ \overline{Br}_{Out} \qquad \textbf{Equation 17}$$

Figure 100 presents the results of this analyses using Equation (17) to calculate P_{LICD*}. Total phosphorus concentrations measured in the mixing tank after less than one day of settling, total phosphorus concentrations measured in the mesocosms after a 2.5 day design HRT, the predicted total phosphorus concentrations for a hydrologically isolated mesocosm study are shown.

Several very significant findings are shown. First, when dilution is accounted for, phosphorus levels in the mixing tanks are very similar to those predicted for a hydrologically isolated mesocosm (P_{LICD*}). Thus, if the mesocosms were hydrologically isolated, the total phosphorus concentrations resulting from LICD would be lower than recorded during this study. Second, for many of the metal dosing treatments, total phosphorus concentrations expected to be achieved in the mesocosms under hydrologically isolated systems are at or below the concentrations achieved in the mixing tanks. Calculations for three of the four metal treatments with PAM dosing levels of 1 mg L^{-1} and for all the aluminum dosing treatments of 400 μM predict that under hydrologically isolated systems, the mesocosms could achieve total phosphorus concentrations less than those achieved in the mixing tanks. For two of the treatments, predicted final phosphorus concentrations (P_{LICD*}) are near or below 10 μg L^{-1}.

As marsh systems are very good at promoting filtration and sedimentation, it is not surprising that accounting for background marsh water increasing mesocosm concentrations would then predict that lower total phosphorus concentrations could be achieved in the mesocosms than in the mixing tanks. The mesocosms operated under a design HRT of 2.5 days whereas the mixing tanks were allowed under one day for settling to occur before grab samples were collected. Both emergent and submergent macrophyte marshes promote particulate removal by filtration and settling in quiescent waters and the mesocosms were essentially marsh communities whereas the mixing tanks were not. Finally, some uptake would be expected in the mesocosms given biological communities present and the assumption that the communities are all phosphorus limited. These three factors support the calculated results shown in Figure 100. Thus, in hydrologically isolated marsh mesocosm systems operated as CFSTRs for a 2.5 day HRT, mean total phosphorus concentrations that can be expected from dosing of metal and polymer blends range from 9 – 29 μg L^{-1}. Mixing tank data also supports this finding with four of the eight metal treatments shown in Figure 100 achieving total phosphorus concentrations of 17 μg L^{-1} or less.

Figure 100. Predicted Total Phosphorus Concentrations for hydrologically isolated CFSTR under LICD.
Total Phosphorus at LICD* is the level anticipated to be achieved in the mesocosms under hydrologically isolated conditions. Dilution of mesocosm water from surrounding marsh water was calculated from bromide tracer data. Bromide data greater than 20 mg L^{-1} or less than 2 mg L^{-1} were excluded. Mean bromide level in dosing lines was 9.2 mg L^{-1} and mean bromide level in mesocosms was 7.10. These values were used to estimate P_{LICD*} using mixing tank and marsh phosphorus concentrations. P_{LICD*} is compared to phosphorus concentrations in the mesocosms. (N=51).

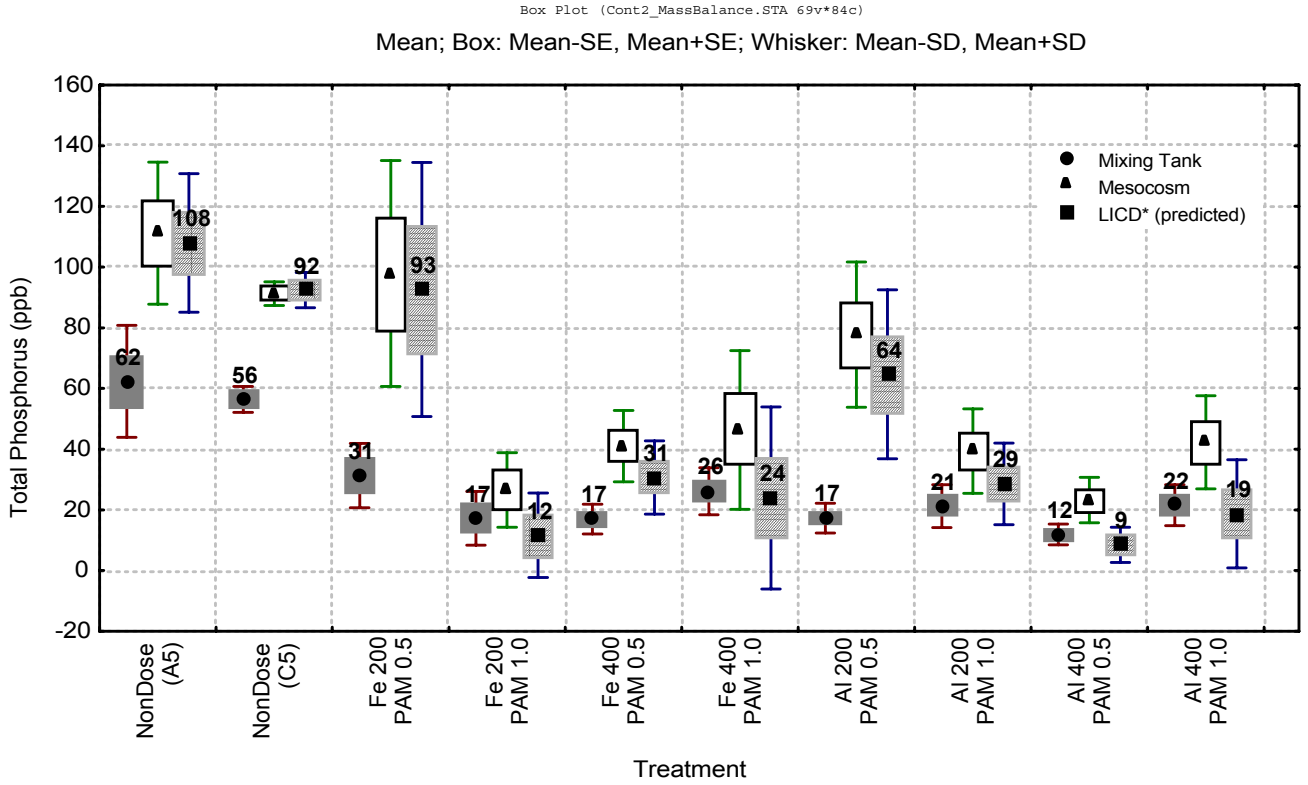

14.2.3.2.5. Determining a marsh removal efficiency for floc settling and biotic uptake

Biotic uptake and floc settling would be expected to occur in all the treatments. The calculations graphed in Figure 100 suggests this with predicted phosphorus concentrations for hydrologically isolated mesocosms being below those for the mixing tanks for many metal polymer blends. In the treatments receiving chemical treatment, dissolved phosphorus is immediately transformed to particulate phosphorus and settling occurs (Figures 28, 35 and 38). Chemical precipitation and subsequent settling of readily settleable precipitates are the primary phosphorus removal mechanisms.

For the remaining particulate and dissolved species, continued removal by biotic uptake and settling likely occurs. This is based to some degree on phosphorus removal in the NonDosed mesocosms. Some phosphorus uptake occurred in the NonDosed Mesocosms (Figure 82). Batch-flow studies in March, July and October 1999 provide insight into the kinetics. Figure 101 shows total and dissolved phosphorus removal over the first four days of both the March and October 1999 batch-flow studies. Only the first four days of data were considered here as dilution, water levels fluctuations and background phosphorus concentrations confounded longer-term trends in the Batch Flow studies. During the March 1999 study, the decrease in total phosphorus occurred over the first two days and concentrations were relatively flat thereafter (Figure 101a). Dissolved phosphorus concentrations decreased linearly over the first three days but were also flattened by the fourth day. Thus, over the first two days, phosphorus removal apparently occurred through biotic uptake and settling as shown by the decrease in both dissolved and total phosphorus. After the second day, biotic conversion from dissolved to particulate phosphorus still occurred though no actual phosphorus removal was occurring in the mesocosms. In October 1999, similar trends were shown at all three sites. Having three sites increased the variance in the data. However, for all the data, total phosphorus uptake occurred mainly by the second day even though a decrease in dissolved phosphorus concentrations occurred over the first four days (Figure 101b).

Biotic uptake is frequently described by:

$$\frac{\partial C}{\partial t} = k_{marsh} C \,. \qquad \textbf{Equation 18}$$

where

k_{marsh} = the phosphorus uptake constant for marshes (Metcalf and Eddy, 1979; Kadlec and Knight, 1994). Thus, higher phosphorus removal rates are expected at higher phosphorus concentrations and as concentrations decline, removal rates decline also. Equation (18) was used to describe phosphorus changes during the field batch studies for the runs described in Figure 101. Table 36

shows that in the non-dosed chambers, Equation (18) did not describe the trends shown in Figure 101 for total phosphorus and 18% of the variance for dissolved phosphorus. Thus, biotic uptake seems to have had some effect on dissolved phosphorus but no effect on total phosphorus during the batch flow mesocosm studies for the time frame shown in this study. This occurs despite some decrease in total phosphorus in the batch flow studies.

Table 36. Biotic uptake of phosphorus in mesocosm studies, February/March 2000.

	Total phosphorus	Dissolved phosphorus
K (d^{-1})	.058	0.366
Standard error	.021	0.028
p-level	0.0064	0.0000
R^2	00.00%	18.03%

These findings suggest several important findings when considering the data from this last mesocosm study which was operated as CFSTRs. First, when phosphorus enters the mesocosms, biotic uptake leads to the speciation change of dissolved to particulate phosphorus and that can occur for many days. Dissolved phosphorus concentrations near 5 $\mu g\ L^{-1}$ can be achieved in the mesocosms solely through biotic uptake. However, this is expected to take time in excess of that which would be acceptable for a treatment wetland. Figure 102 demonstrates this trend for this last demonstration run by showing dissolved phosphorus concentrations through the NonDosed mesocosms. In those mesocosms, dissolved phosphorus concentrations are relatively constant from pumping through the inflow pipes. However in the mesocosms, dissolved phosphorus decreases approximately 25 $\mu g\ L^{-1}$. However, these decreases in dissolved phosphorus concentration do not necessarily correspond to decreases in total phosphorus concentrations. During this same study, phosphorus concentrations in the mesocosms in the NonDosed mesocosms was only slightly less than that in the inflow pipes (Figure 103). Thus, the second finding is that biotic phosphorus uptake may not lead to the phosphorus removal but rather to a change in speciation from dissolved to particulate phosphorus.

Figure 101. Total and dissolved phosphorus changes in Non-dosed mesocosms during Phase II Batch Studies.
Relatively little total phosphorus was removed by biotic uptake.

A) March 1999

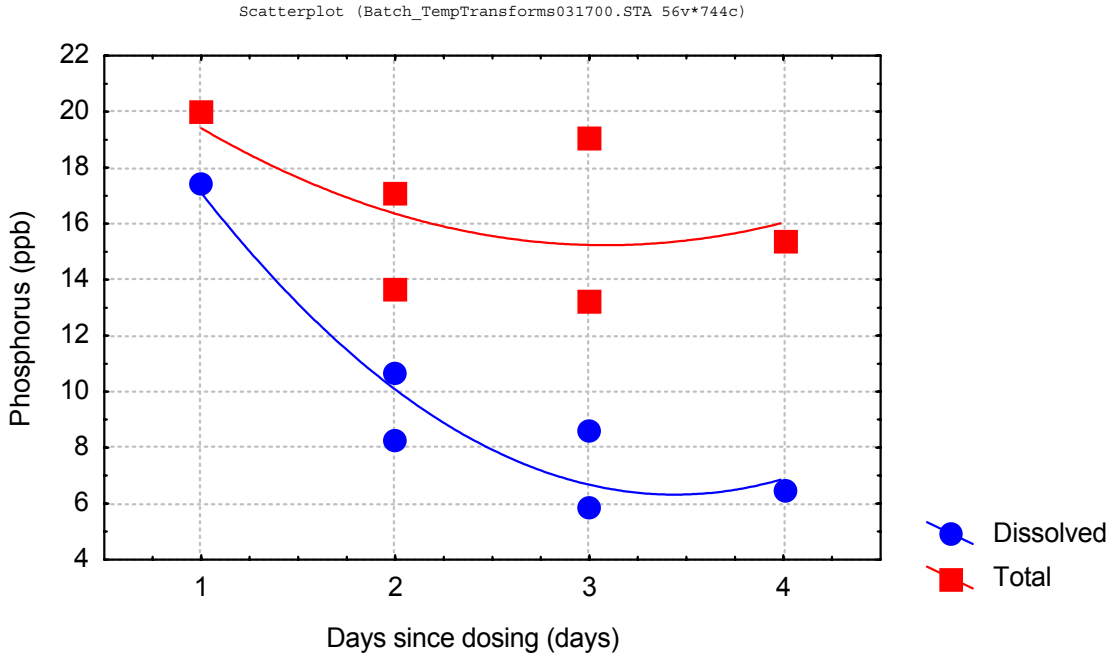

B) October 1999

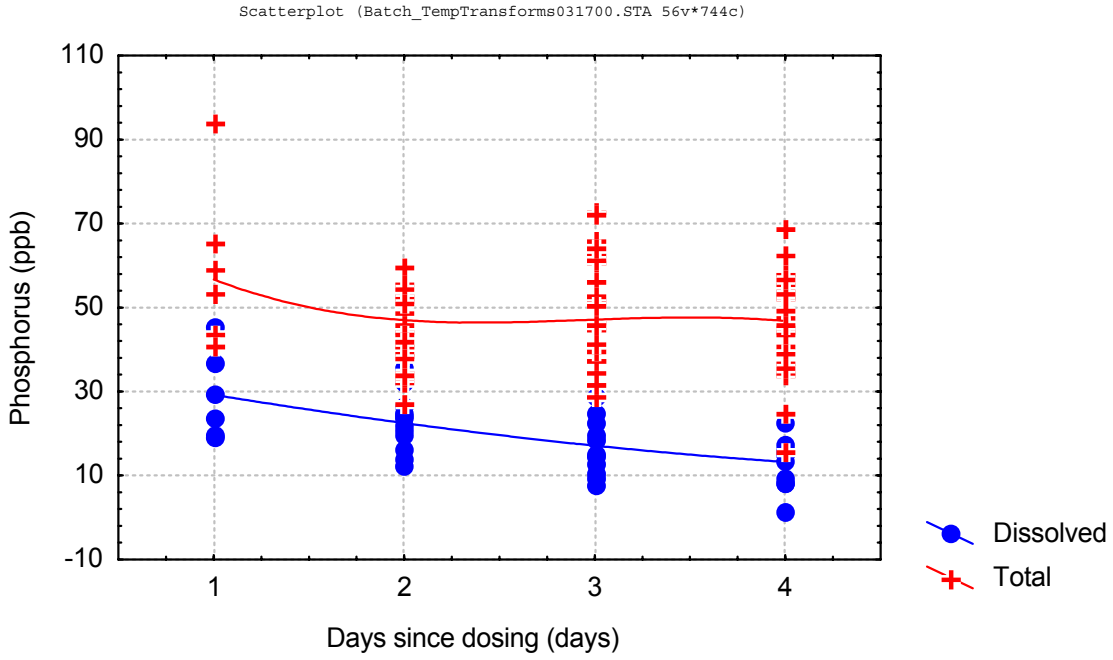

A mass balance model for the mesocosms becomes:

Mass In	=	*Mass out*	+	*Mass removed through chemical precipitation and settling*	+	*Mass removed through biotic uptake and settling*	**Equation 19**

This mass balance equation assumes two mechanisms removing phosphorus during chemical dosing within the marsh. The first is a rapid precipitation as occurred in the mixing tanks and the second is a slower longer term process removing less readily removable particulate phosphorus and dissolved phosphorus. For the purpose of this study and based upon the above findings, biotic removal is considered negligible.

Mass into the mesocosm is defined as:

$$Mass_{In} = Mass_{Pumped} + Mass_{Marsh} =$$

$$P_{In}Q_{In} + P_{Marsh}Q_{Dilution} = P_{In}Q_{in} + P_{Marsh}\frac{(Br_{In} - Br_{Out})}{Br_{Out}}Q_{In} = P_{In}\,{Br_{In}}/{Br_{Out}} \quad \textbf{Equation 20}$$

where

P_{in} = total phosphorus measured at the inflow to the system. Inflow phosphorus because it is pumped from the marsh approximates background phosphorus concentrations in the marsh.

Mass out of the mesocosm is defined as:

$$Mass_{Out} = Q_{Out}P_{Out} = Q_{In}\frac{Br_{In}}{Br_{Out}}P_{Out} \quad \textbf{Equation 21}$$

where

P_{out} = total phosphorus measured in the mesocosm. This assumption is consistent with CFSTR models.

Mass removed through chemical precipitation is:

$$Mass_{LICD} = Q_{In}P_{settleatlve} = Q_{In}PP_{settleable} \quad \textbf{Equation 22}$$

where

$P_{settleable}$ equals settleable phosphorus which is essentially settleable particulate phosphorus ($PP_{settleable}$). $P_{settleable}$ can be defined by combining Equations (5) and (9) to form:

$$P_{settleable} = \left[FTP_{Marsh}(1-\exp(K_{Me}Me_{In}) + PP_{Marsh}\right](1-\exp(K_{PAM}PAM_{In})). \quad \textbf{Equation 23}$$

Mass removed through biotic uptake is assumed to be negligible for the time period considered here. This does not mean that biotic uptake has not occurred and removed phosphorus or that natural processes will not in a larger scale marsh. Rather it suggests that for LICD in the mesocosm studies, chemical precipitation effects are much greater and more describable.

Combining Equations (20) through (23) yields:

$$UTP_{Out} = \frac{\left[UTP_{In}\left(Br_{In}/Br_{Out}\right) - N \times FTP_{In}(1-\exp(K_{Me}[Me_{In}] + PP_{In})(1-\exp(K_{PAM}PAM_{In})\right]}{\left(Br_{In}/Br_{Out}\right)}.$$

Equation 24

K_{ME} and K_{PAM} were determined earlier in the process analyses (Tables 34 and 35). UTP_{In}, Br_{In}, Br_{Out}, FTP_{In}, PP_{In} Me_{In} and PAM_{In} are independent variables, And N the percent phosphorus settled in the mesocosms as compared to the percent predicted to have settled by the mixing tank analyses.

For Iron, this model explains 67% of the variance with the data (Table 37; Figure 104) whereas for aluminum this model explains 78% of the variance (Table 37; Figure 105). Based on the polymer and metal reaction coefficients, approximately 75% of the particulate phosphorus that was expected to settle based upon mixing tank calculations did settle during iron dosing. This result suggests that other factors not considered in the process analyses confounded iron settling in the mesocosms. For aluminum, more phosphorus settled than was expected and this suggests that factors confounding particulate settling differ for the different metals (Table 37).

Table 37. Settling efficiency in mesocosms, February/March 2000.

	Iron	Aluminum
N (%)	0.75	1.08
SE	0.076	0.074
p-value	0.0000	0.0000
R^2	67.09	77.53

Figure 102. Dissolved phosphorus concentrations from pump through mesocosms for Non-dosed mesocosms.

Dissolved phosphorus concentrations decreased from a median near 70 µg L^{-1} to approximately 40 µg L^{-1} once waters entered the mesocosms.

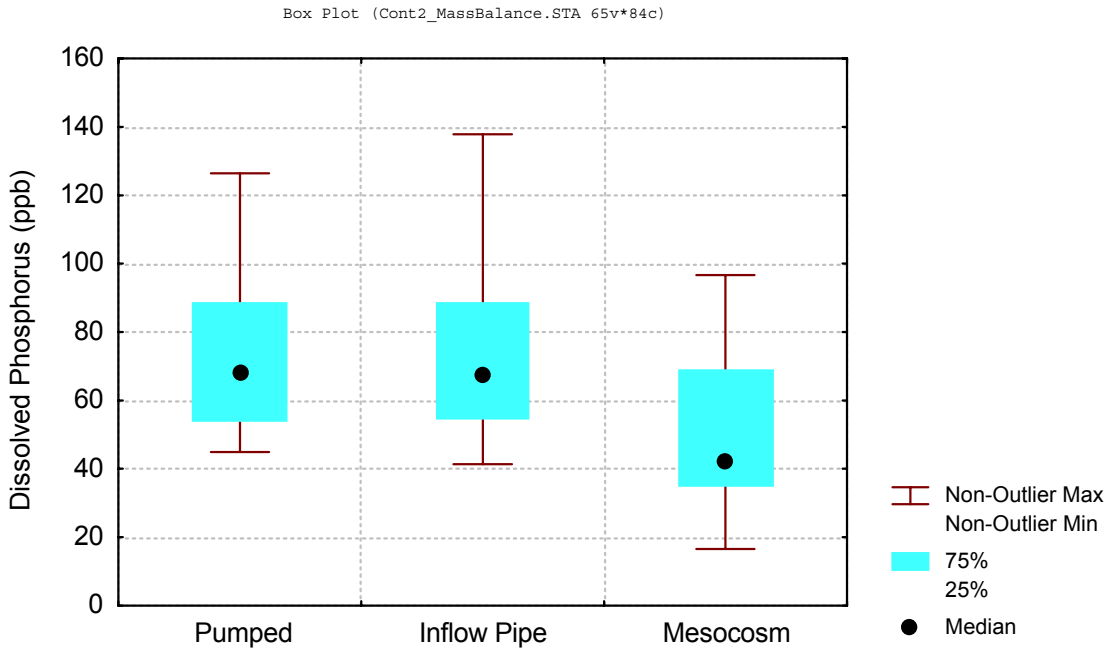

Figure 103. Small differences in total phosphorus concentrations between inflow (background) waters and Non-Dosed mesocosm waters, February/March 2000.

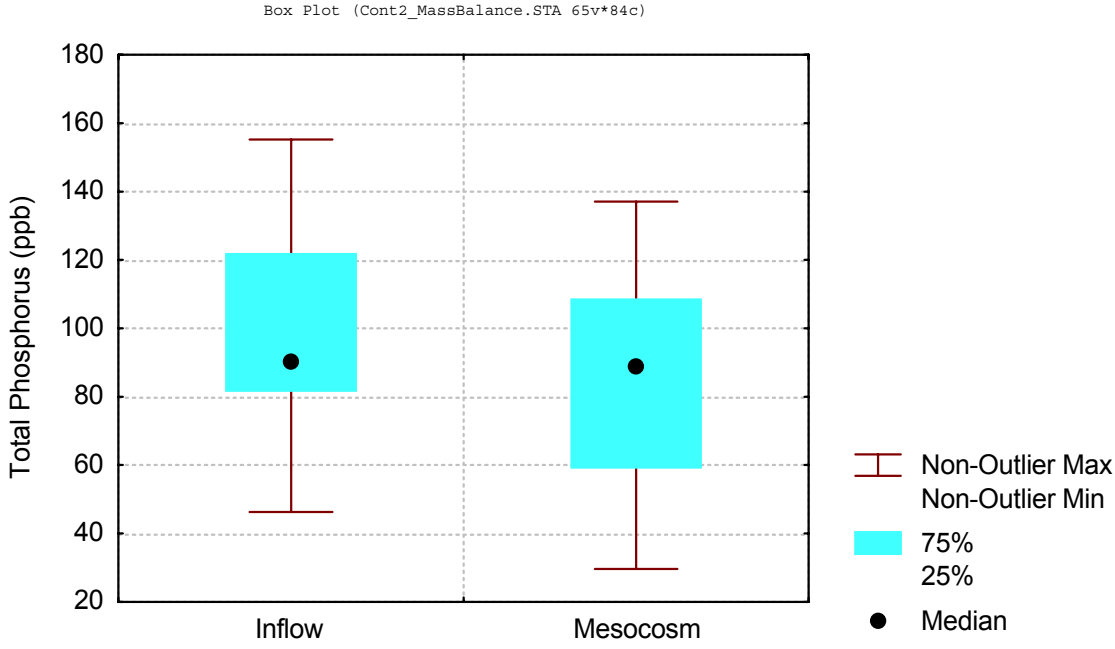

Figure 104. Mass Balance analyses for total phosphorus removal in the mesocosms during February/March 2000 using ferric iron as FPD.
Data for which bromide was below 2 mg L^{-1} or above 20 mg L^{-1} was excluded as well as data in which inflow bromide concentrations were greater than mesocosm concentrations. N = 27.

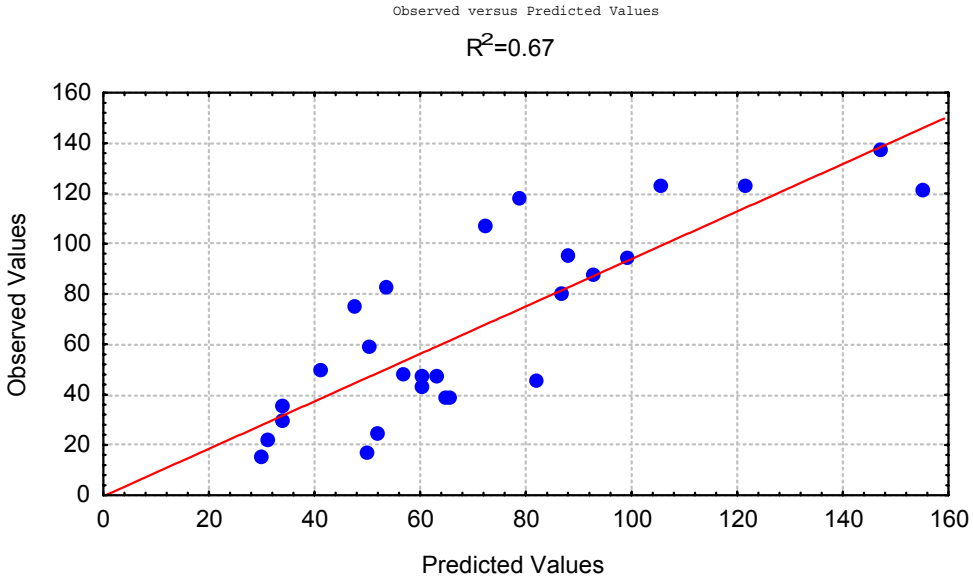

Figure 105. Mass Balance analyses for total phosphorus removal in the mesocosms during February/March 2000 using aluminum as Clarion 4100.
Data for which bromide was below 2 mg L^{-1} or above 20 mg L^{-1} was excluded as well as data in which inflow bromide concentrations were greater than mesocosm concentrations. N = 25.

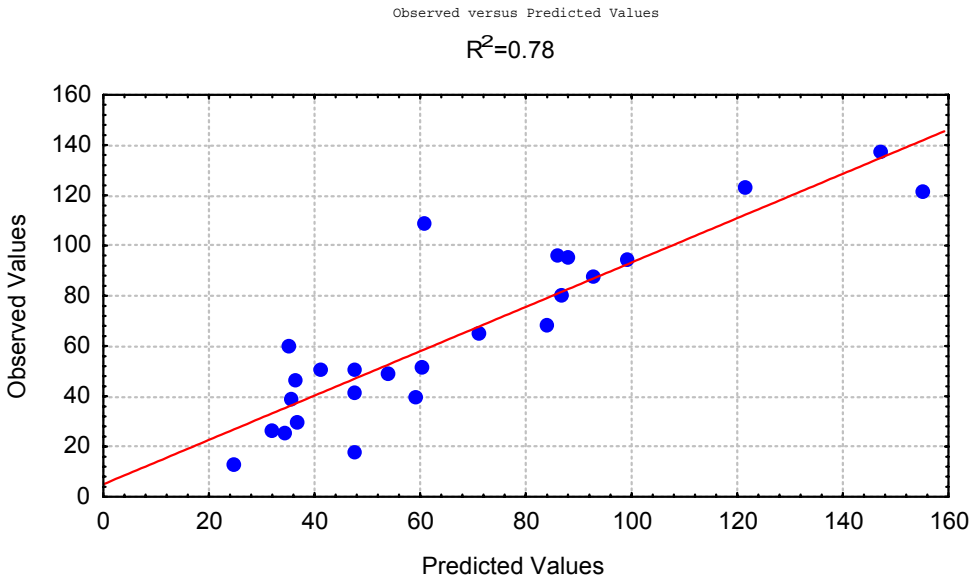

From this process analyses, the following conclusions have been made:

1. The formation of particulate phosphorus following metal dosing has been approximated as exponentially dependent upon metal dosing level. This model explains 82% of the variance for aluminum and 98% of the variance for iron. The model predicts that an iron dose of 5 mg L^{-1} or an aluminum dose of 2 mg L^{-1} would convert half the dissolved phosphorus to particulate phosphorus. This is approximately 100 μM for both metals. This model has been limited by the dosing levels used in this study. Jar test findings have demonstrated that a metal dosing level of 100 μM is as effective as 200 μM in converting dissolved to particulate phosphorus. Moreover, some field studies have shown equivalent phosphorus removal rates for dosing levels of 100 and 200 μM. Therefore, a target metal dose for near complete removal may be as high as 200 μM as generally described in this model or as low as 100 μM as shown in the jar test.
2. Based upon jar test studies, the conversion of poorly-settleable particulate phosphorus to settleable particulate phosphorus using polymers can be described as an exponential relationship dependent upon polymer dosing level. Using mixing tank data, the half-PAM dosing constant was 0.26 mg L^{-1} when added following iron dosing and was 0.17 when added following aluminum dosing. These model results suggest that for iron dosing a minimum PAM dosing concentration of 0.5 mg L^{-1} is required for good settling and for aluminum dosing a minimum PAM dosing concentration of 0.34 mg L^{-1} PAM is required. Data from the field mesocosm studies suggest that these dosing levels may not be conservative enough as PAM dosing levels of 0.5 mg L^{-1} appeared to provide less effective phosphorus removal than PAM dosing levels of 1.0 mg L^{-1}. Thus a minimum PAM dosing concentration of between 0.5 mg L^{-1} and 1.0 mg L^{-1} is recommended in field applications.
3. Mesocosm water was a mix of both pumped chemically dosed water and non-pumped marsh water. Marsh water entered the mesocosms because of diel water level variations in the surrounding marsh and subsequent water level corrections within the mesocosms. This dilution effect is shown by bromide data. Bromide is a conservative tracer.
4. Phosphorus concentrations achieved in the mixing tanks were consistently lower than phosphorus concentrations achieved in the mesocosms. The mixing tanks were hydrologically isolated systems as defined by only having pumped water entering the tanks and having no dilution effects from non-chemically dosed marsh water. The mesocosms were not hydrologically isolated as demonstrated by the bromide data.
5. Because of dilution of chemically dosed water with background marsh waters, phosphorus levels achieved in the mesocosms during this study do not represent minimum phosphorus levels that can be achieved under LICD. Mesocosm dilution with marsh water was incorporated into the data set based upon bromide data to estimate total phosphorus concentrations that can be achieved under hydrologically isolated conditions in a field marsh study. This method predicts that mean total phosphorus concentrations of near 10 μg L^{-1} may be achievable for optimized low intensity metal polymer blends. These

predicted levels are very similar to those levels achieved in the mixing tanks under hydrologically isolated conditions and in some cases represent total phosphorus removal of 80 – 90 % of inflow total phosphorus.

6. Biotic uptake was found to be negligible in the mesocosms for this study as compared to abiotic chemical removal.
7. A steady state mass balance model explained two thirds of the variance for total phosphorus removal under iron addition and three quarters of the variance under aluminum addition. Based upon the model, settling of iron bound particulate phosphorus is somewhat hindered in the marsh whereas settling of aluminum bound particulates is not.

14.2.4. DOC and metal analyses

DOC was sampled at two locations in the mesocosms (C1, C3) as well as the inflow locations and the mixing tanks. The goals for measuring DOC were to assess changes in DOC concentrations that occur under metal dosing and whether those changes persist. Raw data was converted to inflow/outflow data to assess cause and effects of metal dosing and to consider concentration decreases across the system rather than just absolute measures of DOC through the system. Additionally, changes in iron or aluminum concentrations were measured to assess its fate in the water column.

Metal dosing led to immediate decreases in DOC for both aluminum and iron blends as shown by the reductions in DOC in the inflow lines after metal dosing as compared to concentrations entering the NonDosed mesocosms (Figure 106). Chemical dosing at 200 and 400 μM resulted in an approximate 7 mg L^{-1} decrease in DOC for both aluminum and iron dosing blends.

In general, these reductions apparently persisted in the mesocosms. DOC concentrations recorded in the NonDosed mesocosms were higher than background waters. The reason for this is unclear though this could be do in part to DOC diffusion from the sediments. For the NonDosed mesocosms, DOC concentrations in the mesocosms were 5 mg L^{-1} above that found in the inflow water. For both iron and aluminum, the DOC concentrations in the mesocosms were less elevated above inflow concentrations and had less variance (Figure 107).

Figure 106. DOC concentration reductions in inflow pipes following chemical dosing

DOC concentrations in the pipe were measured and it was determined that in situ dosing immediately reduced DOC concentrations. Data shown is for metal dosing levels of 200 and 400 µM during the February-March 2000 study.

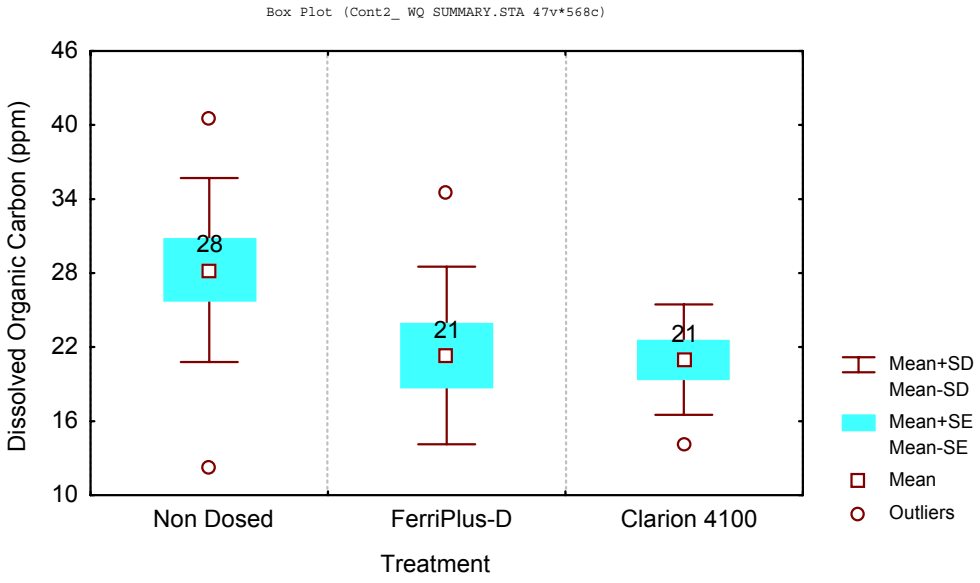

Figure 107. DOC reductions in mesocosms following chemical dosing.

Data is from mesocosms under chemical dosing levels of 0, 200 and 400 µM.

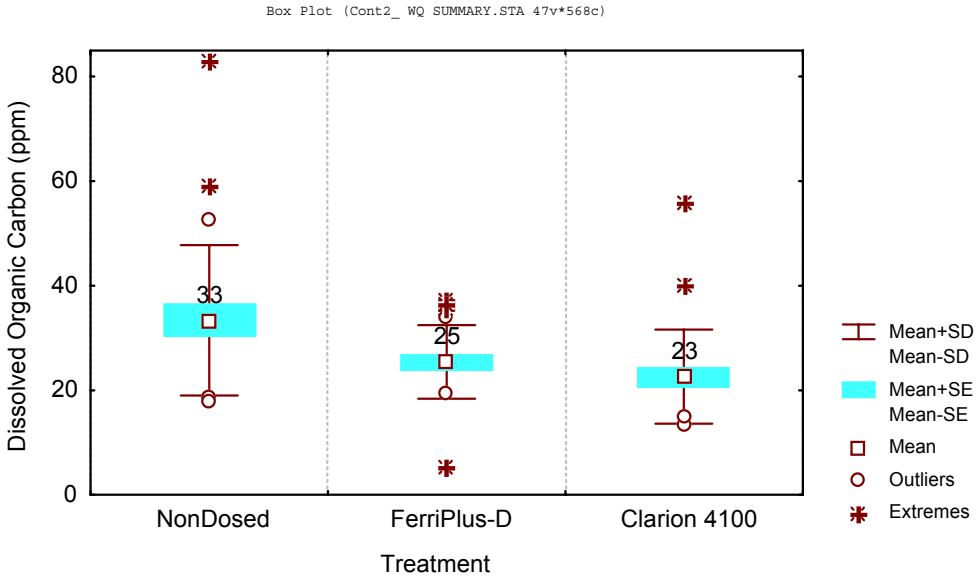

Higher metal dosing levels resulted in lower DOC concentrations for both aluminum and iron dosing, though these effects were greater for iron (Figure 108). This trend persisted in the water column under aluminum dosing with higher dosing aluminum dosing levels achieving lower DOC concentrations (Figure 109). However for iron, the dosing levels of both 200 and 400 μM achieved equivalent DOC concentrations.

Higher PAM dosing levels showed no obvious effect on DOC concentrations immediately after dosing (Figure 110) though DOC concentrations in the water column appeared to slightly decrease with higher PAM dosing levels (Figure 111). These difference were not statistical significant.

Dosing did not affect concentrations of the dissolved metal being dosed. For instance, iron dosing did not increase dissolved iron levels in the water column and aluminum dosing did not increase dissolved aluminum levels in the water column (Figure 112). There were slight increases in total metal for each dosed chemical. However, both metals averaged less than 1 mg L^{-1}.

Aluminum dosing of all levels increased surface water concentrations of total aluminum to generally between 0.3 to 1.3 mg L^{-1} (Figure 113). Residual dissolved aluminum concentrations generally were below 0.2 mg L^{-1} (Figure 114). Increasing dosing levels did not affect residual concentrations of either dissolved or total aluminum. Higher dosing aluminum levels decreased DOC concentrations very linearly (Figure 115) and linearly increased the amount of DOC removed from the water column (Figure 116). In general, for each milligram of aluminum added, one milligram of DOC is removed from the water column (Figure 116). This reduction occurred at pH levels generally around 7 – 7.5 and occurred without any pH manipulations of the treated waters.

Figure 108 Effects on inflow DOC concentrations for different metal dosing levels.
Increasing the metal dosing level from 200 to 400 µM decreased DOC concentrations by approximately 6 mg L^{-1}.

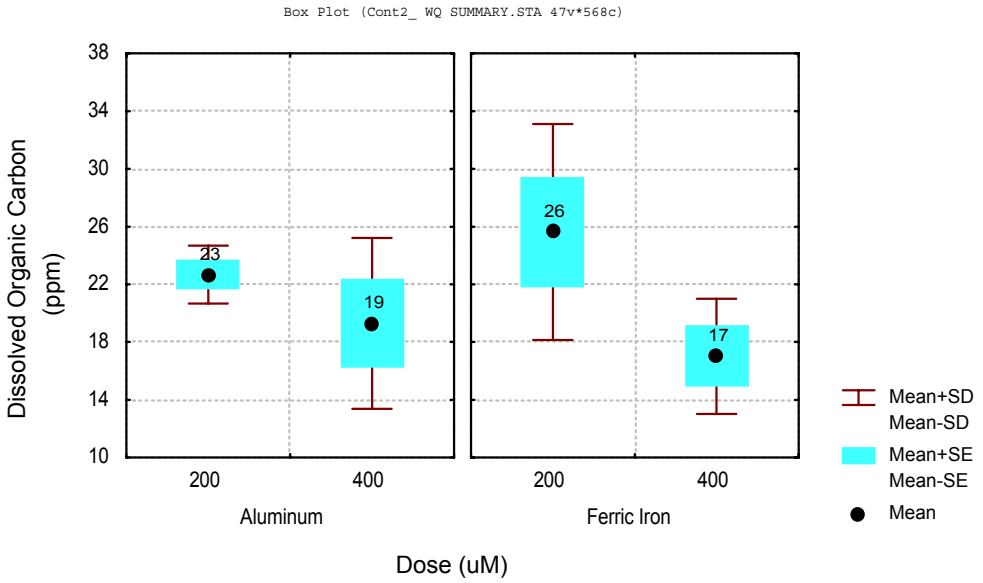

Figure 109. Effects on water column DOC levels for different metal dosing cocentrations.
Data is for iron and aluminum treated mesocosms during February – March 2000 study.

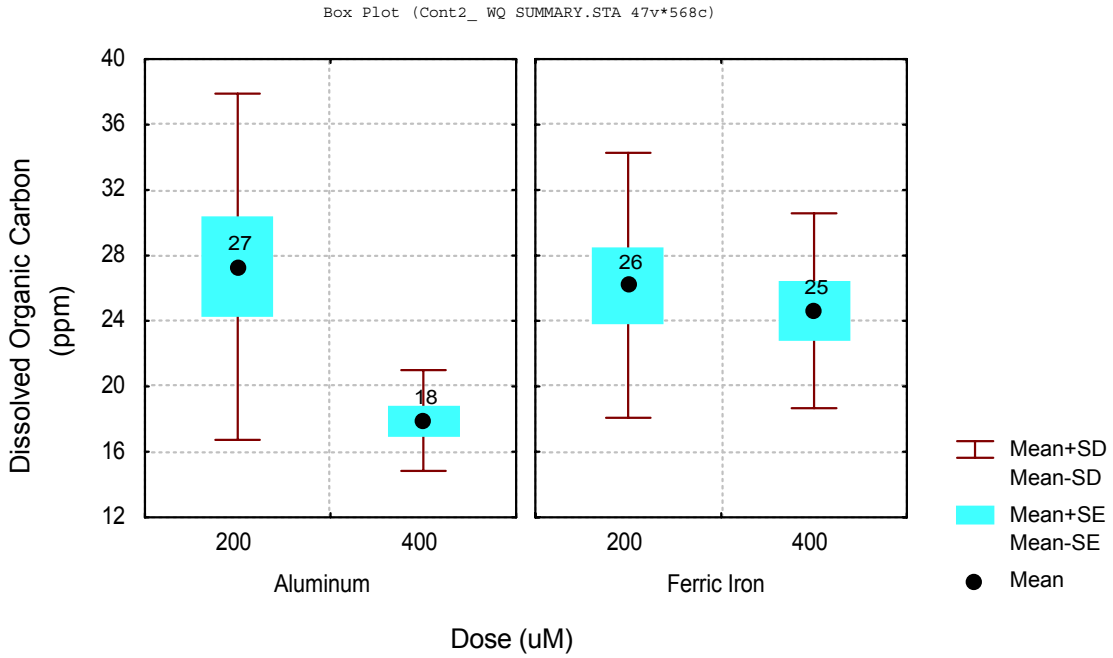

Figure 110. Effects of PAM dosing levels on DOC concentrations in treated inflow.
PAM dosing levels did not initially effect DOC concentrations

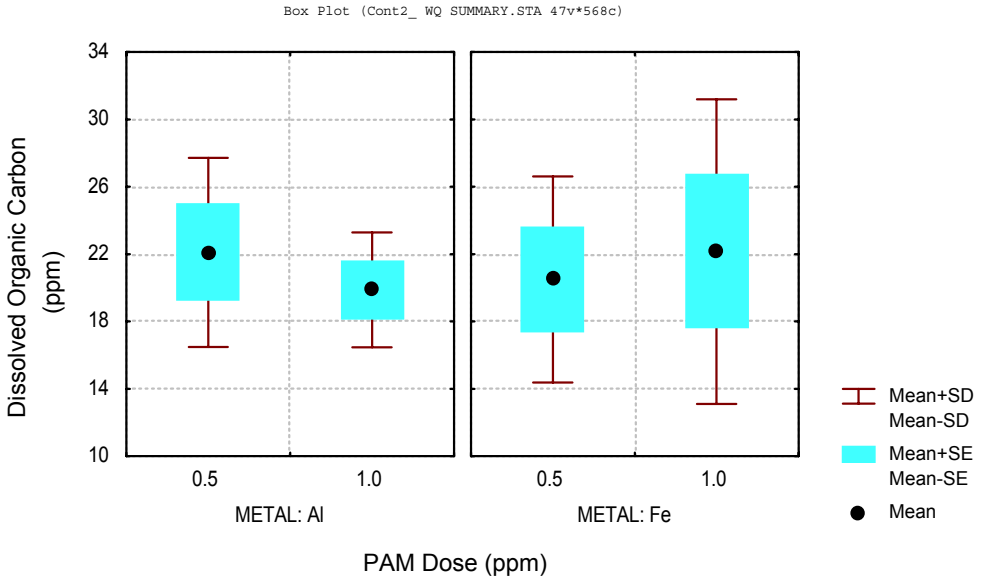

Figure 111. Effects on water column DOC concentrations for higher PAM dosing levels.
Data is for treatments receiving iron or aluminum dosing in February-March 2000 study.

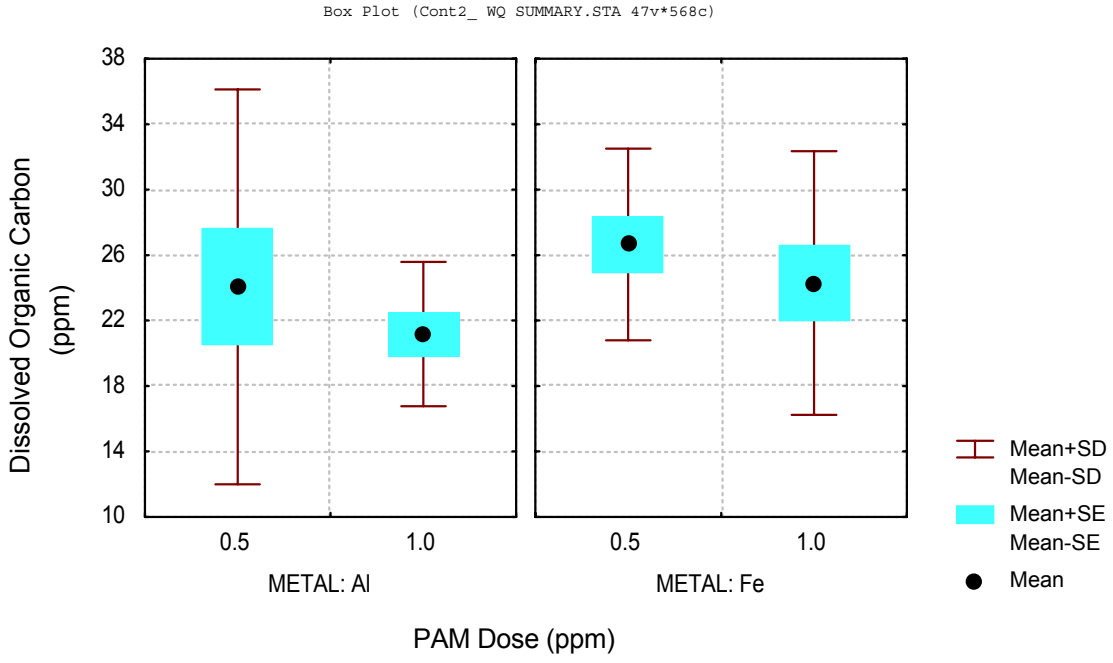

Figure 112. Total and dissolved metal concentrations achieved in the mesocosms for different treatments.

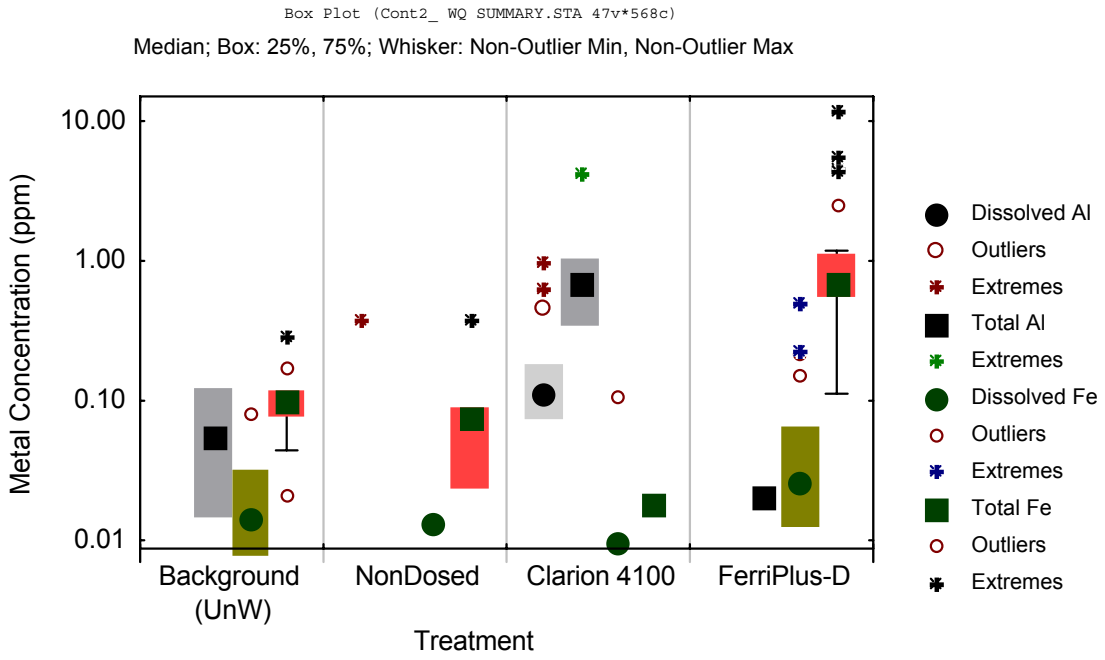

Figure 113. Residual total aluminum concentrations in the water column are independent of aluminum dosing concentration above 2 mg L^{-1}.

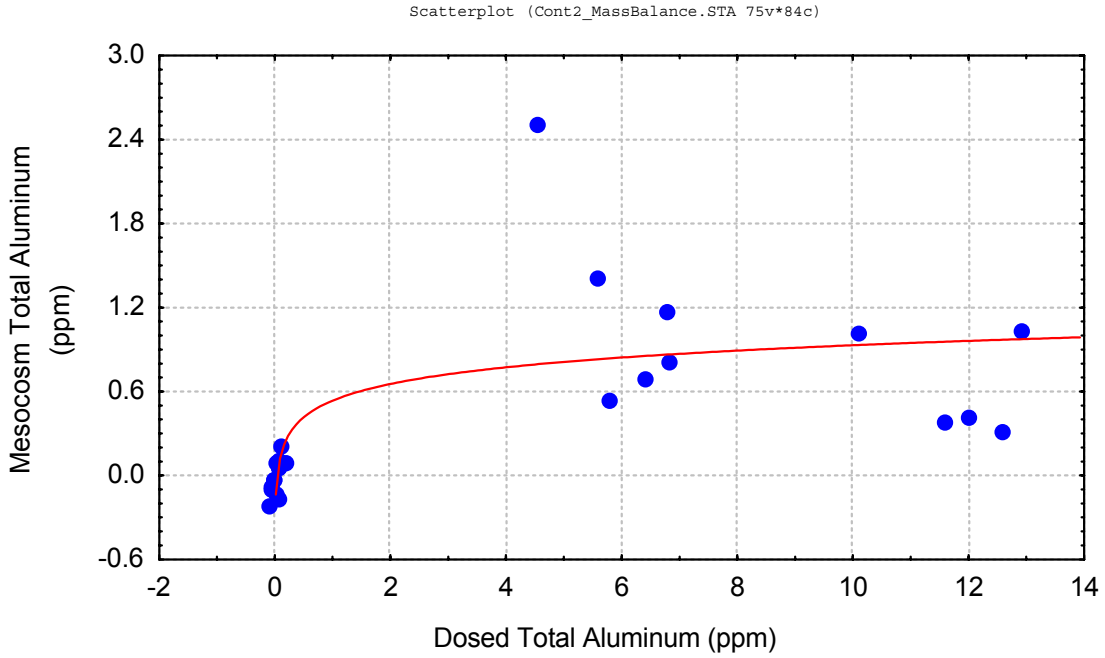

Figure 114. Residual dissolved aluminum concentrations in the water column following aluminum dosing above 2 mg L^{-1}.
Dissolved aluminum concentrations are generally at or below 0.2 mg L^{-1}.

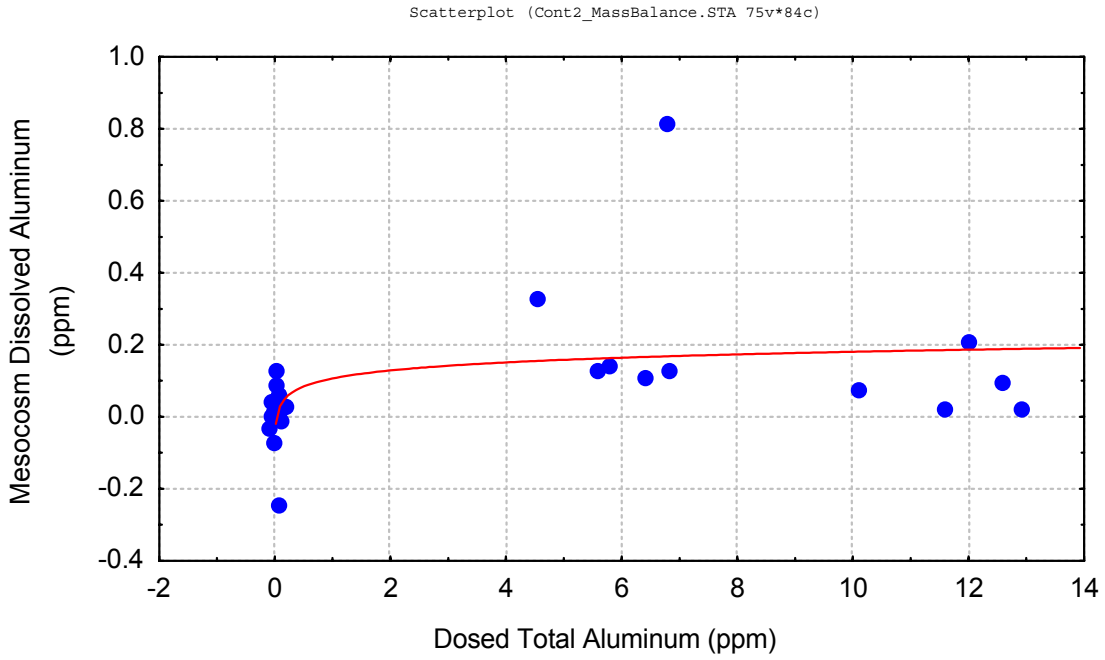

Figure 115. Decreases in mesocosm DOC concentrations with increasing aluminum dosing levels.
Line indicates trend.

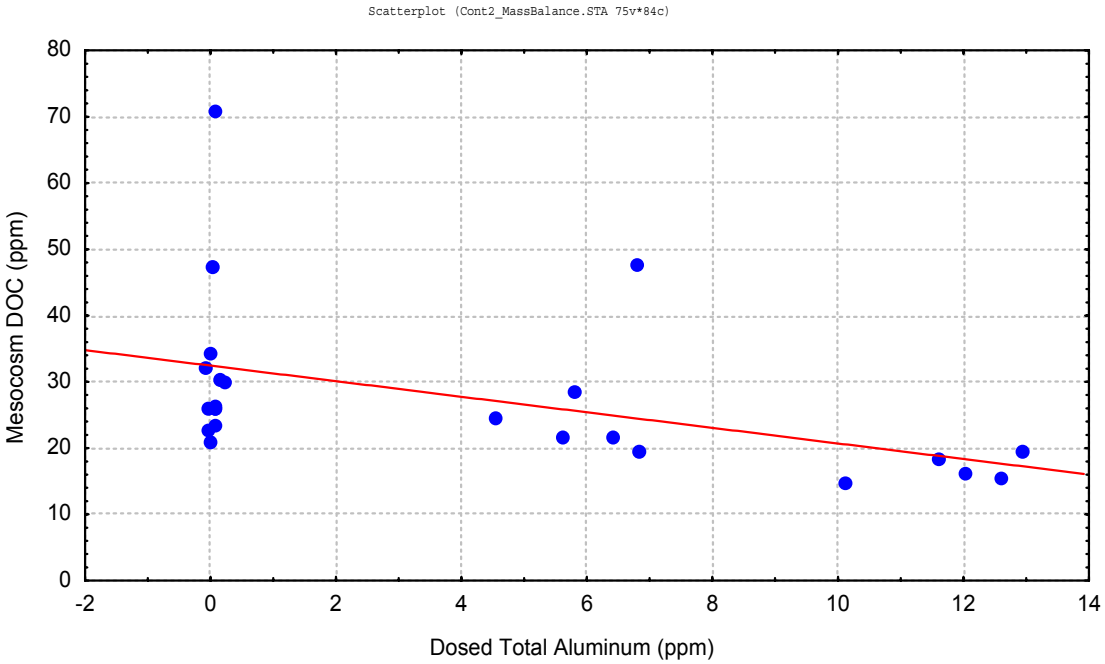

Figure 116. DOC removal as a function of aluminum dosing concentration. Line indicates trend.

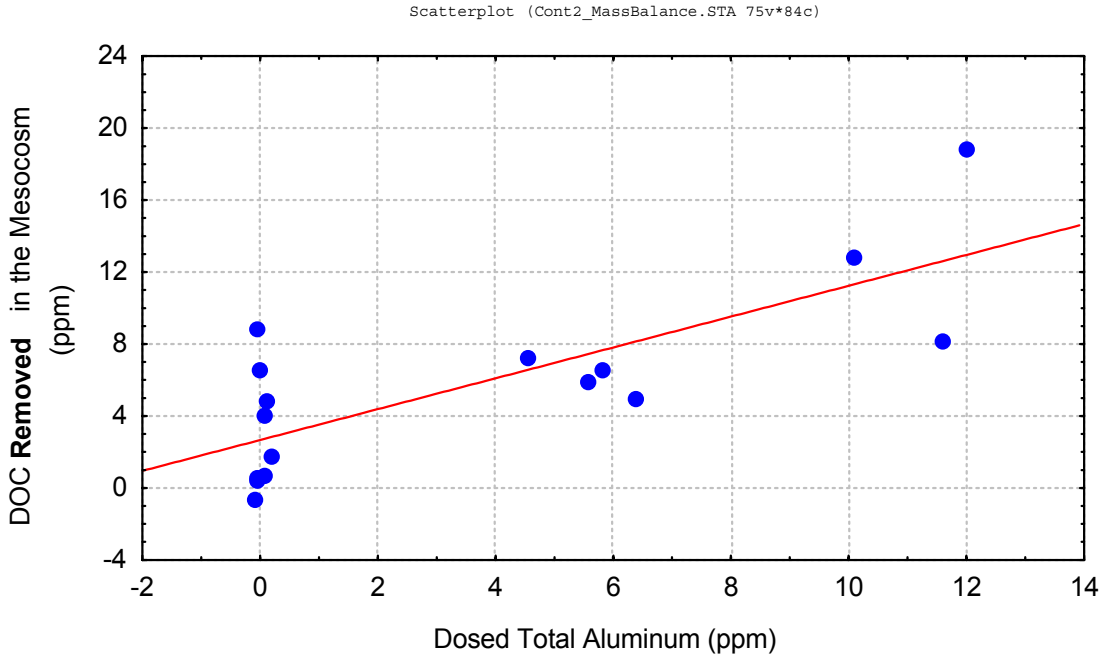

Iron dosing resulted in a residual total iron concentration in the water column of near or less than 1 mg L^{-1} except for a few outliers (Figure 117). Dissolved iron was generally at background and less than 10 µg L^{-1} (Figure 118). Iron generally decreased DOC concentrations in the water column though these effects were not as predictable as for aluminum, suggesting that iron was not settling out metal-organic complexes as well as was aluminum (Figure 119). Nonetheless, DOC was generally removed from the water column under iron dosing and removal generally increased with higher iron dosing level (Figure 120). For each milligram of iron added, approximately 0.4 milligram was removed. DOC removal was less efficient for iron than for aluminum on a weight basis (e.g. grams of DOC removed for grams of metal dosed). However, because a mole of iron is nearly twice as heavy as a mole of aluminum, DOC removal was fairly equivalent on a molar basis.

Figure 117. Residual total iron concentrations in the water column are independent of iron dosing concentration above 5 mg L^{-1}.

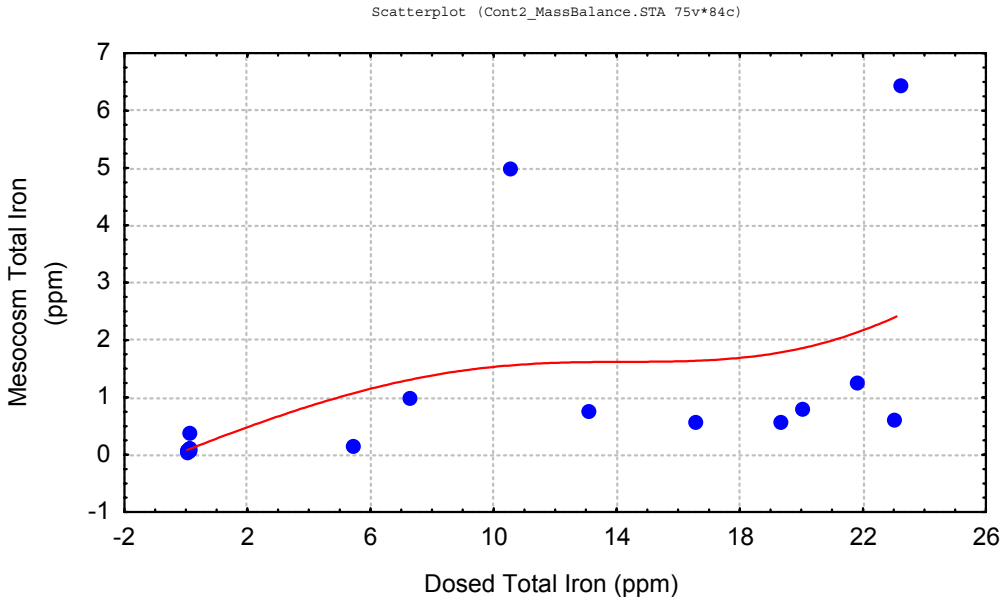

Figure 118. Residual dissolved iron concentrations in the water column are independent of iron dosing concentration.
Dissolved aluminum concentrations are generally at or below 0.1 mg L^{-1}.

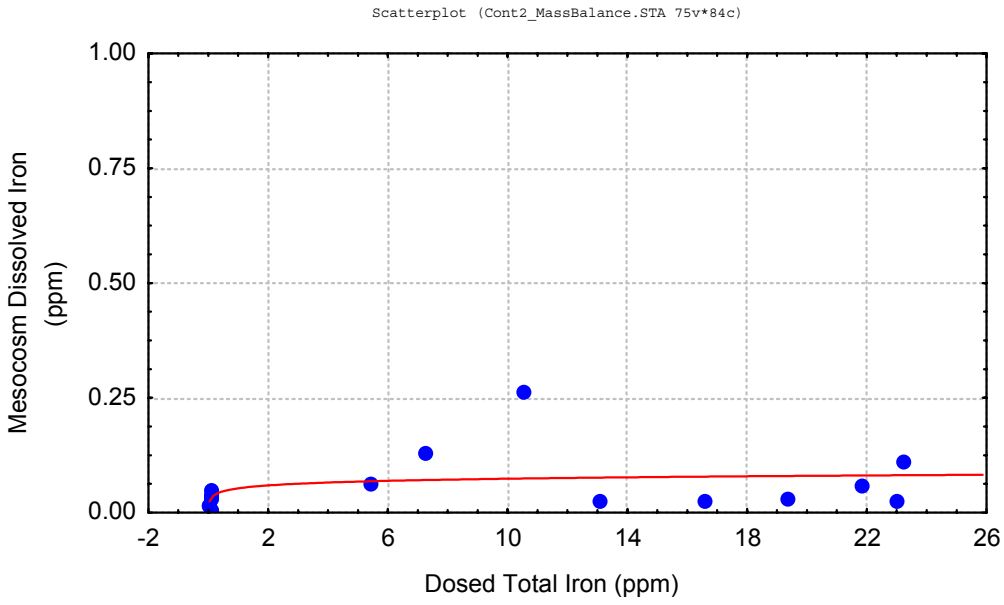

Figure 119. Decrease in mesocosm DOC concentrations with increasing iron dosing levels.
Line indicates trend.

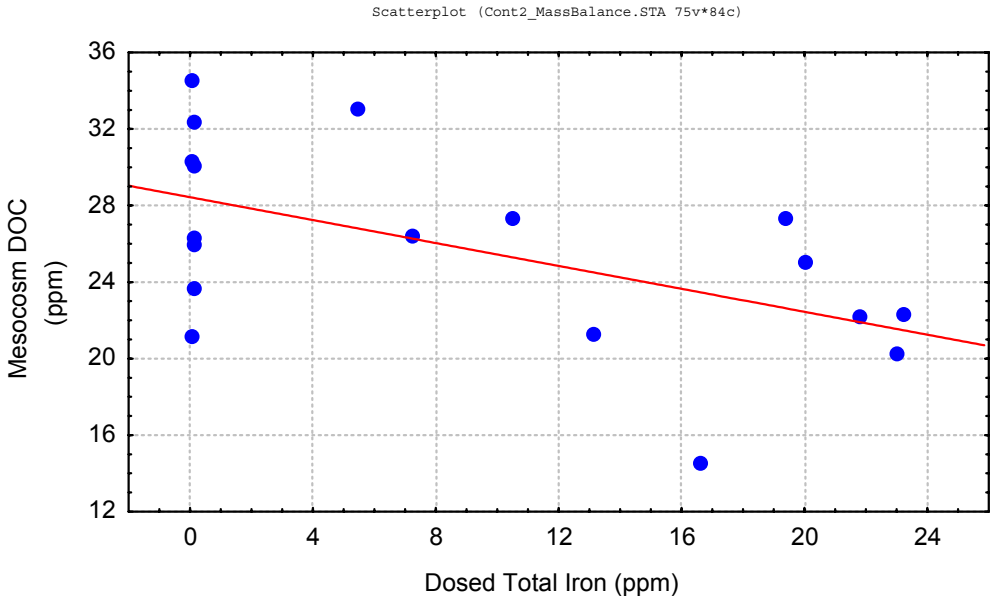

Figure 120. DOC removal as a function of iron dosing level.
Line indicates trend.

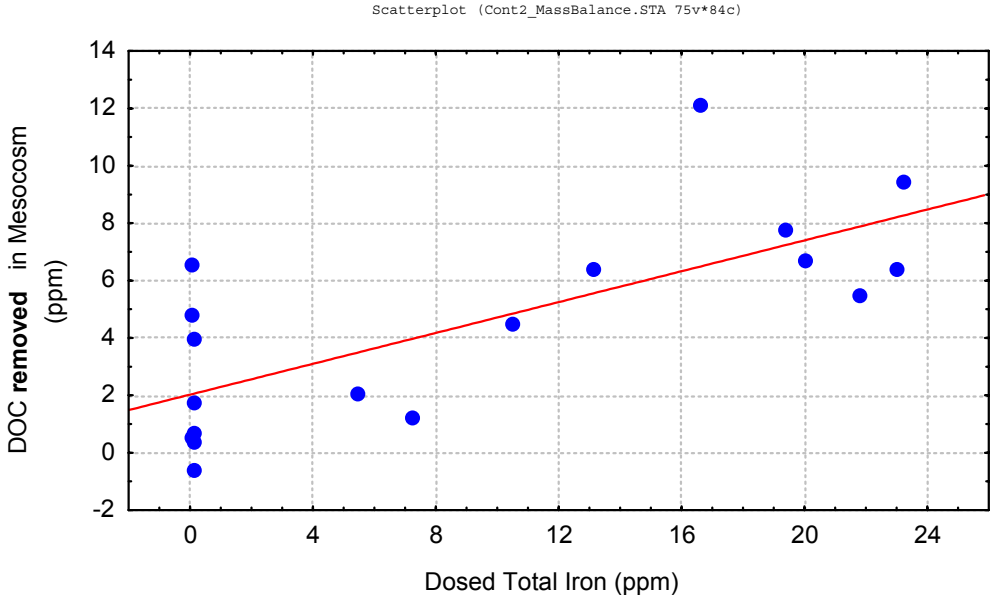

14.2.5. Unattended monitoring data analyses

Unattended monitoring was used to monitor temperature, pH, DO, specific conductivity and turbidity. Turbidity probes were problematic and so this data has not been included in this analysis. Probes were deployed at Site A and began collecting data immediately and through the entire run. Data was collected for approximately one week after dosing ceased.

Metal dosing had no effect on temperature with all treatments averaging approximately 22.5 °C with some diel variation as indicated by the quartile ranges (Figure 121). These temperature characteristics were very similar to background measurements.

Figure 121: Temperature is unaffected by LICD.

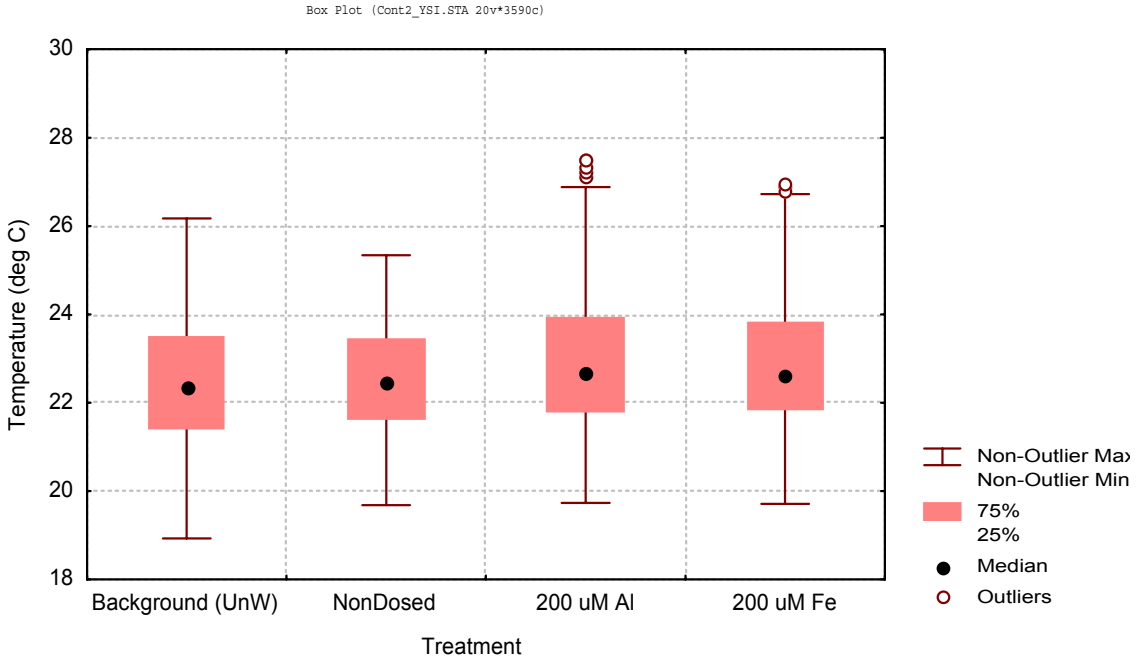

As shown by the differences between dosed and background concentrations, pH was higher in the mesocosms than in background water (Figure 122). This is consistent with Phase 1 findings (Bachand et al., 1999). Metal dosing generally suppressed the pH levels with aluminum having a greater effect than iron. This too is consistent with Phase I findings (Bachand et al. 1999).

Figure 122. pH decreases by 0.2 – 0.4 units with metal dosing concentrations of 200 µM.
Aluminum has a greater effect than iron.

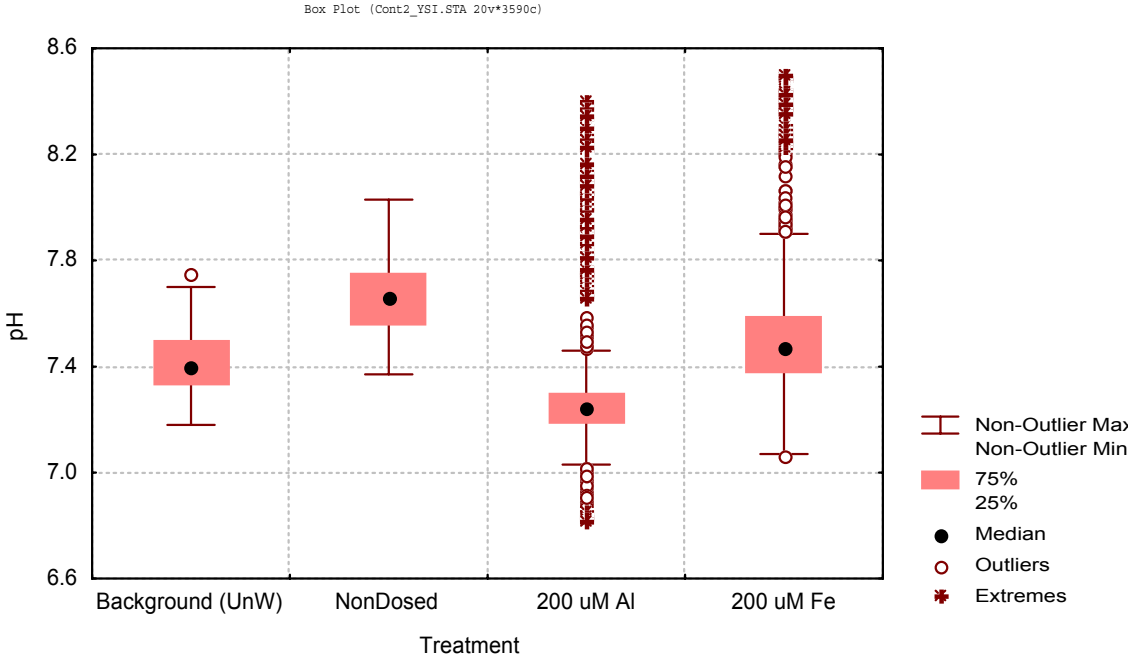

DO concentrations in the NonDosed mesocosm was consistent with background levels and lower than the levels under metal dosing of both iron and aluminum (Figure 123). Higher DO levels under metal dosing was surprising and inconsistent with Phase I findings in which DO was suppressed under metal dosing. Both aluminum and iron treatments showed a general increase in DO concentrations after the initiation of dosing which levels out at around 6 to 10 days after the run began (Figure 124). The NonDosed mesocosm also had a slight increase in that period though it was relatively less. Background concentrations were generally flat. Metal dosed mesocosms also had a much greater diel variation than either the NonDosed or Background mesocosms (Figures 123 and 124). For both, the larger diel variance was an initial characteristic of the run and persisted through the run (Figure 124). Thus, it is unclear the exact mechanisms for this change though the metal dosed mesocosms appear to have greater biofilm and phytoplankton than the NonDosed and Background mesocosms and this algal community may have been stimulated by metal addition.

Figure 123. DO concentrations in iron and aluminum dosed mesocosms (200 µM) were 4 mg L^{-1} higher than background and Non-Dosed levels.

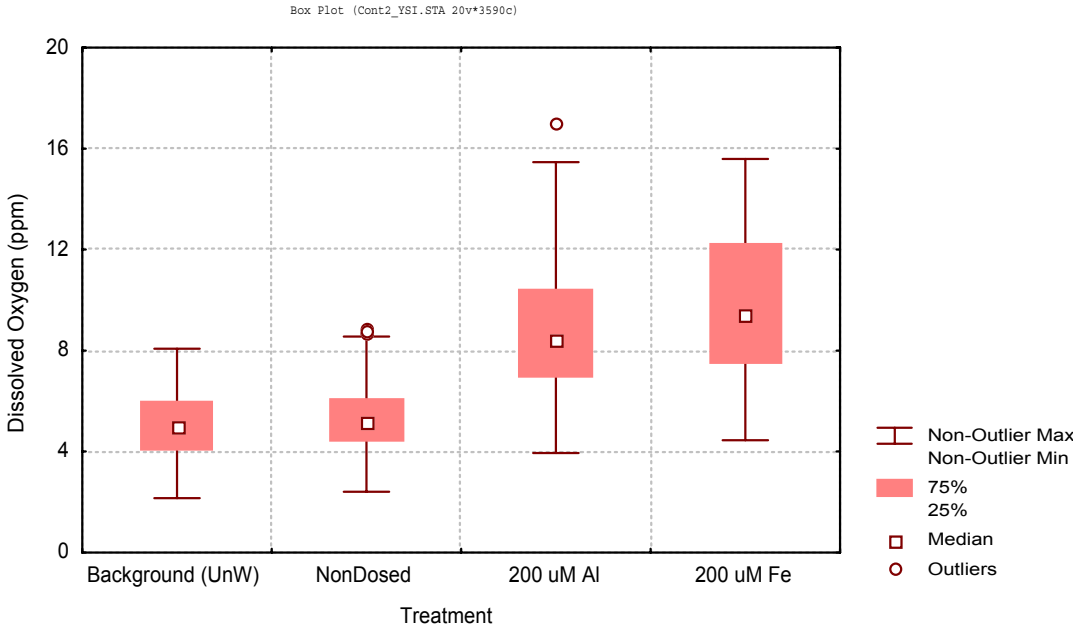

Figure 124. DO concentrations changes over time for different chemical treatments.

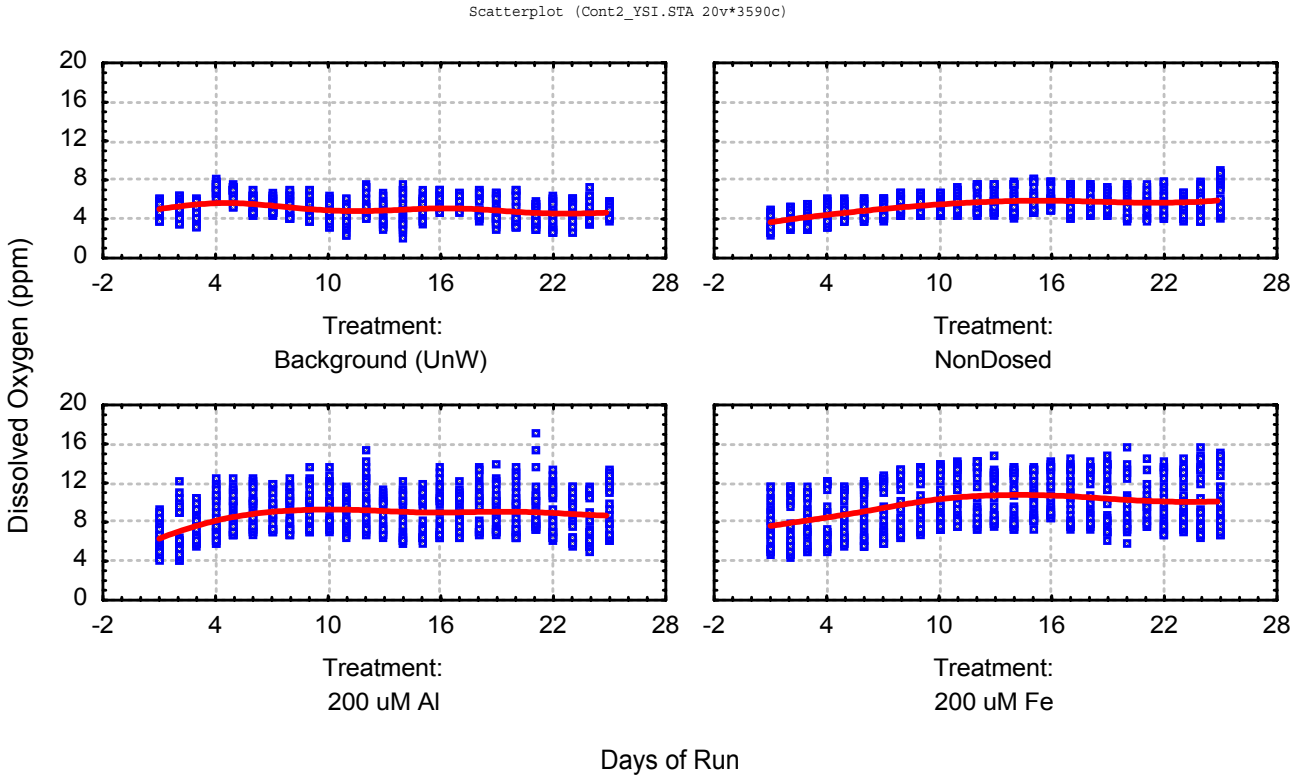

Specific conductivity was unaffected by metal dosing as was the case during Phase I (Figure 125; Bachand et al., 1999).

Figure 125. Iron and aluminum dosing did not affect specific conductivity.

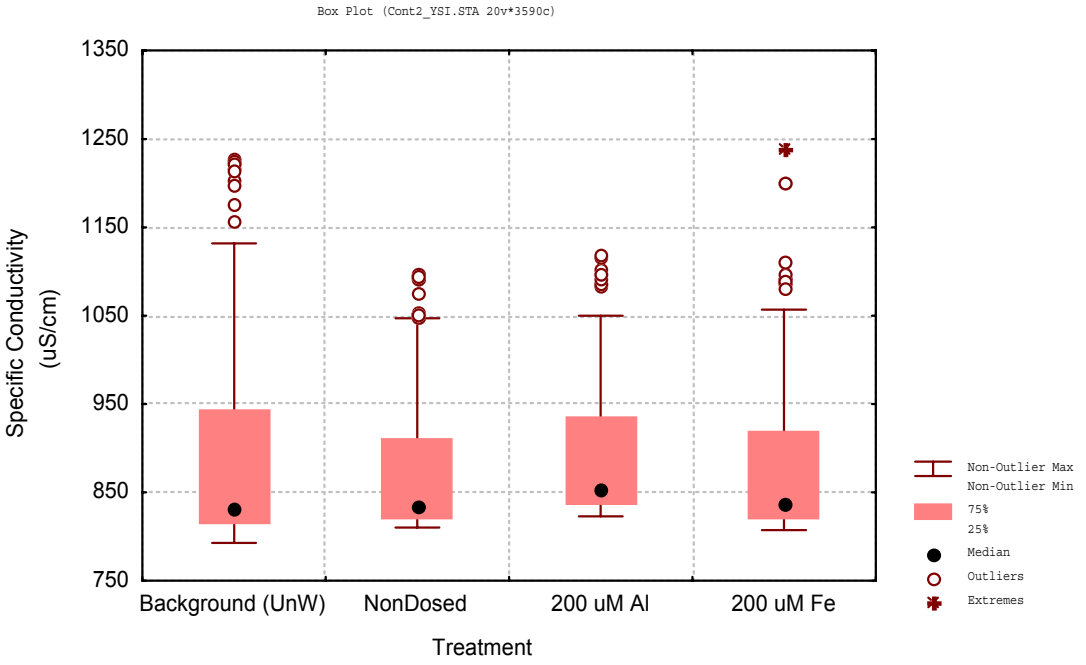

14.2.6. Marsh Readiness effects

Variables specific to marsh readiness and not required as process variables (Table 1; e.g. total nitrogen, dissolved nitrogen, ammonia, nitrate, color, sulfate, silica, chloride, magnesium, sodium, potassium, manganese, alkalinity and total suspended solids) were collected twice during this study. The sampling times for the marsh readiness specific variables corresponded to midway through the study and at the end of the study, both times considered to be generally under steady state conditions. In general, samples were collected at the inflow pipe and within the mesocosm though for alkalinity, silica and TSS only mesocosm samples were considered (Table 38).

Other variables are also considered parameters necessary for determining marsh readiness (e.g. temperaure, DO, pH, specific conductance, turbidiy, total phosphorus, total dissolved phosphorus, dissolved iron and dissolved aluminum).

These variables are also considered process variables in this study (Table 1) and were more intensely sampled (Table 5) to assess the process. Unattended monitoring parameters (e.g. DO, temperature, pH, specific conductance, and turbidity) have been discussed in the previous section. These process variables are not included in this section. Only marsh readiness specific variables are discussed here. Therefore, Table 38 includes the effects of LICD on the sampled parameters specific to marsh readiness. It additionally the effects of LICD on ortho-phosphorus (e.g. soluble reactive phosphorus, SRP). Bachand et al. (1999) demonstrated that ortho-phosphorus was effectively removed at dosing levels of 50, 100 and 200 μM during Phase I. In that study, ortho-phosphorus concentrations were typically reduced to levels below 5 μg L^{-1}. This table presents the ortho-phosphorus results of this study as well.

Metal dosing significantly ($p \sim 0.0000$) decreased ortho-phosphorus to median values of less than 5 μg L^{-1} for both aluminum and iron dosing. Mean values for iron were twice as high. This was due to outliers as expected from the high accompanying standard deviations. These high standard deviations for ortho-phosphorus are inconsistent with the more frequently sampled ortho-phosphorus values during Phase 1 (Bachand et al., 1999). These outliers likely result from contamination as in several cases these values were higher than total dissolved phosphorus or total phosphorus for the same sample.

Metal dosing of aluminum or iron also statistically affected manganese, sulfate, color and alkalinity (Table 38; $p<0.05$). Manganese concentrations increased under iron dosing but not under aluminum dosing (Table 38, Figure 128). Increases in iron were linear with dose (Figure 128). At moderate dosing levels of 200 μM, manganese concentrations averaged 0.012 mg L^{-1} as opposed to 0.008 mg L^{-1} background concentrations, a 50% increase).

Both iron and aluminum dosing increased sulfate concentrations which is not surprising as iron was added as iron sulfate and aluminum was added as aluminum sulfate (Figure 127). The increase in sulfate was greater for aluminum than for iron. At low iron dosing of 200 μM, sulfate concentrations from approximately 45 mg L^{-1} to approximately 55 mg L^{-1}. At the same dosing level for aluminum, sulfate increased to around 90 mg L^{-1}.

Color decreased greatly under both iron and aluminum dosing (Figure 128). Aluminum decreased color more than did iron though both dramatically reduced color from a background level of 120 color units. Iron dosing at 200 μM reduced color to an average of 65 color units and aluminum dosing at the same levels reduced color to under 40 color units. This suggests that both aluminum and iron additions greatly reduced the humic and fulvic acid concentrations in the water column.

Table 38. LICD effects on Marsh Readiness.

Data are for iron and aluminum dosing levels of 200 and 400 µM.

Parameter		NonDosed	Cl 4100	FPD	p-value	Locations
SRP[2]	mean	44.12	2.97	9.63	0.0000	P2, C1
(ug L^{-1})	median	45.45	2.80	4.35		
	SD	23.53	1.77	9.84		
	N	20	19	18		
NOX-N[1]	mean	155	177	195	0.6512	P2, X1, C1, C3
(ug L^{-1})	SD	146	172	172		
	N	28	31	32		
NH_4-N[1]	mean	16.2	16.3	15.6	0.9838	P2, X1, C1, C3
(ug L^{-1})	SD	14.8	16.1	22.1		
	N	27	34	34		
Diss. N[1]	mean	20.3	15.6	19.1	0.0077	P2, X1, C1, C3
(mg L^{-1})	SD	3.6	5.1	8.1		
	N	28	31	32		
Total N[1]	mean	19.4	18.4	19.1	0.8691	P2, X1, C1, C3
(mg L^{-1})	SD	5.1	8.4	8.1		
	N	27	31	35		
Si	mean	6.51	6.25	6.76	0.3622	C1
(mg L^{-1})	SD	1.08	1.17	1.00		
	N	16	8	8		
Ca	mean	62.1	63.9	62.3	0.3403	P2, C1
(mg L^{-1})	SD	3.8	1.1	2.2		
	N	16	16	16		
Mg	mean	16.4	16.4	16.4	0.9916	P2, C1
(mg L^{-1})	SD	0.6	0.4	0.7		
	N	16	16	16		
K	mean	5.9	6.0	5.9	0.9563	P2, C1
(mg L^{-1})	SD	0.7	0.7	0.6		
	N	16	16	16		
Na	mean	89.7	90.9	89.4	0.5391	P2, C1
(mg L^{-1})	SD	3.5	2.6	5.0		
	N	16	16	16		
Cu	mean	0.00319	0.00375	0.00388	0.0500	P2, C1
(mg L^{-1})	SD	0.00179	0.00188	0.00154		
	N	16	16	16		
Mn	mean	0.00694	0.01063	0.01800	0.0015	P2, C1
(mg L^{-1})	SD	0.00573	0.00667	0.01117		
	N	16	16	16		
Zn	mean	0.01631	0.032	0.03725	0.2488	P2, C1
(mg L^{-1})	SD	0.01917	0.04173	0.04314		
	N	16	16	16		
SO_4	mean	55	139	87	0.0032	P2, C1
(mg L^{-1})	SD	51	76	70		
	N	16	16	16		
Cl	mean	126	136	128	0.2852	P2, C1
(mg L^{-1})	SD	12	22	20		
	N	17	16	16		
Color	mean	126	24	49	0.0000	P2, C1
(Color Units)	SD	15	10	27		
	N	16	16	16		
Alkalinity	mean	204	120	167	0.0030	C1
(mg $CaCO_3$ L^{-1})	SD	25	56	41		
	N	8	8	8		
TSS	mean	13.5	3.8	12.3	0.3456	C1
(mg L^{-1})	SD	17.0	8.6	15.5		
	N	8	8	8		

Notes:

1 Nitrogen data was filtered because of contamination during sampling of some vials. Data greater than 2 times the 75% value were excluded:

	75% filtered value (mg L^{-1})	(mg L^{-1})
NOX-N	0.37	0.75
NH_4-N	0.04	0.08
Diss. N	2.26	4.50
Tot. N	2.68	5.00

2 Outliers on SRP skewed mean value. Median values is shown for comparison.

Figure 126: The effects of different iron and aluminum dosing levels on mesocosm manganese concentrations.

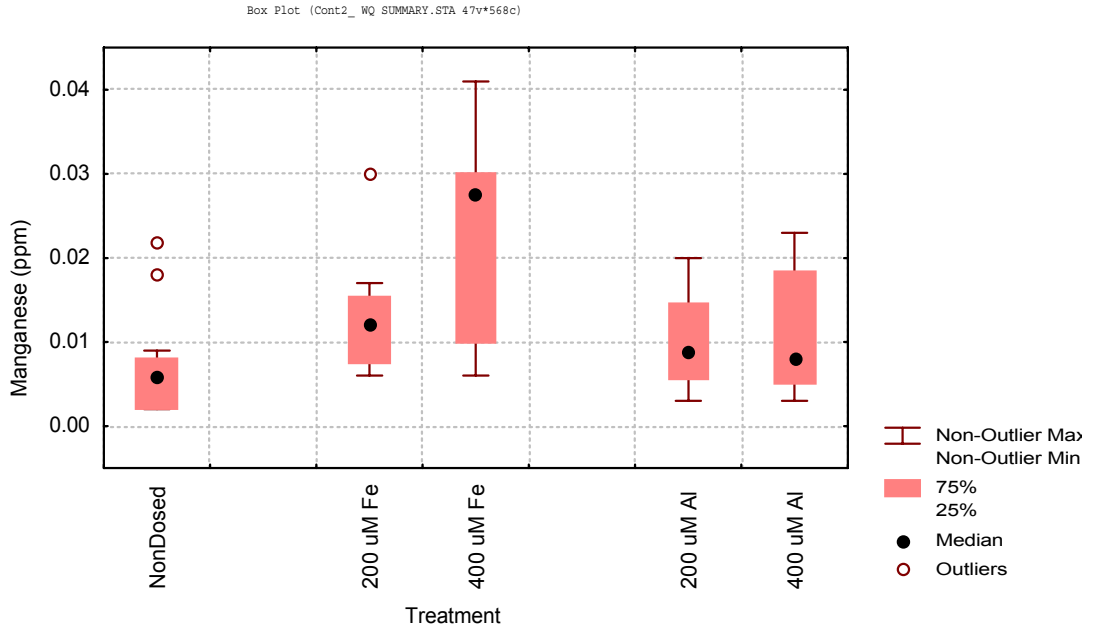

Figure 127: Sulfate concentrations increased with dosing of iron and aluminum coagulants.

Aluminum was dosed as aluminum sulfate. Iron was dosed as ferric sulfate.

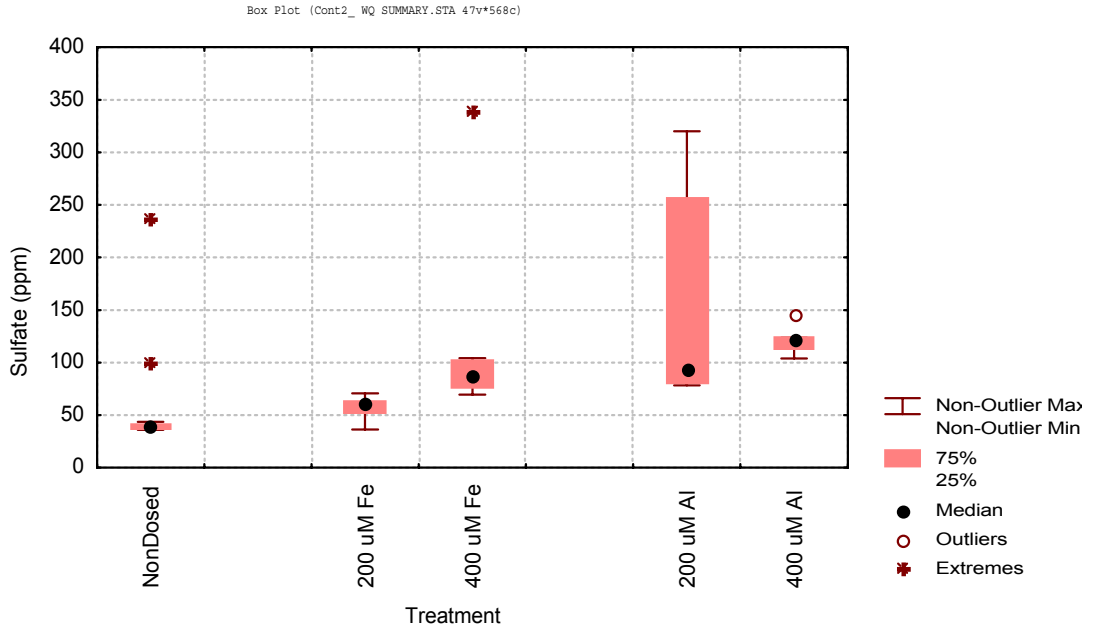

Figure 128: Iron and aluminum treatments decreased color with reductions increasing with dose.

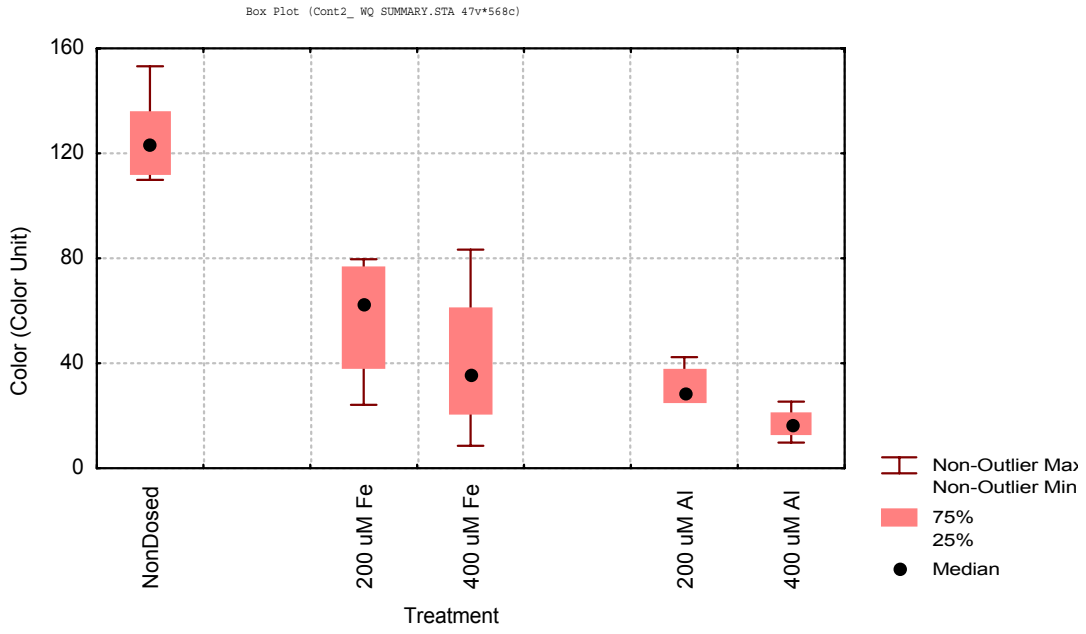

Finally, alkalinity was affected by chemical dosing (Figure 129). Overall, aluminum more greatly decreased alkalinity than ferric iron indicating that aluminum more greatly reduced the buffering capacity of the water. Ferric iron only had a slight affect on alkalinity levels with dosing at 200 µM only negligibly lowering alkalinity levels.

Figure 129: Alkalinity decreased with metal dosing.
Greater decreases in alkalinity resulted from aluminum dosing. Alkalinity decreases at low iron dosing levels were negligible.

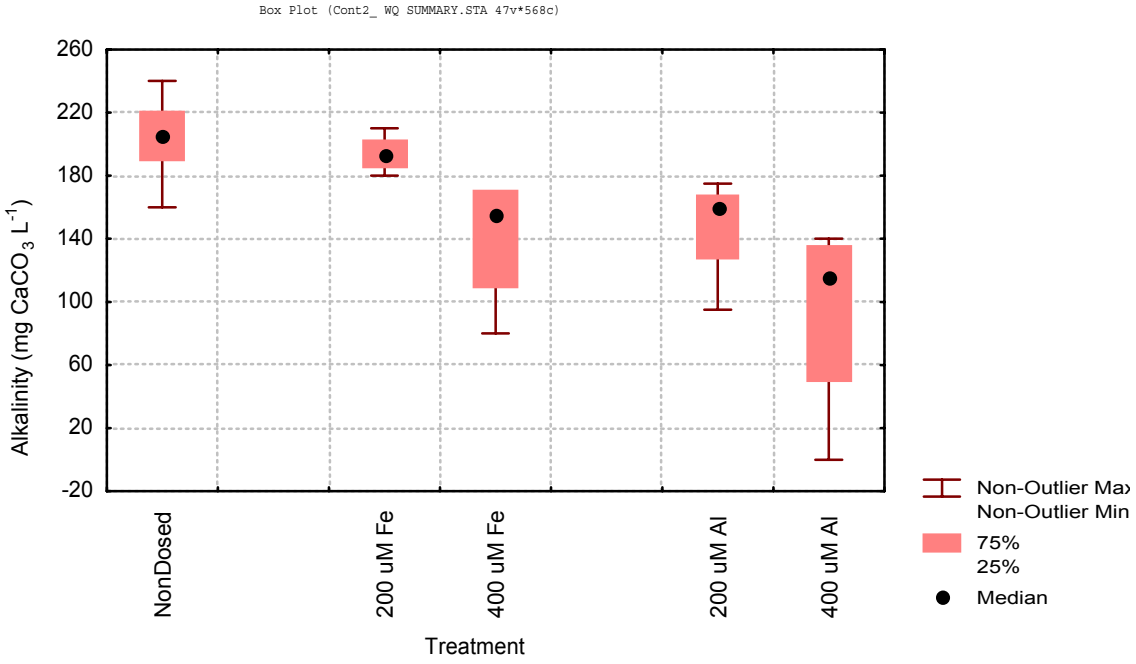

Chemical dosing did not statistically affect calcium, magnesium, potassium, sodium, copper, zinc, chloride or total suspended solids (Table 38). Zinc concentrations slightly increased with chemical dosing though these were not significant ($p=0.2488$). Total suspended solids decreased with aluminum dosing though these were not statistically significant either. Because these parameters were not statistically affected ($p<0.05$), no figures were developed for them. For the most part, chemical dosing did not affect nitrogen levels either. Total nitrogen, ammonia and nitrate concentrations were not affected significantly by chemical dosing. Total dissolved nitrogen concentration was affected significantly ($p=0.0077$) and this was from aluminum dosing. Iron dosing did not affect total dissolved nitrogen concentrations.

14.3. Summary

1. Bromide data demonstrate that LICD dosed water in the mesocosms was diluted with higher phosphorus background waters. Approximately 20% of the mesocosm water was supplied by the marsh through diel marsh water level fluctuations. Phosphorus concentrations achieved in the mesocosms after dosing were thus higher than those that would be achieved under hydrologically isolated conditions as would be the case in larger-scale demonstration projects.
2. LICD effectively decreased dissolved phosphorus concentrations. Dosing immediately decreased dissolved phosphorus concentrations by about 90%.

Aluminum dosing generally decreased dissolved phosphorus concentrations by more with 75% of the dosed inflow waters having dissolved phosphorus concentrations below 10 μg L^{-1} as opposed to below 15 μg L^{-1} for iron dosing. PAM addition did not affect dissolved phosphorus concentrations. Higher metal doses generally had slightly lower dissolved phosphorus concentrations. Determining statistical significance depended greatly upon the statistical test. Overall, higher dosing levels also reduced the variance in the dissolved phosphorus data. Dissolved phosphorus concentrations were generally lower in the mixing tanks with concentrations generally near 5 μg L^{-1}. This data corresponds to water sampled from the mixing tanks under an 18 – 24 hour HRT. Dissolved phosphorus concentrations were slightly higher in the mesocosms and this may partially be attributed to diel dilution of mesocosm with high dissolved phosphorus marsh waters.

3. LICD effectively removed total phosphorus from the water column. Iron dosing levels of 200 μM when used in combination with 20% cationic polymers and PAM dosing levels of 1 mg L^{-1} achieved total phosphorus concentrations in the mixing tanks of 24 μg L^{-1} representing a 77% reduction in total phosphorus. This data represented an 18 – 24 hour HRT. In the mesocosms, the same treatment yielded total phosphorus concentrations of 29 μg L^{-1}. These systems were operated under a 2.5 day HRT and were not hydrologically isolated from the surrounding marsh. When the dilution effect was included in the analyses, LICD yielded mean total phosphorus concentrations of 12 μg L^{-1}. Aluminum dosing at 200 μM in combination with 10% cationic polymer and PAM dosing levels of 1.0 mg L^{-1} resulted in total phosphorus concentrations in the mixing tanks averaging 19 μg L^{-1}. This represented a 82% decrease in total phosphorus. In the mesocosms, total phosphorus concentrations for this treatment yielded an average total phosphorus concentration of 39 μg L^{-1}. When corrected for marsh dilution, LICD yielded total phosphorus concentrations of 28 μg L^{-1}.
4. The addition of PAM in the chemical dosing protocols greatly improved the performance of LICD with regard decreasing total phosphorus concentrations in the water column. With the addition of PAMs, total phosphorus reductions of 82 – 88% were achieved as compared to rates of 21 – 48% achieved in previous studies, both Phase I and Phase II. From the study here, PAM dosing concentrations of 0.5 mg L^{-1} or less are probably too low. For 200 μM dosing of both iron and aluminum, PAM dosing concentrations of 1.0 mg L^{-1} greatly improved phosphorus settling as compared to PAM dosing concentrations of 0.5 mg L^{-1}.
5. Higher metal dosing levels did not necessarily improve performance. For aluminum, greater phosphorus removal from the water column occurred at 400 μM dosing levels as compared to 200 μM levels. However, for iron, this was not the case.
6. Formation of particulate phosphorus after metal dosing can be empirically modeled as an exponential relationship dependent upon metal dosing level. From this model, the metal dosing constant is 4.96 mg L^{-1} (90 μM) for iron and 2.02 mg L^{-1} (75 μM) for aluminum. This model supports the contention

that dosing iron and aluminum at levels below 200 μM may provide effective phosphorus removal.

7. Floc aggregation can be empirically modeled as an exponential relationship depending upon PAM dose. For this model, the PAM dosing constant is 0.26 mg L^{-1} when proceeding iron dosing and 0.17 mg L^{-1} when proceeding aluminum dosing. Twice the PAM dosing constant is an estimate of the PAM dosing concentration necessary for floc aggregation necessary for good phosphorus removal. Thus, a PAM dose of over 0.5 mg L^{-1} is estimated for iron and over 0.34 mg L^{-1} is estimated for aluminum. Given the data from the mesocosms studies in October 1999 and February/March 2000, a minimum PAM dosing concentration of 1 mg L^{-1} is recommended in order to ensure good floc aggregation.
8. Mesocosm data support earlier conclusions that phosphorus removal in the LICD mesocosms is primarily due to chemical precipitation and settling, and not through biotic uptake.
9. LICD lowered DOC concentrations in the water column and these reductions are generally sustained.
10. Dissolved metal concentrations are near background levels after LICD. Total metal concentrations are above background levels for a 2.5 day HRT and generally less than 1 mg L^{-1}. Residual total iron and aluminum concentrations are not dose dependent and would be expected to become lower with longer HRTs and in large-scale systems more resembling PFRs than CFSTRs.
11. LICD did not affect water temperature or specific conductivity. However, LICD had some effects on other standard water quality parameters. Aluminum and ferric iron blends slightly lowered pH and slightly raised DO concentrations. Increases in DO were unexpected and inconsistent with Phase I findings (Bachand et al., 1999). Thus changes in DO apparently depend largely upon the characteristics of the aquatic community where chemical dosing occurs.
12. LICD slightly altered water quality with regard to marsh readiness parameters. Metal dosing did not statistically affect water column concentrations of calcium, magnesium, potassium, sodium, copper, zinc, chloride or total suspended solids. Metal dosing did statistically affect water column concentrations of manganese, sulfate, color and alkalinity. Some of these effects were specific to iron and some specific to aluminum. For instance, though aluminum did not affect manganese, iron dosing increased manganese concentrations from 8 μg L^{-1} to 12 μg L^{-1}. Though both aluminum and ferric iron blends reduced alkalinity, effects under ferric iron dosing were relatively negligible. Both aluminum and ferric iron blends increased sulfate and decreased color. The increase in sulfate resulted from both metal blends having sulfate. The decrease in color represented a removal of humic and fulvic acids from the water column from metal dosing. These changes in marsh readiness parameters were generally minor for dosing concentrations up to 200 μM. At higher dosing concentrations as is being considered by other chemical treatments, these effects will be more consequential.

Chapter 15. Fate of phosphorus in the sediments

The fate of phosphorus from chemical dosing and the long-term effects of LICD on sediment composition and accretion were investigated by collecting and analyzing sediment cores and settled floc. Sediment data was collected during Phase I but analyzed as part of Phase II. Data was collected during the eight month continuous flow study that occurred from August 1998 through February 1999 (Bachand et al., 1999). Additionally, sediment data was collected to assess any changes in sediment quality that might result from LICD. Floc samples were collected during the final field study described in Chapter 14.

15.1. Methods

Sediment samples were collected during Phase I at the initiation and completion of the continuous flow study that occurred at Site A from August 1998 through February 1999 (Bachand et al., 1999). At the initiation of the study, one sediment core was collected at the center of each mesocosm. At the completion, three sediment cores were collected at random locations within each mesocosm. The three sediment cores were partitioned and composited by depth. Partitions were the top ooze layer, 0 – 1 cm, 1 – 2.5 cm and 2.5 – 5 cm. The top ooze layer was much less consolidated and more fluid than the underlying layers. The distinct physical characteristics allowed visual separation of the ooze layer from the underlying sediment. When consolidated, the ooze layer would be on the order of a few millimeters thick. These sediment samples were analyzed for the parameters shown in Table 1.

Floc samples were collected at the conclusion of the continuous flow mesocosm study conducted in February/March 2000. Floc was treated and analyzed as sediments.

15.2. Results

15.2.1. Characterizing sediment cores

Sediment from the top three centimeters for mesocosms receiving 100 and 200 μM dosing was considered in this analysis. This was based on soil data from Bachand et al. (1999) which showed that sediment effects were generally limited to the top few centimeters of the sediment. Data from those top three centimeters (e.g. ooze, 0 – 1 cm., 1 – 2.5 cm) was consistent with marsh readiness data from this report. Soil concentrations in the top three centimeters of magnesium, zinc, copper, calcium, and nitrogen remained unchanged under both iron and aluminum dosing (Table 39). Carbon also remained unchanged and constituted nearly 50% of the sediment (Table 39). Aluminum dosing increased aluminum concentrations in the top three centimeters from approximately 2 - 3 parts per thousand to 4.6 parts per thousand (g kg^{-1}). Iron dosing increased iron concentrations in the top three centimeters to 8.6 ppt (Table 39).

Table 39. Soil Concentrations (top 2.5 cm).
Data from ooze, 0 – 1 cm and 1 – 2.5 cm partitions. For iron and aluminum dosing levels of 100 and 200 μM.

		Aug-98				Feb-99			
Parameter		**UnW**	**NonD.**	**Alum**	**FPD**	**UnW**	**NonD.**	**Alum**	**FPD**
Al	mean	2,461	3,323	3,042	3,110	2,205	2,259	4,602	2,901
(mg kg^{-1})	SD	17	281	523	362	385	564	3,041	383
	N	3	3	6	6	3	3	6	6
Fe	mean	2,108	3,396	2,938	3,007	1,797	2,057	2,136	8,614
(mg kg^{-1})	SD	184	242	499	517	161	551	563	6,961
	N	3	3	6	6	3	3	6	6
Mg	mean	3,417	4,076	4,154	4,146	3,615	3,902	3,820	3,965
(mg kg^{-1})	SD	108	201	414	516	150	431	521	432
	N	3	3	6	6	2	3	6	6
Zn	mean	108	114	112	157	112	109	114	116
(mg kg^{-1})	SD	7	3	8	58	3	10	11	13
	N	3	3	6	6	2	3	6	6
Cu	mean	57	75	81	75	61	62	68	81
(mg kg^{-1})	SD	7	2	10	11	5.7	7	13	26
	N	3	3	6	6	2	3	6	6
Ca	mean	31,430	30,020	30,120	31,610	30,484	34,290	31,750	35,890
(mg kg^{-1})	SD	2,195	664	925	2,989	358	3,048	4,161	8,738
	N	3	3	6	6	2	3	6	6
C	mean	452,746	429,206	418,980	435,808	446,340	468,000	461,305	447,560
(mg kg^{-1})	SD	1,997	1,224	47,241	13,449	30,638	9,766	20,262	29,553
	N	3	3	5	5	3	3	6	6
P	mean	233	919	744	625	323	238	358	412
(mg kg^{-1})	SD	24	102	293	282	171	104	210	199
	N	3	3	6	6	3	3	6	6
N	mean	28,110	28,190	28,600	29,168	29,253	30,793	29,058	28,572
(mg kg^{-1})	SD	306	418	1,672	996	871	3,281	1,095	1,663
	N	3	3	5	5	3	3	6	6

Phosphorus fractionations were conducted on the soil/sediment as well. In background sediments, phosphorus was equally distributed between exchangeable inorganic phosphorus, bicarbonate extractable organic and microbial phosphorus and humic organic phosphorus, in the range of 27 – 30 mg kg^{-1} in the February 1999 samples (Table 40). A larger fraction was bound to calcium (39 mg kg^{-1}) and a smaller fraction to iron and aluminum (4 mg kg^{-1}). In the top five centimeters, there was very little obvious effects on sediment phosphorus speciation from LICD. Phosphorus concentrations of 269 mg kg^{-1} in February 1999 background samples were lower than during August 1998 at 294 mg kg^{-1}. The February 1999 sample had higher concentrations in the very top layer of ooze and then equivalent concentrations throughout the remaining sediment core.

Table 40. Soil Concentrations (top 5 cm).
Values are in mg kg^{-1}. For iron dosing levels of 100 and 200 μM and aluminum dosing levels of 100 μM.

Phosphorus Fraction	Treatment		top	0 - 1 cm	1 - 3 cm	3 - 5 cm	0 - 5 cm
Exchangeable inorg. P	Background	Aug-98	51	27	22	15	21
	Background	Feb-99	136	31	18	33	27
	Fe 100 uM	Feb-99	55	32	26	19	26
	Fe 200 uM	Feb-99	39	38	32	20	30
	Al 100 uM	Feb-99	47	22	17	22	20
Bicarbonate extr. Org. and Micro. P	Background	Aug-98	29	30	23	22	25
(0.5M NaHCO3)	Background	Feb-99	61	26	38	22	29
	Fe 100 uM	Feb-99	73	35	26	22	28
	Fe 200 uM	Feb-99	59	34	18	8	20
	Al 100 uM	Feb-99	65	21	21	21	21
Fe/Al bound inorg. P	Background	Aug-98	7	6	5	4	5
(0.1M NaOH)	Background	Feb-99	14	5	5	3	4
	Fe 100 uM	Feb-99	26	6	4	5	5
	Fe 200 uM	Feb-99	30	8	4	4	5
	Al 100 uM	Feb-99	55	8	4	5	6
Humic organic P	Background	Aug-98	47	54	50	43	49
(0.1M NaOH)	Background	Feb-99	82	28	33	29	30
	Fe 100 uM	Feb-99	43	45	35	21	34
	Fe 200 uM	Feb-99	58	41	24	16	27
	Al 100 uM	Feb-99	273	33	25	31	30
Ca-bound P	Background	Aug-98	39	56	38	27	40
(1M HCL)	Background	Feb-99	130	34	47	34	39
	Fe 100 uM	Feb-99	118	38	27	25	30
	Fe 200 uM	Feb-99	113	49	31	26	35
	Al 100 uM	Feb-99	106	25	24	21	23
Residual P	Background	Aug-98	177	158	138	163	153
(Calculated from difference between	Background	Feb-99	278	151	143	126	140
Total P and fractions)	Fe 100 uM	Feb-99	272	141	148	124	138
	Fe 200 uM	Feb-99	299	154	85	90	110
	Al 100 uM	Feb-99	237	150	138	153	147
Total P	Background	Aug-98	351	331	277	274	294
	Background	Feb-99	701	276	284	246	269
	Fe 100 uM	Feb-99	588	298	267	217	260
	Fe 200 uM	Feb-99	598	324	194	164	227
	Al 100 uM	Feb-99	782	259	229	254	247

In general, metal dosing had only slight effects on phosphorus speciation in the sediments. Both iron and aluminum dosing at 100 μM led to a decrease in calcium bound phosphorus in the top 5 centimeters. In the very top sediment layer, dosing increased aluminum/iron bound phosphorus and decreased exchangeable inorganic phosphorus (Table 40). Total phosphorus concentrations in the sediments were slightly lower and in general metal dosing essentially diluted the background sediments with the accumulation of low phosphorus floc.

Aluminum at 200 μM during this study was not included in this analysis because of operational complications (Bachand et al., 1999). However, sediment data for iron dosing at 200 μM was available. At 200 μM, iron dosing had calcium bound

phosphorus concentrations in the top five centimeters slightly below those found in background sediments. There was a more noticeable decrease in bicarbonate extractable organic and microbial phosphorus than at lower dosing levels. Total phosphorus concentrations in the sediments were lower than at either background concentrations or at concentrations found at iron dosing of 100 μM. Thus, some sediment dilution was again occurring.

In general, metal dosing decreased phosphorus concentrations in the sediments and decreased the amount of readily available phosphorus in the very upper sediments. This is consistent with water data discussed in Chapter 5 in which metal dosing suppressed phosphorus release from the sediments back into the water column. Additionally, approximately one half the phosphorus in the sediments was tightly bound residual phosphorus and this fraction was also not easily available to the water column.

Overall, sediment effects were minor in the top three to five centimeters. The ooze layer appeared more affected by metal dosing suggesting that any effects from LICD on the sediments may not have had sufficient time to penetrate to the deeper sediments. It is difficult to interpret the very top ooze layer though because of difficulty in precisely and accurately collecting those samples.

15.2.2. Calculated Sediment Fluxes from Mass Balance Analysis

Mass balance calculations were conducted to develop a better understanding of water/sediment interactions with regard to LICD. Mass balance calculations were used to determine sediment fluxes in the mesocosms of iron, aluminum, and organic carbon from DOC precipitation and phosphorus. These calculations were conducted for metal dosing levels of 200 and 400 μM and incorporated marsh water dilution effects discussed earlier in the previous chapter. Under aluminum dosing levels of 200 and 400 μM, the average sediment flux of formed precipitates was 1540 mg m^{-2} d^{-1} of which 39% was as aluminum, 60% as carbon from DOC and 0.5% as phosphorus (Figure 130). The same iron dosing levels had an average sediment flux of formed precipitates of 1906 mg m^{-2} d^{-1} of which 60% was as iron, 33% was as carbon from DOC and 0.3% as phosphorus. Both metals removed an equivalent mass of DOC and aluminum generally removed more phosphorus. As these fluxes were collected in the mesocosms, some interference such as the release of DOC from the sediments into the water column could not be measured.

Figure 130. Net iron, aluminum, carbon and phosphorus fluxes to the sediments from mass balance calculations.
Fluxes were calculated based upon changes in water quality in iron and aluminum dosed mesocosms. Calculations use a 2.5 day hydraulic retention time. Data are from aluminum and iron dosing levels of 100 and 200 µM. Calculations cannot distinguish between removal from water column and release from the sediments.

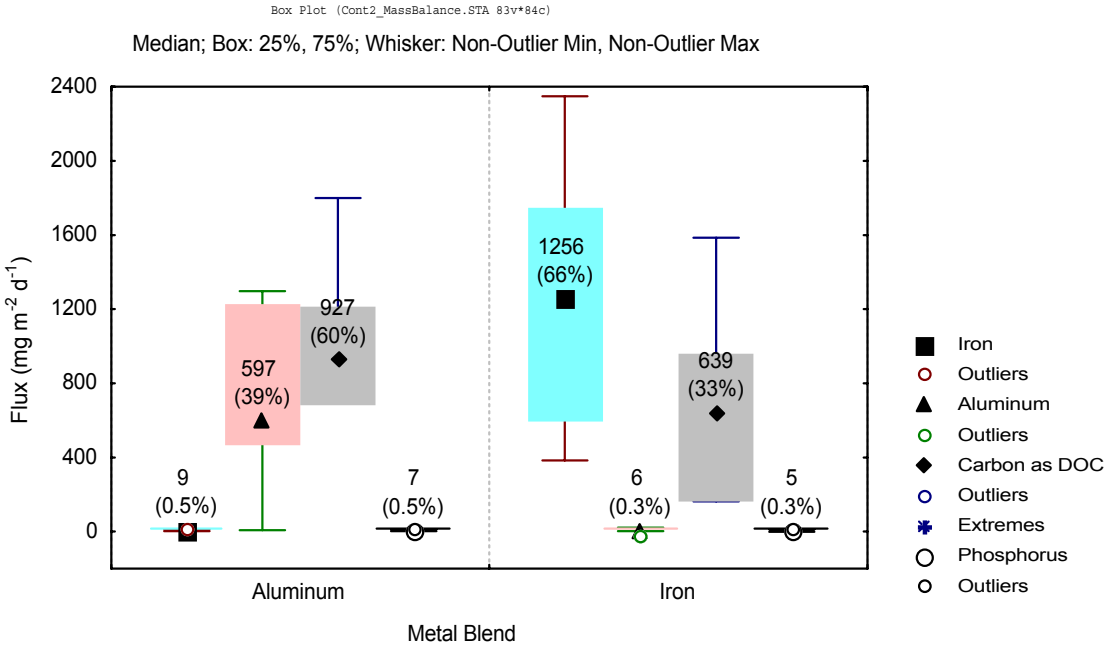

A regression analyses was used to generate a linear relationship between metal dose and metal flux from the water column (Figure 131). This regression fit was excellent and partially reflected that the calculation of flux requires the dosing metal concentration. Because iron and aluminum were much elevated above background concentrations when dosing occurred, minimal interference or confounding mesocosm characteristics affected these calculations. Therefore, these calculations reasonably predict the iron and aluminum fluxes from the water column after dosing. These relationships (Figure 131) incorporate the marsh dilution effect discussed earlier. These relationships were very similar to those determined in Phase I by Bachand et al. (1999) though the higher slope coefficients reflect improved floc aggregation and settling from more optimal coagulant blends.

Figure 131. Metal flux as dependent upon metal dosing level.
A. Iron dosing:

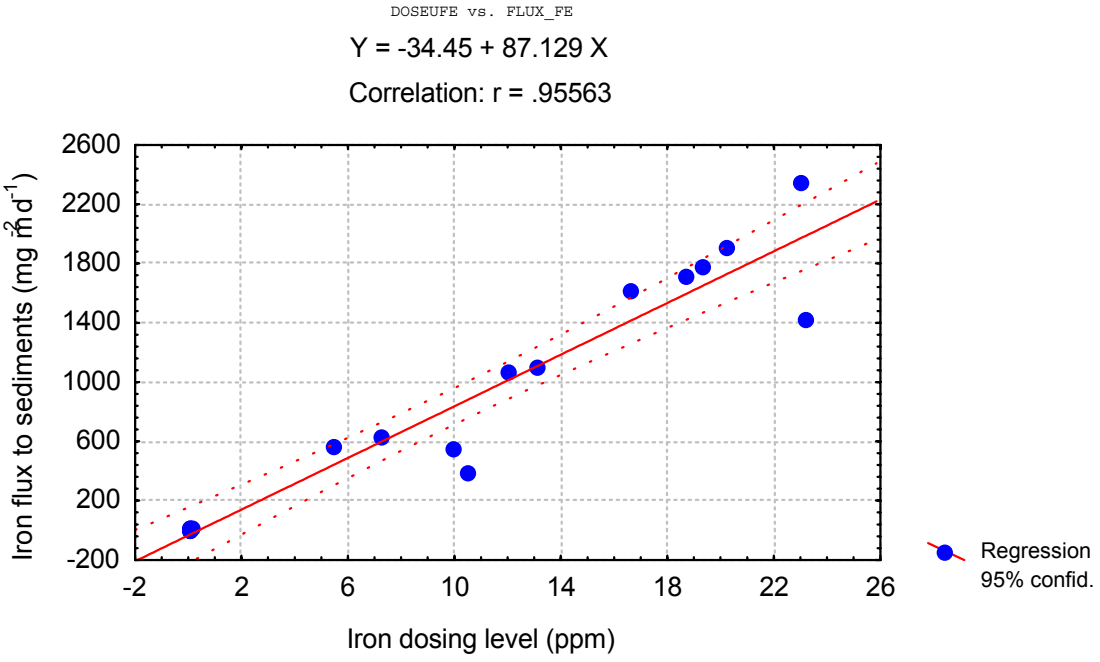

B. Aluminum dosing

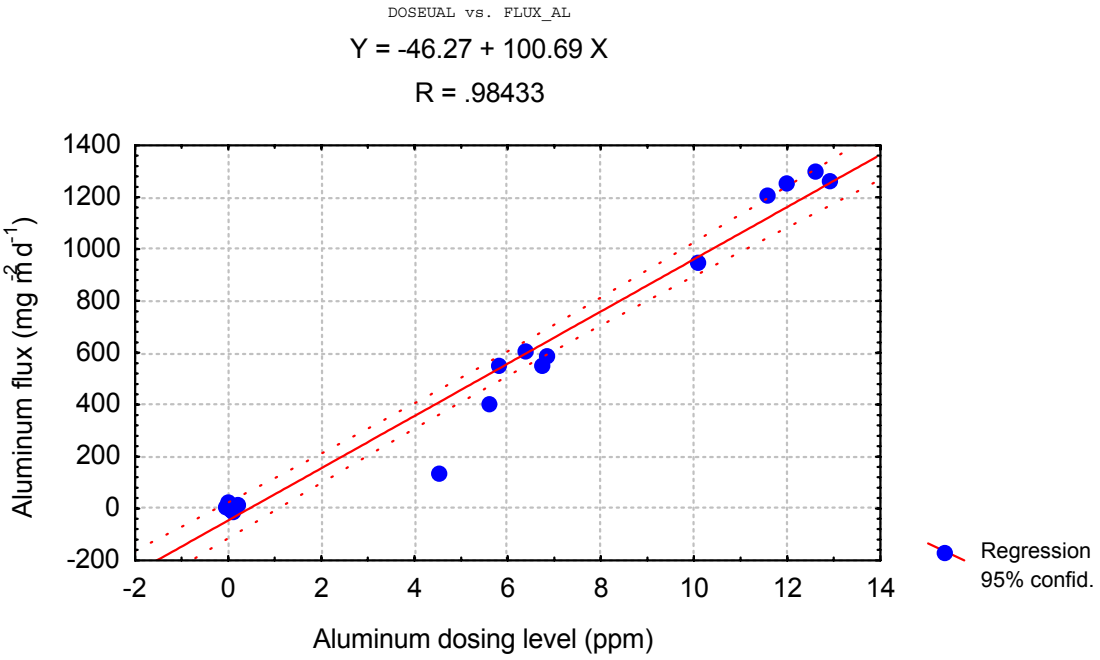

15.2.3. Collection and Analysis of Floc

To determine the chemical composition of the formed floc directly, floc was collected from the mixing tanks during the February/March 2000 study and directly analyzed. This information was considered very important for augmenting sediment data collected in August 1998 and February 1999 and for supplying more precise sedimentation data. This information was then to be integrated with previous sediment data and mass balance data to determine the chemical characteristics of the precipitates formed by LICD.

Floc formed from iron dosing at 200 μM was 26% carbon, 21% iron and 4% calcium. Forty-eight percent of the floc was composed on parameters not directly measured (Table 41). Based on the likelihood that hydroxides formed during precipitation (Snoeyink and Jenkins, 1980) as well as X-ray diffusion evidence from Ullman (1999) showing the likelihood of silica and sulfur in formed crystals, the non-measured constituents likely include sulfur, silica, oxygen and hydrogen. Additionally, iron formed floc had small measured concentrations of phosphorus and magnesium. Phosphorus composed approximately 0.2% of the floc. Floc formed from aluminum dosing at 200 μM was 31% carbon, 11% aluminum, 2.4% calcium, 55% non-measured parameters, and small concentrations of phosphorus and magnesium. Phosphorus composed approximately 0.1% of the floc, half of that of iron precipitates.

Table 41. Chemical analyses of floc formed during February/March 2000 study. Values are in mg kg^{-1}. For iron and aluminum dosing levels of 200 μM.

	Iron Formed Floc			Aluminum Formed Floc		
Mesocosm	**A3**	**C2**	**Average**	**A1**	**C3**	**Average**
Carbon	264,730	261,200	**262,964**	306,860	307,150	**307,001**
Iron	191,823	225,312	**208,567**	2,914	2,182	**2,560**
Aluminum	4,212	1,117	**2,667**	108,864	111,493	**110,185**
Phosphorus	1,972	1,415	**1,696**	772	1,039	**917**
Calcium	39,792	35,871	**37,834**	26,050	22,742	**24,407**
Magnesium	6,030	4,467	**5,251**	4,884	3,504	**4,206**
Others[1]			**481,020**			**550,725**

Notes:
1. Other elements that are likely to be found in any significant mass include oxygen, hydrogen, sulfur and silica (Ullman, 1999).

15.2.4. Estimates of sediment accretion and composition

Sediment accretion rates from LICD were estimated based upon calculated aluminum and iron fluxes (Figure 131). Sediment composition was estimated from the ratios measured in the collected flocs (Table 42). Similarly, peat accretion rates that would be expected in the STAs were developed from WCA-

2A data. In the first five kilometers of WCA-2A, phosphorus concentrations have been equivalent to those at the LICD treatment sites, averaging from 30 – 70 μg L^{-1} (Vaithiyanathan and Richardson, 1997). In that region, Craft and Richardson (1993) found peat accretion rates to average 0.45 cm y^{-1} for a bulk density of 0.09 g cm^{-3}. This corresponds to a peat accumulation rate of 1110 mg dry peat m^{-2} d^{-1}.

15.2.4.1. Composition

For this report, the composition of sediment formed under aluminum and iron dosing was estimated. At dosing concentrations of 200 μM, mineral sediments formed during iron precipitation would comprise between 50 and 80% of the newly accreted sediments depending upon the operating HRT. Organic peat would constitute 20 to 50% of the sediments. In those combined sediments (e.g. LICD- based mineral sediments + peat-based organic sediments), iron would constitute 11 to 17% of the peat. For aluminum dosing at the same concentrations, aluminum precipitates would form between 51 to 80% of the newly accreted sediments, depending upon the operating HRT. Organic peat would constitute 20 to 49% of the sediments. In those combined sediments, aluminum would constitute 6 to 9% of the sediments.

At lower dosing concentrations of 100 μM, the percent of precipitate decreases and the percent of organic peat increases. At 100 μM dosing with iron blends, iron would constitute between 7 and 14% of the newly accreted sediments depending upon HRT. Similarly, with aluminum dosing aluminum would constitute 3 to 7% of the accreted sediments.

Average sediments are composed of approximately 4% iron and 7% aluminum and rocks of the earth crusts are typically 5% iron and 8% aluminum (CRC 1982). Sediment chemistry varies and higher percent iron or aluminum would indicate a prevalence of iron or aluminum oxides, sulfates and metal organic complexes.

Aluminum dosing at either 100 or 200 μM for HRTs of 2.5 to 7.5 days would create sediments with chemistry similar to average sediments which are found worldwide. Iron dosing at 200 μM for a 7.5 day HRT would create sediments with an average iron concentration approximately twice that of the average worldwide sediments. One would eventually expect the formation of iron crystals under those conditions as suggested by ENR sediment analyses conducted by Ullman (1999). Lower iron dosing levels would create sediments with compositions similar to those found worldwide.

Table 42. Estimated Peat accretion rates under LICD.

Table provides estimated peat accretion rates for both chemical addition and natural peat accretion in enriched zones similar to those in WCA-2A.

Dosing Level (uM)	**100**				**100**				**100**			
HRT (days)	**2.5**				**5.0**				**7.5**			
Blend	**Iron**		**Aluminum**		**Iron**		**Aluminum**		**Iron**		**Aluminum**	
	mg m^{-2} d^{-1}	**%**	**mg m^{-2} d^{-1}**	**%**	**mg m^{-2} d^{-1}**	**%**	**mg m^{-2} d^{-1}**	**%**	**mg m^{-2} d^{-1}**	**%**	**mg m^{-2} d^{-1}**	**%**
LICD:												
Mineral sediment	**2163**		**2051**	**65**	**1082**	**49**	**1025**	**48**	**541**	**33**	**513**	**32**
Iron	452	21	0	0	226	10		0	113	21	0	0
Aluminum	0	0	226	11		0	113	5	0	0	56	11
Carbon	569	26	630	31	284	13	315	14	142	26	157	31
Peat accretion:												
Organic sediment	**1110**		**1110**	**35**	**1110**	**51**	**1110**	**52**	**1110**	**67**	**1110**	**68**
Iron	0	0	0	0	0	0	0	0	0	0	0	0
Aluminum	0	0	0	0	0	0	0	0	0	0	0	0
Carbon	488	44	488	44	488	44	488	44	488	44	488	44
Combined sediments	**3273**		**3161**		**2192**		**2135**		**1651**		**1623**	
Iron	452	14	0	0	226	10	0	0	113	7	0	0
Aluminum	0	0	226	7	0	0	113	5	0	0	56	3
Carbon	1057	32	1118	35	773	35	803	38	631	38	646	40
Dosing Level (uM)	**200**				**200**				**200**			
HRT (days)	**2.5**				**5.0**				**7.5**			
Blend	**Iron**		**Aluminum**		**Iron**		**Aluminum**		**Iron**		**Aluminum**	
	mg m^{-2} d^{-1}	**%**	**mg m^{-2} d^{-1}**	**%**	**mg m^{-2} d^{-1}**	**%**	**mg m^{-2} d^{-1}**	**%**	**mg m^{-2} d^{-1}**	**%**	**mg m^{-2} d^{-1}**	**%**
LICD:												
Mineral sediment	**4491**		**4522**		**2245**	**67**	**2261**	**67**	**1123**		**1131**	
Iron	939	21		0	469	21		0	235	21		0
Aluminum		0	497	11		0	249	11		0	124	11
Carbon	1181	26	1388	31	591	26	694	31	295	26	347	31
Peat accretion:												
Organic sediment	**1110**	**34**	**1110**	**35**	**1110**	**51**	**1110**	**52**	**1110**	**67**	**1110**	**68**
Iron	0	0	0	0	0	0	0	0	0	0	0	0
Aluminum	0	0	0	0	0	0	0	0	0	0	0	0
Carbon	488	44	488	44	488	44	488	44	488	44	488	44
Combined sediments	**5601**		**5632**		**3355**		**3371**		**2233**		**2241**	
Iron	939	17	0	0	469	14	0	0	235	11	0	0
Aluminum	0	0	497	9	0	0	249	7	0	0	124	6
Carbon	1670	30	1877	33	1079	32	1183	35	784	35	835	37

Notes

1. Peat accretion rates from Craft and Richardson, 1993
2. Phosphorus in natural peats approximately 0.0125% (Craft and Richardson, 1993)
3. Iron and aluminum composition of peat sediments from Qualls and Richardson, 1995.

15.2.4.2. Preliminary toxicity assessment

From the similar chemical characteristics between the anticipated sediments formed under LICD and that of typical worldwide sediments, we expect that these sediments will not likely be toxic to the biota. In general, naturally forming worldwide sediments are not toxic to biota. That does not mean that in these sediments the diversity and distribution of biota would be the same as found in the unenriched areas of the WCAs or in the Everglades National Park. The biota may differ from those regions. However, in the STAs, we expect that the dominant biota will differ from the unenriched areas of the WCAs as well as the Everglades National Park. The STAs will likely be dominated by cattail and water hyacinth communities. Those communities have dominated the ENRP in regions where vegetation was not first planted. Moreover, in the enriched regions of the WCAs, cattail has become the dominant specie and the specie distribution between the enriched and unenriched areas are quite different (Vaithiyanathan and Richardson, 1999).

Thus, the STAs are likely to have very different biota than further downstream in the unenriched areas of the WCAs and the Everglades National Park and this will likely be caused in large part to the relatively high phosphorus concentrations in the inflow to these systems (Vaithiyanathan and Richardson, 1999). So the more critical question is not will these sediments result in biota different from that historically found in the Everglades but rather will they be toxic to the biota. Because of the similarities with worldwide sediments, we believe the sediments will not be toxic to the biota. The biota will likely be different from that historically found in the Everglades. However, the biota may also be very similar to that found in the ENRP and the enriched areas of the WCAs. Because the STAs are treatment marshes and LICD would be applied in these treatment marshes, we do not expect the formed sediments would adversely affect the biota dominant in those systems. We believe that this preliminary assessment is reasonable and that it supports testing the conceptual model of LICD proposed in this report at the larger scale. At that scale, toxicity testing and other tests on the biota are recommended to provide unequivocal evidence on the effect or lack of effect of LICD on the biota. At that time, an assessment of the biological activity of these formed LICD sediments could be made.

15.3. Summary

A continuous flow mesocosm study was operated as part of Phase I. Chemical dosing occurred from August 1998 through February 1999. After eight months of chemical dosing, sediments were only altered slightly by LICD. Magnesium, zinc, copper, calcium, carbon and nitrogen remained unchanged in the top three centimeters. Aluminum dosing increased aluminum concentrations in the top three centimeters and iron dosing increased iron concentrations in the top three centimeters. These results were consistent with marsh readiness water quality data.

Phosphorus fractions were slightly affected in the top sediments. In general, metal dosing decreased the calcium bound phosphorus concentration, increased the iron and aluminum bound phosphorus and decreased the exchangeable inorganic phosphorus.

Mass balance calculations provided sediment fluxes for organic carbon from DOC, phosphorus, iron and aluminum. Sediment precipitation rates as a sum of those four parameters were 1906 mg m^{-2} d^{-1} under iron dosing levels of 100 and 200 μM. Approximately 60% was iron, 33% was carbon and 0.3% was phosphorus. Sediment precipitation rates as a sum of the same parameters were 1540 mg m^{-2} d^{-1} under aluminum dosing of 100 and 200 μM. Approximately 39% was aluminum, 60% was carbon and 0.5% was phosphorus.

Floc data was collected during the February/March 2000 study to provide more precise data on characteristics of settling floc. Floc formed from iron dosing at 200 μM was 26% carbon, 21% iron, 4% calcium, 0.2% phosphorus and 48% other non-measured parameters (e.g. silica, sulfur, oxygen, hydrogen). Floc formed under 200 μM aluminum dosing was 31% carbon, 11% aluminum, 2.4% calcium, 0.1% phosphorus and 55% non-measured parameters.

Floc data was integrated with aluminum and iron flux data and with WCA-2A peat accretion data to predict sediment accretion rates under LICD and the resulting composition. LICD would increase sediment accretion rates by as low as 50% to as high as 400% depending upon the dosing level and HRT. From a chemical composition standpoint, aluminum dosing at 100 and 200 μM for HRTs of 2.5 to 7.5 days would produce sediments with chemical compositions very similar to average worldwide sediments. Iron dosing concentrations of 200 μM at an HRT of 7.5 days and lower iron dosing concentrations for a broader range of HRTs (5 – 7.5 days) would produce sediment with iron concentrations slightly above concentrations found in average worldwide sediments. Higher concentrations of both iron and aluminum would indicate the formation of amorphous and crystalline metal hydroxides, oxides and sulfides. Based on a comparison of these newly formed sediments with those of worldwide sediments, these sediments are not expected to be toxic to biota. Because these sediments are more mineral than those historically found in the Everglades, the diversity and distribution of the biota is expected to differ from that found in the slough and sawgrass communities in the unenriched areas of the WCAs and the Everglades National Park. However, STA biota is expected to be more similar to cattail and water hyacinth dominated biota such as is found in the enriched areas of the WCAs and found in the ENRP. Thus, with or without implementation of LICD in the STAs, the dominant biota will likely be different from that found historically in the Everglades.

Chapter 16. Conceptual Design

A conceptual design for larger-scale implementation is presented in Figure 132 and specifications are proposed in Table 43. LICD was initially defined as *in situ* marsh dosing of low concentrations of ferric iron or aluminum. Peer Consultants, P.C./Brown and Caldwell (1996) originally hypothesized LICD could enhance the phosphorus removal performance of the STAs by precipitating dissolved phosphorus from solution and aiding settling of both biotic and non-biotic particulates (Figure 1). They hypothesized that in addition to improving the phosphorus removal capabilities of the marsh, it would also ensure more sustainable phosphorus removal. In addition to a chemical component, there was a marsh component as well. Phosphorus removal would also occur through bacterial, algal and macrophyte uptake of phosphorus within the marsh. This study has primarily focused on the *in situ* chemical aspect of LICD, meaning that this study has been conducted on-site with actual ENRP (and STA) waters, sediments and biota. In this environment, we have developed a conceptual design for implementing the LICD at a larger-scale. This conceptual design includes a chemical and biological component and is for the purpose of scaling this concept up from a mesocosm-scale to a macrocosm- or pilot-scale. At the larger scale, the specifications for this technology would be further refined.

16.1. Chemical component

Implementation of this component of LICD requires an understanding that there are several constraints on this technology. First, low chemical concentrations are desired in order to minimize possible environmental and marsh readiness impacts of this technology. Second, phosphorus removal must be optimized for the chemical volumes used. This requires efficient chemical use. Finally, if this technology were implemented upstream of the Everglades, very high water volumes of highly buffered water would be treated. This constraint is one of logistics and limits what can be done with regard to optimizing chemical usage. For instance, lowering pH in these large water volumes is likely unrealistic given the high volumes and the high buffering. Based on these constraints, we have recommended chemicals and mixing regimes for a larger-scale study of LICD.

16.1.1. Chemical dosing

Chemical dosing is recommended in two steps. In the first step, a cationic chemical coagulant blend is dosed. These blends would be iron or aluminum based and may include cationic polymers. Three chemical blends recommended for larger-scale testing are ferric chloride, Ferriplus-D and Clarion 4100, or equivalents. Ferriplus-D is a ferric sulfate based coagulant with 20% by mass of cationic polymer. Clarion 4100 is an aluminum sulfate based coagulant with 10% by mass of cationic polymer. The primary purpose of this first step is to convert most the dissolved phosphorus to particulate phosphorus. Dosing levels of 100 – 200 μM are recommended based upon jar tests and field studies showing

excellent conversion of dissolved to particulate phosphorus at those levels, and based upon the empirical models developed in this study.

The second step includes an anionic coagulant to improve floc aggregation. Superfloc A130 or equivalent is recommended at dosing concentrations of 1 mg L^{-1}. This recommendation is based upon jar tests and field studies, and upon the empirical model developed in this study for floc aggregation and settling. This study has shown very good phosphorus removal. In our final field study, mass balance calculations showed that LICD at PAM concentrations of 1 mg L^{-1} and coagulant dosing concentrations of 200 μM decreased total phosphorus concentrations by about 80% to levels averaging around 20 μg L^{-1}. If PAMs are very effective at promoting floc aggregation, the advantages of preceding its application with cationic polymers may be greatly reduced.

16.1.2. Rapid mixing

Two rapid mixing zones are recommended: one for the addition of metal/cationic polymer blends and one for the addition of PAMs. Rapid mixing is considered critical for efficient and effective chemical use. EPA (1987) in their design manual for phosphorus removal states that chemicals added for phosphorus removal be intimately mixed in order to uniformly disperse the chemicals and ensure efficient application. Industry specialists today continue emphasizing the need for high energy rapid mixing for efficient and effective chemical use (Sims, 1999). The first rapid mixing zone may be accomplished by direct injection into the pump. However, a static mixer or equivalent may be required to mix the chemical coagulant if sufficient mixing energy is not provided by the pump. The second rapid mixing zone for the addition of PAMs is recommended to be a static mixer or equivalent. As with the metal coagulants, PAMs also require high energy rapid mixing to ensure dispersion and provide kinetic energy to the process.

16.1.3. Slow mixing

A slow mixing zone is recommended to improve floc aggregation. The zone may be passively mixed by rapidly flowing inflow or be actively mixed by mechanical mixers. The requirement for active mixing should be tested in the larger-scale system.

Figure 132. Conceptual Model for larger-scale LICD implementation.
Model includes two rapid mixing zones to accommodate blending of metal coagulants and PAMs. A slow mixing zone follows the rapid mixing zones to aid in floc aggregation. Slow mixing may be achievable simply by the dispersion of high energy inflow into low energy quiescent marsh water. The marsh is divided into two zones. The first zone is operated at a HRT of about 2 days and is primarily for settling out large flocs. The second zone is operated at a 3 –5 day HRT and is for biotic uptake and filtering of smaller, less-settleable flocs.

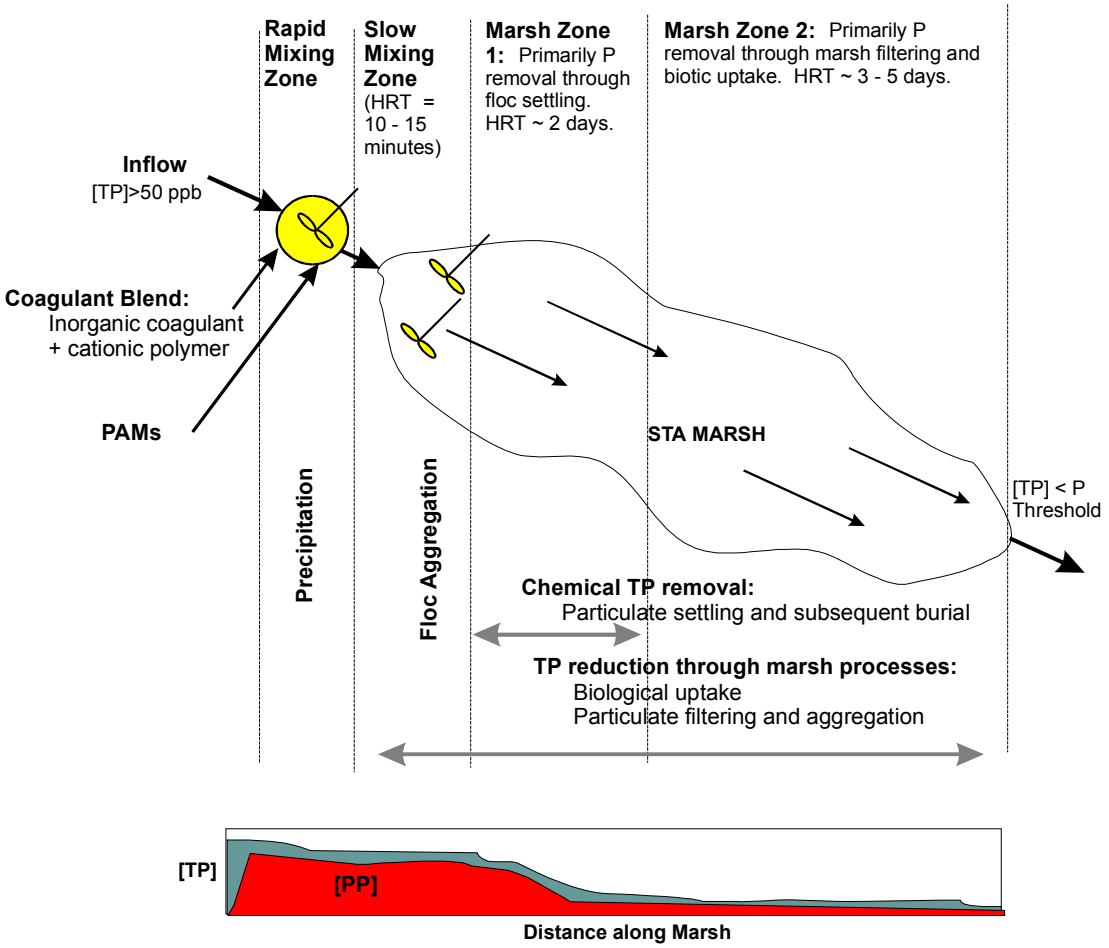

Table 43. Specifications for LICD

Chemical Blends	
Option 1	
Metal	Ferric Iron
Metal Blend	Ferric Chloride
Iron Dose	100 - 200 uM (5.6 -11.2 ppm)
PAM	1 ppm
Option 2	
Metal	Ferric Iron
Metal Blend	FerriPlus-D
Iron Dose	100 - 200 uM (5.6 - 11.2 ppm)
Cationic Polymer	20%
PAM	1 ppm
Option 3	
Metal	Aluminum
Metal Blend	Clarion 4100
Aluminum Dose	100 - 200 uM (2.7 - 5.4 ppm)
Cationic Polymer	10%
PAM	1 ppm
Mixing Protocols	
Rapid Mix Zone 1 for metal blending	
Metal blend injection	Pump
Rapid Mix Zone 2 for PAM blending	
PAM injection	Static Mixer
Slow Mix Zone for Floc Aggregation	
Option 1	Open area downstream of gates
Vegetation	Open water
HRT	15 minutes
Option 2	Mechanical mixers
Vegetation	Open water
HRT	15 minutes
Marsh Area	
LICD Zone	
Vegetation	Emergent or submergent vegetation
HRT	2 Days
Filtering and biotic uptake Zone	
Vegetation	Emergent or submergent
HRT	3 - 5 Days
Total Marsh Area	
Vegetation	Emergent or submergent
HRT	5 - 7 Days

16.2. Marsh component

The marsh is divided into two sections. The first is for a two day HRT in which the bulk of the floc settles. The second is for a 3 – 5 day HRT in which the finer flocs are removed by filtering and some additional phosphorus is removed by biotic uptake. Thus, the marsh experiences a 5 – 7 day HRT.

An emergent marsh is recommended with a design to minimize short-circuiting such that marsh operates closely to a plug flow reactor (PFR). By minimizing short-circuiting, the marsh will likely be modeled as a non-ideal PFR. This design will have several operational advantages over the current completely mixed design that was used for the mesocosm study.

First, as a PFR, the marsh will more efficiently biologically utilize and remove phosphorus than would a Continuous-Flow stirred tank reactor (CFSTR) marsh. Biological uptake of nutrients can be modeled as first-order kinetics (Kadlec and Knight, 1996; Metcalf and Eddy, 1979). For first-order substrate removal kinetics, PFRs are much more efficient at pollutant removal than CFSTRs and this is fundamentally related to the decrease in nutrient concentrations as water passes through the systems (Metcalf and Eddy, 1979). Thus, the reactor kinetics of a larger-scale non-ideal PFR marsh favors more efficient biotic uptake of nutrients than could be achieved in the mesocosm systems given equivalent inflows and operating conditions (e.g. HRT, water depth, plant density). Additionally, marshes have lower hydraulic conductivity and higher resistance to flow than open water systems. This increased resistance is caused by marsh plants. In flow through marsh systems, high plant density and accompanying high frictional resistance lead to more efficient particulate settling and filtering, greater surface area for colonization of biota, and more efficient biological uptake (Bachand and Horne, 2000; Phipps and Crumpton, 1994). These full-scale marsh characteristics should lead to higher particulate settling rates, better filtration and higher biotic uptake rates than can be achieved in the mesocosm systems used in this study. These are the gradient effects associated with large-scale non-ideal plug flow marshes.

16.3. Integration of chemical and marsh components

Florida marshes are phosphorus limited and can decrease total phosphorus to levels at or below 10 $\mu g\ L^{-1}$ (Vaithiyanathan and Richardson, 1997). Dense submerged and emergent marsh vegetation aid with particle filtering and settling. Because Florida marshes can decrease total phosphorus concentrations to 10 $\mu g\ L^{-1}$, a LICD marsh should also be able to achieve the same phosphorus levels.

Because LICD is expected to decrease by approximately 80% the phosphorus load required for treatment by the accompanying marsh, the use of LICD should enable higher flows through the marsh (and shorter HRTs) and lengthen the effective life of the marsh. Vaithiyanathan and Richardson (1997) showed that in

the Water Conservation Areas (WCAs), total phosphorus concentrations under 10 $\mu g\ L^{-1}$ are reached 9 kilometers from the inflow structures. Inflow phosphorus concentrations are decreased by 80% to the range of 25 – 30 $\mu g\ L^{-1}$ 5 to 6 kilometers beyond the inflow structures. Thus, in the WCAs, 55 – 67% of the enriched marsh area is required to decrease the phosphorus loads by 80% to concentration levels in the range of 25 – 30 $\mu g\ L^{-1}$. This data set represents the time periods of 1986 – 1991 and 1993 – 1995. The total phosphorus concentration achieved at this point in the WCAs is similar to concentrations that have been achieved by the LICD mesocosm studies.

With a full-scale LICD marsh, our data suggests that 80% of the load will be removed by LICD and that only 20% of the load will need to be removed by associated marsh processes typical to those in the WCAs. Thus, the WCA data from Vaithiyanathan and Richardson (1997) suggests that marsh area can be decreased by 55 – 67%. Conversely, flows to a LICD marsh can be on the order of 2 to 3 times higher than a treatment wetland without LICD.

In addition to enabling shorter HRTs, an LICD marsh will likely be less apt to become saturated with regard to phosphorus uptake. Richardson and Qian (1999) showed in the WCAs that once phosphorus loading saturate short-term uptake and storage mechanisms as is typical in the enriched zones of the WCAs, a phosphorus front begins moving down the gradient. This sediment saturation with phosphorus is indicated by soil phosphorus concentrations two to three times higher in the enriched zone of the WCAs as compared to the unenriched zones (Vaithiyanathan and Richardson, 1997). These soil concentrations exponentially decrease downstream from inflow structures. In an LICD marsh, the marsh is expected to be less likely to become saturated with regard to phosphorus because chemical processes are expected to decrease the phosphorus load by around 80%. This reduced phosphorus loading will lead to lower water and sediment phosphorus concentrations and effectively extend the marsh life.

If this conceptual model of LICD is applied in a larger-scale non-ideal PFR, we believe that the LICD marsh system has good potential to reduce phosphorus concentrations to near 10 $\mu g\ L^{-1}$. We believe that LICD chemical processes will decrease phosphorus concentrations to around 20 $\mu g\ L^{-1}$ and that the remaining phosphorus removal will occur through typical marsh processes such as settling, filtering and biotic uptake. We believe that a LICD marsh will be able to operate at a HRT approximately 2 to 3 times shorter than a treatment marsh without LICD and that LICD will extend the life of the marsh with regard to phosphorus removal. This conclusion is based upon the performance of LICD in the mesocosm systems under CFSTR conditions; an understanding of reactor kinetics related to wetlands, PFRs and CFSTRs; and WCAs phosphorus removal characteristics (Vaithiyanathan and Richardson, 1997; Craft and Richardson, 1993; Richardson and Qian, 1999).

Effective implementation will require the incorporation of polymers and likely require some consideration of mixing regimes. Given the natural characteristics of the marsh, some of these requirements may be relatively simple and cost-effective to employ. Thus, we recommend testing LICD at a larger-scale with incorporation of polymers and improved mixing regimes.

Chapter 17. Cost Estimate

The SOW for this contract requires a rough estimate of full-scale costs of this technology be outlined. The original proposal anticipated a 3-year study (Richardson et al., 1999) with a Present Worth Analyses completed during the final year under the guidelines detailed in the STSOC (Peer Consultants, P.C./Brown and Caldwell; 1999). For this report, a cost estimate has been developed using the STSOC as a guideline. Cost estimates were developed based upon the 10-year period of record for STA 2. Based upon that record, the average inflow to STA 2 was 464 MGD. This cost estimate assumes that LICD would treat the entire inflow. The 50-year present worth cost was calculated using a net discount rate of 4 percent (Peer Consultants, P.C./Brown and Caldwell, 1999; CRA, 2000).

The detailed cost estimate is presented in two tables. Table 44 presents the LICD treatment system costs excluding chemical costs. This estimate was developed from the conceptual design (Figure 132). Chemical costs were excluded from this table as without further testing at a pilot-scale, exact chemical blends and dosages cannot be determined. Our research from this study has found that several different chemical blends hold good promise in providing the necessary treatment. The most promising include Ferriplus-D, ferric chloride, and Clarion 4100. Jar tests and field studies (Bachand et al, 1999) also suggests that alum may yet provide adequate treatment if used in combination with PAM dosed at a sufficient level. We anticipate that the chemicals will be dosed in a range of 100 – 200 μM and that they will need to be followed by an application of PAM at approximately 1 mg L^{-1}. However, without pilot-scale testing, the exact chemical blend and dosage cannot be determined given that the marsh component could not be adequately tested in this study (See Chapter 16). Table 44 therefore only presents the treatment system equipment and associated O&M costs. These costs have been developed from conservative estimates. Cost information has been used from several sources including the STSOC, Kemiron (2000), General Chemical (2000), Cytec (2000) and CRA (2000). Cost information and assumptions are noted for line items in Table 44. Equipment costs are not expected to vary greatly between the different potential chemical dosing scenarios, as the chemical dosing ranges are similar. This conservative cost should accommodate any differences in costs associated with different chemical dosing regimes and provide a reasonable rough estimate of LICD treatment system costs at the full-scale.

From Table 44, the 50-year present worth is approximately $177 million dollars with about 9% that due to the LICD equipment, operations and maintenance, and the remainder associated with the STA. Costs associated with LICD include the costs associated with chemical delivery and mixing, and some modifications of the STAs to provide adequate mixing and vegetation control.

Table 45 estimates chemical costs for different possible dosing scenarios. Chemical cost information for this estimate has been provided by Kemiron (2000), Cytec (2000) and General Chemical (2000), as well as from the STSOC. Chemical costs can potentially be the largest costs associated with LICD. 50-year present worth ranges from approximately $90 to 630 million dollars depending upon chemical blend and dosing level. Ferric chloride is approximately one third the costs of FerriPlus-D and alum is approximately one third the costs of Clarion 4100. Thus, savings for these metal/cationic polymer blends depends upon achieving equivalent phosphorus removal results at lower metal dosing levels. If lower metal dosing levels can be achieved, then in addition to direct material costs savings, additional benefits such as lower sediment production and less potential environmental effects are likely to follow.

PAM also adds cost to the process. For 1 mg L^{-1} dosing level, the added 50-year present worth is approximately $2 million dollars. Flocculation and settling was greatly improved in both the lab and the field with the addition of PAM as a flocculent aid. In jar test studies, ferric chloride was nearly as effective at removing phosphorus as FerriPlus-D when sufficient PAM dosing levels were used. However, in the field, insufficient PAM dosing levels greatly hindered phosphorus removal by ferric chloride. Effective laboratory dosing levels of 0.25 mg L^{-1} were one-fourth the effective field dosing levels of 1 mg L^{-1}, suggesting that mixing inefficiencies compromised PAM effectiveness in the field. Obviously, improvements to chemical mixing enhance the effectiveness of PAM would result in large costs savings.

This may also be true with the metal blends. Field data suggested that mixing of metal blends was less effective in the field than in the lab. This is suggested by higher resulting total phosphorus concentrations achieved in the field as opposed to the lab for equivalent metal dosing levels and higher residual metal concentrations after chemical dosing. Better phosphorus removal and lower residual metal concentrations achieved in field studies when using metal/cationic polymer blends suggests that these blends better offset field mixing inefficiencies than either alum or ferric chloride alone. However, that is apparently achieved at a higher materials cost. Thus, improvements in mixing that further enhance the effectiveness of chemical dosing should also reduce chemical costs greatly.

Table 45 thus suggests a reasonable range of potential chemical costs, depending upon the field implementation of LICD. If chemicals are inadequately mixed, then metal/cationic blends at the higher dosing concentrations will be required and will result in higher costs. More effective mixing may enable either lower dosing concentrations of metal/cationic polymer blends or the use of alum or ferric chloride. In all cases, PAMs are likely required though improved mixing may enable lower dosing concentrations.

A summary of the 50-year present worth is presented in Table 46. Predicted costs to treat a million gallons range from approximately 30 - 100 dollars.

Testing at the pilot-scale is necessary to further refine chemical dosing specifications and to develop a more precise estimate of the 50-year present worth for full-scale LICD implementation.

Table 44. LICD Treatment System Cost Estimate.

Development of 50-Year Present Worth for LICD Treatment System. Costs do not include chemical costs.

	Item/Task	Unit	Unit cost	Quantity	Costs		
					LICD	STA	Total
1	**Capital costs**						
1.1.1	Equipment[1]	$	-	NA			
1.1.2	Residuals management[12]	$/MGD	-	NA			
1.1.3	Chemical feed system[2]	$/MGD	3,000	464	$ 1,392,000	$ -	$ 1,392,000
1.2	Freight		-	NA			
1.3	Installation		-	NA			
1.4	Instrumentation[3,14]		-	L.S	$ 30,000	$ -	$ 30,000
1.5	Electrical controls						$ -
1.5.1	Electrical controls[3,15]		-	L.S	$ 15,000	$ -	$ 15,000
1.5.2	Electrical power distribution[3,13]	$/mile	80,000	0.5	$ 40,000	$ -	$ 40,000
1.6	Civil Work- water control structures						$ -
1.6.1	84" culvert open[3]	$/structure	20,000	NA			
1.6.2	84" culvert with gate[3]	$/structure	35,000	NA			
1.6.3	With gates[3]	$/structure	300,000	NA			
1.6.4	Without gates[3]	$/structure	150,000	NA			
1.7.1	Canals (digging - no blasting)						
1.7.1.1	Canals- Deep excavation[3]	$/cubic yard	3.50	NA			
1.7.1.2	Canals- Shallow excavation[5,3,16]	$/cubic yard	2.50	119335	$ -	$ 298,338	$ 298,338
1.7.2	Canals- Including blasting	$/cubic yard					$ -
1.7.2.1	Canals- Deep excavation[6]	$/cubic yard	6.17	57433	$ 76,372	$ -	$ 76,372
1.7.2.2	Canals- Shallow excavation[3]	$/cubic yard	3.50	NA			
1.8.1	Levees (no blasting)						
1.8.1.1	Internal- 7' (4.5' SWD)[3]	$/mile	390,000	NA			
1.8.1.3	External- 8' (4.5' SWD)[5,3,17]	$/mile	485,000	18	$ -	$ 8,730,000	$ 8,730,000
1.8.1.4	External- 9' (4.5' SWD)[3]	$/mile	562,000	NA			
1.8.1.5	External-10' (4.5' SWD)[3]	$/mile	703,000	NA			
1.9.1	STA Influent pumping station[7]	$/cfs	9,000	3000	$ -	$ 27,000,000	$ 27,000,000
1.9.2	STA effluent pumping station[8]	$/cfs	10,500	2000	$ -	$ 21,000,000	$ 21,000,000
1.9.3	Pumping stations- Seepage, 60-500 cfs[3,5]	$/cfs	9,900	500	$ -	$ 4,950,000	$ 4,950,000
1.10	Interior land preparation						
1.10.1	Disking	$/acre	60	NA			
Subtotal					$ 1,553,372	$ 61,978,338	$ 63,531,710
Construction contingencies[4,18]					$ 310,674	$ 12,395,668	$ 12,706,342
Subtotal, construction costs					$ 1,864,047	$ 74,374,005	$ 76,238,052
Engineering and Design costs[4,19]					$ 279,607	$ 11,156,101	$ 11,435,708
1.11	Land						
1.11.1	Natural System[9]	$acre	4,655	5000	$ -	$ 23,275,000	$ 23,275,000
TOTAL CAPITAL COSTS					**$ 2,143,654**	**$ 108,805,106**	**$ 110,948,759**
PRESENT WORTH - CAPITAL COST					**$ 2,143,654**	**$ 108,805,106**	**$ 110,948,759**

2	**OPERATING COSTS (per year)**							
2.1	Labor[20]	hr	30	NA				
2.2.1	Maintenance (spare parts, etc.)[20]	$/unit	23,000	NA				
2.2.2	Maintenance (water control structures)[3]	$/unit	12,000	0	$ -	$ -	$	-
2.2.3	Maintenance (building)[3]	$/unit	12,000	1	$ 12,000	$ -	$	12,000
2.2.4	Maintenance- Levees[4]	$/mile	1,530	18	$ -	$ 27,540	$	27,540
2.2.5	Maintenance (vegetation control)[6,4,21]	$/acre						
2.2.5.1	STA		22	5000	0	$ 110,000	$	110,000
2.2.5.2	Slow Mixing Zone		44	2.97	$ 131	$ -	$	131
2.2.6	Maintenance - Seepage pump station[4,25]	$/unit	110,000	1	$ -	$ 110,000	$	110,000
2.2.7	Maintenance - Influent/effluent pump station[4,26]	$/unit	520,000	2	$ -	$ 1,040,000	$	1,040,000
2.2.8	Maintenance - chemical feed system	$/unit	75,000	1	$ 75,000	$ -	$	75,000
2.3	**Chemicals**	**SEE CHEMICAL WORKSHEETS FOR VARIOUS DIFFERENT CHEMICAL BLENDS**						
2.4	Solids disposal[12]	Tons	50	NA				
2.5	Sampling and monitoring[3]	yr			$ 500,000	$ -	$	500,000
TOTAL OPERATING COSTS					**$ 587,131**	**$ 1,287,540**	**$**	**1,874,671**
PRESENT WORTH - OPERATING COSTS					**$ 12,623,310**	**$ 27,682,110**	**$**	**40,305,420**
3	**Demolition/Replacement Costs**							
3.1	Demolition costs[1,4]			NA				
3.2	Restoration of levees[3]	$/yard	3	156790.8	$ -	$ 470,372	$	470,372
3.4	Clearing and grubbing							
3.4.1	Light folliage[3,4]	$/acre	300	5000	$ -	$ 1,500,000	$	1,500,000
3.4.2	Forest/heavy brushes	$/acre	1,500		$ -	$ -	$	-
3.5	Replacement items							
3.5.1	Seepage pumping stations[22,4]	Lump sum			$ -	$ 2,475,000	$	2,475,000
3.5.3	STA pumping stations[22,4]	Lump sum			$ -	$ 24,000,000	$	24,000,000
3.5.4	Chemical feed system[23,4]	Lump sum			$ 835,200	$ -	$	835,200
TOTAL DEMOLITION/REPLACEMENT COSTS					$ 835,200	$ 28,445,372	$	29,280,572
PRESENT WORTH - DEMOLITION/REPLACEMENT COSTS					$ 835,200	$ 28,445,372	$	29,280,572
4	**Salvage Costs**							
4.1	Salvage Cost[3]	$acre	4,655	5000	$ -	$ 23,275,000	$	23,275,000
TOTAL SALVAGE COSTS					**$ -**	**$ 23,275,000**	**$**	**23,275,000**
PRESENT WORTH - SALVAGE COSTS					**$ -**	**$ 3,272,465**	**$**	**3,272,465**
5	**Lump Sum/ Contingency Items**							
5.1	Telemetry	Lump sum			$ -	$ 100,000	$	100,000
5.1.1	Pump Stations[24,3]	$/unit	50,000		$ -	$ -	$	-
5.1.2	Water Control Structures[24,3]	$unit	25,000		$ -	$ -	$	-
5.2	FPL Improvements[24,3]	Lump sum	-		$ -	$ -	$	-
5.3	Administrative facilities	Lump sum	-		$ 100,000	$ -	$	100,000
TOTAL LUMP SUM ITEMS					**$ 100,000**	**$ 100,000**	**$**	**200,000**
50-YEAR PRESENT WORTH								
CAPITAL COST					$ 2,143,654	$ 108,805,106	$	110,948,759
OPERATING COST					$ 12,623,310	$ 27,682,110	$	40,305,420
DEMOLITION/REPLACEMENT COST					$ 835,200	$ 28,445,372	$	29,280,572
SALVAGE COST					$ -	$ 3,272,465	$	3,272,465
LUMP SUM COST					$ 100,000	$ 100,000	$	200,000
TOTAL					$ 15,702,163	$ 161,760,123	$	177,462,286

Notes

1	LICD requires no chemical treatment plant or associated equipment (e.g. concrete tanks, clarifier plates, mechanical scrapers, treatment plant piping,excavation). Mixers (e.g. rapid, slow) may be required and that cost is included with the chemical feed system costs.
2	Chemical feed system costs based upon Chemical Treatment Solids Separation (CTSS) estimate by CRA (2000). CRA (2000) estimated that Chemical feed system would be equal to 2.5% of the CTSS Equipment Costs. For PostSTA treatment, Equipment costs are estimated by CRA (2000) as $60,300/ mgd. Thus, chemical feed costs are estimated as $1500/mgd. This estimate has been doubled to account for rapid and slow mixers such that chemical
3	Cost estimated by CRA (2000) for CTSS Unit Cost Summary.
4	Costs estimated from Peer Consultants, P.C./Brown and Caldwell (1999).
5	Quantity estimated from CRA (2000).
6	Slow mixing zone excavation is assumed to prevent vegetation colonization. Costs assumed to be equivalent ot that for deep canal excavation including blasting. Vegetation maintenance may also be required.
7	Pump flows calculated for 3 standard deviations. Costs are estimated from Peer Consultants, P.C./Brown and Caldwell (1999) for pump stations designed for flows in excess of 2000 cfs.
8	Pump flows calculated for 2 standard deviations. Wetland provides flow buffering and outflows from the STAs are lower than inflows (CRA, 2000). Costs are estimated from Peer Consultants, P.C./Brown and Caldwell (1999) for pump stations designed for flows in excess of 1200 cfs.
9	Assumes water depth of 2 ft.
10	Clar+Ion 4100 is registered by General Chemical and is composed of Alum + 10% cationic polymer. Pricing information provided by e-mail
11	E-Mail memorandum from Chris Lind, General Chemical Corporation, October 26, 2000. Alum price is a conservative estimate and likely would be lower in full-scale operation. This price has previously been provided to SFWMD district.
12	Assumed not applicable. Formed sediments to stay in marsh and expected to accrete one foot every 35 - 50 years. No solids are expected to be
13	To be provided from nearby power station. For instance, for STA-2, power provided from STA-2 effluent pump station.
14	Assumed to be 10% of chemical feed system costs.
15	Assumed to be 5% of chemical feed system costs.
16	Perimeter seepage canal.
17	Perimeter levee.
18	20% of capital costs
19	15% of construction costs
20	Included in maintenance of pumps and equipment
21	Assumed same vegetation control in slow mixing zone as typically required for Flow Equalization Basin.
22	50% of cost replaced once at 25 years.
23	60% of cost replaced every 10 years.
24	Accounted for.
25	Based upon seepage pump station for STA 2 (Peer Consultants, P.C./Brown and Caldwell, 1999).
26	Based upon G335 in STA 2 (3000,244; Peer Consultants, P.C./Brown and Caldwell, 1999).

Table 45. LICD Chemical Cost Estimate

Chemical blends are proposed blends that should be further tested at a pilot scale before full-scale implementation.

Descriptor	Ferric chloride + PAM		FerriPlus-D + PAM		Alum + PAM		Clar+ion 4100 + PAM	
Metal Blend	**Ferric chloride**		**FerriPlus-D6[4]**		**Alum**		**85**	
Unit	$/Dry ton[6]		$/Wet ton[4]		$/Dry ton[6]		$/wet ton[5]	
Unit Costs	180		264		150		180	
Dose	Low[1]	High[2]	Low[1]	High[2]	Low[1]	High[2]	Low[1]	High[2]
tons/yr	11500	23000	35,000	70,000	21,000	42,000	76,200	152,400
Subtotal ($)	2,070,000	4,140,000	9,240,000	18,480,000	3,150,000	6,300,000	13,716,000	27,432,000
PAM								
Unit	$/Dry ton	$/Dry ton	$/Dry ton	$/Dry ton	$/Dry ton	$/Dry ton	$/Dry ton	$/Dry ton
Unit Costs[7]	2,940	2,940	2,940	2,940	2,940	2,940	2,940	2,940
Tons	708	708	708	708	708	708	708	708
Subtotal ($)	2,081,814	2,081,814	2,081,814	2,081,814	2,081,814	2,081,814	2,081,814	2,081,814
Total Chemical Costs ($)	**4,151,814**	**6,221,814**	**11,321,814**	**20,561,814**	**5,231,814**	**8,381,814**	**15,797,814**	**29,513,814**
50-YEAR PRESENT WORTH ($)	**89,264,001**	**133,769,001**	**243,419,001**	**442,079,001**	**112,484,001**	**180,209,001**	**339,653,001**	**634,547,001**

Notes

1 100 uM dose.
2 200 uM dose
3 Present Worth based upon 50 year of operation at 464 mgd flows.
4 Ferriplus-D is registered by Kemiron. FerriPlus-D is ferric sulfate + 20% cationic polymer. Pricing information provided by communications with Kemiron (2000). FerriPlus-D price is a conservative estimate and likely would be lower in full-scale operati
5 Clar+Ion 4100 is registered by General Chemical and is composed of Alum + 10% cationic polymer. Pricing information provided by General Chemical Corporation (2000) based upon bid pricing.
6 Peer Consulting (1999)
7 Cytec Industries (2000).

Table 46. 50-Year Present Worth Summary

Treatments	Ferric chloride + PAM		FerriPlus-D + PAM		Alum + PAM		Clar+ion 4100 + PAM	
	Ferric chloride		FerriPlus-D[3]		Alum		Clar+Ion 4100[4]	
Dose	Low[2]	High[2]	Low[2]	High[2]	Low[2]	High[2]	Low[2]	High[2]
Treatment System costs excluding chemicals ($)[6]								
Capitol	110,948,759	110,948,759	110,948,759	110,948,759	110,948,759	110,948,759	110,948,759	110,948,759
Operating	40,305,420	40,305,420	40,305,420	40,305,420	40,305,420	40,305,420	40,305,420	40,305,420
Demo/Replacement	29,280,572	29,280,572	29,280,572	29,280,572	29,280,572	29,280,572	29,280,572	29,280,572
Salvage	3,272,465	3,272,465	3,272,465	3,272,465	3,272,465	3,272,465	3,272,465	3,272,465
Lump Sum	200,000	200,000	200,000	200,000	200,000	200,000	200,000	200,000
SubTotal	177,462,286	177,462,286	177,462,286	177,462,286	177,462,286	177,462,286	177,462,286	177,462,286
Chemical Costs ($)								
	89,264,001	133,769,001	243,419,001	442,079,001	112,484,001	180,209,001	339,653,001	634,547,001
Plant + Chemical Costs ($)								
	266,726,287	311,231,287	420,881,287	619,541,287	289,946,287	357,671,287	517,115,287	812,009,287
$/MGals Treated[1]	31.50	36.75	49.70	73.16	34.24	42.24	61.07	95.89

Notes

1 Assumes 50 years of treatment at average treated flow of 464 MGD.
2 Low dose = 100 uM. High dose = 200 uM.
3 Registered by Kemiron.
4 Registered by General Chemical.
5 Generic equivalent to Clar+Ion 4100 manufactured in-house. Price per ton based upon Raw Material costs.
6 Treatment system costs are assumed to be equal for all chemical treatment options.

Chapter 18. Conclusion

LICD is composed of a mix of chemical and biological processes. These processes are:

- Precipitation (chemical)
- Floc Aggregation (chemical)
- Settling/Filtering (chemical/biological)
- Uptake (biological)
- Burial (biological/chemical)

Implementing LICD requires an appreciation of these processes and an understanding that *in situ* chemical addition requires optimization of chemical blends and performance in order to minimize accretion of these sediments in the marsh.

Earlier Phase I studies showed that aluminum and iron dosing levels of 100 – 200 μM very effectively and sustainably decreased water column concentrations of dissolved phosphorus (Bachand et al., 1999). Seventy-five percent of the decrease occurred immediately after chemical dosing by the near immediate conversion of dissolved phosphorus to particulate phosphorus. LICD also decreased total phosphorus concentrations with aluminum dosing levels of 100 and 200 μM decreasing total phosphorus 33 – 50% below background phosphorus concentrations of 40 – 45 μg L^{-1} (Bachand et al., 1999). As LICD was never considered a stand-alone technology and the accompanying marsh would remove some phosphorus, these results were very promising. Bachand et al. (1999) recommended investigating management practices to improve chemical utilization and create a more robust, reliable and effective technology. First year Phase II studies was a mix of laboratory and field studies. Laboratory studies consisted of a series of eight jar tests and field studies consisted of three mesocosm studies. All experimental studies for Phase II were conducted from April 1999 through March 2000.

18.1. Conclusions from Jar Test Studies

Jar tests were conducted to better understand the various chemical processes associated with phosphorus removal by LICD. These processes were primarily precipitation, floc aggregation and floc settling. From the jar test studies, the following conclusions were drawn:

1. Chemical doses of 100 and 200 μM provide similar results with regard to phosphorus removal

Generally, total phosphorus removal in jar tests is slightly better for aluminum and iron dosing concentrations of 200 μM as opposed to 100 μM. However, both dosing concentrations have achieved total phosphorus concentrations at or near

10 μg L^{-1} and have provided similar results. This is especially true when polymers are introduced into the chemical blends.

2. Both cationic and anionic polymers greatly improve the effectiveness of LICD with regard to phosphorus removal from the water column.

Cationic polymer blends generally outperformed pure metal coagulants. Ferric iron with 20% cationic polymers was the most promising iron blend and Alum with 10% polymer was the most promising aluminum blend. Metal/cationic polymer blends generally had lower turbidity, lower dissolved phosphorus and lower total phosphorus concentrations than metals alone. One obvious and important role of cationic polymers is more effective and efficient conversion of dissolved phosphorus to particulate phosphorus. When followed by anionic polymers (PAMs), floc aggregation and settling rates were further improved. The use of PAMs accelerated settling rates and floc settling was complete in the jar tests sometimes immediately after mixing ceased and generally within the first ten minutes. This improvement was dramatic for iron blends but less so for aluminum blends. Using PAMs with ferric iron blends decreased the need for using cationic polymers. Thus, ferric iron blends were most improved by the addition of PAMs and only slightly so by the use of cationic polymers. Aluminum blends were most improved by the use of cationic polymers and only slightly so by the use of PAMs. Using metal/cationic/anionic blends led to total phosphorus concentrations near or under 10 μg L^{-1} for both ferric iron and aluminum blends.

3. ***Proper mixing protocols are likely beneficial.***

Longer rapid mixing and the addition of a slow mixing period improved floc settling characteristics. The addition of additional inline mixers and a slow mixing tank in the *in situ* process should lead to decreased total phosphorus concentrations in the water column through improved chemical mixing and floc aggregation.

4. Calcium is ineffective at improving phosphorus removal

Calcium either alone or in combination with iron and aluminum is ineffective at improving floc settling rates or total phosphorus removal.

5. Iron/aluminum blends provide no additional benefits.

Ferric iron/aluminum blends do not improve performance over ferric iron or aluminum alone.

Overall, jar tests showed that under effective mixing regimes, metal/ polymer combinations improved floc aggregation and increased settling at all metal dosing levels. Achieving mean total phosphorus concentrations at or very near 10 μg L^{-1} were achievable in the jar tests at metal dosing levels of 100 – 200 μM when proper consideration was given to identifying the blend components.

18.2. Conclusions from mesocosm studies

Field studies followed the jar tests in order to validate the jar test findings and discern environmental effects on and from LICD. From the field studies as well as a review of relevant publications, the following conclusions have been drawn with regard to LICD and chemical treatments in general:

1. PAMs can greatly improve in situ total phosphorus removal from the water column.

PAM utilization at dosing levels of 1 mg L^{-1} greatly improved phosphorus removal. When PAMs were used at a lower dose of 0.5 mg L^{-1}, iron dosing at 200 μM only decreased total phosphorus concentrations 20% from 129 μg L^{-1} to 103 μg L^{-1}. This trend was similar for aluminum at 200 μM (5.6 mg L^{-1}), with PAM dosing at 1 mg L^{-1} resulting in mean phosphorus concentrations in the mesocosms of 39 μg L^{-1} as opposed to only 77 μg L^{-1} when the lower PAM dose was utilized. In general, PAMs greatly improved settling and this was most apparent at lower metal doses. In previous mesocosm studies at metal dosing concentration of 200 μM, decreases in water column total phosphorus concentrations of only 21 to 48% had been achieved (Bachand et al, 1999). This finding is very important for LICD process development efforts as metal dosing levels of 100 and 200 μM have effectively and consistently converted dissolved phosphorus to particulate phosphorus (Bachand et al., 1999). However, hindered settling of pin floc was identified as a problem for settling the particulate phosphorus. PAMs apparently convert the pin floc formed under metal dosing to larger aggregates that settle more effectively. Thus, *in situ* PAM dosing of 1 mg L^{-1} holds promise for effective total phosphorus removal metal dosing levels below 200 μM.

2. Cationic polymers/metal blends outperform metals alone.

In situ application of cationic polymer blends improved the removal of dissolved and total phosphorus from the water column for both ferric iron and aluminum blends. Cationic polymer blends of 20% for iron and 10% for aluminum result in dissolved phosphorus concentrations in the mesocosms of between 5 and 10 μg L^{-1}. These dissolved phosphorus concentrations have been achieved *in situ* with metal dosing levels as low as 100 μM. Consistently, cationic polymer/metal blends more effectively convert dissolved phosphorus to particulate phosphorus than metals alone.

The more effective conversion of dissolved to particulate phosphorus may also have led to more settleable flocs. When a 20% cationic polymer was used in combination with ferric iron, improved total phosphorus removal occurred than when ferric iron was used alone. When a 10% cationic polymer was used in combination with aluminum greater removal of total phosphorus also occurred.

For aluminum dosing, cationic polymers/alum blends have clear and easily identifiable benefits over the use alum alone. Consistent with the jar test studies, Clarion 4100 outperforms alum alone with regard to the removal of both dissolved

and total phosphorus from the water column. For iron dosing, the benefits of the cationic blends are less clear. Generally, ferric chloride and FerriPlus-D decrease dissolved phosphorus to the same levels of below 10 μg L^{-1}. FerriPlus-D appears to have better total phosphorus removal in the absence of sufficient PAM concentrations for optimum phosphorus removal. However, at adequate PAM concentrations, jar test studies suggests that ferric chloride is as effective as FerriPlus-D with regard to total phosphorus removal and that has not been field validated at this time.

3. Total phosphorus concentrations of 12 μg L^{-1} may be achievable by the chemical component of LICD. When incorporating the biological (marsh) component of LICD and maintaining non-ideal PFR conditions, total phosphorus concentrations of 10 μg L^{-1} may be possible.

A LICD marsh will incorporate both a chemical and biological component for phosphorus removal. The chemical component of LICD was primarily tested in these *in situ* mesocosm studies. In the mesocosm studies, LICD effectively removed total phosphorus from the water column. In the final field study with background total phosphorus concentrations averaging between 105 and 128 μg L^{-1}, iron dosing levels at 200 μM with 20% cationic polymers and then followed by PAM dosing at 1 mg L^{-1} decreased total phosphorus concentrations in the mixing tanks to 24 μg L^{-1}. This represented a 77% reduction in total phosphorus for an 18 – 24 hour HRT. In the mesocosms, the same treatment yielded total phosphorus concentrations of 29 μg L^{-1}. These systems were operated under a 2.5 day HRT and were **not hydrologically** isolated from the surrounding marsh. With mass balance calculations incorporating dilution effects, LICD yielded mean total phosphorus concentrations of **12 μg L^{-1}**. Aluminum dosing at 200 μM in combination with 10% cationic polymer and PAM dosing levels of 1.0 mg L^{-1} resulted in total phosphorus concentrations in the mixing tanks averaging 19 μg L^{-1}. This represented a 82% decrease in total phosphorus. In the mesocosms, total phosphorus concentrations for this treatment yielded an average total phosphorus concentration of 39 μg L^{-1}. When corrected for marsh dilution, aluminum dosing at 200 μM yielded total phosphorus concentrations of 28 μg L^{-1}. These results primarily reflect the chemical component of LICD and not the spatial marsh effects such as biotic uptake and effective filtering.

In larger-scale non-ideal PFR marsh, better performance is expected and achieving outflow concentrations below 10 μg L^{-1} may be possible. More favorable PFR kinetics (Metcalf and Eddy, 1979); improved particulate filtering and settling because of high frictional resistance from emergent vegetation; and greater plant surface area provided for colonization by attached biota (Phipps and Crumpton, 1994) should enhance biological uptake of phosphorus. These uptake rates should be higher than were possible in the CFSTR mesocosm systems. In the larger-scale marsh, the design and management should minimize short-circuiting in order to maintain non-ideal PFR conditions.

This conclusion is supported by data from the WCAs. Florida marshes are phosphorus limited and the WCAs achieve total phosphorus to levels at or below 10 $\mu g\ L^{-1}$ (Vaithiyanathan and Richardson, 1997). Because Florida marshes can decrease total phosphorus concentrations alone to 10 $\mu g\ L^{-1}$, than a LICD marsh should also be able to achieve the same phosphorus levels. Because LICD is expected to decrease by approximately 80% the phosphorus load required for treatment by the accompanying marsh, the use of LICD should enable higher flows through the marsh (and shorter HRTs) and lengthen the effective life of the marsh. Based on phosphorus removal and sediment data from the WCA (Craft and Richardson, 1993; Vaithiyanathan and Richardson, 1997; Richardson and Qian, 1999), we believe that an LICD marsh can operate at a HRT 2 to 3 times shorter than a treatment wetland without LICD. Moreover, from these same data and sediment analyses from this study, we expect that a LICD marsh will be more sustainable with regard to phosphorus removal because the sediments will have lower phosphorus concentrations than a marsh without LICD. This should help minimize phosphorus saturation of the sediments and lengthen the life of the marsh with regard to phosphorus removal.

4. Near total removal of dissolved phosphorus occurs

LICD effectively decreased dissolved phosphorus concentrations. Dosing immediately decreased dissolved phosphorus concentrations by about 90%. Aluminum dosing generally decreased dissolved phosphorus concentrations by more with 75% of the dosed inflow waters having dissolved phosphorus concentrations below 10 $\mu g\ L^{-1}$ as opposed to below 15 $\mu g\ L^{-1}$ for iron dosing. Though cationic polymers improve the conversion of dissolved to particulate phosphorus and results in lower dissolved phosphorus concentrations, PAM additions have no obvious effect on the process. Higher metal doses generally had slightly lower dissolved phosphorus concentrations. Determining statistical significance depended greatly upon the statistical test. Overall, higher dosing levels also reduced the variance in the dissolved phosphorus data.

In the final field study, mixing tank data was collected in addition to mesocosm data. Dissolved phosphorus concentrations were generally lower in the mixing tanks with concentrations generally near 5 $\mu g\ L^{-1}$. This data corresponds to water sampled from the mixing tanks under an 18 – 24 hour HRT. Dissolved phosphorus concentrations were slightly higher in the mesocosms and this was partially attributed to diel dilution of mesocosm with high dissolved phosphorus marsh waters. Thus, in a hydrologically isolated system, dissolved phosphorus concentrations of 5 $\mu g\ L^{-1}$ are likely as have been predicted by the various jar test studies.

5. LICD is likely the most cost-effective chemical treatment alternative

LICD requires low metal dosing concentrations and minimal infrastructure as compared to other treatment technologies. Dosing levels for the larger-scale LICD marsh system will likely be in the range of 100 – 200 μM with the blending of cationic polymers and the addition of PAM concentrations of 1 $mg\ L^{-1}$. If larger-

scale systems using the conceptual design presented here can verify the performance we predict (See Conclusion #3 above), we expect the low chemical doses and the minimal infrastructure requirements will make LICD a very competitive chemical treatment alternative.

6. ***Floc formed under metal dosing is approximately 10 – 20 % metal depending upon the metal used.***

Aluminum dosing leads to precipitates composed primarily of aluminum, carbon and non-measured parameters which likely include oxygen, sulfur, hydrogen and silica. Aluminum floc formed at dosing levels of 200 μM were 31% carbon, 11% aluminum, 2.4% calcium, 0.1% phosphorus and 55% non-measured parameters. Iron precipitates are similar in composition though they have iron instead of aluminum as their predominant metal. Iron flocs formed at dosing levels of 200 μM were 26% carbon, 21% iron, 4% calcium, 0.2% phosphorus and 48% non-measured parameters.

7. ***Sediments formed have excess phosphorus storage capacity and prevent the loss of phosphorus from the sediments back into the water column.***

Phosphorus concentrations in the formed floc range from approximately 0.1 to 0.2%. The iron:phosphorus ratio in background sediments is approximately 4:1 and the aluminum:phosphorus ratio is similar. In the formed flocs, the iron:phosphorus ratios and the aluminum:phosphorus ratios are twenty times higher at approximately 100:1. These high ratios suggest that the flocs when settled create a sediment with excess phosphorus storage capacity. Operational mesocosm data supports the contention. During periods of rising water in which phosphorus-rich pore waters were being flushed from the sediments into surface waters, non-dosed mesocosms experienced a sharp rise in water column phosphorus concentrations whereas LICD treated mesocosms did not. This difference was attributed to sediments formed during LICD capping the peat soils and creating a boundary which hindered or prevented the transport of phosphorus upward through the peat sediments into the water column. Iron appeared to create a more effective barrier than did aluminum. This phenomenon occurred at metal dosing levels of 100 μM.

8. ***Dosing levels of 200 μM for both iron and aluminum form sediments with characteristics similar to sediments throughout the world. Based upon this comparison, these formed sediments are not expected to be toxic or harmful to the biota.***

Sediments formed during LICD will be a mixture of sediments formed through precipitation and sediments formed by natural processes of peat accretion. For both iron and aluminum dosing, the resulting sediments will have a higher mineral content than typical in the peat sediments typically found in the Everglades. For aluminum, dosing levels of 100 – 200 μM for HRTs ranging from 2.5 to 7.5 days will create sediments with an aluminum content similar or below that of average worldwide sediments. Iron dosing levels of 200 μM for an HRT of

7.5 days and dosing levels of 100 μM for an HRT of greater than 5 days will create sediments with an average iron concentration in the range of twice that of average worldwide sediments. Both sediments would have a higher percentage of metal oxides, sulfides and hydroxides than the typical Everglade peat soils and likely result in the formation of crystals in some areas. Changes in sediment composition would be constrained to the LICD marsh as little residual iron or aluminum remains in the water column.

From the similar chemical characteristics between the anticipated sediments formed under LICD and that of typical worldwide sediments, we expect that these sediments will not likely be toxic to the biota. In general, naturally forming worldwide sediments are not toxic to biota. That does not mean that in these sediments the diversity and distribution of biota would be the same as found in the unenriched areas of the WCAs or in the Everglades National Park. The biota may differ from those regions. However, we believe this will be the case with the STAs regardless of the presence or absence of LICD. In the non-planted areas of the ENRP and in the enriched areas of WCAs, the biota is dominated by water hyacinth and cattail as opposed to the sawgrass and slough communities in the unenriched areas of the WCAs and in Everglades National Park. This is due in large part to elevated phosphorus concentrations (Vaithiyanathan and Richardson, 1999). The STAs will have elevated phosphorus concentrations and therefore will likely continue to have biota similar to the non-planted areas of the ENRP and the enriched WCA areas.

So the more critical question is not will these sediments result in biota different from that historically found in the Everglades but rather will they be toxic to the biota. Because of the similarities with worldwide sediments, we believe the sediments will not be toxic to the biota. The biota will likely be different from that historically found in the Everglades. However, the biota may also be very similar to that found in the ENRP and the enriched areas of the WCAs. Because the STAs are treatment marshes and LICD would be applied in these treatment marshes, we expect the formed sediments will not adversely affect the biota dominant in those systems. We believe that this preliminary assessment is reasonable and that it supports testing the conceptual model of LICD proposed in this report at the larger scale. At that scale, toxicity testing and other tests on the biota are recommended to provide unequivocal evidence on the effect or lack of effect of LICD on the biota. At that time, an assessment of the biological activity of these formed LICD sediments could be made.

9. Sediment accretion will increase under LICD and those sediments will be more mineral rich.

Depending upon LICD dosing levels, sediment accretion rates are predicted to be 50 – 400% of those in the enriched areas of the WCA-2A. At a metal dosing level of 100 μM for a LICD marsh operated at a 7.5 day HRT, sediment accretion rates are predicted to average 1650 mg m^{-2} d^{-1} and be approximately 50% higher than rates in the enriched area of the WCA-2A. This corresponds to a rate of 6.7

mm y-1 as compared to 4.5 mm y-1 in the enriched area, assuming a bulk density of 0.09 g cm-3. At a metal dosing level of 200 μM operated at a 7.5 day HRT, sediment accretion rates would be approximately twice that of the enriched area of the WCA-2A. At a 200 μM dosing rate, it would take 34 years to raise the marsh elevation by one foot. At a dosing rate of 100 μM, it would take 46 years. Without chemical dosing, the marsh bed will raise by one foot over 68 years.

10. LICD will slightly affect the marsh water characteristics . Dosing levels at and below 200 μM minimally affect the marsh readiness of the water. Dosing levels above 200 μM in this or other technologies may require additional post-treatment beyond that necessary for phosphorus removal in order to maintain marsh readiness of the outflows.

LICD does not affect temperature, specific conductance, calcium, magnesium, hardness, potassium, sodium, copper, zinc, chloride or TSS. LICD slightly lowers pH with aluminum dosing more greatly affecting pH levels. This may be in part do to changes in alkalinity. LICD decreases alkalinity. Iron less affects pH and alkalinity than does aluminum with the effects from iron relatively negligible. LICD slightly affects DO concentrations. In this study, DO slightly increased though in earlier studies it slightly decreased (Bachand et al., 1999). Thus, LICD slightly effects DO concentrations though the effect depends upon the aquatic community in the region affected by chemical dosing. Iron dosing increases manganese concentrations. Both iron and aluminum blends increased sulfate (both blends were sulfate based) and decreased color representing a removal of humic and fulvic acids from the water column. Overall, changes in marsh readiness were relatively negligible at both 200 and 400 μM and would be even less at lower metal dosing concentrations. However, there are some concerns with water quality effects even at 400 μM dosing levels. Aluminum dosing at 400 μM decreased alkalinity by nearly half from approximately 200 mg CaCO3 L-1 to around 100 mg CaCO3 L-1. This represents a large decrease in the waters buffering capacity. Dosing concentrations above 400 μM could therefore have a large effect on pH and require post-treatment to artificially increase the alkalinity of the water.

11. LICD increased residual metal concentrations in the water column above those of background concentrations. Inefficient chemical use may elevate iron and aluminum concentrations in downstream waters.

Iron and aluminum dosing increased the residual total iron and aluminum concentrations above background levels. Earlier mesocosm studies gave total aluminum concentrations in the water column generally ranging from 0.4 – 1.6 mg L^{-1} and total iron concentrations generally ranging from 1 – 6 mg L^{-1} (Bachand et al., 1999). The metal concentration in the water column depended upon dosing level and the efficiency of the metal utilization during chemical addition. Thus, inefficient utilization led to higher residual concentrations in the water column. Residual dissolved metal concentrations were lower for both metals. Typically for aluminum, residual dissolved aluminum was in the range of

0.5 mg L^{-1} whereas for iron, residual dissolved iron was sometimes as high as 2 mg L^{-1}.

Improved chemical utilization through better mixing regimes and the incorporation of polymers have decreased residual metal concentrations in the water column. In the most recent field study, residual dissolved aluminum and iron were at background levels. Residual total iron and aluminum concentrations were less than 1 mg L^{-1}. The mesocosms were operated at a 2.5 day HRT. Longer HRTs in a larger-scale marsh that can leverage marsh settling characteristics should provide additional removal of both iron and aluminum.

Inefficient chemical usage by this or other technologies could lead to unnecessarily high residual metal concentrations in surface waters and negatively affect downstream waters.

12. Higher metal dosing levels do not necessarily improve phosphorus removal rates from the water column.

Jar test studies suggests that only marginal improvement in phosphorus removal is achieved at higher metal dosing levels and that greater improvements can be achieved through the use of polymers. Phase I findings also suggests that *in situ* metal dosing at 200 μM is at best only negligibly better that metal dosing levels at 100 μM (Bachand et al., 1999). Phase II mesocosm studies show that great improvements in phosphorus removal can be achieved with the incorporation of PAMs and cationic polymers. However, again, higher metal dosing levels do not necessarily lead to better phosphorus removal. Increasing iron dosing levels from 200 to 600 μM in the most recent field study did not improve phosphorus removal. Increasing aluminum dosing levels from 200 to 400 μM did provide slightly better phosphorus removal. The primary mechanism of metal dosing with regard to phosphorus removal appears to be the conversion of dissolved to particulate phosphorus. That task is completed at relatively low metal dosing concentrations, generally at or below 100 μM. Once that task has been completed, the role of metals increasing floc size and floc settling characteristics is not clear and somewhat problematic. Greater improvements in improving floc settling characteristics can result from the incorporation of polymers. Thus, using higher and higher metal dosing levels is not likely to be a very efficient or economic approach towards improving phosphorus removal from the water column. That approach may also lead to problems with marsh readiness of the water with regard to pH and alkalinity and may also lead to a carry over of aluminum and iron particulates into downstream marshes.

13. Formation of particulate phosphorus and floc aggregation can be empirically modeled as exponential relationships

The conversion of dissolved phosphorus to particulate phosphorus can be empirically modeled as an exponential relationship dependent upon metal dose. The conversion of non-settleable floc to settleable floc can be empirically modeled as an exponential relationship dependent upon PAM dosing level.

14. Effective implementation of LICD will require recognition of the underlying chemical processes and principles required for effective phosphorus removal.

Inefficient chemical dosing in LICD and other chemical dosing technologies has implications outside of costs and achieved phosphorus removal. High iron or aluminum dosing levels may cause problems with regard to marsh readiness and lead to the carry over of aluminum and iron into downstream waters. Higher and higher metal dosing levels do not necessarily lead to better phosphorus removal and thus may provide no added function aside from increasing costs of materials and sludge management. Developing proper dosing methodologies requires an understanding of the precipitation process and the mechanisms involved in forming settleable or filterable floc. That necessity has been the impetus for the extensive jar test studies conducted in this study. More emphasis needs to be placed on jar testing and laboratory studies in the chemical treatment technologies. Incorporation of this approach is most critical for technologies interested in settling phosphorus from the water column as opposed to filtering it.

15. An HRT of 5 – 7.5 days is recommended to optimize phosphorus removal and minimally affect the sediments.

For LICD, an HRT of 5 to 7.5 days is recommended for optimal phosphorus removal. Approximately 2 days are expected to be needed for precipitating settleable flocs formed by chemical dosing. Three to five additional days are expected to be required for marsh filtering of less settleable flocs and biotic uptake of phosphorus. In a large-scale marsh which is hydrologically isolated and can be approximated by a plug flow reactor model, phosphorus concentrations in the outflow are expected to be near 10 $\mu g\ L^{-1}$. This hypothesis is based upon results from the most recent field study and data from the WCA-2A which shows that the WCA can achieve phosphorus concentrations at and below 10 $\mu g\ L^{-1}$ (Vaithiyanathan and Richardson, 1997). The chemical precipitation zone (2 day HRT) of the LICD marsh would be expected to remove 75 – 80% of the phosphorus load and the remaining phosphorus load would be removed through filtering and biotic uptake in the biotic zone of the LICD marsh. Thus, results from the LICD mesocosm and jar test studies and data from the WCA-2A suggest that 10 $\mu g\ L^{-1}$ is achievable in an LICD marsh.

Chapter 19. References

Bachand, P.A.M., P. Vaithiyanathan, R.G. Qualls and C.J. Richardson. 1999. Low Intensity Chemical Dosing of Stormwater Treatment Areas: An Approach to Enhance Phosphorus Removal Capacity of Stormwater Treatment Areas. Phase I. Final Report for FDEP Contract WM694. December 1999.

Bachand, P.A.M. and A.J. Horne. 2000. Denitrification in constructed free-water surface wetlands: II. Effects of vegetation and temperature. Ecological Engineering 14(1-2):17-32.

Berger, B.B. 1987. Control of Organic Substances in Water and Wastewater. Noyes Data Corporation, Park Ridge, NJ.

Craft, C.B. and C.J. Richardson. 1993. Peat accretion and N, P, and organic C accumulation in nutrient-enriched and unenriched Everglades peatlands. Ecological Applications 3(3):446-458.

CRC. 1982. Handbook of Chemistry and Physics. 62nd Edition. CRC Press. Boca Raton, Fl.

Cytec, 2000. Personal communications regarding pricing.

DUWC, 1999. Phase II Low Intensity Chemical Dosing (LICD): Development of Management Practices Year One. Scope of Work submitted by Duke University Wetland Center for Contract No. WM720 with Florida Department of Environmental Protection, Tallahassee, FL.

EPA. 1987. Design Manual, Phosphorus Removal. EPA/625/1-87/-001. U.S. Environmental Protection Agency, Office of Research and Development, Center for Environmental Research Information. Cincinnati, OH.

FDEP. 1997. Phase I Procedures for Evaluating the Potential for Effects to Everglades Biota from Discharges from Pilot Testing of Supplemental Technologies. Everglades Technical Series Number 1. Everglades Technical Support Section, Division of Water Facilities, Florida Department of Environmental Protection. November 26, 1997.

General Chemical, 2000. Personal communications with Chris Lind regarding pricing and products.

Kadlec, R.H. and R.L. Knight. 1996. Treatment Wetlands. CRC Press, NY.

Kemiron, 2000. Personal communications with Fred Sims regarding pricing, methods and design.

Metcalf and Eddy, 1979. Wastewater Engineering: Treatment, Disposal and Reuse. McGraw-Hill Book Company, NY.

Nearhoof, F.L. et al. 1999. Draft: Everglades Phosphorus Criterion Technical Support Document - WCA-2. Florida Department of Environmental Protection, Tallahassee, FL. Current Draft is September 1999.

Peer Consultants, P.C. / Brown and Caldwell. 1996. Desktop evaluation of alternative technologies final report. In Appendix L, Vol. II Final Programmatic Environmental Impact Statement. Florida's Everglades Program Everglades Constructions Project. US Army Corps of Engineers, Jacksonville, FL.

Peer Consultants, P.C. / Brown and Caldwell. 1999. Technical Memorandum. Basis for cost estimates of full scale alternative treatment (supplemental) technology facilities. Contract No. C-E008 – A12 presented to South Florida Water Management District. August.

Phipps, R.G. and W.G. Crumpton. 1994. Factors affecting nitrogen loss in experimental wetlands with different hydrologic loads. Ecological Engineering 3(4): 381-398.

Qualls, R.G. and C.J. Richardson. 1995. Forms of soil phosphorus along a nutrient enrichment gradient in the Northern Everglades. Soil Science 160(3): 183-198.

Richardson, C.J., P.A.M. Bachand, P. Vaithiyanathan, and Robert G. Qualls. 1997. Low Intensity Chemical Dosing of Stormwater Treatment Areas: An approach to enhance phosphorus removal capacity of Stormwater Treatment Areas, Phase I. Scope of Work for Contract No. WM694 with Florida Department of Environmental Protection, Tallahassee, FL.

Richardson, C.J., P. Vaithiyanathan, J.R. Stevenson, R.S. King, C.A. Stow, R.G. Qualls and S.Q. Song. 1999. The ecological basis for a Phosphorus threshold in the Everglades: Directions for sustaining ecosystem structure and function. Report to the Everglades Agricultural Area Environmental Protection District. Duke Wetland Center Publication 99-05

Richardson, C.J. and S.S. Qian. 1999. Long-term phosphorus assimilative capacity in freshwater wetlands: A new paradigm for sustaining ecosystem structure and function. Environmental Science and Technology 33(10):1545 – 1551.

SFWMD. 1999. Everglades Consolidated Report. South Florida Water Management District, West Palm Beach, Fl.

Sims, F. 1999. Phone conversations on methods to improve mixing and floc aggregation in the mesocosm study. Kemiron. Bartow, Fl.

Snoeyink, V.L. and D. Jenkins. 1980. Water Chemistry. John Wiley and Sons, Inc, NY, NY.

StatSoft. 1998. STATISTICA for Windows [Computer program manual]. Tulsa, OK: StatSoft, Inc., 2300 East 14th Street, Tulsa, OK.

Ullman, J.L. 1999. Characterization of iron in a constructed wetland following metal dosing for phosphorus removal from agricultural runoff. Master Thesis, Duke University.

Vaithiyanathan, P. and C.J. Richardson. 1997. Nutrient profiles in the everglades: examination along the eutrophication gradient. The Science of the Total Environment 205:81-95.

Vaithiyanathan, P and C.J. Richardson. 1999. Macrophyte species changes in the Everglades: Examination along a Eutrophication gradient. Journal of Environmental Quality 28:1347 – 1358.

Walker, W.W. 1995. Design basis for Everglades stormwater treatment areas. Water Resources Bulletin, 31: 671-685.

White, F.M. 1979. Fluid Mechanics. McGraw-Hill Book Company. N.Y.

Zimmerman, S. 1999. Phone conversations and recommendations on providing sufficient mixing in mixing tanks. Robert E. Mason. Charlotte, NC.

APPENDIXES

Appendix A. Database Description for Access File FDEP_PH2_Database

Table: MDLs and PQLs summary. See Appendix C which is the QAPP for this project

Grab Sample	Parameter	MDL	PQL	Unit
Surface Water				
	Dissolved reactive phosphate (PO_4-P)	0.002	0.006	mg L^{-1}
	Total dissolved P (TDP)	0.002	0.006	mg L^{-1}
	Total P in water (TP)	0.002	0.006	mg L^{-1}
	Dissolved Al	0.19	0.57	mg L^{-1}
	Total Al.	0.19	0.57	mg L^{-1}
	Dissolved Fe	0.08	0.24	mg L^{-1}
	Total Fe	0.08	0.24	mg L^{-1}
	Br	0.006	0.018	mg L^{-1}
	DOC	0.73	2.19	mg L^{-1}
Sediment/Soil				
	Total Phosphorus	23	69	mg kg^{-1}
	Total C	14	42	µg
	Total N	36	108	µg
	Total Al	48	144	mg kg^{-1}
	Total Fe	20	60	mg kg^{-1}
	Ca	5	15	mg kg^{-1}
	Cu	1.3	3.9	mg kg^{-1}
	Mg	0.5	1.5	mg kg^{-1}
	Zn	0.8	2.4	mg kg^{-1}
	Extractable forms of Phosphorus	0.9	2.7	mg kg^{-1}
	Extractable forms of Fe	4.8	14.4	mg kg^{-1}
	Extractable forms of Al	11	33	mg kg^{-1}

Table: Data Qualifiers

Data Qualifier	*Description*
A	Reported value is the calculated average of lab or field replicates.
BC	Reported value is blank corrected.
D#	Sample diluted by this factor (#). Reported value is the calculated result multiplied by same factor.
I	Reported value is between the lab MDL and lab PQL.
ID	The identification of this sample is questionable because the container label is damaged, or indecipherable.
J#	Reported value is estimated for reason #: 1) no quality control criteria exist for this analyte. 2) reported value didn't meet any of the established quality control criteria for precision and accuracy. 3) matrix interference prevented accurate determination. 4) improper lab or field protocols used.
K	Off-scale low. Reported value is below lowest standard on nonlinear calibration curve; actual value is known to be lower.
L	Off-scale high. Reported value is beyond the range of highest standard on nonlinear curve; sample can not be diluted.
M	Analyte detected but not quantified. Actual value is less than reported value. Reported value is the lab PQL.
NR	Sample with this tracking number not received.
O#	Sample received but analysis not performed for reason #: 1) analyte not required for this sample. 2) sample volume less than minimum required for analysis. 3) instrument configuration inappropriate for sample range. 4) contamination known or suspected, sample rejected. 5) sample container not found at time of analysis. 6) operator error 7) other
OD	Reported value is based on oven-dry weight.
Q	Sample analyzed after holding time expired.
QC	Percent recovery of external QC standard exceeded documented value by more than 10%.
R	Significant rain in past 48 hours.
RE	Reported value is from an analysis that was repeated for this sample.
T	Reported value is less than lab MDL, and is reported only per request of PI.
U	Analyte not detected. Reported value is the lab MDL.
V	The analyte was detected in both the sample and the blank.
Y	The sample was not preserved or was improperly preserved. (Note: this designation applies as well to samples arriving in cracked or leaking tubes.)
*	Not analyzed due to interference.
!	Reported value deviates from historical range.
?	Data is rejected, presence or absence of analyte can not be determined owing to unacceptable quality control criteria.
PRD	Values recorded by YSI probes before field deployment.
POD	Values recorded by YSI probes after field recovery

Table: CR10X_Hourly

Properties

Description: CR10X Hourly data
RecordCount: 13488

Columns

Name	Type	Size	Description
ID	Number (Long)	4	
ArrayID	Number (Long)	4	CR10X Array ID
Site	Number (Long)	4	Site Code (1 = A, 2 = B. 3 = C)
YEAR	Number (Double)	8	Year
DAY	Number (Double)	8	Julian Day
HRMIN	Number (Double)	8	Recording time
1H_GAL1	Number (Double)	8	One hour volume to M1 (gallons)
1H_GAL2	Number (Double)	8	One hour volume to M2 (gallons)
1H_GAL3	Number (Double)	8	One hour volume to M3 (gallons)
1H_GAL4	Number (Double)	8	One hour volume to M4 (gallons)
1H_GAL5	Number (Double)	8	One hour volume to M5 (gallons)
1H_GAL6	Number (Double)	8	One hour volume to M6 (gallons)
1H_GAL7	Number (Double)	8	One hour volume to M7 (gallons)
1H_GAL8	Number (Double)	8	One hour volume to M8 (gallons)
1H_GAL9	Number (Double)	8	One hour volume to all mesocosms (gallons)
H20DR_FT	Number (Double)	8	Distance from ultrasonic probe to water level (ft)
H20DC_FT	Number (Double)	8	Temp. corrected distance from ultrasonic probe to water level (ft)
H20EL_FT	Number (Double)	8	Water elevation (ft)
ETO_INHR	Number (Double)	8	Hourly evapotranspiration (in/hr)
RAIN_IN	Number (Double)	8	Hourly precipitation data (in/hr)
TMP_FAVE	Number (Double)	8	Average air temperature (°F)
RH_AVE	Number (Double)	8	Average relative humidity (%)
VPKPAAVE	Number (Double)	8	Average vapor pressure (KPa)
KWM2AVE	Number (Double)	8	Average solar radiation (kW/M^2)
WS MPH	Number (Double)	8	Average wind speed (mph)
WIND_DIR	Number (Double)	8	Average wind direction (degrees)
WDIR_SD	Number (Double)	8	Wind direction standard deviation (degrees)
CR10VAVE	Number (Double)	8	CR10X power (V)
PMP_VAVE	Number (Double)	8	System power (V)
PMP_VMIN	Number (Double)	8	Minimum system power (V)
DATE	Date/Time	8	Date
TIME	Date/Time	8	Time
DQ	Text	50	Data Qualifier
DOWNLOAD	Date/Time	8	Download Date

Table: PH2:DosingSchedule

Properties

Description: Phase I Mesocosm Dosing Schedule
RecordCount: 31

Columns

Name	Type	Size	Description
order	Number (Long)	4	
Ph1	Number (Integer)	2	Phase I Data Label
RunNo	Number (Double)	8	Run Number
Model	Text	255	Batch or Continuous Flow Reactor Model
Site	Text	255	Mesocosm Site at which data collected
Meso	Number (Double)	8	Mesocosm identifier
MesoCode	Text	50	Mesocosm identifier
Trade	Text	255	Trade Name for dosed chemical
Metal	Text	50	Metal (e.g. Fe or Al)
Dose_uM	Number (Double)	8	Dosing level (uM)
Me_ppm	Number (Double)	8	Dosing level (ppm)

Table: Ph2:SampleIDs

Properties

Description: Phase 1 Sample ID descripitions for water quality data
RecordCount: 184

Columns

Name	Type	Size	Description
Smpl ID	Text	255	Sample ID
SiteCode	Text	255	Mesocosm site at which data collected
MesoCode	Text	255	Mesocosm identifier
LocCode	Text	255	Sample location identifier
RepCode	Text	255	Replicate identifier
Site	Text	50	Site Name
Mesocosm	Text	50	Mesocosm Name
Location	Text	50	Sampling location description
Replicate	Text	50	Replicate Name

Table: PH2:SoilData

Properties

Description: Phase 1 Soil Data.
RecordCount: 1523

Columns

Name	Type	Size	Description
TrackNo	Text	255	Tracking Number
Smpl ID	Text	255	Sample ID
AbrSmplID	Text	255	Abreviated sample ID for database utilities
Date	Date/Time	8	Date
Matrix	Text	50	Matrix (SO = soil/sediment)
SiteCode	Text	255	Site Code
MesoCode	Text	255	Mesocosm Code
DepthCode	Text	255	Depth Code for partitioning sample core
Depth (cm)	Text	50	Depth from which sample was collected from core (range in cm)
ParaCode	Text	255	Sampled parameter identifier code
Parameter	Text	50	Sampled parameter description
Fraction	Text	255	Sampled parameter fraction
ParaFracCode	Text	255	Parameter fraction code for database utilities
SoilConc ugg	Number (Double)	8	Soil concentration (ug/g^{-1})
DQ	Text	255	Data Qualifier

Table: PH2:SW_WaterQual

Properties

Description: Phase 1 Surface Water Quality Sample Summary
RecordCount: 1377

Columns

Name	Type	Size	Description
Ph1	Number (Integer)	2	Phase I
TrackNo	Text	255	Tracking Number
Smpl ID	Text	255	Sample ID
WkDay	Number (Double)	8	Weeks (for Continuous) or Days (for Batch) since initiation of Chemical dosing for given Run Number.
SiteCode	Text	255	Site Code
Site	Text	50	Site Name
MesoCode	Text	255	Mesocosm Code
Mesocosm	Text	50	Mesocosm Name
LocCode	Text	255	Location Code for water sampling
Location	Text	50	Description of water sampling location
RepCode	Text	255	Replicate Code (A = Field Replicate 1, B= Field Replicate 2)
Replicate	Text	50	Replicate Name
FOP ppb	Number (Double)	8	Filtered ortho-phosphate (ppb)
FOP DQ	Text	255	and data qualifier
FTP ppb	Number (Double)	8	Filtered total phosphorus (ppb)
FTP DQ	Text	255	and data qualifier
UTP ppb	Number (Double)	8	Unfiltered total phosphorus (ppb)
UTP DQ	Text	255	and data qualifier
FOC ppm	Number (Double)	8	Filtered organic carbon (ppm)
FOC DQ	Text	255	and data qualifier
FAL ppm	Number (Double)	8	Filtered total aluminum (ppm)
FAL DQ	Text	255	and data qualifier
UAL ppm	Number (Double)	8	Unfiltered total aluminum (ppm)
UAL DQ	Text	255	and data qualifier
FFE ppm	Number (Double)	8	Filtered total iron (ppm)
FFE DQ	Text	255	and data qualifier
UFE ppm	Number (Double)	8	Unfiltered total iron (ppm)
UFE DQ	Text	255	and data qualifier
FBr ppm	Number (Double)	8	Filtered total bromide (ppm)
FBr DQ	Text	255	and data qualifier
Year	Number (Long)	4	Year
Month	Text	50	Month
Date	Date/Time	8	Sample date
JulDay	Number (Double)	8	Julian Day
Model	Text	255	Model (Cont. = Continuous flow reactor study; Batch = Batch Flow reactor study)
RunNo	Number (Double)	8	Experimental Run Number

Table: PH2:SW_WaterQual Blanks

Properties

Description: Phase I Surface Water Quality Blank Data
RecordCount: 284

Columns

Name	Type	Size	Description
TrackNo	Text	255	Tracking Number
Smpl ID	Text	255	Sample ID (e.g. Blank Name):
			FLBlK — Field blank
			PBLK — Pump blank
			DIBLK — DI water blank
			DIPBLK — Dip blank
			PCEBLK — Pre-cleaned equipment blank
			FCEBL1 — Field-cleaned equipment blank 1
			FCEBL2 — Field-cleaned equipment blank 2
FOP ppb	Number (Double)	8	Filtered ortho-phosphate (ppb)
FOP DQ	Text	255	and data qualifier
FTP ppb	Number (Double)	8	Filtered total phosphorus (ppb)
FTP DQ	Text	255	and data qualifier
UTP ppb	Number (Double)	8	Unfiltered total phosphorus (ppb)
UTP DQ	Text	255	and data qualifier
FOC ppm	Number (Double)	8	Filtered organic carbon (ppm)
FOC DQ	Text	255	and data qualifier
FAL ppm	Number (Double)	8	Filtered total aluminum (ppm)
FAL DQ	Text	255	and data qualifier
UAL ppm	Number (Double)	8	Unfiltered total aluminum (ppm)
UAL DQ	Text	255	and data qualifier
FFE ppm	Number (Double)	8	Filtered total iron (ppm)
FFE DQ	Text	255	and data qualifier
UFE ppm	Number (Double)	8	Unfiltered total iron (ppm)
UFE DQ	Text	255	and data qualifier
FBr ppm	Number (Double)	8	Filtered total bromide (ppm)
FBr DQ	Text	255	and data qualifier
RunNo	Number (Double)	8	Experimental Run Number
Date	Date/Time	8	Sample Date

Table: YSI

Properties

Description: Phase I YSI Data
RecordCount: 17695

Columns

Name	Type	Size	Description
ID	Number (Long)	4	
Sitecode	Text	255	Site Code
MesoCode	Text	50	Mesocosm Code
ProbeCode	Text	255	Probe Code
Startdate	Date/Time	8	Deployment Date
Date	Date/Time	8	Recording date
Time	Date/Time	8	Recording time
Temp	Number (Double)	8	Water temperature (°F)
SpC uScm	Number (Double)	8	Specific conductivity (uS/cm)
DO%	Number (Double)	8	Dissolved oxygen (% saturation)
Do mgl	Number (Double)	8	Dissolved oxygen (ppm)
pH	Number (Double)	8	pH
Orp mV	Number (Double)	8	Redox (Data not calibrated)
Turb NTU	Number (Double)	8	Turbidity (NTU)
Batt V	Number (Double)	8	YSI Battery Voltage (V)
Time Rnd	Date/Time	8	Recording time rounded to the hour if needed
Notes	Text	255	Data Qualifier
Depth ft	Number (Double)	8	Water depth (ft)

Table: YSIprobe_code

Properties

Description: Probe identification codes.
RecordCount: 6

Columns

Name	Type	Size	Description
ProbeCode	Text	255	Probe Code
SerialNo	Text	255	Probe serial number

Appendix B. Scope of Work for FDEP Contract No. WM720

Appendix C. QAPP

Appendix D. Database

(Database “FDEP_PH2_Database.mdb” is included on attached CD-Rom)